

Multi-Channel Communications

R. Michael Buehrer

November 14, 2022

Part I

Preliminaries

Notation

The notation used in this manuscript is listed in the following tables. More specifically, Tables 1 and 2 describe the general notation used in this text. Tables 3 and 4 represent the English letter variables used in the text while Table 6 describe the Greek variables used in the manuscript.

Symbol	Meaning	Notes
$\tilde{x}(t)$	complex function	This notation will always indicate a complex function. However, at times we may have complex functions without this notation. Depends on context.
$\tilde{x}^*(t)$	complex conjugate	if $\tilde{x}(t) = a(t) + jb(t)$ then $\tilde{x}^*(t) = a(t) - jb(t)$
$E\{x(t)\}$ $E\{\mathbf{x}\}$	expectation of random process $x(t)$ expectation of random vector \mathbf{x}	If not clear from the context, the variable over which the expectation is taken will be made clear by using a subscript. e.g., $E_\lambda\{\mathbf{x}\}$ indicates expectation over λ
$\mathcal{F}\{x(t)\}$ $\mathcal{F}^{-1}\{X(f)\}$ $\mathcal{F}\{x[n]\}$ $\mathcal{F}^{-1}\{X[k]\}$	Fourier Transform of $x(t)$ Inverse Fourier Transform of $X(f)$ Discrete Transform of $x[n]$ Inverse Discrete Transform of $X[k]$	$X(f) = \mathcal{F}\{x(t)\} = \int_{-\infty}^{\infty} x(t)e^{-j2\pi ft}dt$ $x(t) = \mathcal{F}^{-1}\{X(f)\} = \int_{-\infty}^{\infty} X(f)e^{j2\pi ft}df$ $X[k] = \mathcal{F}\{x[n]\} = \sum_{n=0}^{N-1} x[n]e^{-j\frac{2\pi}{N}kn}$ $x[n] = \mathcal{F}^{-1}\{X[k]\} = \sum_{k=0}^{N-1} X[k]e^{j\frac{2\pi}{N}kn}$ In matrix notation, $\mathbf{X} = \mathbf{D}_N \mathbf{x}$, where \mathbf{D}_N defined below $\mathbf{x} = \mathbf{D}_N^H \mathbf{X}$ where $\mathbf{x}, \mathbf{X} \in \mathcal{C}^N$
\mathbf{v}	column vector	$\bar{\mathbf{v}}$ will also be used when bold isn't clear if size of vector isn't clear from context $\mathbf{v}^{a \times 1}$ will indicate the size
$[\mathbf{v}]_i$	i th element of vector	
\mathbf{H}	matrix	If size isn't clear from context, $\mathbf{H}^{m \times n}$ will be used to indicate an $m \times n$ matrix
$[\mathbf{H}]_{i,j}$	$\{i,j\}$ th element of matrix \mathbf{H}	
$\mathbb{R}^{m \times n}$	set of all $m \times n$ real matrices	
$\mathcal{C}^{m \times n}$	set of all $m \times n$ complex matrices	
$\mathbf{I}^{m \times m}$	$m \times m$ identity matrix	
$\mathbf{0}^{m \times n}$	$m \times n$ matrix of zeros	
$span(\mathcal{S})$	set of vectors spanned by \mathcal{S}	
$col(\mathbf{A})$	space spanned by columns of \mathbf{A}	column space of \mathbf{A}
$row(\mathbf{A})$	space spanned by rows of \mathbf{A}	row space of \mathbf{A}
$vec(\mathbf{A})$	stacked columns of matrix \mathbf{A}	converts an $m \times n$ matrix to an $mn \times 1$ vector
\mathbf{u}^T \mathbf{A}^T	transpose of \mathbf{u} transpose of \mathbf{A}	
$\ \mathbf{u}\ _p$	p -norm of \mathbf{u}	$\ \mathbf{u}\ $ is the 2-norm

Table 1: General Notation Used in the Class (Part 1 of 2)

Symbol	Meaning	Notes
\mathbf{A}^*	element by element conjugate of \mathbf{A}	
\mathbf{A}^H	conjugate transpose of \mathbf{A}	
\mathbf{A}^{-H}	conjugate transpose of \mathbf{A}^{-1}	$\mathbf{A}^{-H} = (\mathbf{A}^{-1})^H$
\mathbf{A}^\dagger	pseudo-inverse of \mathbf{A}	$\mathbf{A}^\dagger = (\mathbf{A}^T \mathbf{A})^{-1} \mathbf{A}^T$ $\mathbf{A}^\dagger = (\mathbf{A}^H \mathbf{A})^{-1} \mathbf{A}^H$ if \mathbf{A} is complex
$\mathbf{A}^{1/2}$	matrix square root	
$\text{trace}(\mathbf{A})$	trace of \mathbf{A}	sum of diagonal elements
$R(\mathbf{A})$	rank of \mathbf{A}	
$\text{row}(\mathbf{A})$	row space of \mathbf{A}	
$\text{col}(\mathbf{A})$	column space of \mathbf{A}	
$\dim(\mathbf{A})$	dimension of \mathbf{A}	number of vectors in any basis
$\lambda(\mathbf{A})$	eigenvalues of \mathbf{A}	also called the spectrum of \mathbf{A} $\lambda_{\min}, \lambda_{\max}$ are min and max eigenvalues $\lambda_k(\mathbf{A})$ is the k th eigenvalue of \mathbf{A}
$\sigma(\mathbf{A})$	singular values of \mathbf{A}	$\sigma_{\min}, \sigma_{\max}$ are min and max singular values
$\ \mathbf{A}\ _F$	Frobenius norm of \mathbf{A}	
\mathbf{A}^{-1}	inverse of \mathbf{A}	
$ \mathcal{V} $	cardinality of set \mathcal{V}	sets will generally use cal font
$\nabla f(\mathbf{x})$	gradient of function $f(\mathbf{x})$	argument is a vector \mathbf{x} ; output is scalar

Table 2: General Notation Used in the Class (Part 2 of 2)

Symbol	Meaning	Notes
$\mathbf{a}(\theta)$	array factor	also array manifold vector
$\mathbf{A}(\bar{\theta})$	Matrix of array factors	$\mathbf{A}(\bar{\theta}) = [\mathbf{a}_1 \mathbf{a}_2 \dots \mathbf{a}_N]$
B	bandwidth	
C	capacity	
d	distance	scalar
D	Directivity	
\mathbf{D}_N	DFT matrix, $[\mathbf{D}]_{m,n} = e^{-j2\pi(m-1)(n-1)/N}$	\mathbf{D}_N^H is IDFT matrix
$\mathbf{D}_{(LL)}$	first L rows and columns of N -point DFT matrix ($L \times L$ matrix)	\mathbf{D}_N also known as Fourier matrix
$\mathbf{D}_{(NL)}$	first L columns DFT matrix ($N \times L$ matrix)	
f	frequency	
f_c	center (or carrier) frequency	
f_d	max Doppler frequency	$f_d = \frac{v}{\lambda}$
f_o	digital frequency offset	$f_o = f_{co}T_{eff}$ (f_{co} = cont. time)
f_{sa}	sampling frequency	$f_{sa} = \frac{1}{T_{sa}}$
Δf	sub-carrier spacing in OFDM	
$f_X(x)$	pdf of random variable X	
$F_X(x)$	cdf of random variable X	
G_r	Receive Antenna Gain	scalar when in dB use $G_r(dB)$
G_t	Transmit Antenna Gain	scalar when in dB use $G_t(dB)$
$G(\theta)$	Array Factor	gain pattern due to array
$g_A(\theta)$	individual element pattern	gain pattern due to element
$h(\tau, t), \mathbf{H}(\tau, t)$	channel impulse response	if time-invariant, t is dropped if narrowband, τ is dropped can be scalar or vector or matrix if matrix, size is $M_r \times N_t$ complex baseband channel
$\tilde{h}(\tau, t)$		complex baseband channel sample
\tilde{h}		\tilde{h} and \tilde{a} are essentially the same
$H(f, t)$	time-varying frequency response	$\mathcal{F}\{h(t, \tau)\}$
\mathbf{H}	channel matrix	complex channel samples
\mathbf{H}_w	white channel matrix	channel elements are iid complex GRV
$H(X)$	entropy of random variable X	context differentiates from channel functions
$I(x; y)$	mutual information between x and y	
$J_o(\tau)$	zeroth-order Bessel function of the first kind	
K	Number of users	Used in multi-user systems
L	diversity order	Number of branches in a diversity system (could be equal to M_r)
M_r	number of receive antennas	

Table 3: Variables Used in the Class (Part 1 of 3)

Symbol	Meaning	Notes
n	path loss exponent	scalar
n	noise (sample)	scalar or vector
$n(t)$	noise function	typically AWGN
$n_i(t)$	noise function on i th rx antenna	typically AWGN
N	number of components	typically multipath components
N_{cp}	samples in cyclic prefix	Number of sub-carriers in OFDM
N_s	number of signals in the environment	
N_t	number of transmit antennas	
P_r	Received Power	scalar when in dB use $P_r(\text{dB})$
P_t	Transmit Power	scalar when in dB use $P_t(\text{dB})$
$p(t)$	pulse shape	
$r(t)$	received signal with noise	$r[k]$ is the sampled signal
$r_i(t)$	received signal with noise on i th antenna	
$\mathbf{r}(t)$	received signal on all antennas	if sampled, \mathbf{r}
$R(\tau)$	auto-correlation function of a random process	
\mathbf{R}_{tx}	transmit side correlation matrix	
\mathbf{R}_{rx}	of the random channel vector	seen across the transmit antennas
\mathbf{R}	receive side correlation matrix	
R_b	of the random channel vector	seen across the receive antennas
R_s	correlation matrix	$E\{\text{vec}(\mathbf{H})\text{vec}(\mathbf{H})^H\}$
R_{st}	bit rate	
R_{ofdm}	symbol rate	
	space-time symbol rate	
	OFDM symbol rate	

Table 4: Variables Used in the Class (Part 2 of 3)

Symbol	Meaning	Notes
$s_{i,k}$	symbol transmitted from the i th antenna during k th time slot	o
$S(f)$ $S_A(\theta)$	Power Spectral Density of Random Process Azimuthal Power Spectral Density	Fourier Transform of $R(\tau)$ power per received angle $P_r = \int_{-\pi}^{\pi} S_A(\theta) G(\theta) d\theta$ $G(\theta)$ is the receive antenna gain $\mathcal{F}\{\tilde{R}(\tau)\}$
$S_D(f)$	Doppler Spectrum	
t	time	
T_s T_{sa}	symbol duration sample time/duration	$T_{sa} = \frac{1}{f_{sa}}$
T_o T_{eff} T_{cp} T_w	OFDM symbol duration effective OFDM symbol duration cyclic prefix duration window duration	$T_o = T_{eff} + T_{cp} + T_w$ $T_{eff} = 1/\Delta f$
$U[a, b]$	uniform distribution	range is [a,b]
v or \mathbf{v}	velocity	scalar or vector
w or \mathbf{w}	weights	scalar or vector
$x(t)$ $x_i(t)$ $\mathbf{x}(t)$	transmit signal transmit signal from i th antenna is transmit signal from multiple antennas	Will also use $\bar{x}(t)$ for this vector
z	decision statistic	after channel compensation

Table 5: Variables Used in the Class (Part 3 of 3)

Symbol	Meaning	Notes
α	magnitude of single channel	$\tilde{\alpha}$ is complex channel $\alpha e^{j\phi}$ h will sometimes also be used for the single antenna channel
γ	SNR	
$\delta(t)$	impulse function	
Δ	distance	
ΔX	change in X	
ϵ	error	e.g. in the adaptation of antenna weights
η	decision statistic	before channel compensation ($z = \alpha^* \eta$)
ψ	general angle of an array	$\psi = \frac{2\pi d}{\lambda} \sin(\theta)$
λ	wavelength	scalar
λ	eigenvalue of a square matrix	context clarifies
μ	mean	
μ_i	i th moment about zero	
ν	discrete symbol time	represents discrete time
∇	gradient	$\hat{\nabla}$ is the estimated gradient
Ω_A	Solid Beam Angle	
ϕ	phase	
$\phi(\omega)$	Characteristic Function	$E_\gamma \{ e^{j\omega\gamma} \}$
Φ	angle-of-departure	defined relative to array normal
$\Phi(s)$	Moment Generating Function	$E_\gamma \{ e^{s\gamma} \}$
$\rho(d)$	spatial correlation	measured at distance d
θ	angle-of-arrival	defined relative to array normal
σ_n	noise standard deviation	
σ_A	AOA standard deviation	
σ	singular value of a matrix	context clarifies
$\Sigma_{\mathbf{x}}$	covariance matrix of the vector \mathbf{x}	$\Sigma_{\mathbf{x}} = E \{ \mathbf{x} \mathbf{x}^H \} - E \{ \mathbf{x} \} E \{ \mathbf{x} \}^H$
τ	delay	
ζ	element angle	defined for a circular array
ψ	array variable	$= \frac{2\pi d}{\lambda} \sin(\theta)$

Table 6: Greek Variables Used in the Class

Chapter 1

Matrix Theory: Basic Definitions

1.1 Introduction

Multi-channel communications by its nature involves the consideration of multiple channels simultaneously, whether they be in time, space or frequency. These channels may be separate at the time of transmission, but mixed upon reception. Or they may stay orthogonal throughout. In either case, vector and matrix notation is a convenient way to represent multiple channels both at the transmitter and receiver. Further, matrix theory is very convenient in describing the characteristics of these signals and the wireless channels that carry them. Thus, in this chapter we will provide a brief overview of vectors and matrices, with an emphasis on those concepts that are important to understanding MIMO and OFDM. For a more complete treatment of the topic of Linear Algebra and Matrix Analysis, please see [1]. In this section we will specifically discuss the following:

- Definitions
- Vector Spaces
- Functions of Matrices and Vectors
- Matrix Inversion
- Matrix Factorization (LU, LDU, Cholesky)
- Singular Value and Eigenvalue Decomposition

1.2 Basic Definitions

An n -element column vector is a group of n elements in vertical form:

$$\mathbf{v}^{n \times 1} = \begin{bmatrix} v_1 \\ v_2 \\ \vdots \\ v_n \end{bmatrix}$$

An n -element row vector is a group of n elements in horizontal form:

$$\mathbf{v}^{1 \times n} = \begin{bmatrix} v_1 & v_2 & v_3 & \cdots & v_n \end{bmatrix}$$

If not specified, assume that any lower case bold letter is a column vector and any upper case bold letter is a matrix.

A matrix $\mathbf{V}^{m \times n}$ is defined as an $m \times n$ array of mn elements:

$$\mathbf{V}^{m \times n} = \begin{bmatrix} v_{11} & v_{12} & v_{13} & \cdots & v_{1n} \\ v_{21} & v_{22} & v_{23} & \cdots & v_{2n} \\ v_{31} & v_{32} & v_{33} & \cdots & v_{3n} \\ \vdots & \vdots & \vdots & \vdots & \vdots \\ v_{m1} & v_{m2} & v_{m3} & \cdots & v_{mn} \end{bmatrix}$$

$\Re^{m \times n}$ represents the set of all $m \times n$ real matrices.

$\mathcal{C}^{m \times n}$ is the set of all complex matrices of dimension $m \times n$. Note that $\mathcal{C} \in \{\Re^{m \times n} + j\Re^{m \times n}\}$.

Example 1.2.1. Consider modulation symbols s_i transmitted from four different transmitters using the same pulse shape and received at four different receivers over the same frequency band. If there is independent noise generated at each receiver, how can we use matrix notation to represent the matched filter outputs assuming independent channels h_{ij} between the i th receiver and j th transmitter? How would we represent the received signal if the transmit and receive frequency bands were mutually orthogonal?

Solution: We can write the transmitted symbols as a vector $\mathbf{s} = [s_1, s_2, s_3, s_4]^T$. The channel between four transmitters and five receivers can be written as a 4×4 matrix with h_{ij} as the (i, j) th element:

$$\mathbf{H} = \begin{bmatrix} h_{1,1} & h_{1,2} & h_{1,3} & h_{1,4} \\ h_{2,1} & h_{2,2} & h_{2,3} & h_{2,4} \\ h_{3,1} & h_{3,2} & h_{3,3} & h_{3,4} \\ h_{4,1} & h_{4,2} & h_{4,3} & h_{4,4} \end{bmatrix} \quad (1.1)$$

The matched filter outputs and the noise samples can both be written as 5×1 vectors $\tilde{\mathbf{r}}$ and \mathbf{n} respectively. That gives the following representation:

$$\mathbf{r} = \mathbf{H}\mathbf{s} + \mathbf{n} \quad (1.2)$$

If the frequency bands are orthogonal, the equation would be the same but we would have a different definition for the channel matrix \mathbf{H} . Specifically, it would be diagonal:

$$\mathbf{H} = \begin{bmatrix} h_{1,1} & 0 & 0 & 0 \\ 0 & h_{2,2} & 0 & 0 \\ 0 & 0 & h_{3,3} & 0 \\ 0 & 0 & 0 & h_{4,4} \end{bmatrix} \quad (1.3)$$

1.3 Vector Measures

Two column vectors \mathbf{u} and \mathbf{v} (with equal length) are said to be **orthonormal** if

$$\mathbf{u}^T \mathbf{v} = 0$$

and

$$\mathbf{u}^T \mathbf{u} = \mathbf{v}^T \mathbf{v} = 1$$

The p -norm of a vector \mathbf{v} is defined as

$$\|\mathbf{v}\|_p = \left(\sum_{i=1}^n |v_i|^p \right)^{1/p}$$

Example 1.3.1. Consider the vectors $\mathbf{u}_1 = \begin{bmatrix} 1 \\ 1 \\ 1 \\ 1 \end{bmatrix}$ and $\mathbf{v}_1 = \begin{bmatrix} 1 \\ -1 \\ 1 \\ -1 \end{bmatrix}$. Are they orthonormal? How about

$$\mathbf{u}_2 = \begin{bmatrix} 0.5 \\ 0.5 \\ 0.5 \\ 0.5 \end{bmatrix} \text{ and } \mathbf{v}_2 = \begin{bmatrix} 0.5 \\ -0.5 \\ 0.5 \\ -0.5 \end{bmatrix} \text{ ? What is the 2-norm of } \mathbf{v}_1?$$

Solution: It is straightforward to show that $\mathbf{u}_1^T \mathbf{v}_1 = 0$. Thus, the two vectors are orthogonal. However, $\|\mathbf{u}_1\|_2 = 2$ and $\|\mathbf{v}_1\|_2 = 2$. Thus, neither vector has unit norm and the two vectors are NOT orthonormal.

On the other hand $\mathbf{u}_2^T \mathbf{v}_2 = 0$, $\|\mathbf{u}_2\|_2 = 1$ and $\|\mathbf{v}_2\|_2 = 1$. Thus \mathbf{u}_2 and \mathbf{v}_2 are orthonormal.

1.3.1 Vector Spaces

A set of vectors \mathcal{V} is defined as a vector space over \mathcal{F} when basic vector addition and scalar multiplication properties hold. The most fundamental are the closure properties:

- $\mathbf{x} + \mathbf{y} \in \mathcal{V}$ for all $\mathbf{x}, \mathbf{y} \in \mathcal{V}$
- $\alpha\mathbf{x} \in \mathcal{V}$ for all $\alpha \in \mathcal{F}$ and $\mathbf{x} \in \mathcal{V}$.

Simple example: the set \mathbb{R}^n of real vectors of length n is a vector space over \mathbb{R} .

A **subspace** is defined as a non-empty set of vectors taken from a vector space that also forms a separate vector space.

1.3.2 Linear Independence

A set of vectors $\mathcal{S} = \{\mathbf{v}_1, \mathbf{v}_2, \mathbf{v}_3, \dots, \mathbf{v}_n\}$ is said to be **linearly independent** when the only set of coefficients α_i that satisfy the equation

$$\alpha_1\mathbf{v}_1 + \alpha_2\mathbf{v}_2 + \alpha_3\mathbf{v}_3 + \dots + \alpha_n\mathbf{v}_n = \mathbf{0}$$

is $\alpha_1 = \alpha_2 = \alpha_3 = \dots = \alpha_n = 0$.

Alternatively, a set of vectors is linearly independent if none of them can be written as a linear combination of finitely many other vectors in the collection.

A set of vectors which is not linearly independent is called **linearly dependent**.

1.3.3 Span

A set of vectors \mathcal{S} is said to **span** the vector space \mathcal{V} if every vector in \mathcal{V} can be generated from a linear combination of the vectors in \mathcal{S} .

We denote this relationship by $\mathcal{V} = \text{span}(\mathcal{S})$ or \mathcal{S} spans \mathcal{V} .

If a set of vectors \mathcal{S} is a spanning set and is also **linearly independent** it is said to be a **basis** for the vector space \mathcal{V} .

Example 1.3.2. The unit vectors $\left\{ \mathbf{e}_1 = \begin{pmatrix} 1 \\ 0 \\ 0 \end{pmatrix}, \mathbf{e}_2 = \begin{pmatrix} 0 \\ 1 \\ 0 \end{pmatrix}, \mathbf{e}_3 = \begin{pmatrix} 0 \\ 0 \\ 1 \end{pmatrix} \right\}$ span \mathbb{R}^3 .

That is, we can construct any vector in \mathbb{R}^3 using a weighted sum of \mathbf{e}_1 , \mathbf{e}_2 , and \mathbf{e}_3 .

NOTE: These vectors also form a basis for \mathbb{R}^3 .

1.4 Matrices

1.4.1 Matrix Addition

Consider two matrices \mathbf{A} and \mathbf{B} which are $m \times n$ matrices. The sum of two matrices is defined as the sum of the individual elements:

$$\mathbf{A} + \mathbf{B} = \begin{bmatrix} A_{11} + B_{11} & A_{12} + B_{12} & \cdots & A_{1n} + B_{1n} \\ A_{21} + B_{21} & A_{22} + B_{22} & \cdots & A_{2n} + B_{2n} \\ \vdots & \vdots & \ddots & \vdots \\ A_{m1} + B_{m1} & A_{m2} + B_{m2} & \cdots & A_{mn} + B_{mn} \end{bmatrix}_{m \times n}$$

1.4.2 Scalar Multiplication

When multiplying a matrix \mathbf{A} by a scalar α the result is that every element in the matrix is multiplied by that scalar. In other words:

$$\alpha\mathbf{A} = \begin{bmatrix} \alpha A_{11} & \alpha A_{12} & \cdots & \alpha A_{1n} \\ \alpha A_{21} & \alpha A_{22} & \cdots & \alpha A_{2n} \\ \vdots & \vdots & \ddots & \vdots \\ \alpha A_{m1} & \alpha A_{m2} & \cdots & \alpha A_{mn} \end{bmatrix}$$

1.4.3 Matrix Multiplication

The multiplication of two matrices requires that the number of columns of the first matrix is the same as the number of rows of the second matrix. Given the $m \times n$ matrix \mathbf{A} and the $n \times k$ matrix \mathbf{B} , the multiplication of the two matrices is defined as

$$\mathbf{AB} = \begin{bmatrix} \sum_{i=1}^n A_{1i}B_{i1} & \sum_{i=1}^n A_{1i}B_{i2} & \cdots & \sum_{i=1}^n A_{1i}B_{ik} \\ \sum_{i=1}^n A_{2i}B_{i1} & \sum_{i=1}^n A_{2i}B_{i2} & \cdots & \sum_{i=1}^n A_{2i}B_{ik} \\ \vdots & \vdots & \ddots & \vdots \\ \sum_{i=1}^n A_{mi}B_{i1} & \sum_{i=1}^n A_{mi}B_{i2} & \cdots & \sum_{i=1}^n A_{mi}B_{ik} \end{bmatrix}_{m \times k}$$

Note that in general, $\mathbf{AB} \neq \mathbf{BA}$. In fact, both products can only be formed when the two matrices are square with the same dimensions.

However, if \mathbf{A} , \mathbf{B} and \mathbf{AB} are all symmetric and \mathbf{A}, \mathbf{B} , both are of the same dimensions, then $\mathbf{AB} = \mathbf{BA}$. Alternatively, if \mathbf{A}, \mathbf{B} are of the same dimensions and diagonal, then $\mathbf{AB} = \mathbf{BA}$.

1.4.4 Matrix Transpose

The transpose of a matrix is the matrix obtained by interchanging the rows and columns of that matrix.

The transpose of the $m \times n$ matrix \mathbf{A} is a $n \times m$ matrix denoted as \mathbf{A}^T . That is:

$$\mathbf{A}^T = \begin{bmatrix} A_{11} & A_{21} & \cdots & A_{m1} \\ A_{12} & A_{22} & \cdots & \alpha A_{m2} \\ \vdots & \vdots & \cdots & \vdots \\ A_{1n} & A_{2n} & \cdots & A_{mn} \end{bmatrix}_{n \times m}$$

From this definition, it should be clear that $(\mathbf{A}^T)^T = \mathbf{A}$.

1.4.5 Matrix Conjugate

The conjugate of a matrix is the element-by-element conjugate. We will denote the conjugate of the matrix \mathbf{A} as \mathbf{A}^* :

$$\mathbf{A}^* = \begin{bmatrix} A_{11}^* & A_{12}^* & \cdots & A_{1n}^* \\ A_{21}^* & A_{22}^* & \cdots & A_{2n}^* \\ \vdots & \vdots & \cdots & \vdots \\ A_{m1}^* & A_{m2}^* & \cdots & A_{mn}^* \end{bmatrix}_{m \times n}$$

1.4.6 Matrix Hermitian

The conjugate transpose \mathbf{A}^H (sometimes called the **Hermitian** of \mathbf{A}) is then:

$$\mathbf{A}^H = \begin{bmatrix} A_{11}^* & A_{21}^* & \cdots & A_{m1}^* \\ A_{12}^* & A_{22}^* & \cdots & \alpha A_{m2}^* \\ \vdots & \vdots & \cdots & \vdots \\ A_{1n}^* & A_{2n}^* & \cdots & A_{mn}^* \end{bmatrix}_{n \times m}$$

1.4.7 Matrix Definitions

A **symmetric matrix** is one for which $\mathbf{A} = \mathbf{A}^T$. A **Hermitian matrix** is one for which $\mathbf{A} = \mathbf{A}^H$. It is straightforward to show that

$$\begin{aligned} (\mathbf{AB})^T &= \mathbf{B}^T \mathbf{A}^T \\ (\mathbf{AB})^H &= \mathbf{B}^H \mathbf{A}^H \end{aligned}$$

Because of these facts, $\mathbf{A}^T \mathbf{A}$ and $\mathbf{A} \mathbf{A}^T$ are symmetric matrices:

$$(\mathbf{A}^T \mathbf{A})^T = \mathbf{A}^T (\mathbf{A}^T)^T = \mathbf{A}^T \mathbf{A}$$

Similarly, for a complex matrix \mathbf{A} , $\mathbf{A}^H \mathbf{A}$ is a Hermitian matrix.

Important Matrix Measures

The **trace** of an $n \times n$ matrix is the sum of its diagonal elements. That is

$$\text{trace}(\mathbf{A}) = A_{11} + A_{22} + \dots + A_{nn} = \sum_{i=1}^n A_{ii}$$

The **Frobenius norm** of a matrix is defined as

$$|\mathbf{A}|_F = \sqrt{\sum_{i=1}^m \sum_{j=1}^m |A_{ij}|^2}$$

Later we will also discuss the **rank** and **determinant** of a matrix.

The Matrix Inverse

For a square matrix \mathbf{A} of size $n \times n$, the matrix \mathbf{B} that satisfies the conditions

$$\mathbf{AB} = \mathbf{I}_n$$

and

$$\mathbf{BA} = \mathbf{I}_n$$

where \mathbf{I}_n is an $n \times n$ identity matrix is called the **inverse** of \mathbf{A} , denoted $\mathbf{B} = \mathbf{A}^{-1}$.

For a matrix to be invertible it must be square, but not all square matrices are invertible.

A matrix that is not invertible is called a **singular matrix**. If it is invertible, it is **nonsingular**.

Properties of the Matrix Inverse

For two square nonsingular matrices \mathbf{A} and \mathbf{B} of the same dimensions:

- $(\mathbf{A}^{-1})^{-1} = \mathbf{A}$
- \mathbf{AB} is also nonsingular
- $(\mathbf{AB})^{-1} = \mathbf{B}^{-1}\mathbf{A}^{-1}$
- $(\mathbf{A}^{-1})^T = (\mathbf{A}^T)^{-1}$

The Matrix Inversion Lemma

A very handy identity is the matrix inversion lemma (also known as the Woodberry matrix identity) which states

$$(\mathbf{A} + \mathbf{BCD})^{-1} = \mathbf{A}^{-1} - \mathbf{A}^{-1}\mathbf{B}(\mathbf{C}^{-1} + \mathbf{D}\mathbf{A}^{-1}\mathbf{B})^{-1}\mathbf{D}\mathbf{A}^{-1} \quad (1.4)$$

Orthogonal Matrices

An orthogonal matrix is defined to be a real matrix $\mathbf{P}_{n \times n}$ whose columns (or rows) constitute an orthonormal basis for \mathcal{R}^n . Note that the following properties hold:

- \mathbf{P} has orthonormal columns
- \mathbf{P} has orthonormal rows
- $\mathbf{P}^T \mathbf{P} = \mathbf{P} \mathbf{P}^T = \mathbf{I}$
- $\mathbf{P}^{-1} = \mathbf{P}^T$
- $\|\mathbf{Px}\|_2 = \|\mathbf{x}\|_2$ for every $\mathbf{x} \in \mathcal{R}^n$

Unitary Matrices

A unitary matrix is defined to be a complex matrix $\mathbf{U}_{n \times n}$ whose columns (or rows) constitute an orthonormal basis for \mathcal{C}^n . Note that the following properties hold:

- \mathbf{U} has orthonormal columns
- \mathbf{U} has orthonormal rows
- $\mathbf{U}^H \mathbf{U} = \mathbf{U} \mathbf{U}^H = \mathbf{I}$
- $\mathbf{U}^{-1} = \mathbf{U}^H$
- $\|\mathbf{Ux}\|_2 = \|\mathbf{x}\|_2$ for every $\mathbf{x} \in \mathcal{C}^n$

Example 1.4.1. Consider the matrix $\mathbf{A} = \begin{bmatrix} 10 & 2 & 9 \\ -1 & 4 & 12 \\ 20 & 25 & -10 \end{bmatrix}$. What is $\text{trace}(\mathbf{A})$? What is $|\mathbf{A}|_F$? Is \mathbf{A} orthogonal?

Solution: We can easily find that $\text{trace}(\mathbf{A}) = 4$ and $|\mathbf{A}|_F = 38.4$. Further, it is easy to see that $\mathbf{A}^T \mathbf{A} \neq \mathbf{I}$, thus \mathbf{A} is not orthogonal.

Example 1.4.2. Consider the matrix $\mathbf{B} = \begin{bmatrix} -0.5 & -0.5 & \sqrt{2}/2 \\ \sqrt{2}/2 & -\sqrt{2}/2 & 0 \\ 0.5 & 0.5 & \sqrt{2}/2 \end{bmatrix}$.

What is $\text{trace}(\mathbf{B})$? What is $|\mathbf{B}|_F$? Is \mathbf{B} orthogonal? What is the inverse of \mathbf{B} ?

Solution: Calculating the trace we find that $\text{trace}(\mathbf{B}) = -0.5$ and $|\mathbf{B}|_F = 1.73$. Further, it is easy to show

that $\mathbf{B}^T \mathbf{B} = \mathbf{I}$ and $\mathbf{B}\mathbf{B}^T = \mathbf{I}$. Also, since \mathbf{B} is orthogonal,

$$\mathbf{B}^{-1} = \mathbf{B}^T = \begin{bmatrix} -0.5 & \sqrt{2}/2 & 0.5 \\ -0.5 & -\sqrt{2}/2 & 0.5 \\ \sqrt{2}/2 & 0 & \sqrt{2}/2 \end{bmatrix} \quad (1.5)$$

Null Space

The **null space** of an $m \times n$ matrix \mathbf{A} is the set X of $n \times 1$ vectors \mathbf{x} such that $\mathbf{Ax} = \mathbf{0}$. The *left-hand null space* of \mathbf{A} is the set of $m \times 1$ vectors \mathbf{y} such that $\mathbf{A}^T \mathbf{y} = \mathbf{0}$. In other words, the left-hand null space of \mathbf{A} is the null space of \mathbf{A}^T .

Example 1.4.3. Consider the matrix $\mathbf{A} = \begin{bmatrix} 10 & 2 & 9 \\ -1 & 4 & 12 \\ 20 & 25 & -10 \end{bmatrix}$. Is the vector $\mathbf{v} \begin{bmatrix} 1 \\ -1 \\ 1 \end{bmatrix}$ in the null space of \mathbf{A} ?

Solution: Taking \mathbf{Av} we get

$$\mathbf{A} = \begin{bmatrix} 10 & 2 & 9 \\ -1 & 4 & 12 \\ 20 & 25 & -10 \end{bmatrix} \begin{bmatrix} 1 \\ -1 \\ 1 \end{bmatrix} = \begin{bmatrix} 17 \\ 7 \\ -15 \end{bmatrix} \quad (1.6)$$

Thus, \mathbf{v} is not in the null space of \mathbf{A} .

1.5 Matrix Factorization

1.5.1 The LU Factorization

If \mathbf{A} is an $n \times n$ matrix that is non-singular and all leading principal submatrices \mathbf{A}_k are nonsingular, \mathbf{A} can be factored into the product \mathbf{LU} where \mathbf{L} is lower triangular (all zeros above the diagonal) and \mathbf{U} is upper triangular (all zeros below the diagonal). That is

$$\mathbf{A} = \mathbf{LU} = \begin{bmatrix} L_{11} & 0 & 0 & \cdots & 0 \\ L_{21} & L_{22} & 0 & \cdots & 0 \\ \vdots & \vdots & \vdots & \ddots & \vdots \\ L_{n1} & L_{n2} & L_{n3} & \cdots & L_{nn} \end{bmatrix} \begin{bmatrix} U_{11} & U_{12} & U_{13} & \cdots & U_{1n} \\ 0 & U_{22} & U_{23} & \cdots & U_{2n} \\ \vdots & \vdots & \vdots & \ddots & \vdots \\ 0 & 0 & 0 & \cdots & U_{nn} \end{bmatrix} \quad (1.7)$$

Note that $L_{ii} = 1 \forall i$ and $U_{ii} \neq 0 \forall i$.

1.5.2 The LDU Factorization

The **LU** factorization can be converted to a factorization with ones on the diagonals of both the lower and upper triangular matrices by factoring **U**:

$$\mathbf{U} = \begin{bmatrix} U_{11} & 0 & 0 & \cdots & 0 \\ 0 & U_{22} & 0 & \cdots & 0 \\ \vdots & \vdots & \vdots & \vdots & \vdots \\ 0 & 0 & 0 & \cdots & U_{nn} \end{bmatrix} \begin{bmatrix} 1 & U_{12}/U_{11} & U_{13}/U_{11} & \cdots & U_{1n}/U_{11} \\ 0 & 1 & U_{23}/U_{22} & \cdots & U_{2n}/U_{22} \\ \vdots & \vdots & \vdots & \vdots & \vdots \\ 0 & 0 & 0 & \cdots & 1 \end{bmatrix}$$

Thus, a matrix that can be factored in an **LU** factorization can also be factored as $\mathbf{A} = \mathbf{LDU}$ where **L** and **U** are upper and lower triangular matrices respectively with 1's on their diagonals and **D** is a diagonal matrix.

1.5.3 Cholesky Factorization

If an $n \times n$ matrix **A** that has an **LDU** factorization is symmetric, the **LDU** factorization is $\mathbf{A} = \mathbf{LDL}^T$. Such a matrix is called **positive definite** if all of the diagonal values of **D** are greater than zero.

A positive definite matrix can also be factored as $\mathbf{A} = \mathbf{R}^T \mathbf{R}$ where **R** is upper triangular with all positive diagonal entries. This factorization is known as the **Cholesky factorization** of **A**. Note that $\mathbf{R} = \mathbf{D}^{1/2} \mathbf{L}^T$.

Example 1.5.1. Consider the matrix $\mathbf{A} = \begin{bmatrix} 10 & 2 & 9 \\ -1 & 4 & 12 \\ 20 & 25 & -10 \end{bmatrix}$. Calculate an LU factorization of **A**. Determine the LDU factorization of **A**. **Solution:** Using Matlab, we can find the LU factorization:

$$\mathbf{L} = \begin{bmatrix} 1 & 0 & 0 \\ -0.1 & 1 & 0 \\ 2 & 5 & 1 \end{bmatrix} \quad (1.8)$$

$$\mathbf{U} = \begin{bmatrix} 10 & 2 & 9 \\ 0 & 4.2 & 12.9 \\ 0 & 0 & -92.5 \end{bmatrix} \quad (1.9)$$

Now, the LDU factorization is similar, but we factor a diagonal out of \mathbf{U} .

$$\mathbf{L} = \begin{bmatrix} 1 & 0 & 0 \\ -0.1 & 1 & 0 \\ 2 & 5 & 1 \end{bmatrix} \quad (1.10)$$

$$\mathbf{U} = \begin{bmatrix} 1 & 0.2 & 0.9 \\ 0 & 1 & 3.1 \\ 0 & 0 & 1 \end{bmatrix} \quad (1.11)$$

$$\mathbf{D} = \begin{bmatrix} 10 & 0 & 0 \\ 0 & 4.2 & 0 \\ 0 & 0 & -92.5 \end{bmatrix} \quad (1.12)$$

1.5.4 Rank of a Matrix

An important measure of a matrix is its **rank**.

There are many ways to define rank, but a basic definition is as follows: The rank of a matrix \mathbf{A} , denoted $R(\mathbf{A})$ the number of linearly independent rows of the matrix or the number of linearly independent columns of the matrix (note that they are the same).

Alternatively, the rank is the number of non-zero rows in the matrix after it has been transformed to row-echelon form.

Rank is also equal to the number of non-zero singular values (to be discussed shortly) of \mathbf{A} .

Notes on $R(\mathbf{A})$

- The rank of \mathbf{A} is the dimension of the column space of \mathbf{A} (which is the same as the dimension of the row space of \mathbf{A}).
- If \mathbf{A} is a square matrix of size $n \times n$ and $R(\mathbf{A}) = n$, then we say that \mathbf{A} has **full rank**.
- If the rank of an $m \times n$ matrix \mathbf{A} is greater than or equal to n , the null space is empty.
- For a full-rank square matrix, the null space is empty.
- If \mathbf{A} is an $m \times n$ matrix, then $\dim(\text{col}(\mathbf{A})) + \dim(\text{nul}(\mathbf{A})) = n$ where $\dim(\mathcal{S})$ is the dimension (i.e., the number of vectors in any basis) of the space \mathcal{S} .
- If \mathbf{A} is an $m \times n$ matrix, then $\text{row}(\mathbf{A}) = \text{col}(\mathbf{A}^T)$ and $\text{col}(\mathbf{A}) = \text{row}(\mathbf{A}^T)$.
- Note that for an $m \times n$ matrix \mathbf{A} ,

$$R(\mathbf{A}) = R(\mathbf{A}^T) = R(\mathbf{A}\mathbf{A}^T) = R(\mathbf{A}^T\mathbf{A})$$

- For a square $n \times n$ matrix \mathbf{A} , it is non-singular only if the rank of \mathbf{A} is n . In other words $R(\mathbf{A}) = n$ if \mathbf{A} is non-singular.
- A diagonal matrix \mathbf{A} which has non-zero values on the diagonal is full rank.
- It can be shown that $R(\mathbf{A} + \mathbf{B}) \leq R(\mathbf{A}) + R(\mathbf{B})$.
- Based on the preceding two properties adding a diagonal matrix to any matrix will make it full rank.

1.5.5 Row and Column Spaces

Rank can also be defined in terms of the row or column space of \mathbf{A} .

The **row space** of an $m \times n$ matrix, \mathbf{A} , denoted by $\text{row}(\mathbf{A})$ is a vector space which is the set of all linear combinations of the row vectors of \mathbf{A} .

The **column space** of an $m \times n$ matrix, \mathbf{A} , denoted by $\text{col}(\mathbf{A})$ is the set of all linear combinations of the column vectors of \mathbf{A} .

If \mathbf{A} is an $m \times n$ real matrix, then $\text{col}(\mathbf{A})$ is a subspace of \Re^m and $\text{row}(\mathbf{A})$ is a subspace of \Re^n .

More specifically, $\text{col}(\mathbf{A})$ is the span of the columns of \mathbf{A} and $\text{row}(\mathbf{A})$ is the span of the rows of \mathbf{A} .

1.5.6 Singular Value Decomposition

For each $m \times n$ matrix \mathbf{A} , there are orthogonal matrices $\mathbf{U}^{m \times m}$ and $\mathbf{V}^{n \times n}$ and a diagonal matrix $\mathbf{D}^{r \times r} = \text{diag}(\sigma_1 \sigma_2 \dots \sigma_r)$ such that

$$\mathbf{A} = \mathbf{U} \begin{pmatrix} \mathbf{D} & \mathbf{0} \\ \mathbf{0} & \mathbf{0} \end{pmatrix} \mathbf{V}^T$$

The values $\sigma_1, \sigma_2, \dots, \sigma_r$ are called the non-zero singular values of \mathbf{A} . When $r < p = \min\{m, n\}$, \mathbf{A} also has $p - r$ zero singular values.

This factorization is known as the **singular value decomposition** of \mathbf{A} and the columns in \mathbf{U} and \mathbf{V} are called the left and right singular vectors of \mathbf{A} .

Note that r is the *rank* of \mathbf{A} . Further, we will define the maximum singular value as σ_{\max} and the minimum singular value as σ_{\min} .

Note that \mathbf{U} and \mathbf{V} are orthogonal matrices.

If \mathbf{A} is $n \times n$ and nonsingular, we can write the SVD of \mathbf{A} as

$$\mathbf{A} = \mathbf{UDV}^T$$

and the SVD of the inverse of \mathbf{A} can be written

$$\mathbf{A}^{-1} = \mathbf{V}\mathbf{D}^{-1}\mathbf{U}^T$$

The SVD provides valuable information about the matrix \mathbf{A}

- The unit vectors of \mathbf{U} (i.e., the left singular vectors) that correspond to the non-zero singular values span the range of \mathbf{A} .
- The singular vectors corresponding to the zero singular values span the null space of \mathbf{A} .

Singular values define the matrix 2-norm. For an $m \times n$ matrix \mathbf{A} :

$$\|\mathbf{A}\|_2 = \max_{\|\mathbf{x}\|_2=1} \|\mathbf{Ax}\|_2$$

To interpret this, we say that for any $n \times 1$ vector \mathbf{x} with a unit norm, the matrix norm of \mathbf{A} is the maximum norm possible after transforming \mathbf{x} by \mathbf{A} . Further it can be shown that

$$\max_{\|\mathbf{x}\|_2=1} \|\mathbf{Ax}\|_2 = \sigma_{max}.$$

Thus, $\|\mathbf{A}\|_2 = \sigma_{max}$

The *condition number* of a matrix κ is the ratio of the largest to smallest singular value of a matrix. That is

$$\kappa = \frac{\max_i \sigma_i}{\min_i \sigma_i}$$

1.5.7 The Pseudo-Inverse

The pseudo inverse (sometimes called the Moore-Penrose psuedoinverse) of an $m \times n$ matrix \mathbf{A} with rank is $R(\mathbf{A}) = \min(m, n)$ is defined as

$$\mathbf{A}^\dagger = (\mathbf{A}^T \mathbf{A})^{-1} \mathbf{A}^T$$

If $R(\mathbf{A}) < \min(m, n)$, then the pseudo inverse can be defined through the SVD of \mathbf{A} . Specifically,

if $\mathbf{A} = \mathbf{U} \begin{pmatrix} \mathbf{D} & \mathbf{0} \\ \mathbf{0} & \mathbf{0} \end{pmatrix} \mathbf{V}^T$ is the SVD of \mathbf{A} , then the pseudo inverse is defined as

$$\mathbf{A}^\dagger = \mathbf{V} \begin{pmatrix} \mathbf{D}^{-1} & \mathbf{0} \\ \mathbf{0} & \mathbf{0} \end{pmatrix} \mathbf{U}^T$$

Thus, when considering the psuedoinverse of \mathbf{A} , the singular values of the inverse are equal to $\frac{1}{\sigma_i}$ where σ_i are the non-zero singular values of \mathbf{A} .

Additionally, the right singular vectors of \mathbf{A}^\dagger are the left singular vectors of \mathbf{A} and vice-versa.

Example 1.5.2. Consider the matrix $\mathbf{A} = \begin{bmatrix} 3 & 4 & 1 \\ 2 & 6 & 4 \\ 1 & 1 & 0 \end{bmatrix}$. Determine a SVD for \mathbf{A} . What does the SVD tell us?

Solution: The SVD is written as $\mathbf{UDV}^T = \mathbf{A}$. Using Matlab we can find one possible solution:

$$\mathbf{U} = \begin{bmatrix} -0.54 & 0.75 & -0.37 \\ -0.83 & -0.55 & 0.09 \\ -0.13 & 0.36 & 0.92 \end{bmatrix}$$

$$\mathbf{D} = \begin{bmatrix} 8.9 & 0 & 0 \\ 0 & 2.1 & 0 \\ 0 & 0 & 0 \end{bmatrix}$$

$$\mathbf{V} = \begin{bmatrix} -0.38 & 0.72 & 0.58 \\ -0.82 & 0.03 & -0.58 \\ -0.43 & -0.69 & 0.58 \end{bmatrix}$$

We can see that the rank of \mathbf{A} is two and it is a singular matrix. There are only two modes, one much stronger than the other.

Example 1.5.3. Consider the matrix $\mathbf{B} = \begin{bmatrix} 3 & 2 & 1 \\ 2 & 6 & 1 \\ 1 & 1 & 1 \end{bmatrix}$. Determine a SVD for \mathbf{B} . What does the SVD tell us? Provide an SVD for \mathbf{B}^{-1} .

Solution: The SVD is written as $\mathbf{UDV}^T = \mathbf{B}$. Using Matlab we can find one possible solution:

$$\begin{aligned}\mathbf{U} &= \begin{bmatrix} -0.45 & 0.82 & -0.35 \\ -0.87 & -0.5 & -0.04 \\ -0.21 & 0.28 & 0.94 \end{bmatrix} \\ \mathbf{D} &= \begin{bmatrix} 7.3 & 0 & 0 \\ 0 & 2.1 & 0 \\ 0 & 0 & 0.58 \end{bmatrix} \\ \mathbf{V} &= \begin{bmatrix} -0.45 & 0.82 & -0.35 \\ -0.87 & -0.50 & -0.04 \\ -0.21 & 0.28 & 0.94 \end{bmatrix}\end{aligned}$$

We can see that the rank of \mathbf{B} is three (i.e., it is non-singular). There are three modes, although the third is very weak. Further, we can find $\mathbf{B}^{-1} = \mathbf{VD}^{-1}\mathbf{U}^T$.

1.5.8 Eigenvalues and Eigenvectors

For an $n \times n$ matrix \mathbf{A} , the scalars λ and $n \times 1$ vectors $\mathbf{x} \neq \mathbf{0}$ satisfying

$$\mathbf{Ax} = \lambda\mathbf{x}$$

are called the **eigenvalues** and **eigenvectors** of \mathbf{A} . The set of distinct eigenvalues $\lambda(\mathbf{A})$ is known as the **spectrum** of \mathbf{A} .

Some additional notes on eigenvalues and eigenvectors:

- * The absolute value of the maximum eigenvalue is also known as the **spectral radius** of \mathbf{A} .
- * The eigenvectors corresponding to distinct eigenvalues is a linearly independent set.
- * If no eigenvalue of \mathbf{A} is repeated, then \mathbf{A} is diagonalizable.
- * Symmetric and Hermitian matrices have real eigenvalues.

1.5.9 Eigenvalues vs Singular Values

For $\mathbf{A} \in \mathcal{C}^{m \times n}$ with $R(\mathbf{A}) = r$:

- * The nonzero eigen values of $\mathbf{A}^H\mathbf{A}$ and $\mathbf{A}\mathbf{A}^H$ are equal and positive.
- * The nonzero singular values of \mathbf{A} are equal to the positive square roots of the non-zero eigenvalues of $\mathbf{A}^H\mathbf{A}$

1.5.10 Eigen Decomposition

A square $n \times n$ matrix \mathbf{A} that has n linearly independent eigenvectors can be factorized into

$$\mathbf{A} = \mathbf{Q}\Lambda\mathbf{Q}^{-1} \quad (1.13)$$

where the i column of \mathbf{Q} corresponds to the i th eigenvector of \mathbf{A} and Λ is diagonal with the i th element of the diagonal equal to the i th eigenvalue of \mathbf{A} . If \mathbf{A} is also symmetric, then

$$\mathbf{A} = \mathbf{Q}\Lambda\mathbf{Q}^T$$

Positive Definite Matrices

If $\lambda_i > 0 \forall i$, then we can set $\mathbf{B} = \Lambda^{1/2}\mathbf{Q}^T$ and

$$\mathbf{A} = \mathbf{B}^T\mathbf{B} \quad (1.14)$$

Such a matrix when \mathbf{B} is non-singular is termed **positive definite**. In other words, consider the eigenpair (λ, \mathbf{x}) :

$$\mathbf{Ax} = \lambda\mathbf{x} \quad (1.15)$$

Multiplying both sides by \mathbf{x}^T and solving for λ gives

$$\begin{aligned} \mathbf{x}^T\mathbf{Ax} &= \mathbf{x}^T\lambda\mathbf{x} \\ \lambda &= \frac{\mathbf{x}^T\mathbf{Ax}}{\mathbf{x}^T\mathbf{x}} \end{aligned}$$

Continuing,

$$\begin{aligned} \lambda &= \frac{\mathbf{x}^T\mathbf{B}^T\mathbf{Bx}}{\mathbf{x}^T\mathbf{x}} \\ &= \frac{\|\mathbf{Bx}\|_2^2}{\|\mathbf{x}\|_2^2} \end{aligned}$$

If \mathbf{B} is non-singular all eigenvalues will be positive and thus we say that \mathbf{A} is **positive definite**.

However, if \mathbf{B} is singular, all of the eigenvalues will be non-negative and we say that \mathbf{A} is **positive semi-definite**.

Notes on Eigendecomposition

The matrix \mathbf{B} in the previous decomposition is not unique.

However, there is only one upper triangular matrix with positive diagonals \mathbf{R} such that $\mathbf{A} = \mathbf{R}^T\mathbf{R}$. This is known as the **Cholesky Factorization** of \mathbf{A} as discussed above.

For a square matrix, the inverse of a matrix can be found from its eigendecomposition. Specifically,

$$\mathbf{A}^{-1} = \mathbf{Q}\Lambda^{-1}\mathbf{Q}^{-1}$$

Formal Definition of Positive Definiteness

If a matrix \mathbf{A} is Hermitian, it is **positive definite** if for any vector $\mathbf{x} \neq \mathbf{0}$

$$\mathbf{x}^H \mathbf{A} \mathbf{x} > 0$$

\mathbf{A} is **semipositive definite** if for any vector \mathbf{x}

$$\mathbf{x}^H \mathbf{A} \mathbf{x} \geq 0$$

\mathbf{A} is **negative definite** if for any vector $\mathbf{x} \neq \mathbf{0}$

$$\mathbf{x}^H \mathbf{A} \mathbf{x} < 0$$

Note that \mathbf{A} is positive definite if and only if all of its eigenvalues are positive.

Hermitian Matrices

If the $n \times n$ matrix \mathbf{A} is Hermitian, its eigenvalues are real and we can decompose \mathbf{A} as

$$\mathbf{A} = \mathbf{U} \Lambda \mathbf{U}^H$$

where

$$\mathbf{U} = [\mathbf{u}_1 \mathbf{u}_2 \dots \mathbf{u}_n]$$

are the orthogonal eigenvectors. This means that \mathbf{U} is unitary. Further, the diagonal matrix Λ is made up of the eigenvalues of \mathbf{A} . Note that since \mathbf{U} is unitary, we can also write:

$$\mathbf{U}^H \mathbf{A} \mathbf{U} = \Lambda$$

Further,

$$\mathbf{A} \mathbf{U} = \mathbf{U} \Lambda$$

which means that for any eigenvector \mathbf{u}_i we can write

$$\mathbf{A} \mathbf{u}_i = \lambda_i \mathbf{u}_i \tag{1.16}$$

Interpreting Eigenvalues

The eigenvectors are somewhat arbitrary. Any orthonormal basis will suffice. Once the eigenvectors are chosen, the eigenvalues tell us the real information about the matrix.

To see this consider a symmetric $n \times n$ matrix \mathbf{A} . The eigendecomposition can be written as

$$\mathbf{A} = \mathbf{Q} \Lambda \mathbf{Q}^T$$

Now consider the matrix applied to an arbitrary vector \mathbf{x} :

$$\begin{aligned} \mathbf{y} &= \mathbf{A} \mathbf{x} \\ &= \mathbf{Q} \Lambda \mathbf{Q}^T \mathbf{x} \end{aligned}$$

Let us consider the multiplication steps one at a time. The product $\mathbf{z}_1 = \mathbf{Q}^T \mathbf{x}$ can be written as

$$\mathbf{z}_1 = \begin{bmatrix} \mathbf{q}_1^T \mathbf{x} \\ \mathbf{q}_2^T \mathbf{x} \\ \vdots \\ \mathbf{q}_n^T \mathbf{x} \end{bmatrix}$$

Thus, the i th element of \mathbf{z}_1 is the inner product of the input vector \mathbf{x} with the i th eigenvector. We can think of this as correlation (how much of each eigenvector is in \mathbf{x}).

Next, we have

$$\begin{aligned} \mathbf{z}_2 &= \Lambda \mathbf{Q}^T \mathbf{x} \\ &= \lambda \mathbf{z}_1 \\ &= \begin{bmatrix} \lambda_1 \mathbf{q}_1^T \mathbf{x} \\ \lambda_2 \mathbf{q}_2^T \mathbf{x} \\ \vdots \\ \lambda_n \mathbf{q}_n^T \mathbf{x} \end{bmatrix} \end{aligned} \tag{1.17}$$

Thus, the next step is to weight each inner product with the appropriate eigenvalue. (We are weighting each correlation measure by their relative importance as determined by the eigenvalues.

Finally,

$$\begin{aligned} \mathbf{y} &= \mathbf{Q} \mathbf{z}_2 \\ &= \mathbf{Q} \begin{bmatrix} \lambda_1 \mathbf{q}_1^T \mathbf{x} \\ \lambda_2 \mathbf{q}_2^T \mathbf{x} \\ \vdots \\ \lambda_n \mathbf{q}_n^T \mathbf{x} \end{bmatrix} \\ &= \sum_{i=1}^n \lambda_i (\mathbf{q}_i^T \mathbf{x}) \mathbf{q}_i \end{aligned}$$

Thus, we see that the output is the weighted sum of the eigenvectors. The weighting is the product of the correlation of the input with each eigenvector and the eigenvalue of interest. Thus, we can think of the matrix multiplication process as a decomposition, followed by a weighting, followed by a synthesis.

Example 1.5.4. What does the previous analysis tell us about the eigenvalues of an $n \times n$ identity matrix?

Example 1.5.5. Consider the matrix $\mathbf{B} = \begin{bmatrix} 3 & 2 & 1 \\ 2 & 6 & 1 \\ 1 & 1 & 1 \end{bmatrix}$. Determine an eigen decomposition for

B. What does the decomposition tell us? Compare to the SVD of this matrix. What does this suggest about the SVD and eigen decomposition of symmetric matrices?

Solution: The eigen decomposition is written as $\mathbf{Q}\Lambda\mathbf{Q}^T = \mathbf{B}$. Using Matlab we can find one possible solution:

$$\mathbf{Q} = \begin{bmatrix} -0.35 & 0.82 & 0.45 \\ -0.04 & -0.5 & 0.87 \\ 0.94 & 0.28 & 0.21 \end{bmatrix}$$

$$\Lambda = \begin{bmatrix} 0.58 & 0 & 0 \\ 0 & 2.1 & 0 \\ 0 & 0 & 7.3 \end{bmatrix}$$

We can see that the eigenvalues are equal to the singular values. Further, we see from the SVD that $\mathbf{U} = \mathbf{V}$. Also, we can see that the eigen decomposition and the SVD are the same for \mathbf{B} . For symmetric matrices we can conclude that the two decompositions are the same.

Example 1.5.6. Consider the matrix $\mathbf{C} = \begin{bmatrix} 3 & 2 & -1 \\ 2 & 6 & -1 \\ -1 & -1 & -1 \end{bmatrix}$. Determine an eigen decomposition

for \mathbf{C} . What does the decomposition tell us? Compare to the SVD of this matrix. What does this suggest about the SVD and eigen decomposition of symmetric matrices?

Solution: The eigen decomposition is written as $\mathbf{Q}\Lambda\mathbf{Q}^T = \mathbf{B}$. Using Matlab we can find one possible solution:

$$\mathbf{Q} = \begin{bmatrix} -0.35 & 0.82 & 0.45 \\ -0.04 & -0.5 & 0.87 \\ 0.94 & 0.28 & 0.21 \end{bmatrix}$$

$$\Lambda = \begin{bmatrix} 0.58 & 0 & 0 \\ 0 & 2.1 & 0 \\ 0 & 0 & 7.3 \end{bmatrix}$$

We can see that the eigenvalues are equal to the singular values. Further, we see from the SVD that $\mathbf{U} = \mathbf{V}$. Also, we can see that the eigen decomposition and the SVD are the same for \mathbf{B} . For symmetric matrices we can conclude that the two decompositions are the same.

1.5.11 Range Space

The **range space** of an $m \times n$ matrix \mathbf{A} is the set of $m \times 1$ vectors \mathbf{Y} generated as $\mathbf{y} = \mathbf{Ax}$ when $\mathbf{x} \in \Re^n$.

The range space is denoted as $col(\mathbf{A})$ and is a subspace of \Re^m .

$col(\mathbf{A})$ is the space spanned by the columns of \mathbf{A} , also called the column space of \mathbf{A} .

$col(\mathbf{A}^T)$ is the space spanned by the rows of \mathbf{A} , also called the row space of \mathbf{A} , denoted as $row(\mathbf{A})$.

1.5.12 Using the Matrix Inverse

A system of n linear equations in n unknowns can be written as a single matrix equation as

$$\mathbf{Ax} = \mathbf{b}$$

where \mathbf{x} is an n -dimensional vector of the n unknowns, \mathbf{A} is the $n \times n$ matrix of coefficients, and \mathbf{b} is an $n \times 1$ vector.

If the matrix \mathbf{A} is nonsingular, the solution is given by

$$\mathbf{x} = \mathbf{A}^{-1}\mathbf{b}$$

Note: In general, computing the inverse is a computationally intensive operation, and thus solving systems of equations are typically done in other ways.

1.5.13 DFT Matrix

The DFT matrix (also called the Fourier matrix), denoted \mathbf{D}_N , is an $N \times N$ matrix where the elements are defined as $[\mathbf{D}]_{m,n} = e^{-j2\pi(m-1)(n-1)/N}$. Note that multiplying an N -element column vector \mathbf{x} by \mathbf{D}_N creates the DFT of \mathbf{x} . That is the DFT of a vector \mathbf{x} is defined as

$$X[k] = \mathcal{F}\{x[n]\} = \sum_{n=0}^{N-1} x[n]e^{-j\frac{2\pi}{N}kn} \quad (1.18)$$

This can be written as

$$\mathbf{X} = \mathbf{D}_N \mathbf{x} \quad (1.19)$$

where $\mathbf{x}, \mathbf{X} \in \mathcal{C}^N$. Similarly, \mathbf{D}_N^H is the IDFT matrix since $\mathbf{x} = \mathbf{D}_N^H \mathbf{X}$.

\mathbf{D}_N^H is IDFT matrix

1.5.14 Circulant Matrices

A *circulant* matrix is a matrix entirely defined by any of its rows, as all other rows are simply circular shifts of that first row with offsets defined by the row indices. Alternatively a circulant matrix is described by any of its columns with all other columns simply circular shifts of the first column. Note that \mathbf{D}_N is a circulant matrix.

Note that if an $N \times N$ matrix \mathbf{A} is circulant, the following important properties hold:

- * The eigenvectors of \mathbf{A} equal the columns of the DFT matrix \mathbf{D}_N .
- * The eigenvalues of \mathbf{A} equal the entries of $\mathbf{D}_N \mathbf{a}$ where \mathbf{a} is any column of \mathbf{A} . In other words, the eigenvalues are the DFT of any of the columns.

1.5.15 The Kronecker Product

The Kronecker product is analogous to the outer product in vector multiplication. Specifically, if we have an $N \times M$ matrix \mathbf{A} and a $K \times T$ \mathbf{B} the Kronecker product is an $NK \times MT$ matrix \mathbf{C} :

$$\mathbf{C} = \mathbf{A} \otimes \mathbf{B} = \begin{bmatrix} [\mathbf{A}]_{1,1}\mathbf{B} & \cdots & [\mathbf{A}]_{1,M}\mathbf{B} \\ \vdots & \ddots & \vdots \\ [\mathbf{A}]_{N,1}\mathbf{B} & \cdots & [\mathbf{A}]_{N,M}\mathbf{B} \end{bmatrix} \quad (1.20)$$

Note that the Kronecker product has the following properties:

- * $(\mathbf{A} \otimes \mathbf{B})^* = \mathbf{A}^* \otimes \mathbf{B}^*$
- * $(\mathbf{A} \otimes \mathbf{B})^{-1} = \mathbf{A}^{-1} \otimes \mathbf{B}^{-1}$

Part II

Multi-Input Multi-Output Transmission and Reception

Chapter 2

The MIMO Wireless Channel

2.1 Introduction

In this chapter, we describe the various effects of the wireless channel, with an emphasis on the *spatial* channel, since that is of primary importance in MIMO systems. We start by describing the three primary propagation effects: (1) the impact of distance, (2) the impact of motion, and (3) the impact of multipath. The first effect is primarily a large-scale effect (i.e., we notice its impact over large distances - say greater than 10m), while the second and third effects are small-scale effects (their effects are noticed over small distances - say smaller than a few meters). In a later chapter we will revisit the wireless channel with a focus on frequency selectivity as it is of primary importance when studying OFDM. For more complete treatments of the wireless channel, including the MIMO channel, please see [4], Chapter 3, [5], Chapter 3, as well as classic discussions of the SISO channel in [6, 7, 9].

2.2 Basic Propagation Effects

2.2.1 Impact of Distance

Consider a sinusoidal transmit signal at frequency f in a single dimension measured by a perfect antenna at a distance d from the transmitter. The measured electric field (ignoring polarization) is

$$\begin{aligned} E(f, t, d) &= \frac{\cos(2\pi f(t - d/c))}{d} \\ &= \frac{1}{d} \cos(2\pi f t - \phi(d)) \end{aligned} \tag{2.1}$$

where $\phi(d) = \frac{2\pi f d}{c}$ and c is the speed of light.

From this equation, we can see that the sinusoidal field is attenuated and phase shifted depending on the distance d . The phase shift is of marginal consequence, but the attenuation due to distance is a major effect. This inverse relationship to distance results in a power loss relative to d^2 . Specifically, it can be shown that the received signal power P_r in a free-space environment (i.e.,

in the absence of objects) can be written as

$$P_r = P_t G_t G_r \left(\frac{\lambda}{4\pi d} \right)^2 \quad (2.2)$$

where P_t is the transmit power, G_t and G_r are the transmit and receive antenna gains along the direction of the signal propagation, and $\lambda = c/f$ is the wavelength of transmission. This is known as the Friis Transmission Formula. From this equation we can see that the received signal power decreases with d^2 . Additionally, for constant antenna gains, the received power also decreases with frequency.

The above received power formula applies only to free-space. However, it has been found empirically that in more complicated environments, the large scale path loss increases with d^n where n is the termed the path loss exponent and is generally $2 < n < 5$. In other words,

$$P_r = P_o \left(\frac{d_o}{d} \right)^n \quad (2.3)$$

where P_o is a reference power received at reference distance d_o . The reference distance is generally smaller than the distance being characterized d .

Path loss is a *large scale* effect in that it doesn't change significantly over small distances (say one meter). Changes in the received signal power over smaller distances (or time) is due to the impact of multipath and Doppler shift. These *small scale* effects will be discussed next.

2.2.2 Movement and Doppler Shift

Again consider a sinusoidal transmit signal, but with a mobile receiver¹. Now if the receive antenna (starting from distance d_o) moves with velocity v away from the transmit antenna, the measured field is

$$\begin{aligned} E(f, t, d) &= \frac{\cos(2\pi f(t - \frac{d_o + vt}{c}))}{d_o + vt} \\ &= \frac{1}{d_o + vt} \cos(2\pi(f - f_d)t - \phi_o) \end{aligned} \quad (2.4)$$

where $f_d = \frac{fv}{c} = \frac{v}{\lambda}$ is the *Doppler Shift* and $\phi_o = \frac{2\pi f d_o}{c}$. For small changes in distance,

$$E(f, t, d) \approx \frac{1}{d_o} \cos(2\pi(f - f_d)t - \phi_o) \quad (2.5)$$

And the primary impact that we observe due to movement is a Doppler shift. Note that in general, the shift in frequency due to movement is $f_i = f_d \cos(\theta)$ where $f_d = \frac{v}{\lambda}$ is the maximum Doppler shift and θ is the angle of arrival of the signal relative to the velocity. In the case above, $\theta = 180^\circ$ resulting in the largest negative shift of f_d . Had the receiver been moving *towards* the transmitter ($\theta = 0$), the frequency shift would have been positive f_d .

¹Although we focus on a mobile receiver, a mobile transmitter and static receiver would cause the same effect.

2.2.3 Multipath

The third major effect due to the wireless channel is multipath. That is, because the transmitter and receiver are not located in free space, the receiver will observe multiple versions of the signal which have been reflected, scattered or diffracted by objects in the environment. The multiple copies of the signal will arrive at different relative delays and relative strengths. The difference in delay will cause two primary effects. If the delay is large relative to the modulated symbol time, the received signal will experience *inter-symbol interference or ISI*. We will discuss this effect in more detail later. Secondly, due to the fact that the carrier frequency is typically large (hundreds of MHz to tens of GHz), even small delay differences will cause substantial phase differences between the two sinusoids. The phase differences can (and will) cause destructive interference.

To see this, consider the situation depicted in Figure 2.1. In this example there is a perfect reflector located $d_r = 10\text{m}$ from the transmitter which is transmitting a continuous tone signal at frequency f . We examine the magnitude of the received E-field at various distances d between the transmitter and receiver. The received E-field can be written as (note the negative sign due to the perfect reflector):

$$E(f, t, d) = \frac{\cos(2\pi f(t - \frac{d}{c}))}{d} - \frac{\cos(2\pi f(t - \frac{2d_r - d}{c}))}{2d_r - d}$$

Thus, at the receiver we have the sum of two sinusoids with the same frequency, f , but different gains and phases. The phase difference is

$$\begin{aligned} \Delta\phi &= \frac{2\pi f(2d_r - d)}{c} + \pi - \frac{2\pi f d}{c} \\ &= \frac{4\pi f(d_r - d)}{c} + \pi \end{aligned} \tag{2.6}$$

Thus:

- * When $\Delta\phi = 2k\pi$ for integer k , the two sinusoids will add *constructively* and the signal due to two paths is larger than without multipath.
- * When $\Delta\phi = k\pi$ for odd integer k , the two signals add *destructively*.
- * Thus a pattern of constructive/destructive interference is created that gradually attenuates due to longer distances. Specifically, the peak received magnitude will decay with $\frac{1}{d}$.

To make this more concrete, consider an example where $t = 0.01$, $f = 2\text{GHz}$, $c = 2.98 \times 10^8$ and $d_r = 10\text{m}$. The magnitude of the E-field is plotted in Figure 2.2. We can see that there are repeating patterns of constructive and destructive interference. Note that because the reflection is immediately behind the receiver, changing the distance dm causes a $2d/\lambda$ change in the phase difference. As a result, we see the pattern repeat at multiples of $\lambda/2 = 0.075\text{m}$ in this case. Additionally, the overall received signal amplitude is decaying at $\frac{1}{d}$ as expected. (This corresponds to a power decay of $\frac{1}{d^2}$).

Of course, if there is multipath and receiver movement, the phase relationship of the two paths will vary with time due to the time varying phase of each multipath component (i.e., their respective frequency shifts).

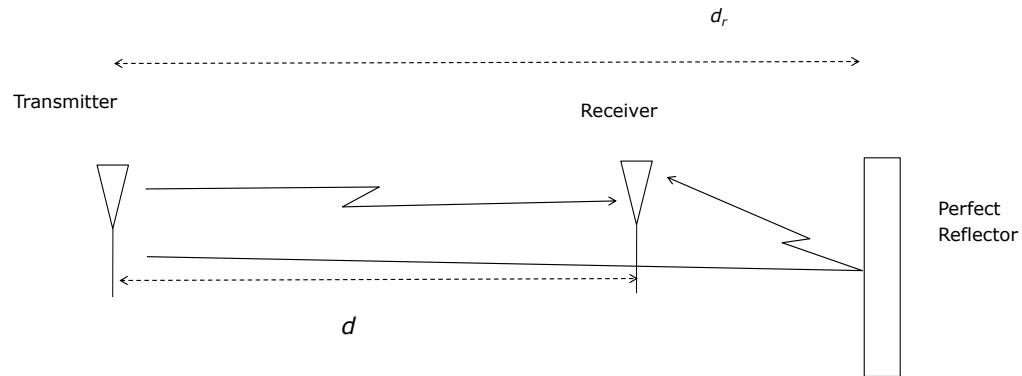


Figure 2.1: Example of Multipath with a Perfect Reflector

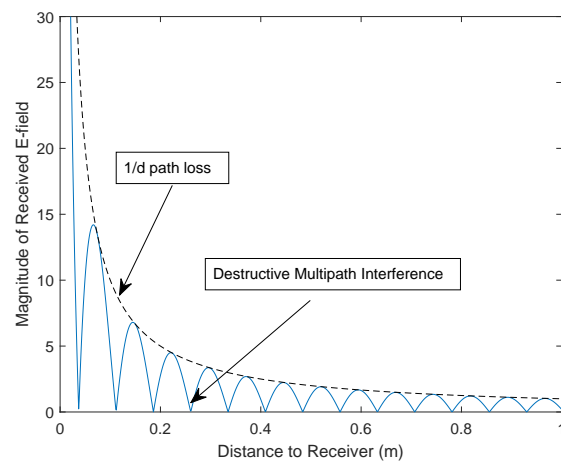


Figure 2.2: Example of Multipath Interference with a Perfect Reflector. Note that the electric field strength (plotted for a fixed time versus distance) decays with distance and experiences destructive multipath interference at multiples of half the wavelength.

2.2.4 Small and Large Scale Effects

The first propagation effect discussed (attenuation vs distance) is typically termed a *large scale effect* whereas the second and third propagation effects are termed *small scale effects*. The reason for this is that the attenuation over distance doesn't change appreciably over small relative distance changes, whereas the small scale effects do. For example consider Figure 2.3. The figure shows the magnitude of the received E-field for the example in Figure 2.2 when the receiver is moving towards the reflector at $v = 5\text{m/s}$ and $d_r = 150\text{m}$. The overall attenuation due to distance is clearly seen in left hand plot which shows the received signal magnitude over 50m. However, the impact of multipath and Doppler is not visible. On the right, when the magnitude is viewed over a short distance (less than a meter) the attenuation due to distance is not discernible, but the multipath/Doppler effects clearly are. Thus, we refer to the effects which are discernible over large distances as large scale effects, and those which are discernible over short distances as small scale effects.

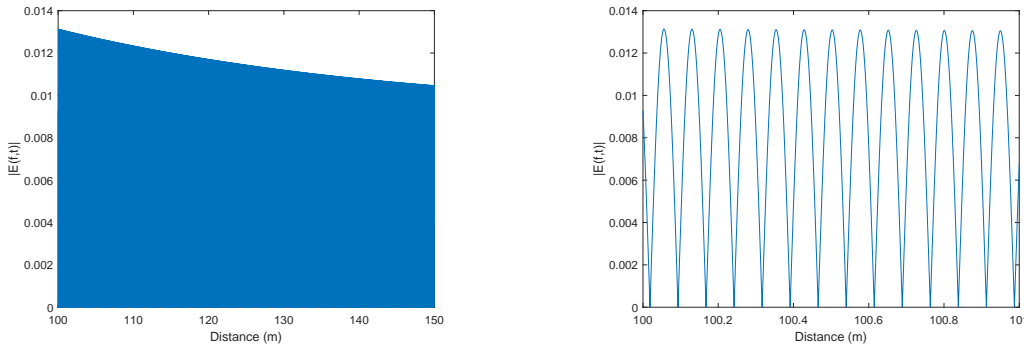


Figure 2.3: Large vs Small Scale Propagation Effects: The magnitude of the received E-field at a given distance when there is a perfect reflector placed at 150m from the transmitter and the receiver is traveling away from the transmitter (and towards the reflector) at 5m/s.

2.3 The General Wireless Channel in Complex Baseband

Thus, there are two dominant small-scale effects in the wireless channel: multipath and Doppler. In general, the received signal is a superposition of scaled and time-delayed versions of the transmit signal where the scaling, delay and number of multipath components is time-varying. This general scenario is shown in Figure 2.4. Together, multipath and Doppler result in the phenomenon known as *fading*, time-varying signal strength due to the changing phase relationships between multipath components.

At bandpass we can write the transmit and receive signals (ignoring noise):

$$x(t) = \Re \{ \tilde{x}(t)e^{j2\pi f_c t} \} \quad (2.7)$$

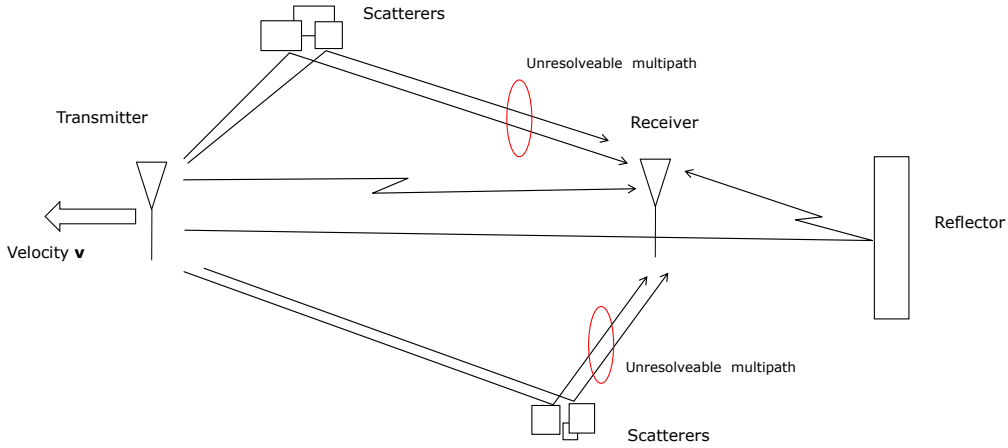


Figure 2.4: Depiction of the General Wireless Channel

$$r(t) = \Re \left\{ \sum_{i=1}^{N(t)} \alpha_i(t) \tilde{x}(t - \tau_i(t)) e^{j(2\pi f_c(t - \tau_i(t)) + \phi_i)} \right\} \quad (2.8)$$

Let $\phi_i(t) = 2\pi f_c \tau_i(t) + \phi_i$. Then,

$$r(t) = \Re \left\{ \left(\sum_{i=1}^{N(t)} \alpha_i(t) e^{j\phi_i(t)} \tilde{x}(t - \tau_i(t)) \right) e^{j2\pi f_c t} \right\} \quad (2.9)$$

Assuming a linear, time-varying channel, from linear system theory we can write represent the channel by its time-varying impulse response. Thus, the complex baseband received signal $\tilde{r}(t)$ can be written as the convolution of the complex baseband of the input and channel impulse responses. Thus, the received signal we can written as:

$$r(t) = \Re \left\{ \left[\underbrace{\int_{-\infty}^{\infty} \tilde{h}(\tau, t) \tilde{x}(t - \tau) d\tau}_{\tilde{r}(t)} \right] e^{j2\pi f_c t} \right\} \quad (2.10)$$

Which means that

$$\tilde{h}(\tau, t) = \sum_{i=1}^{N(t)} \tilde{\alpha}_i(t) \delta(\tau - \tau_i(t)) \quad (2.11)$$

is the time-varying impulse response of the channel in complex baseband and $\tilde{\alpha}_i(t) = \alpha_i(t) e^{j\phi_i(t)}$

is the complex channel gain of the i th multipath component. Further, the time-varying transfer function of the channel is

$$\tilde{H}(f, t) = \int_{-\infty}^{\infty} \tilde{h}(\tau, t) e^{-j2\pi f\tau} d\tau \quad (2.12)$$

2.4 Random Channels

In general it is impossible to know the channel $\tilde{h}(\tau, t)$ in advance or with certainty. Thus, when characterizing system performance we rely on statistical characterizations of the channel. There are three aspects of this statistical characterization which dictate link performance: delay spread, Doppler spread, and angle spread. Delay spread is a measure of the range of delays τ_i . If the delay spread is large (larger than the signal's modulated symbol duration T_s) inter-symbol interference occurs. In the frequency domain, we observe *frequency selective* fading since the channel transfer function is not flat over the signal bandwidth. In other words, the signal experiences different gains at different frequencies. This distortion is particularly harmful to signal detection. On the other hand if $\tau_i(t) \ll T_s, \forall i, t$, the fading experienced by the signal is termed *flat fading* and ISI is absent.

Doppler spread represents the range of Doppler shifts f_i experienced by the various multipath components. Clearly, from our previous discussion $-f_d < f_i < f_d$. Thus, the mobile velocity and transmit frequency dictate the Doppler spread. Doppler spread results in time-domain selectivity. If $f_d \propto \frac{1}{T_s}$ we term the fading *fast* fading. On the other hand, if $f_d \ll \frac{1}{T_s}$, the fading is termed *slow* fading.

Angle spread is a measure of the range of angles-of-arrival of the various multipath components. Clarke's model (which we will discuss next) assumes that the angle spread is 2π . Angle spread dictates spatial fading which we will discuss later in this chapter. In general, the larger the angle spread, the more spatially selective the channel is.

2.4.1 Spatial Selectivity and Correlation

Define the received signal power as a function of angle-of-arrival θ as the power spectrum $S_A(\theta)$. Then, assuming that all multipath components have equal gain, we can write the complex baseband received signal (without noise) in terms of the transmit signal $x(t)$ as

$$y(t) = \int_{-\pi}^{\pi} \sqrt{S_A(\theta)} G(\theta) x(t - D(\theta)/c) d\theta \quad (2.13)$$

where $G(\theta)$ is the normalized receive antenna gain and $D(\theta)$ is the delay due to the angle-of-arrival θ and c is the speed of light. Assuming the transmit signal is a sinusoid, at complex baseband the signal is a constant $x(t - D(\theta)/c) = x e^{-j\phi(\theta)}$. Further, assuming an omni-directional antenna with normalized gain pattern $G(\theta) = 1$

$$y(t) = y = h_o x \quad (2.14)$$

where h_o is the channel:

$$h_o = \int_{-\pi}^{\pi} \sqrt{S_A(\theta)} e^{-j\phi(\theta)} d\theta \quad (2.15)$$

Now, if we consider another point in space, d meters away, we find the channel to be

$$h_1 = \int_{-\pi}^{\pi} \sqrt{S_A(\theta)} e^{-j[\phi(\theta) + 2\pi d/\lambda \sin(\theta)]} d\theta \quad (2.16)$$

where θ is defined relative to a line normal to the line connecting the two points². The correlation of the channels between those two points can be found as

$$\rho(d) = E \left\{ \int_{-\pi}^{\pi} \int_{-\pi}^{\pi} \sqrt{S_A(\theta_1)} e^{-j\phi(\theta_1)} \sqrt{S_A(\theta_2)} e^{j[\phi(\theta_2) + 2\pi d/\lambda \sin(\theta_2)]} d\theta_1 d\theta_2 \right\} \quad (2.17)$$

where the expectation is over $\phi(\theta)$. Making the reasonable assumption that $\phi(\theta)$ is uniformly distributed over $[-\pi, \pi]$, the expectation is zero unless $\theta_1 = \theta_2$, thus

$$\rho(d) = \int_{-\pi}^{\pi} S_A(\theta) e^{j2\pi d/\lambda \sin(\theta)} d\theta \quad (2.18)$$

Thus, we can see that the power azimuth spectrum directly controls the spatial correlation. We will show later that the larger the spread of the power azimuth spectrum, the faster the signal decorrelates in space.

2.4.2 Temporal Selectivity and Correlation

This result can also be used to determine the temporal correlation. Specifically, if we assume that the receiver is moving at velocity v , after τ seconds the receiver has moved $v\tau$ meters. Thus, using a simple substitution of variables we can calculate the temporal correlation $\tilde{R}(\tau)$ as

$$\tilde{R}(\tau) = \int_{-\pi}^{\pi} S_A(\theta) e^{j2\pi \frac{v}{\lambda} \tau \sin(\theta)} d\theta \quad (2.19)$$

$$= \int_{-\pi}^{\pi} S_A(\theta) e^{j2\pi f_d \tau \sin(\theta)} d\theta \quad (2.20)$$

We see that the temporal correlation at time delay τ depends directly on the maximum Doppler spread $f_d = \frac{v}{\lambda}$. Later we will see that, as one would expect, larger f_d leads to faster decorrelation in time.

2.4.3 Frequency Selectivity and Correlation

The power delay profile $\phi_h(\tau)$ is defined as the expected power of the channel impulse response as a function of delay τ :

$$\phi_h(\tau) = E \left\{ \tilde{h}(\tau, t) \tilde{h}^*(\tau, t) \right\} \quad (2.21)$$

$$= E \left\{ |\tilde{h}(\tau, t)|^2 \right\} \quad (2.22)$$

²It should be noted that this definition of the direction of arrival is somewhat different than the definition we used for determining the Doppler shift. In that case, the AOA was defined relative to the velocity.

Using this definition, we can write the frequency correlation (assuming wide sense stationarity) as

$$R_h(\Delta f) = \mathbb{E} \left\{ \tilde{H}(f, t) \tilde{H}^*(f + \Delta f, t) \right\} \quad (2.23)$$

$$= \mathbb{E} \left\{ \int_{-\infty}^{\infty} \tilde{h}(\tau, t) e^{-j2\pi f \tau} d\tau \int_{-\infty}^{\infty} \tilde{h}^*(\tau, t) e^{j2\pi(f+\Delta f)\tau} d\tau \right\} \quad (2.24)$$

$$= \int_{-\infty}^{\infty} \int_{-\infty}^{\infty} \mathbb{E} \{ h(\tau_1, t) h^*(\tau_2, t) \} e^{j2\pi[(f+\Delta f)\tau_2 - f\tau_1]} d\tau_1 d\tau_2 \quad (2.25)$$

Now, assuming uncorrelated scattering,

$$\mathbb{E} \{ h(\tau_1, t) h^*(\tau_2, t) \} = 0 \quad \tau_1 \neq \tau_2 \quad (2.26)$$

Thus,

$$R_h(\Delta f) = \int_{-\infty}^{\infty} \mathbb{E} \{ |h(\tau, t)|^2 \} e^{j2\pi \Delta f \tau} d\tau \quad (2.27)$$

$$= \int_{-\infty}^{\infty} \phi_h(\tau) e^{j2\pi \Delta f \tau} d\tau \quad (2.28)$$

2.5 Narrowband Fading

In the early days of mobile communication, the signal bandwidth was fairly small. Thus, a common assumption in channel modeling was that the channel bandwidth was significantly larger than the signal bandwidth (i.e., fading was flat). As data rates increased, this assumption was no longer valid and the channel was observed to be frequency selective. Many developed channel models made the narrowband assumption. While, clearly that is not valid for modern communication systems, the advent of OFDM made the narrowband channel models relevant again. Specifically, since OFDM transmits a large number of narrowband signals, each narrowband signal will typically experience flat fading, and the narrowband assumption becomes valid. For the remainder of Part II, we will make the narrowband assumption in order to focus on the spatial effects of the channel which dominate MIMO link performance. We will however, revisit this narrowband assumption when we examine OFDM.

2.6 Clarke's Model for SISO Channels

Let us assume that the transmit signal is $x(t) = \cos(2\pi f_c t)$. The received signal is comprised of a large number of multipath components arriving from different directions θ_i with respect to the velocity vector \mathbf{v} and thus each has a different Doppler shift:

$$f_i = \frac{v}{\lambda} \cos(\theta_i) \quad (2.29)$$

Clarke's Model [7, 9] makes a *Narrowband Assumption* that $\delta(\tau - \tau_i) = \delta(\tau - \tau_o) \forall i$ (see Figure 2.5). In other words, the difference in time-of-arrival of all multipath components is very small relative to the symbol duration and thus unresolvable. This is equivalent to the channel having a bandwidth that is much greater than the signal bandwidth (i.e., we assume that the signal is narrow relative to the channel).

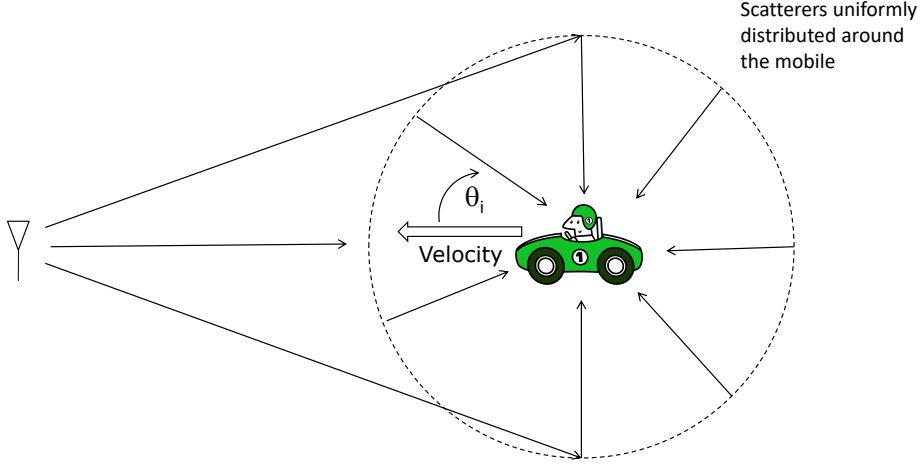


Figure 2.5: Scenario Assumed in Jakes/Clarke's Model. Scatterers causing multipath at the mobile receiver are uniformly distributed in angle around the mobile. θ_i is the angle-of-arrival of i th multipath component relative to the mobile velocity.

With a sinusoidal transmit signal (constant at baseband), we have

$$r(t) = \sqrt{2P_{avg}} \sum_{i=1}^N c_i \cos(2\pi f_c t + 2\pi f_i t + \phi_i) \quad (2.30)$$

where the P_{avg} is the average received power, $\sum_i c_i^2 = 1$ and ϕ_i is assumed to be random and uniformly distributed over $[0, 2\pi]$ or deterministic and equally spaced over $[0, 2\pi]$. We can re-write this as

$$r(t) = \sqrt{P_{avg}} \sum_{i=1}^N [c_i \cos(2\pi f_i t + \phi_i) \cos(2\pi f_c t) - c_i \sin(2\pi f_i t + \phi_i) \sin(2\pi f_c t)] \quad (2.31)$$

Thus, in complex baseband

$$\begin{aligned} \tilde{r}(t) &= \sqrt{P_{avg}} \sum_{i=1}^N [c_i \cos(2\pi f_i t + \phi_i) + j c_i \sin(2\pi f_i t + \phi_i)] \\ &= \sqrt{P_{avg}} \sum_{i=1}^N c_i e^{j(2\pi f_i t + \phi_i)} \\ &= \sqrt{P_{avg}} \sum_{i=1}^N c_i e^{j(2\pi f_d \cos(\theta_i) t + \phi_i)} \end{aligned} \quad (2.32)$$

where $f_d = \frac{v}{\lambda}$ is the maximum Doppler shift. Further, in this model we typically set $c_i = \frac{1}{\sqrt{N}}$.

From the above development we can see that $\tilde{h}(\tau, t) \approx \tilde{\gamma}(t)\delta(\tau)$ and thus $\tilde{r}(t) \approx \tilde{\gamma}(t)\tilde{x}(t)$.

2.6.1 Rayleigh and Rician Fading

From the Central Limit Thereom, as $N \rightarrow \infty$ the real ($\tilde{r}_I(t)$) and imaginary ($\tilde{r}_Q(t)$) portions of $\tilde{r}(t)$ tend towards Gaussian random processes. Further, since ϕ_i is uniformly distributed, they will be independent Gaussian random processes with equal power $P_{avg}/2$. In this case, the magnitude of the complex baseband channel $\alpha(t)$

$$\alpha(t) = \sqrt{\tilde{r}_I^2(t) + \tilde{r}_Q^2(t)} \quad (2.33)$$

will be *Rayleigh Distributed* and we have what is called the *Rayleigh Channel* or *Rayleigh Fading*. Specifically, if we let

$$\sigma^2 = \frac{P_{avg}}{2} = E\{\tilde{r}_I^2(t)\} = E\{\tilde{r}_Q^2(t)\} \quad (2.34)$$

we have the distribution of the envelope:

$$f_\alpha(x) = \begin{cases} \frac{x}{\sigma^2} \exp\left(-\frac{x^2}{2\sigma^2}\right) & 0 \leq x \leq \infty \\ 0 & \text{else} \end{cases} \quad (2.35)$$

Note that we can write the impulse response for this model as

$$\tilde{h}(\tau, t) = \left\{ \frac{1}{\sqrt{N}} \sum_{i=1}^N e^{-j(2\pi f_i t + \phi_i)} \right\} \delta(\tau) \quad (2.36)$$

which is a narrowband model (no frequency selectivity) but is also time-varying.

For a Rician channel, there is a direct LOS component. Specifically, if $\tilde{h}^{Ra}(t)$ is a unit power Rayleigh fading channel, then a Rician fading channel can be written as

$$\tilde{h}^{Ri}(t) = \sqrt{\frac{K}{K+1}} + \sqrt{\frac{1}{K+1}} \tilde{h}^{Ra}(t) \quad (2.37)$$

where $\tilde{h}^{Ri}(t)$ is a unit power Rician fading channel where the K -factor is the ratio of the power of the direct LOS component and the diffuse (Rayleigh) component. Note that $K \rightarrow \infty$ results in an AWGN channel and $K \rightarrow 0$ results in a Rayleigh channel. An example plot of Rayleigh and Ricean distributions is given in Figure 2.6 for a Ricean K -factor of $K = 10$. We can see that the probability of low amplitudes (close to zero) is much smaller for the Ricean channel due to the strong LOS component.

2.6.2 Temporal Correlation in Clarke's Model

We typically define the autocorrelation function of the received signal (assuming that the signal is wide sense stationary) as

$$R(\tau) = E\{r(t)r(t+\tau)\} \quad (2.38)$$

or in complex baseband

$$\tilde{R}(\tau) = E\{\tilde{r}(t)\tilde{r}^*(t+\tau)\} \quad (2.39)$$

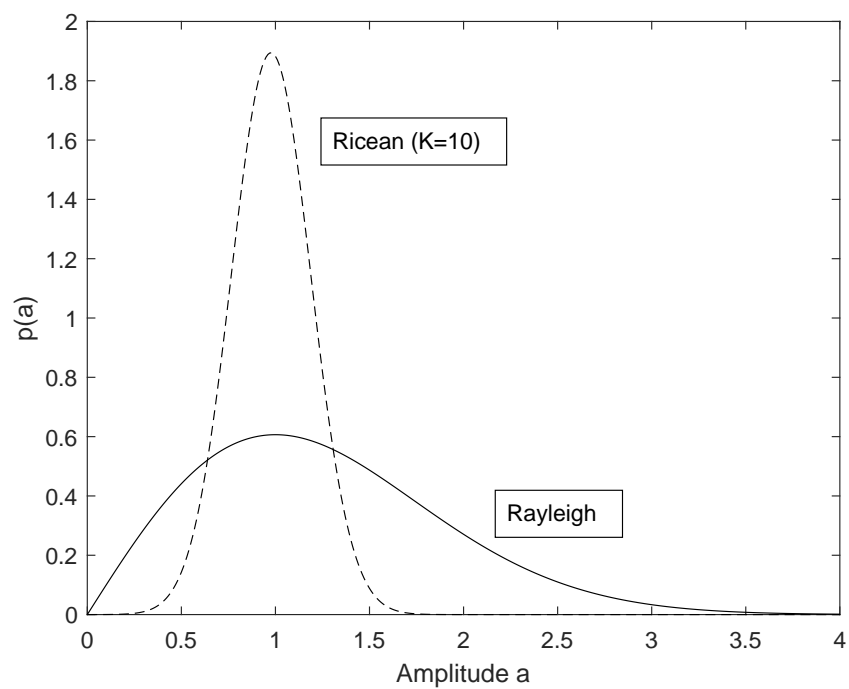


Figure 2.6: Rayleigh and Ricean ($K=10$) Probability Density Functions for Unit Average Energy.

where for Clarke's model, the expectation is over c_i , θ_i and ϕ_i . Assuming a sinusoidal transmit signal (to highlight the impact of the channel) we have

$$\begin{aligned}\tilde{R}(\tau) &= \text{E} \{ \tilde{r}(t)\tilde{r}(t+\tau) \} \\ &= \text{E} \left\{ \left(\frac{1}{\sqrt{N}} \sum_{i=1}^N e^{-j(2\pi f_i t + \phi_i)} \right) \left(\frac{1}{\sqrt{N}} \sum_{k=1}^N e^{j(2\pi f_k(t+\tau) + \phi_k)} \right) \right\} \\ &= \text{E} \left\{ \frac{1}{N} \sum_{i=1}^N \sum_{k=1}^N e^{-j(2\pi f_d \cos(\theta_i)t - 2\pi f_d \cos(\theta_k)t + \phi_i - \phi_k)} \right\}\end{aligned}\quad (2.40)$$

Taking the expectation over uniform distribution of θ_i , θ_k , ϕ_i and ϕ_k , we find that the expectation is zero for $i \neq k$. Thus, we have

$$\begin{aligned}\tilde{R}(\tau) &= \text{E} \left\{ \frac{1}{N} \sum_{i=1}^N e^{-j2\pi f_d \cos(\theta_i)\tau} \right\} \\ &= \frac{1}{N} \sum_{i=1}^N \int_0^{2\pi} \frac{1}{2\pi} e^{-j2\pi f_d \cos(\theta_i)\tau} d\theta_i \\ &= \frac{1}{2\pi} \int_0^{2\pi} e^{-j2\pi f_d \cos(\theta)\tau} d\theta \\ &= J_o(2\pi f_d \tau)\end{aligned}\quad (2.41)$$

where J_o is the zeroth order modified bessel function of the first kind. Note that all N integrals are the same since θ_i are i.i.d.

Alternatively, we can use the expression in (2.20) to determine temporal correlation using $S_A(\theta) = \frac{1}{2\pi}$:

$$\tilde{R}(\tau) = \int_{-\pi}^{\pi} \frac{1}{2\pi} e^{j2\pi f_d \tau \sin(\theta)} d\theta \quad (2.42)$$

$$= J_o(2\pi f_d \tau) \quad (2.43)$$

This function is plotted versus τf_d in Figure 2.7. If the maximum Doppler frequency f_d increases, the temporal correlation will change faster. Alternatively, for a lower maximum Doppler frequency, the temporal correlation is higher for a specific delay.

2.6.3 Doppler Power Spectrum for Clarke's Model

The total power at the mobile can be written as the integral of the azimuthal power spectrum $S_A(\theta)$:

$$P_r = \int_{-\pi}^{\pi} S_A(\theta) G(\theta) d\theta \quad (2.44)$$

where $G(\theta)$ is the receive antenna gain. We would like to translate this to Doppler Power Spectrum $S_D(f)$. Now $f = f_d \cos(\theta)$. Thus, two angles contribute to f , $\pm\theta$. What we want is

$$P_r = \int_{-f_d}^{f_d} S_D(f) df \quad (2.45)$$

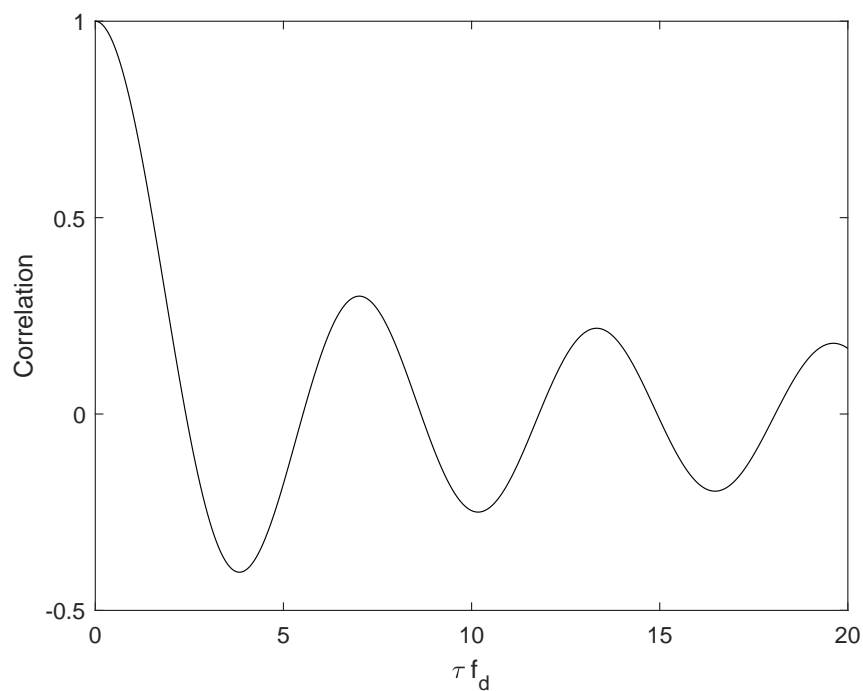


Figure 2.7: Temporal Correlation in Jakes/Clarkes Model. Note that the plot is normalized by the maximum Doppler frequency f_d .

Now, to convert from θ to f :

$$\theta = \cos^{-1} \left(\frac{f}{f_d} \right) \quad (2.46)$$

$$d\theta = -\frac{1}{f_d} \frac{1}{\sqrt{1 - (f/f_d)^2}} \quad (2.47)$$

Thus,

$$\begin{aligned} P_r &= \int_{-f_d}^{f_d} \left\{ S_A \left(\left| \cos^{-1} \left(\frac{f}{f_d} \right) \right| \right) G \left(\left| \cos^{-1} \left(\frac{f}{f_d} \right)^{-1} \right| \right) + \right. \\ &\quad \left. S_A \left(- \left| \cos^{-1} \left(\frac{f}{f_d} \right) \right| \right) G \left(- \left| \cos^{-1} \left(\frac{f}{f_d} \right)^{-1} \right| \right) \right\} \frac{-df}{f_d \sqrt{1 - (f/f_d)^2}} \end{aligned} \quad (2.48)$$

Thus,

$$\begin{aligned} S_D(f) &= \frac{1}{f_d \sqrt{1 - (f/f_d)^2}} S_A \left(\left| \cos^{-1} \left(\frac{f}{f_d} \right) \right| \right) G \left(\left| \cos^{-1} \left(\frac{f}{f_d} \right)^{-1} \right| \right) + \dots \\ &\quad S_A \left(- \left| \cos^{-1} \left(\frac{f}{f_d} \right) \right| \right) G \left(- \left| \cos^{-1} \left(\frac{f}{f_d} \right)^{-1} \right| \right) \end{aligned} \quad (2.49)$$

For a uniform distribution in angle and a dipole antenna:

$$\begin{aligned} S_A(\theta) &= \frac{1}{2\pi} \\ G(\theta) &= \frac{3}{2} \end{aligned}$$

we have

$$S_D(f) = \begin{cases} \frac{3}{2\pi f_d \sqrt{1 - (f/f_d)^2}} & |f| \leq f_d \\ 0 & \text{else} \end{cases} \quad (2.50)$$

Finally, it can be shown that there is a close relationship between the Doppler spectrum and the correlation function. Specifically,

$$S_D(f) = \mathcal{F} \left\{ \tilde{R}(\tau) \right\} \quad (2.51)$$

An example for $f_d = 100\text{Hz}$ is plotted in Figure 2.8.

2.7 General Matrix Channel

Up to this point, we have considered a SISO channel (i.e., one transmit antenna and one receive antenna). Now, we will expand our discussion to a MIMO channel. Consider a set of N_t signals sent from N_t antennas written in vector complex baseband form as

$$\tilde{\mathbf{x}}(t) = \begin{bmatrix} \sum_{i=-\infty}^{\infty} s_{1,i} p(t - iT) \\ \sum_{i=-\infty}^{\infty} s_{2,i} p(t - iT) \\ \vdots \\ \sum_{i=-\infty}^{\infty} s_{N_t,i} p(t - iT) \end{bmatrix} \quad (2.52)$$

where $p(t)$ is the pulse shape used, $s_{j,i}$ is the i th symbol in time sent from the j th antenna. Let the channel between any transmit/receive pair be a slow, flat fading channel so that the received

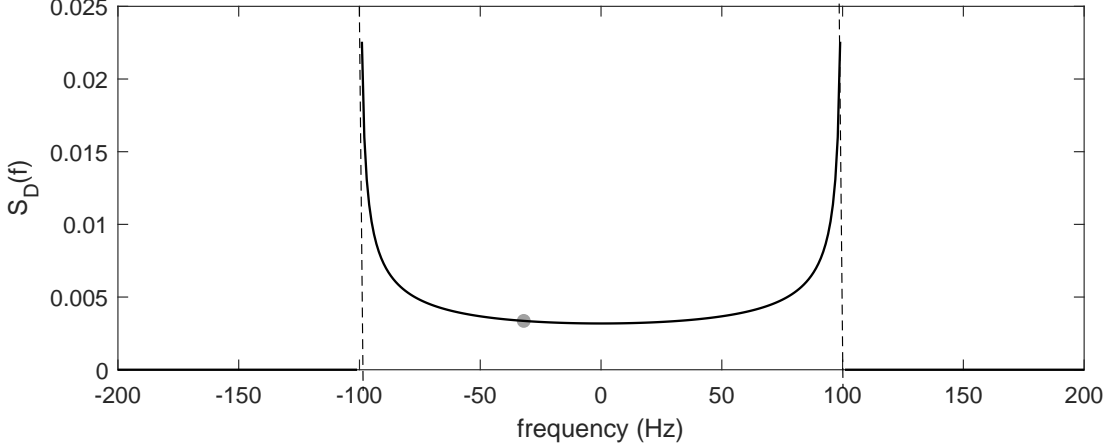


Figure 2.8: Doppler Spectrum in Jakes/Clarkes Model. Note that the plot assumes that the maximum Doppler frequency is $f_d=100\text{Hz}$.

signal on the i th receive antenna is

$$\tilde{r}_i(t) = \sum_{k=1}^{N_t} \int_{-\infty}^{\infty} \tilde{h}_{i,k}(\tau, t) x_k(t - \tau) d\tau + \tilde{n}_i(t) \quad (2.53)$$

$$= \sum_{k=1}^{N_t} \sum_{m=-\infty}^{\infty} \tilde{h}_{i,k}[mT] s_{k,i} p(t - mT) + \tilde{n}_i(t) \quad (2.54)$$

where $h_{i,k}(\tau, t)$ is the channel impulse response between the k th transmit antenna and the i th receive antenna. Our assumption that the channel is flat (i.e., the Narrowband Assumption) means that the transmit signal is not distorted (no inter-symbol interference) and experiences a single time-varying gain. The assumption that the channel is slow means that the channel remains constant over a symbol. Thus, for any particular symbol, the received symbol on the i antenna from k th transmitter can be written as $h_{i,k}[mT] s_{k,m} p(t - mT)$. $\tilde{n}_i(t)$ is the noise process observed on the i th receive antenna (generally assumed to be white Gaussian noise).

The received signal during the m th time slot is passed through a matched filter and sampled:

$$r_i[m] = \int_{(m-1)T/2}^{mT/2} \tilde{r}_i(t) p(t - mT) dt \quad (2.55)$$

$$= \sum_{k=1}^{N_t} s_{k,m} \tilde{h}_{i,k}[m] + \tilde{n}_i[m] \quad (2.56)$$

where $x[n] = x(nT)$. Dropping the dependence on time (and again remembering the Narrowband Assumption), we have

$$\tilde{r}_i = \sum_{k=1}^{N_t} s_k \tilde{h}_{i,k} + \tilde{n}_i \quad (2.57)$$

$$= \tilde{\mathbf{h}}_i^T \mathbf{s} + \tilde{n}_i \quad (2.58)$$

where \mathbf{s} is a vector of symbols transmitted from N_t antennas and $\tilde{\mathbf{h}}_i$ is the complex channel coefficients seen at the i th receiver from each of the N_t antennas. If there are M_r receive antennas, we can write the vector of received signals (after matched filtering and sampling) as:

$$\tilde{\mathbf{r}} = \tilde{\mathbf{H}}\mathbf{s} + \tilde{\mathbf{n}} \quad (2.59)$$

where $\tilde{\mathbf{r}}$ is the receive signal vector, \mathbf{s} is the vector of transmit symbols, $\tilde{\mathbf{n}}$ is a vector of complex AWGN noise samples with $E\{\tilde{\mathbf{n}}\} = \mathbf{0}^{M_r \times 1}$ and $E\{\tilde{\mathbf{n}}\tilde{\mathbf{n}}^H\} = \sigma^2 \mathbf{I}$, and $\tilde{\mathbf{H}}$ is the $M_r \times N_t$ channel matrix. $[\tilde{\mathbf{H}}]_{i,j}$ is the complex channel coefficient from the j th transmit antenna to the i th receive antenna.

If all transmit/receive channels are independent Rayleigh faded channels $\tilde{\mathbf{H}}$ is a matrix of independent complex Gaussian random variables, i.e., $\tilde{\mathbf{H}} = \tilde{\mathbf{H}}_w$.

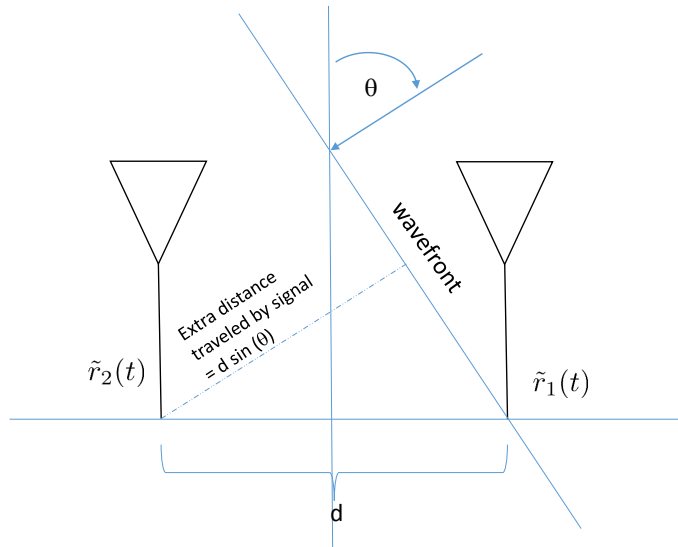


Figure 2.9: Wavefront impinging on two antennas (plane-wave assumption). Note that θ is defined here to be relative to the array normal.

2.8 Spatial Correlation

Consider a single multipath component received at two antennas $\tilde{r}_1(t)$ and $\tilde{r}_2(t)$ separated by distance d . The correlation between the two received signals (ignoring noise) can be written as

$$\rho(d) = E\{\tilde{r}_1(t)\tilde{r}_2^*(t)\} \quad (2.60)$$

For a single multipath component arriving from angle θ (note that we have temporarily defined θ to be relative to the array normal as shown in Figure 2.9) we have

$$\tilde{r}_2(t) = \tilde{r}_1(t)e^{-j2\pi\frac{d}{\lambda}\sin(\theta)} \quad (2.61)$$

Thus, we have

$$\rho(d) = E\left\{\tilde{r}_1(t)\tilde{r}_1^*(t)e^{j2\pi\frac{d}{\lambda}\sin(\theta)}\right\} \quad (2.62)$$

Clearly, the overall correlation will depend on the angular distribution of the arriving multipath. Assuming that the received signal is wide-sense stationary, that $E\{|\tilde{r}_1(t)|\} = P_r$ and the angle of arrival is uniformly distributed on $[0, 2\pi)$:

$$\begin{aligned} \rho(d) &= P_r E\left\{e^{j2\pi\frac{d}{\lambda}\sin(\theta)}\right\} \\ &= \int_{-\pi}^{\pi} \frac{1}{2\pi} e^{j2\pi\frac{d}{\lambda}\sin(\phi)} d\phi \\ &= J_o\left(\frac{2\pi d}{\lambda}\right) \end{aligned} \quad (2.63)$$

where we assumed in the second step that $P_r = 1$. NOTE: The imaginary part is zero. We could have also arrived at this result by using $S_A(\theta) = \frac{1}{2\pi}$ in (2.18).

Now, consider a Gaussian distribution³ for $S_A(\theta)$ with central angle θ_o and standard deviation σ_A

$$\begin{aligned} \rho(d) &= \int_{-\pi}^{\pi} S_A(\theta) e^{j2\pi d/\lambda\sin(\theta)} d\theta \\ &= \int_{-\pi}^{\pi} e^{j2\pi\frac{d}{\lambda}\sin(\theta)} \frac{1}{\sqrt{2\pi}\sigma} \exp\left(-\frac{(\theta - \theta_o)^2}{2\sigma_A^2}\right) d\theta \end{aligned}$$

Let $z = \frac{\theta - \theta_o}{\sigma_A}$ and $dz = \frac{d\theta}{\sigma_A}$.

$$\begin{aligned} \rho(d) &= \frac{1}{\sqrt{2\pi}} \int_{-\pi}^{\pi} e^{j2\pi\frac{d}{\lambda}\sin(\sigma_A z + \theta_o)} \exp\left(-\frac{z^2}{2}\right) dz \\ &= \frac{1}{\sqrt{2\pi}} \int_{-\pi}^{\pi} e^{j2\pi\frac{d}{\lambda}(\sin(\sigma_A z)\cos(\theta_o) + \cos(\sigma_A z)\sin(\theta_o))} \exp\left(-\frac{z^2}{2}\right) dz \end{aligned}$$

Assuming relatively small angle spread $\sigma_A z$ will be small where $\exp -z^2/2$ is significant. Thus, we can make the approximation

$$\begin{aligned} \sin(\sigma_A z) &\approx \sigma_A z \\ \cos(\sigma_A z) &\approx 1 \end{aligned}$$

³We note that the distribution is *approximately* Gaussian since it has finite support. Technically it is a truncated Gaussian, but we assume that σ_A is small enough that the assumption is valid.

Thus,

$$\begin{aligned} \rho(d) &\approx \frac{1}{\sqrt{2\pi}} \int_{-\pi}^{\pi} e^{j2\pi \frac{d}{\lambda}(\sigma_A z \cos(\theta_o) + \sin(\theta_o))} \exp\left(-\frac{z^2}{2}\right) dz \\ &= \frac{e^{j2\pi \frac{d}{\lambda} \sin(\theta_o)}}{\sqrt{2\pi}} \int_{-\pi}^{\pi} e^{j2\pi \frac{d}{\lambda} \sigma_A z \cos(\theta_o)} \exp\left(-\frac{z^2}{2}\right) dz \end{aligned} \quad (2.64)$$

$$= e^{j2\pi \frac{d}{\lambda} \sin(\theta_o)} e^{-\left(\frac{(2\pi \frac{d}{\lambda} \sigma_A \cos(\theta_o))^2}{2}\right)} \quad (2.65)$$

As an example, consider $\sigma_A = 5^\circ$ with a central AOA of zero. (In the equation above, σ is defined in radians. For this example $\sigma_A = 0.0873$ radians.) The spatial correlation is clearly much higher (for the same separation distance) for the Gaussian distribution. In general, we can show an inverse relationship between angular spread (some measure of the width of the angle power distribution) and spatial correlation. That is, for a given separation distance, a smaller angular spread results in higher correlation. The separation required to obtain a specific correlation (magnitude)

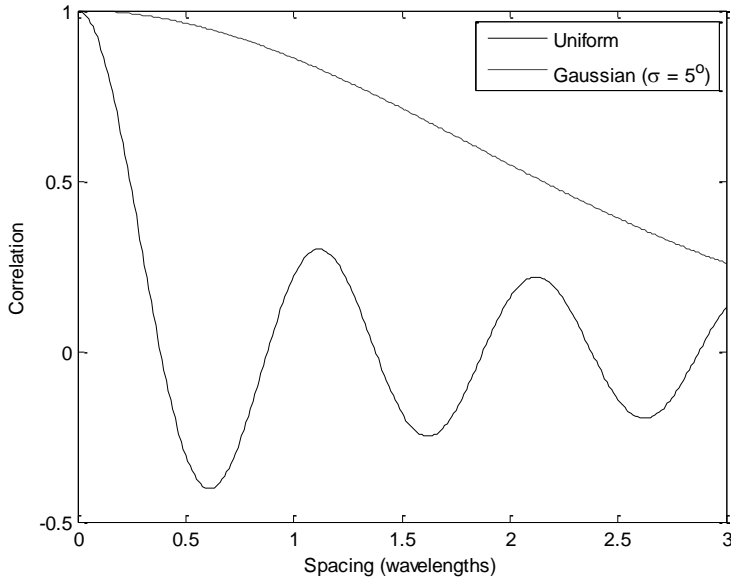


Figure 2.10: Spatial Correlation for Uniform Distribution and Gaussian Distribution ($\sigma = 5^\circ$)

can be found by taking the magnitude of (2.65) and solving for $\frac{d}{\lambda}$:

$$\begin{aligned} |\rho(d)| &\approx e^{-\left(\frac{(2\pi \frac{d}{\lambda} \sigma_A \cos(\theta_o))^2}{2}\right)} \\ -\ln(|\rho(d)|) &= \frac{(2\pi \frac{d}{\lambda} \sigma_A \cos(\theta_o))^2}{2} \\ \frac{d}{\lambda} &= \frac{\sqrt{-2 \ln(|\rho(d)|)}}{2\pi \sigma_A \cos(\theta_o)} \end{aligned} \quad (2.66)$$

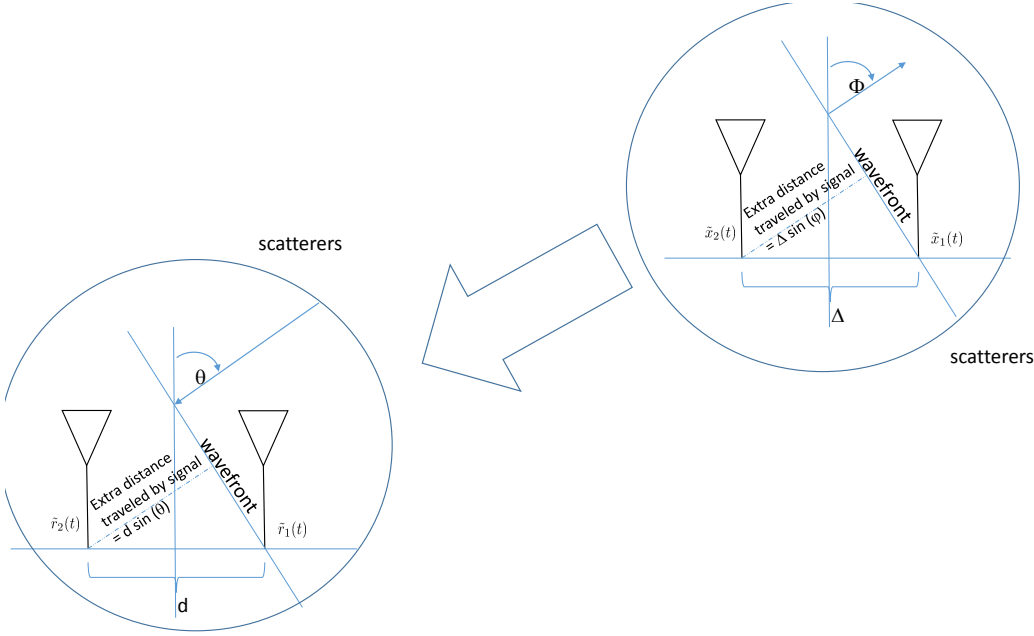


Figure 2.11: Assumed Geometry for Spatial Jakes Model

2.9 Matrix (Spatial) Version of Clarke's Model

Clarke's narrowband SISO model discussed earlier can be extended to a MIMO channel. To understand this, we will first extend Clarke's model to SIMO channels and then MISO channels. We can then combine those two models into a full MIMO model.

2.9.1 Clarke's Model for SIMO Channels

For SIMO channels, there is a single transmit antenna and multiple receive antennas. The received signal is then an $M_r \times 1$ vector as is the channel $\tilde{\mathbf{h}}$:

$$\tilde{\mathbf{r}}(t) = \tilde{\mathbf{h}}(t)x(t) + \tilde{\mathbf{n}}(t) \quad (2.67)$$

where $x(t)$ is the scalar transmit signal and $\tilde{\mathbf{n}}(t)$ is AWGN with zero mean and covariance \mathbf{I}_{M_r} (i.e., independent noise). The vector channel is

$$\tilde{\mathbf{h}}(t) = \begin{bmatrix} \tilde{h}_1(t) \\ \tilde{h}_2(t) \\ \vdots \\ \tilde{h}_{M_r}(t) \end{bmatrix} \quad (2.68)$$

Now, to see what $\tilde{h}_i(t)$ is let us consider transmitting a tone at a wavelength λ , which in complex baseband is $\tilde{x}(t) = 1$, the received signal on the first antenna based on the i th multipath component is

$$\tilde{r}_1(t) = e^{j(2\pi f_i t + \phi_i)} + \tilde{n}_1(t) \quad (2.69)$$

where $f_i = \frac{v}{\lambda} \cos(\theta_i)$ is the Doppler shift due to velocity v of the i th component which is arriving from angle θ_i . Assuming a linear array with the first element serving as the phase reference⁴, the same multipath component at the second antenna d m away can be written as

$$\tilde{r}_2(t) = e^{j(2\pi f_i t + \phi_i - 2\pi \frac{d}{\lambda} \sin(\theta_i))} + \tilde{n}_2(t) \quad (2.70)$$

Generalizing we can write the received vector based on the i th multipath component as

$$\tilde{\mathbf{r}}(t) = \begin{bmatrix} e^{j(2\pi f_i t + \phi_i)} + \tilde{n}_1(t) \\ e^{j(2\pi f_i t + \phi_i - 2\pi \frac{d}{\lambda} \sin(\theta_i))} + \tilde{n}_2(t) \\ e^{j(2\pi f_i t + \phi_i - 2\pi \frac{2d}{\lambda} \sin(\theta_i))} + \tilde{n}_3(t) \\ \vdots \\ e^{j(2\pi f_i t + \phi_i - 2\pi \frac{(M_r-1)d}{\lambda} \sin(\theta_i))} + \tilde{n}_{M_r}(t) \end{bmatrix} \quad (2.71)$$

The vector SIMO channel (again making a Narrowband Assumption) is then the normalized sum of N multipath components:

$$\tilde{\mathbf{h}}(t) = \frac{1}{\sqrt{N}} \sum_{i=1}^N e^{j(2\pi f_i t + \phi_i - 2\pi \frac{d}{\lambda} \sin(\theta_i))} \quad (2.72)$$

where \mathbf{d} is a vector of distances from the first antenna and we define

$$e^{\mathbf{x}} = \begin{bmatrix} e^{[\mathbf{x}]_1} \\ e^{[\mathbf{x}]_2} \\ \vdots \\ e^{[\mathbf{x}]_n} \end{bmatrix} \quad (2.73)$$

$[\mathbf{x}]_i$ is the i th element of the length n vector \mathbf{x} . The covariance matrix for this channel is

$$\mathbf{R}_{rx} = E \left\{ \tilde{\mathbf{h}}(t_o) \tilde{\mathbf{h}}^H(t_o) \right\} \quad (2.74)$$

and the expectation is over the random angles of arrival at time t_o . However, the channel is can be shown to be ergodic and thus the expectation can also be taken over time t for a fixed set of AOAs.

2.9.2 Clarke's Model for MISO Channels

The MISO extension of Clarke's model is similar to the SIMO case. The received signal can be written as a scalar

$$\tilde{r}(t) = \tilde{\mathbf{h}}^T(t) \tilde{\mathbf{x}}(t) + \tilde{n}(t) \quad (2.75)$$

where $\tilde{\mathbf{h}}(t)$ is now an $N_t \times 1$ vector. The transmit signal $\tilde{\mathbf{x}}(t)$ is also an $N_t \times 1$ vector. We will discuss what such a transmit vector might be later in the text. The vector channel in this case can be written as

$$\tilde{\mathbf{h}}(t) = \frac{1}{\sqrt{N}} \sum_{i=1}^N e^{j(2\pi f_i t + \phi_i - 2\pi \frac{\Delta}{\lambda} \sin(\Phi_i))} \quad (2.76)$$

⁴The extension to other array geometries is straight-forward. The key is defining the phase reference point.

where Δ is the vector of distances of the transmit antennas from the first (reference) antenna, again assuming a linear array. Φ_i is the angle of departure of the i th component from the transmit array. Note that the Doppler shift $f_i = \frac{v}{\lambda} \cos(\theta_i)$ and θ_i is the angle of arrival assuming that the receiver is in motion. If the transmitter is in motion, θ_i should be replaced by Φ_i .

2.9.3 Clarke's Model for MIMO Channels

Now, let's consider the scenario depicted in Figure 2.11. If we consider a sinusoidal transmit signal and examine one multipath component from the first transmit antenna to the first receive antenna:

$$\tilde{r}_{11}(t) = e^{j(2\pi f_i t + \phi_i)} \quad (2.77)$$

where $f_i = \frac{v}{\lambda} \cos(\theta_i)$ assuming that the array baseline is perpendicular to the velocity vector and that the receiver is mobile (not the transmitter). Note that if the velocity were due to the transmitter movement, the angle-of-arrival θ_i should be replaced by the angle of departure at the transmitter, Φ_i . If we have a uniformly spaced linear array, the received signal at the other antennas can be written:

$$\begin{aligned} \tilde{r}_{21}(t) &= e^{j(2\pi f_i t + \phi_i - 2\pi \frac{d}{\lambda} \sin(\theta_i))} \\ \tilde{r}_{31}(t) &= e^{j(2\pi f_i t + \phi_i - 2\pi \frac{2d}{\lambda} \sin(\theta_i))} \\ &\vdots \\ \tilde{r}_{M_r 1}(t) &= e^{j(2\pi f_i t + \phi_i - 2\pi \frac{(M_r - 1)d}{\lambda} \sin(\theta_i))} \end{aligned} \quad (2.78)$$

Similarly, we can write the signal from the multiple transmit antennas (assuming a uniform linear array with spacing Δ) and a departure angle Φ_i seen at first receive antenna:

$$\begin{aligned} \tilde{r}_{12}(t) &= e^{j(2\pi f_i t + \phi_i - 2\pi \frac{\Delta}{\lambda} \sin(\Phi_i))} \\ \tilde{r}_{13}(t) &= e^{j(2\pi f_i t + \phi_i - 2\pi \frac{2\Delta}{\lambda} \sin(\Phi_i))} \\ &\vdots \\ \tilde{r}_{1N_t}(t) &= e^{j(2\pi f_i t + \phi_i - 2\pi \frac{(N_t - 1)\Delta}{\lambda} \sin(\Phi_i))} \end{aligned} \quad (2.79)$$

In general,

$$x_{ab}(t) = e^{j(2\pi f_i t + \theta_i - \frac{2\pi}{\lambda} (a-1)d \sin(\phi_i) - \frac{2\pi}{\lambda} (b-1)\Delta \sin(\Phi_i))} \quad (2.80)$$

If we define the $M_r \times 1$ vector

$$\mathbf{d} = \begin{bmatrix} 0 \\ d \\ 2d \\ \vdots \\ (M_r - 1)d \end{bmatrix} \quad (2.81)$$

and $N_t \times 1$ vector

$$\bar{\Delta} = \begin{bmatrix} 0 \\ \Delta \\ 2\Delta \\ \vdots \\ (N_t - 1)\Delta \end{bmatrix} \quad (2.82)$$

we can write one component in the matrix channel as

$$\mathbf{H}_i(t) = \underbrace{e^{j(2\pi f_i t + \phi_i)}}_{\text{scalar, time-varying component}} \underbrace{e^{-j\left(\frac{2\pi}{\lambda} \mathbf{d} \sin(\theta_i)\right)}}_{\text{rx antennas}} \underbrace{e^{-j\left(\frac{2\pi}{\lambda} \bar{\Delta}^T \sin(\Phi_i)\right)}}_{\text{tx antennas}} \quad (2.83)$$

$$\begin{bmatrix} e^{x_1} \\ e^{x_1} \\ e^{x_1} \\ \vdots \\ e^{x_N} \end{bmatrix}$$

Note that for a length N column vector \mathbf{x} , we define $e^{\mathbf{x}} =$

is a scalar (representing the time varying component), the second term is $M_r \times 1$ (representing the impact of the receive antennas) and the third term is $1 \times N_t$ (representing the impact of the transmit antennas) meaning that each multipath component results in an $M_r \times N_t$ term in the sum. Finally, the narrowband Clarke's $M_r \times N_t$ Matrix channel can be written as

$$\begin{aligned} \mathbf{H}(t) &= \sqrt{\frac{1}{N}} \sum_{i=1}^N \mathbf{H}_i(t) \\ &= \sqrt{\frac{1}{N}} \sum_{i=1}^N e^{j(2\pi f_i t + \phi_i)} e^{-j\left(\frac{2\pi}{\lambda} \mathbf{d} \sin(\theta_i)\right)} e^{-j\left(\frac{2\pi}{\lambda} \bar{\Delta}^T \sin(\Phi_i)\right)} \end{aligned} \quad (2.84)$$

where $f_i = \frac{v}{\lambda} \cos(\theta_i)$ (assuming that the receiver is moving). The distribution of θ_i and Φ_i depend on many factors. Typical assumptions include uniform (mobile), Gaussian, Laplacian (base station). The angle spread of the distribution determines the spatial correlation.

2.10 Matrix Correlation

Define matrix channel $\mathbf{H} = \begin{bmatrix} h_{11} & \dots & \dots & h_{1N_t} \\ h_{21} & \dots & \dots & h_{2N_t} \\ \vdots & & & \vdots \\ h_{M_r1} & \dots & \dots & h_{M_rN_t} \end{bmatrix}$. We define the stacked vector

$$\mathbf{h}_{st} = \text{vec}\{\mathbf{H}\} = \begin{bmatrix} h_{11} \\ h_{21} \\ \vdots \\ h_{M_r1} \\ h_{12} \\ h_{22} \\ \vdots \\ h_{M_r2} \\ \vdots \\ h_{M_rN_t} \end{bmatrix} \quad (2.85)$$

The correlation matrix is defined as

$$\mathbf{R} = \mathbb{E}\{\mathbf{h}_{st}\mathbf{h}_{st}^H\} \quad (2.86)$$

2.10.1 Kronecker Model

The Kronecker model assumes that

$$\mathbf{R} = \mathbf{R}_{tx} \otimes \mathbf{R}_{rx} \quad (2.87)$$

where \mathbf{R}_{tx} is the correlation across transmit antennas (termed *transmit correlation*), \mathbf{R}_{rx} is the correlation across receive antennas (termed *receive correlation*), and \otimes is the Kronecker product.

2.10.2 Example

Define a 2×2 channel matrix with $\mathbb{E}\{|h_{i,j}|^2\} = 1$

$$\mathbf{H} = \begin{bmatrix} h_{11} & h_{12} \\ h_{21} & h_{22} \end{bmatrix} \quad (2.88)$$

Determine the full correlation matrix \mathbf{R} if the correlation between receive antennas is ρ and the correlation between transmit antennas is λ with and without the Kronecker assumption.

First, we can write

$$\mathbf{R}_{rx} = \mathbb{E}\left\{\begin{bmatrix} h_{11} \\ h_{21} \end{bmatrix} \begin{bmatrix} h_{11}^* & h_{21}^* \end{bmatrix}\right\} = \begin{bmatrix} 1 & \rho \\ \rho^* & 1 \end{bmatrix} \quad (2.89)$$

$$\mathbf{R}_{rx} = \mathbb{E} \left\{ \begin{bmatrix} h_{12} \\ h_{22} \end{bmatrix} \begin{bmatrix} h_{12}^* & h_{22}^* \end{bmatrix} \right\} = \begin{bmatrix} 1 & \rho \\ \rho^* & 1 \end{bmatrix} \quad (2.90)$$

$$\mathbf{R}_{tx} = \mathbb{E} \left\{ \begin{bmatrix} h_{11} \\ h_{12} \end{bmatrix} \begin{bmatrix} h_{11}^* & h_{12}^* \end{bmatrix} \right\} = \begin{bmatrix} 1 & \lambda \\ \lambda^* & 1 \end{bmatrix} \quad (2.91)$$

$$\mathbf{R}_{tx} = \mathbb{E} \left\{ \begin{bmatrix} h_{21} \\ h_{22} \end{bmatrix} \begin{bmatrix} h_{21}^* & h_{22}^* \end{bmatrix} \right\} = \begin{bmatrix} 1 & \lambda \\ \lambda^* & 1 \end{bmatrix} \quad (2.92)$$

However, this doesn't completely define the channel correlation. We can see this by looking at \mathbf{R} :

$$\mathbf{R} = \mathbb{E} \left\{ \begin{bmatrix} h_{11} \\ h_{21} \\ h_{12} \\ h_{22} \end{bmatrix} \begin{bmatrix} h_{11}^* & h_{21}^* & h_{12}^* & h_{22}^* \end{bmatrix} \right\} = \begin{bmatrix} 1 & \rho & \lambda & ? \\ \rho^* & 1 & ? & \lambda \\ \lambda^* & ? & 1 & \rho \\ ? & \lambda^* & \rho^* & 1 \end{bmatrix} \quad (2.93)$$

Thus, without the Kronecker assumption, we cannot complete the correlation matrix. The Kronecker Model thus assumes that

$$\mathbf{R} = \begin{bmatrix} \mathbf{R}_{rx} & \lambda \mathbf{R}_{rx} \\ \lambda^* \mathbf{R}_{rx} & \mathbf{R}_{rx} \end{bmatrix} \quad (2.94)$$

$$= \begin{bmatrix} 1 & \rho & \lambda & \lambda\rho \\ \rho^* & 1 & \lambda\rho^* & \lambda \\ \lambda^* & \lambda^*\rho & 1 & \rho \\ \lambda^*\rho^* & \lambda^* & \rho^* & 1 \end{bmatrix} \quad (2.95)$$

Thus, with the Kronecker assumption, we can complete the correlation matrix.

2.11 Conclusion

Overcoming the wireless channel is the dominant challenge in wireless communications. Understanding multipath fading is a key to understanding the benefits (and thus prevalence) of MIMO-OFDM communications. In this chapter we have examined the key aspects of the MIMO wireless channel including the temporal, spatial and frequency statistics of the channel. We have primarily focused on the first two aspects, but will return to the frequency statistics later in this manuscript.

Chapter 3

Introduction to MIMO

3.1 Introduction

What is MIMO communications? As we have already defined it, MIMO is “Multi-input Multi-Output” communications, i.e., a communication system that uses multiple antennas at the transmitter and/or receiver. In this brief chapter, we will first introduce the primary uses of multiple antennas at the transmitter and receiver. In the previous chapter we spent considerable time examining the wireless channel, especially that wireless channel in the presence of multiple antennas. It is the wireless channel that motivates the use of multiple antennas in modern communication systems. However, there are benefits to MIMO even in the absence of multipath, as we will discuss in this chapter. Specifically, there are four primary benefits to the use of MIMO: (a) average SNR gain, (b) diversity gain, (c) spatial multiplexing, and (d) interference mitigation. While the second and third benefits are exclusive to the multipath channel, the first and last gains can be obtained even in the absence of multipath.

We will begin by looking at uses of multiple antennas at the receiver only (commonly referred to as SIMO - single input, multiple output links). When we have multiple antennas at the receiver but only a single antenna at the transmitter, we can use those multiple receive antennas for three purposes: (1) SNR gain, (2) diversity gain, and (3) interference mitigation. Note that spatial multiplexing is not possible in SIMO, as we will discuss later. These three gains are not necessarily mutually exclusive when applied at the receiver. For example, SNR gain and diversity gain can typically be obtained simultaneously (note that this is not always the case at the transmitter). On the other hand, diversity gain and mitigation of interference cannot necessarily be obtained simultaneously.

It is also important to note that the relationship between the channel and the antenna array plays a major role in the gains obtainable. Specifically, in order for diversity gain to be realized, the antennas must be spaced at distances greater than the spatial coherence distance.

After discussing the use of multiple antennas at the receiver, we will discuss the use of multiple antennas at the transmitter only (MISO links). Generally speaking, the same gains can be ob-

tained (i.e., SNR gain, diversity gain and interference mitigation) using multiple antennas at the transmitter, although channel knowledge is required at the transmitter.

Finally, we will discuss spatial multiplexing which requires multiple antennas at both the transmitter and receiver. For MIMO channels, SNR gain, diversity gain and interference mitigation are all possible. However, unlike the MISO and SIMO cases, MIMO also offers the opportunity to increase throughput through spatial multiplexing, *i.e.*, the transmission of multiple parallel data streams (i.e., independent data signals in the same frequency band at the same time). Note that in this chapter we are simply introducing the concepts. We will explore each of these topics in greater detail in the following chapters.

3.2 Multiple Antennas at the Receiver (SIMO)

Our first discussion will focus on the use of multiple antennas at the receiver, the so-called “single input multiple output” or SIMO system. We first briefly investigate the benefit in the absence of multipath (at least absence at the receiver).

3.2.1 SIMO in the Absence of Multipath - Receive Beamforming

The first case to consider is the absence of multipath at the receiver, *i.e.*, where the multiple antennas are located. This case represents a plane wave arriving at the array and is shown in Figure 3.1. More specifically, consider that the channel is constant (*i.e.*, non time-varying) and equal to $\tilde{\alpha}\tilde{\mathbf{h}}$. The received signal (in complex baseband) at multiple antennas can be written as a vector

$$\tilde{\mathbf{r}}(t) = \tilde{\alpha}\tilde{\mathbf{h}}x(t) + \mathbf{n}(t) \quad (3.1)$$

where $\tilde{\alpha} = \alpha e^{j\phi}$ represents the impact of the channel between the transmitter and receive antenna array, $\mathbf{n}(t)$ is a complex vector Gaussian random process representing AWGN with zero mean and $E\{\mathbf{n}(t)\mathbf{n}^H(t)\} = \sigma^2\mathbf{I}$, and the transmit signal is a pulse modulated pulse stream $x(t) = \sum_{i=-\infty}^{\infty} s_i p(t - iT)$, $E\{|s_i|^2\} = 1$, $\int_{-\infty}^{\infty} p^2(t)dt = 1$. The vector $\tilde{\mathbf{h}}$ represents the impact of the receive array. More specifically, h_i ($|h_i| = 1$) is a complex phasor representing the phase shift observed at the i th antenna. At the output of a matched filter at the ν th symbol time we have

$$\tilde{\mathbf{r}}[\nu] = \tilde{\alpha}s_\nu\tilde{\mathbf{h}} + \mathbf{n}[\nu] \quad (3.2)$$

The SNR at each antenna is the same and found to be

$$\gamma_i = \frac{E\{|r_i|^2\}}{\sigma^2} = \frac{|\tilde{\alpha}|^2}{\sigma^2} \quad (3.3)$$

Consider that we have a plane wave impinging on a uniform linear array (*i.e.*, the antennas are evenly spaced in a line). The channel vector elements are then

$$h_i = e^{-j2\pi\frac{d}{\lambda}(i-1)\sin(\theta)} \quad (3.4)$$

where θ is defined according to Figure 3.1, *i.e.*, relative to the normal of the array. Now in receive beamforming, we combine the outputs of each antenna using a set of complex weights. That is, let the output from each antenna be weighted with a vector of weights \mathbf{w} to give a decision variable

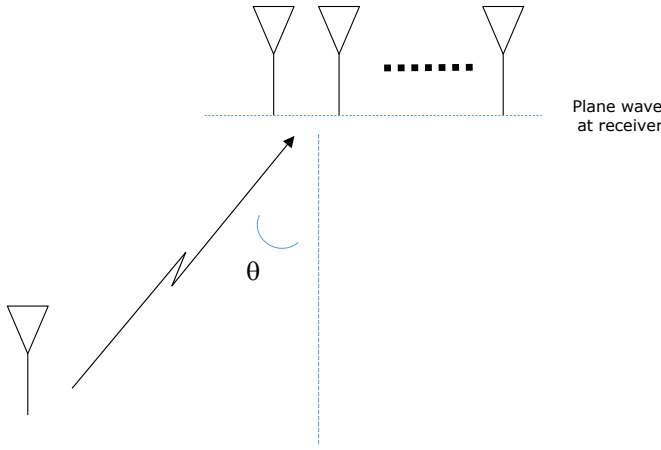


Figure 3.1: Signal Received at a Uniform Linear Array (SIMO) in Absence of Multipath

$z[\nu]$:

$$z[\nu] = \mathbf{w}^H \tilde{\mathbf{r}}[\nu] \quad (3.5)$$

The weights are typically chosen to optimize some criterion, as we will discuss in a later chapter. For now, let $\mathbf{w} = \tilde{\mathbf{h}}\tilde{\alpha}$:

$$\begin{aligned} z[\nu] &= \tilde{\alpha}^* \sum_{i=1}^{M_r} e^{j2\pi\frac{d}{\lambda}(i-1)\sin(\theta)} r_i \\ &= M_r |\tilde{\alpha}|^2 s_\nu + \tilde{\alpha}^* \underbrace{\sum_{i=1}^{M_r} e^{j2\pi\frac{d}{\lambda}(i-1)\sin(\theta)} n_i[\nu]}_{GRV(0, M_r |\tilde{\alpha}|^2 \sigma^2)} \end{aligned} \quad (3.6)$$

The SNR the resulting output is then found to be

$$\gamma = \frac{M_r^2 |\tilde{\alpha}|^4}{M_r \sigma^2 |\tilde{\alpha}|^2} = \frac{M_r |\tilde{\alpha}|^2}{\sigma^2} \quad (3.7)$$

Thus, we obtain an SNR improvement of M_r , which is typically called **beamforming gain**. Note that this provides the maximum SNR at the output of the combiner, as we will show later. Thus, in the absence of multipath and interference at the receiver, we can still obtain a benefit from the use of multiple antennas at the receiver.

3.2.2 SIMO Irrespective of Multipath - Interference Mitigation

A second benefit of using multiple antennas at the receiver is interference mitigation. This benefit can be achieved irrespective of the presence of multipath, and uses the degrees of freedom to

mitigate interference. To see this, consider the received signal on two antennas $r_1(t)$, $r_2(t)$ as

$$\begin{aligned} r_1(t) &= h_1 s(t) + h_1^i(t) i(t) + n_1(t) \\ r_2(t) &= h_2 s(t) + h_2^i(t) i(t) + n_2(t) \end{aligned}$$

where $s(t)$ is the signal of interest and $i(t)$ is an interfering signal. h_1 and h_2 represent the static channel between the transmitter of interest and the two receive antennas, while h_1^i and h_2^i represent the static channel between the interfering transmitter and the two receive antennas. $n_i(t)$ represents AWGN on the i th receive antenna. The two receive antennas could be used for SNR gain or diversity gain as discussed above. However, in this case, the interference $i(t)$ may be very detrimental to performance, and mitigating its effects may provide much bigger gains than either SNR or diversity gain.

If we combine the two signals with weights w_1 and w_2

$$r_T(t) = w_1 r_1(t) + w_2 r_2(t) \quad (3.8)$$

we can choose the weights to mitigate the interference. An obvious choice (assuming that we knew or could estimate the interference channel) would be to choose

$$\begin{aligned} w_1 &= -h_2^i \\ w_2 &= h_1^i \end{aligned}$$

which results in

$$\begin{aligned} r_T(t) &= -h_2^i r_1(t) + h_1^i r_2(t) \\ &= (-h_2^i h_1 + h_1^i h_2) s(t) + (-h_2^i h_1^i + h_2^i h_1^i) i(t) + (-h_2^i + h_1^i) n(t) \\ &= (-h_2^i h_1 + h_1^i h_2) s(t) + (-h_2^i + h_1^i) n(t) \end{aligned} \quad (3.9)$$

Thus, we can see that the interference is eliminated. We can then apply the gain $((-h_2^i h_1 + h_1^i h_2))^{-1}$ to eliminate the effects of the channel on the desired signal. This allows proper detection, but note that it does not allow for SNR gain, or as we will show in the next section, diversity gain. This is a general truth in MIMO communications: the degrees of freedom can be used for various gains, but not for all gains simultaneously. Thus, the system designer must consider what the best use of the antennas are.

3.2.3 SIMO For Combatting Multipath - Receive Diversity

Now let's consider the case where there is rich multipath scattering at the receiver. In this case we write the received signal vector as

$$\tilde{\mathbf{r}}(t) = x(t)\tilde{\mathbf{h}} + \mathbf{n}(t) \quad (3.10)$$

where

$$\tilde{\mathbf{h}} = \begin{bmatrix} \tilde{\alpha}_1 \\ \tilde{\alpha}_2 \\ \vdots \\ \tilde{\alpha}_{M_r} \end{bmatrix} \quad (3.11)$$

and $\mathbf{n}(t)$ is a complex vector Gaussian random process with zero mean and $E\{\mathbf{n}(t)\mathbf{n}^H(t)\} = \sigma^2\mathbf{I}$,

$$x(t) = \sum_{n=-\infty}^{\infty} s_n p(t - nT) \quad (3.12)$$

At the output of M_r matched filters sampled at the optimal symbol time we have

$$\tilde{\mathbf{r}}[\nu] = s_v \tilde{\mathbf{h}} + \mathbf{n}[\nu] \quad (3.13)$$

The SNR on the i th antenna is

$$\gamma_i = \frac{|\tilde{\alpha}_i|^2}{\sigma^2} \quad (3.14)$$

Using Maximal Ratio combining (we will describe this in detail in a later chapter):

$$z_\nu = \mathbf{w}^H \tilde{\mathbf{r}}[\nu] \quad (3.15)$$

where $\mathbf{w} = \tilde{\mathbf{h}}$. The SNR after MRC is

$$\begin{aligned} \gamma &= \frac{\left(E \left\{ \sum_{i=1}^{M_r} |\tilde{\alpha}_i|^2 s_\nu \middle| x_\nu \right\} \right)^2}{\sigma^2 \sum_{i=1}^{M_r} |\tilde{\alpha}_i|^2} \\ &= \frac{\left(\sum_{i=1}^{M_r} |\tilde{\alpha}_i|^2 \right)^2}{\sigma^2 \sum_{i=1}^{M_r} |\tilde{\alpha}_i|^2} \\ &= \frac{\sum_{i=1}^{M_r} |\tilde{\alpha}_i|^2}{\sigma^2} \end{aligned}$$

The SNR now benefits from both diversity and SNR gain. We will determine the statistics of this later, but for now we can say that the fading statistics of the combined channel are much less severe than an individual channel, provided that the channels are independent.

3.3 Multiple Antennas at the Transmitter (MISO)

The benefits of using multiple antennas at the receiver can generally be realized by using multiple antennas at the transmitter, albeit with more difficulty due to the channel knowledge required. That is, whereas at the receiver we can usually estimate the channel to determine the optimal antenna weights, that knowledge is more difficult to obtain at the transmitter.

3.3.1 MISO in the Absence of Multipath - Transmit Beamforming

In general, the gains discussed above for the SIMO channel are also applicable to the MISO channel. To see this, let's consider the received signal

$$\tilde{r}(t) = \tilde{\alpha} \mathbf{w}^H \tilde{\mathbf{h}} x(t) + n(t) \quad (3.16)$$

where $x(t) = \sum_{n=-\infty}^{\infty} s_n p(t - nT)$, $n(t)$ is complex Gaussian random process with power σ^2 , and again the vector channel is defined as $h_i = e^{-j2\pi\frac{d}{\lambda}(i-1)\sin(\theta)}$ (not including the scalar fading term).

If at the transmitter we choose

$$w_i = \frac{1}{\sqrt{N_t}} e^{-j2\pi\frac{d}{\lambda}(i-1)\sin(\theta)} \quad (3.17)$$

where the term $\frac{1}{\sqrt{N_t}}$ is due to normalizing the transmit power. Note that choosing the weights requires knowledge of the angle-of-departure θ *at the transmitter*. When applying this at the receiver, we can estimate θ . This is more difficult to obtain at the transmitter. At the output of a pulse matched filter sampled at the optimal symbol time

$$r[\nu] = \tilde{\alpha} \underbrace{\mathbf{w}^T \tilde{\mathbf{h}}}_G x_\nu + n[\nu] \quad (3.18)$$

Now $G = \sum_{i=1}^{N_t} w_i h_i = \frac{N_t}{\sqrt{N_t}} = \sqrt{N_t}$. Thus, the SNR at the receiver is

$$\gamma = \frac{N_t |\tilde{\alpha}|^2}{\sigma^2} \quad (3.19)$$

where N_t is again the **beamforming gain**.

Similarly, we can show that diversity gain is achievable using multiple transmit antennas and even interference mitigation is possible (typically termed interference avoidance) using multiple antennas at the transmitter instead of the receiver. However, knowledge of the appropriate channels is required at the transmitter instead of the receiver, which typically requires some form of feedback or time division duplexing.

3.4 True MIMO - Exploiting Multipath through Spatial Multiplexing

When the link has multiple antennas at both the transmitter and receiver, another type of benefit is possible: spatial multiplexing. Spatial multiplexing is the transmission of multiple simultaneous data streams in the same frequency band. To see this, consider the received signal $r_i(t)$ on M_r receive antennas (written in vector form)

$$\tilde{\mathbf{r}}(t) = \mathbf{H}\mathbf{x}(t) + \mathbf{n}(t) \quad (3.20)$$

where

$$x_i(t) = \sum_{n=-\infty}^{\infty} s_{i,n} p(t - nT) \quad (3.21)$$

and \mathbf{H} is the static matrix channel (assuming flat fading) between N_t transmit antennas and M_r receive antennas. At the output of M_r matched filters sampled at the optimal sampling time:

$$\tilde{\mathbf{r}}[\nu] = \mathbf{H}\mathbf{x}[\nu] + \mathbf{n}[\nu] \quad (3.22)$$

where $\mathbf{x}[\nu] = \begin{bmatrix} s_{1,\nu} \\ \dots \\ s_{N_t,\nu} \end{bmatrix}$. If the channel matrix \mathbf{H} is known *and is square*, we could formulate

$$\mathbf{z}[\nu] = \mathbf{H}^{-1}\tilde{\mathbf{r}}[\nu] = \mathbf{x}[\nu] + \mathbf{H}^{-1}\mathbf{n}[\nu] \quad (3.23)$$

Note, if \mathbf{H} is not square, we could still use the pseudo-inverse. However, as we will show later, there are actually better ways to do the signal processing at the receiver. The problem with this approach is that \mathbf{H} could be singular or poorly conditioned (very common case). Thus, the noise power can be enhanced since it is pre-multiplied by \mathbf{H}^{-1} . This can be seen in Figure 3.2 where we plot an example received QPSK constellation in a SISO channel (left) and MIMO channel (right). Clearly the constellation on the right is more spread out (i.e., adversely affected by noise) due to the application of the matrix inverse. This would lead to a higher BER in the MIMO case, relative to the SISO case. However, downside is counterbalanced by the fact that $N_t = M_r$ parallel channels are transmitted in the same frequency band/time slot. More sophisticated processing will also reduce the negative impact.

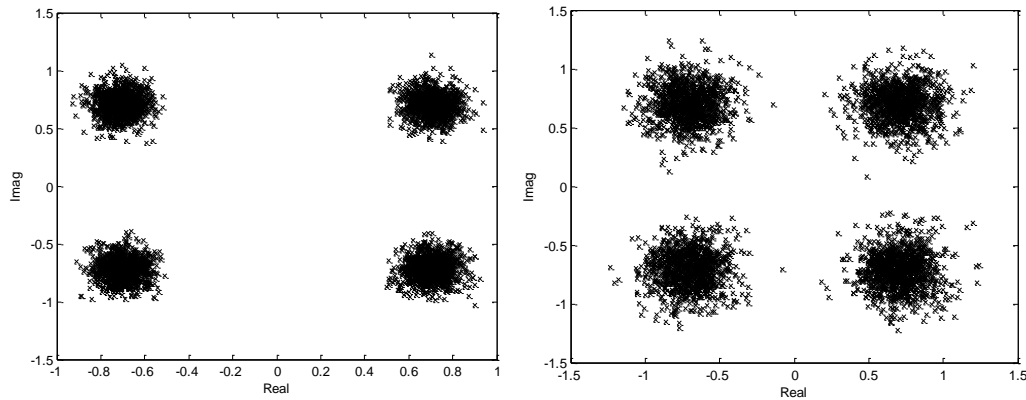


Figure 3.2: Example QPSK Constellation Received in SISO (left) and MIMO (right) Channels

3.4.1 More General Matrix Channel

Again, consider the received signal

$$\tilde{\mathbf{r}}[\nu] = \mathbf{H}\mathbf{x}[\nu] + \mathbf{n}[\nu] \quad (3.24)$$

where \mathbf{H} is an $M_r \times N_t$ matrix channel and $E\{\mathbf{n}(t)\mathbf{n}^H(t)\} = \sigma^2\mathbf{I}$. Now, using the psuedo-inverse and assuming that $rank(\mathbf{H}) = N_t$, we can create the decision variables as

$$\mathbf{z}[\nu] = \mathbf{T}\tilde{\mathbf{r}}[\nu] \quad (3.25)$$

with

$$\mathbf{T} = (\mathbf{H}^H \mathbf{H})^{-1} \mathbf{H}^H \quad (3.26)$$

which results in

$$\begin{aligned} \mathbf{z}[\nu] &= (\mathbf{H}^H \mathbf{H})^{-1} \mathbf{H}^H \tilde{\mathbf{r}}[\nu] \\ &= (\mathbf{H}^H \mathbf{H})^{-1} \mathbf{H}^H \mathbf{H} \mathbf{x}[\nu] + (\mathbf{H}^H \mathbf{H})^{-1} \mathbf{H}^H \mathbf{n}[\nu] \end{aligned} \quad (3.27)$$

$$= \mathbf{x}[\nu] + (\mathbf{H}^H \mathbf{H})^{-1} \mathbf{H}^H \mathbf{n}[\nu] \quad (3.28)$$

Now,

$$\mathbf{E} \left\{ (\mathbf{H}^H \mathbf{H})^{-1} \mathbf{H}^H \mathbf{n}[\nu] ((\mathbf{H}^H \mathbf{H})^{-1} \mathbf{H}^H \mathbf{n}[\nu])^H \right\} = (\mathbf{H}^H \mathbf{H})^{-1} \mathbf{H}^H \mathbf{E} \left\{ \mathbf{n}[\nu] \mathbf{n}^H[\nu] \right\} \mathbf{H} (\mathbf{H}^H \mathbf{H})^{-H} \quad (3.29)$$

$$= (\mathbf{H}^H \mathbf{H})^{-1} \mathbf{H}^H (\sigma^2 \mathbf{I}) \mathbf{H} (\mathbf{H}^H \mathbf{H})^{-H} \quad (3.30)$$

$$= \sigma^2 \underbrace{(\mathbf{H}^H \mathbf{H})^{-1} \mathbf{H}^H \mathbf{H}}_{\mathbf{I}} (\mathbf{H}^H \mathbf{H})^{-H} \quad (3.31)$$

$$= \sigma^2 (\mathbf{H}^H \mathbf{H})^{-H} \quad (3.32)$$

where \mathbf{A}^{-H} is the Hermitian of the inverse \mathbf{A} . In general, the diagonal elements of the matrix $(\mathbf{H}^H \mathbf{H})^{-H}$ will be greater than 1 resulting in noise enhancement.

3.5 Conclusions

In this brief chapter we have quickly summarized the primary benefits of employing multiple antennas at the receiver (SIMO), at the transmitter (MISO) or both (MIMO). Again, in SIMO and MISO channels SNR gains, diversity gains, and interference mitigation are all possible depending on the nature of the multipath and size the antenna array used. Further, in the case of MIMO we can also achieve a spatial multiplexing gain. In the MIMO case we can also achieve combinations of these gains, although we cannot obtain the full benefit of all gains simultaneously. There is always some trade-off that must be considered.

Chapter 4

MIMO Link Capacity

For many years the primary use of multiple antennas in a fading environment was to *combat* multipath fading. Specifically, multiple antennas were a primary source of diversity which mitigated the effect of fading. But in the last 20 years it was realized that multiple antennas were also a means for *exploiting* multipath. Specifically, as we will show in this chapter, the use of multiple antennas at the transmitter and receiver allows for an increase in spectral efficiency (i.e., capacity) in the presence of rich scattering.

4.1 Entropy and Uncertainty

To understand channel capacity, we must first describe a couple of basic concepts in information theory [2]. First, the measure of uncertainty of a random variable X that is used in information theory is known as *entropy*. For continuous random variables this is termed differential entropy and is defined as

$$\begin{aligned} H(X) &= -E \{ \log f_X(x) \} \\ &= - \int_{S_X} f_X(x) (\log f_X(x)) dx \end{aligned} \tag{4.1}$$

where $f_X(x)$ is the probability density function of X and S_X is the support of X . Mutual information between two random variables X and Y is the reduction in uncertainty of one random variable when observing the other. Note that the base of log determines the units of information. When we use base 2, the units are in *bits*, while when we used base e , the units are *nats*. Formally, mutual information is defined as

$$\begin{aligned} I(X; Y) &= H(X) - H(X|Y) \\ &= H(Y) - H(Y|X) \end{aligned}$$

Example 4.1.1. Find the differential entropy of a (scalar) complex Gaussian random variable in bits.

Solution: The differential entropy of a complex Gaussian random variable with mean μ_x and variance σ_x^2 is

$$\begin{aligned} H(X) &= -E \{ \log_2 f_X(x) \} \\ &= -E \left\{ \log_2 \left(\frac{1}{\pi \sigma_x^2} e^{-\frac{|x-\mu_x|^2}{\sigma_x^2}} \right) \right\} \\ &= \log_2(\pi \sigma_x^2) - E \left\{ \left(-\frac{|x-\mu_x|^2}{\sigma_x^2} \right) \right\} \log_2(e) \\ &= \log_2(\pi \sigma_x^2) + \log_2(e) \\ &= \log_2(e \pi \sigma_x^2) \end{aligned}$$

Note that the mean is irrelevant. Only the variance determines the differential entropy. Further, it can be shown that this is the maximum possible differential entropy for any random variable. In other words, $H(X) \leq \log_2(e \pi \sigma_x^2)$ for all possible X .

Example 4.1.2. Find the differential entropy of a complex Gaussian random vector in bits.

Solution: The differential entropy of a complex Gaussian random vector with mean $\bar{\mu}_x$ and covariance matrix Σ_x is

$$\begin{aligned} H(X) &= -E \{ \log_2 f_{\mathbf{X}}(\mathbf{x}) \} \\ &= -E \left\{ \log_2 \left(\frac{1}{\det(\pi \Sigma_x)} e^{-(\mathbf{x}-\bar{\mu}_x)^H \Sigma_x^{-1} (\mathbf{x}-\bar{\mu}_x)} \right) \right\} \\ &= \log_2(\det(\pi \Sigma_x)) - E \{ -(\mathbf{x}-\bar{\mu}_x)^H \Sigma_x^{-1} (\mathbf{x}-\bar{\mu}_x) \} \\ &= \log_2(\det(e \pi \Sigma_x)) \end{aligned} \tag{4.2}$$

Example 4.1.3. Find the mutual information in bits between random variables X and Y where $y = x + n$ when X and N are both zero-mean complex Gaussian random variables with variances σ_x^2 and σ^2 respectively.

Solution: The mutual information is defined as

$$I(X; Y) = H(Y) - H(Y|X) \tag{4.3}$$

Since X and N are both Gaussian, Y is also Gaussian. Thus we have:

$$H(Y) = \log_2(e \pi \sigma_y^2)$$

Further, if X is known, Y is a Gaussian random variable with mean x and variance σ^2 . Thus,

$$H(Y|X) = \log_2(e \pi \sigma^2)$$

Thus, the mutual information is

$$\begin{aligned}
 I(X; Y) &= \log_2(e\pi\sigma_y^2) - \log_2(e\pi\sigma^2) \\
 &= \log_2\left(\frac{e\pi\sigma_y^2}{e\pi\sigma^2}\right) \\
 &= \log_2\left(\frac{\sigma_x^2 + \sigma^2}{\sigma^2}\right) \\
 &= \log_2(1 + \gamma)
 \end{aligned} \tag{4.4}$$

where $\gamma = \frac{\sigma_x^2}{\sigma^2}$ is the ratio of the variances. Note that this is the mutual information for the model $y = x + n$ if n is known to be Gaussian but x can be chosen to follow any distribution. In other words, we achieve the maximum mutual information if x is also Gaussian as that makes y Gaussian.

4.2 Capacity

We are interested in a measured known as *capacity* which is the maximum mutual information provided by a channel. Consider a random channel input X and a random channel output Y where $y = x + n$. Further, assume that X has a distribution $f_X(x)$ and Y has a distribution $f_Y(y)$. The uncertainty of the input X is the entropy, defined above. As also mentioned above, the mutual information between the input X and channel output Y is the reduction in uncertainty in one random variable due to observation of the other. In our case, we observe the output Y and are interested in the input X . Mutual information can also be seen as a measure of the dependence of two random variables. For continuous random variables, using the definitions above, the mutual information for two continuous random variables X and Y can be written as

$$I(X; Y) = \int_{S_X, S_Y} f_{X,Y}(x, y) \log\left(\frac{f_{X,Y}(x, y)}{f_X(x)f_Y(y)}\right) dx dy \tag{4.5}$$

where S_X and S_Y are the supports for the random variables X and Y respectively. The capacity of a channel is the maximum mutual information where the maximization occurs over the distribution of the input:

$$C = \max_{f_X(x)} I(X; Y) \tag{4.6}$$

If $y = x + n$ and n has a complex Gaussian distribution, the capacity of the channel is achieved when X also has a complex zero-mean Gaussian distribution as discussed above. Further, using the example above, the capacity is well-known to be (in bits per channel use):

$$C = \log_2\left(1 + \frac{P}{\sigma^2}\right) \tag{4.7}$$

where $P = \sigma_x^2$ and σ^2 is the variance of the noise n . Now, if we have a continuous time AWGN channel with bandpass bandwidth B and AWGN power spectral density $\frac{N_o}{2}$, the output after bandpass to baseband conversion, can be represented by samples taken at a rate of $1/B$. Thus, the capacity of this channel is

$$C = B \log_2(1 + \gamma) \tag{4.8}$$

where $\gamma = \frac{P}{N_o B}$ is the signal-to-noise ratio and the capacity is measured in bits per second (b/s). The capacity C/B (b/s/Hz) for an AWGN channel is plotted in Figure 4.1. We can see that for an SNR of 15dB, we can obtain a spectral efficiency of 5b/s/Hz.

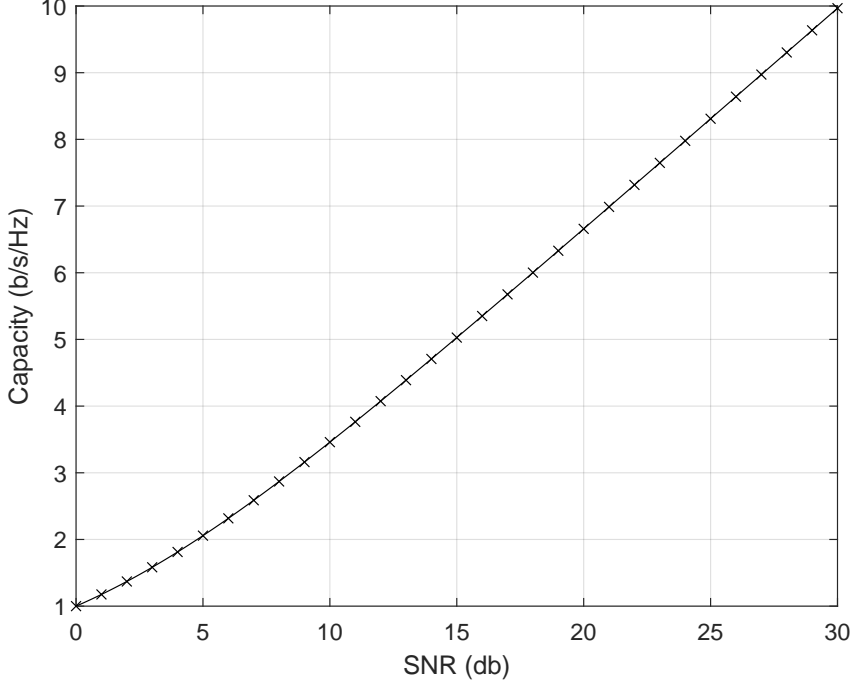


Figure 4.1: Channel Capacity (b/s/Hz) versus SNR in an AWGN Channel

4.3 Channel Capacity in MISO and SIMO Channels

For a fixed scalar channel h , [NOTE: Although we don't use the tilde notation here, we can assume that all vectors can be either real or complex.] we have (at the output of a pulse-matched filter):

$$y = hx + n \quad (4.9)$$

where x is the transmit symbol (i.e., the channel input) and n is AWGN (zero mean, variance σ^2). Shannon's capacity theorem above still applies for a fixed value of h . Specifically, the maximum error free transmission rate (i.e., capacity) is

$$C = B \log_2 (1 + \gamma|h|^2) \text{ b/s} \quad (4.10)$$

where B is the system bandwidth, $\gamma = \frac{\mathbb{E}\{|x|^2\}}{\sigma^2}$ (i.e., SNR). Note that B has two effects since $\sigma^2 = N_o B$. In terms of spectral efficiency we have

$$\frac{C}{B} = \log_2 (1 + \gamma|h|^2) \text{ b/s/Hz} \quad (4.11)$$

Now, if we transmit on one antenna, but receive the signal on M_r antennas the received signal vector is

$$\mathbf{y} = \tilde{\mathbf{h}}x + \mathbf{n} \quad (4.12)$$

where $\tilde{\mathbf{h}}$ is the $M_r \times 1$ fixed channel vector. Despite the multiple receive antennas, the channel still permits only a single input. The received vector \mathbf{y} has M_r dimensions, but the information is only along $\tilde{\mathbf{h}}$. Thus, we can project \mathbf{y} along $\tilde{\mathbf{h}}$ and retain all of the information while rejecting $M_r - 1$ dimensions of the noise vector \mathbf{n} :

$$\begin{aligned} z &= \tilde{\mathbf{h}}^H \mathbf{y} \\ &= \tilde{\mathbf{h}}^H \tilde{\mathbf{h}} x + \tilde{\mathbf{h}}^H \mathbf{n} \end{aligned}$$

This corresponds to a SISO channel with SNR $\frac{E\{|x|^2\}\tilde{\mathbf{h}}^H \tilde{\mathbf{h}}}{\sigma^2}$. Thus, the capacity that corresponds to a SISO channel with a modified SNR:

$$\frac{C}{B} = \log_2 \left(1 + \gamma \sum_{i=1}^{M_r} |h_i|^2 \right) b/s/Hz \quad (4.13)$$

On the other hand, if we transmit the signal from N_t antennas (without channel knowledge) but only have one output (i.e., one receive antenna), the received signal is

$$y = \tilde{\mathbf{h}}^T \mathbf{x} + n \quad (4.14)$$

Again, this is similar to a SISO channel, except that the input is now a vector \mathbf{x} which is projected onto a channel $\tilde{\mathbf{h}}$. Without channel knowledge, the optimal transmit signal is a Gaussian random vector with covariance $\Sigma_x = \frac{E\{|x|^2\}}{N_t} \mathbf{I}$. Again, the capacity is the similar to SISO channels with a modified SNR. However, unlike the SIMO case there is a normalizing power constant $1/\sqrt{N_t}$ since we must split the power over multiple antennas:

$$\frac{C}{B} = \log_2 \left(1 + \frac{\gamma}{N_t} \sum_{i=1}^{N_t} |h_i|^2 \right) b/s/Hz \quad (4.15)$$

We can also see this by viewing the received signal as $y = v + n$ where $v = \sum_{i=1}^{N_t} h_i x_i$ for fixed values of h_i . Capacity is maximized by making v Gaussian with the power constraint that $\sum_i \sigma_{x_i}^2 = 1$. Without knowledge of h_i , we simply use equal power in each transmit signal and thus $\sigma_{x_i}^2 = \frac{1}{N_t}$.

For M_r receive antennas, capacity goes up due to increased capture of signal energy. For N_t transmit antennas, capacity doesn't necessarily go up since the transmit power is fixed regardless of the number of antennas.

Now, if the transmitter has channel knowledge in the MISO case, we can transmit $\frac{\tilde{\mathbf{h}}}{\|\tilde{\mathbf{h}}\|} x$ and receive

$$y = \left(\frac{\tilde{\mathbf{h}}}{\|\tilde{\mathbf{h}}\|} \right)^H \tilde{\mathbf{h}} x + n \quad (4.16)$$

Now in this case we again have a modified AWGN SISO channel and the capacity (using a Gaussian distribution for x) is

$$\frac{C}{B} = \log_2 \left(1 + \gamma \sum_{i=1}^{N_t} |h_i|^2 \right) b/s/Hz \quad (4.17)$$

which is equivalent to the SIMO case.

4.4 Fading Channels

The previous sections assumed that the channel was *static*. However, in fading channels the channel is not assumed to be constant, but time-varying. The capacity in the fading case differs substantially from the static channel case. The capacity of the fading channel depends on the information available. There are two primary cases of interest:

1. The channel is known by the receiver.
2. The channel is known by the transmitter and receiver.

We already saw that in the case of MISO channels, knowledge of the channel made a difference in the channel capacity. That is also true for fading channels, although the gain achieved depends on the distribution of the channel.

4.4.1 Channel Known at the Receiver

There are two definitions of capacity that are relevant in fading channels when the transmitter does not know the channel (but the receiver does). Those two definitions are

1. Ergodic (Shannon) Capacity
2. Outage Capacity

Because the transmitter does not know the channel, the rate cannot be adapted relative to the channel. As a result, we must pick a constant rate for transmission. There are two general assumptions applied to understanding the capacity in this case. The first assumption is that the channel varies quickly allowing for a sufficiently long code word to experience all channel states. In this case, the constant rate is known as the *ergodic* or Shannon capacity and is defined as

$$C_{erg} = \int_0^{\infty} B \log_2(1 + \gamma)p(\gamma)d\gamma \quad (4.18)$$

where $p(\gamma)$ is the distribution of the SNR due to channel fading. Note that although this is the AWGN capacity averaged over the SNR distribution we cannot think of this as the rate being modified to match the channel conditions. The transmitter in fact does not know the channel and thus cannot adapt the rate. The rate is fixed. If it is fixed at a rate equal to the ergodic capacity or lower, a bit error rate approaching zero can be achieved. Thus, to achieve this capacity, the transmitter and receiver must know the distribution of the channel to determine this rate, although the transmitter doesn't know the channel at any given instant. As an example consider the ergodic capacity of a Rayleigh fading channel shown in Figure 4.2. Again, noting a 15dB SNR (average in the fading case), we can see that as opposed to the 5b/s/Hz achievable in an AWGN channel, the ergodic capacity in the case of Rayleigh fading is only 4.3b/s/Hz. Thus, there is a nearly 15% reduction in the capacity due to fading.

On the other hand, if the channel varies slowly, such that a code word experiences a constant channel, the capacity will depend on specific channel conditions. Again, since the rate cannot be adapted (since the transmitter does not know the channel), the receiver will experience an outage whenever the channel capacity is less than the constant rate chosen by the transmitter. Thus,

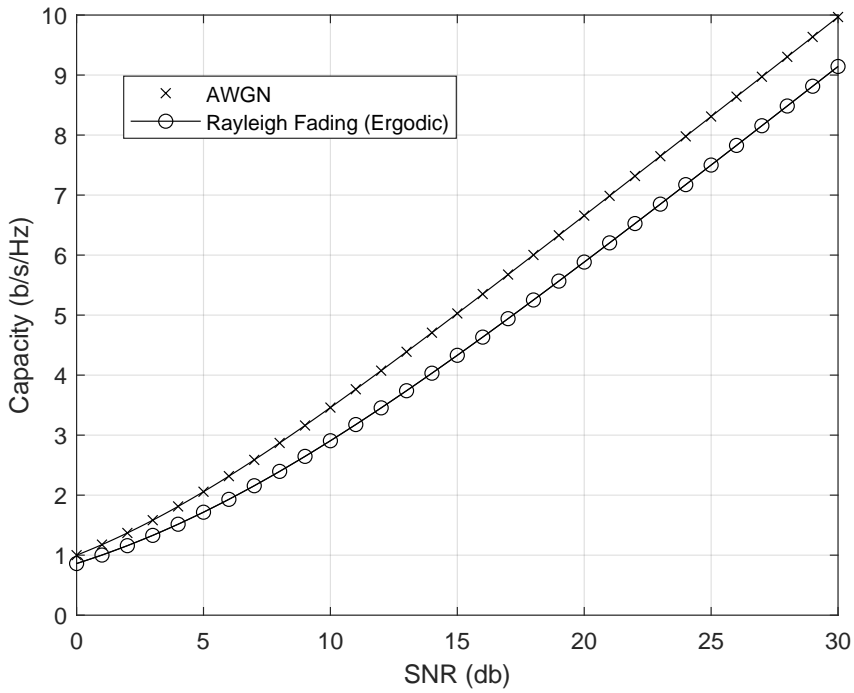


Figure 4.2: Ergodic Capacity (b/s/Hz) versus SNR in an Rayleigh Fading Channel

the higher the rate chosen, the higher the outage probability. If the distribution is known the transmitter can choose the constant rate based on a desired outage probability. This is known as the *outage capacity*. For formally, we define the $p \times 100\%$ outage capacity as the capacity C_{out} that satisfies

$$p = \Pr \{ B \log_2(1 + \gamma) < C_{out} \} \quad (4.19)$$

As an example, consider a Rayleigh fading channel with an average SNR of 15dB. The probability of outage versus outage capacity is plotted in Figure 4.3. For example, if a 1% outage is desired, the capacity is approximately 0.4b/s/Hz. On the other hand if a 10% outage probability can be tolerated, the capacity is a good bit higher at approximately 2.1 b/s/Hz. The outage capacity for 1% and 10% outage probabilities are compared with the ergodic capacity and AWGN capacity in Figure 4.4. We can see that for moderate to low outage probabilities the outage capacity is significantly lower than the ergodic capacity in a Rayleigh fading channel. This can be ameliorated by adding antennas at the transmitter or receiver as we will see shortly.

4.4.2 Channel Known at the Transmitter and Receiver

When the transmitter has knowledge of the channel there are two options that the transmitter can choose:

1. Adapt rate only
2. Adapt power and rate

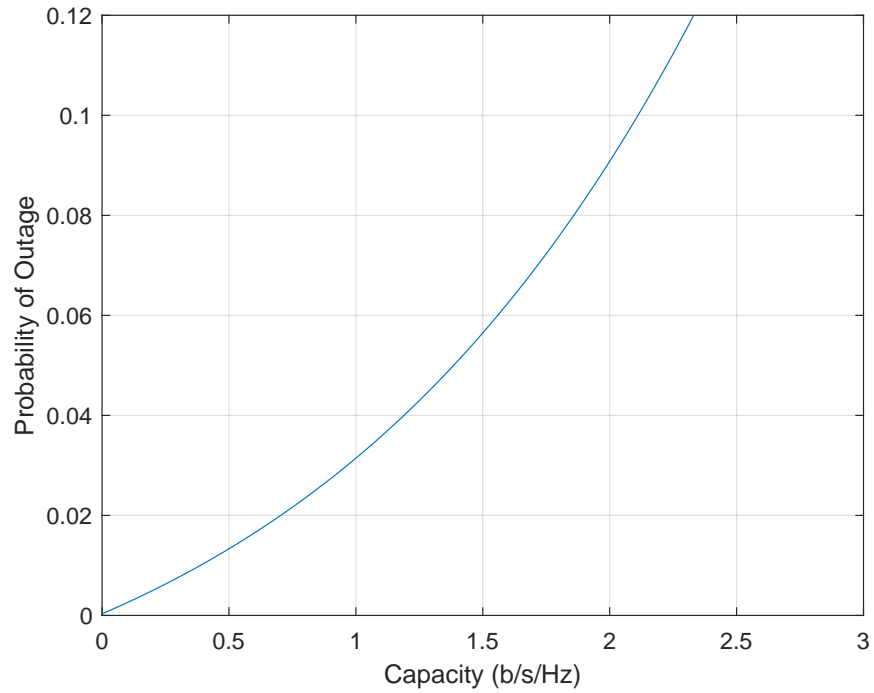


Figure 4.3: Outage Capacity (b/s/Hz) versus Outage Probability in an Rayleigh Fading Channel (average SNR = 15dB)

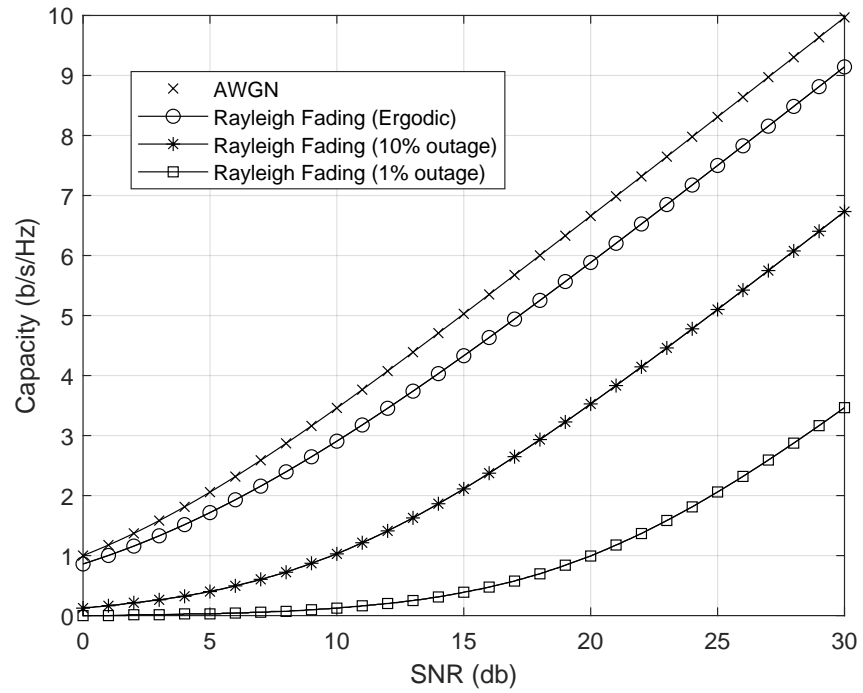


Figure 4.4: Capacity (b/s/Hz) versus SNR in an AWGN or Rayleigh Fading Channel

In the case where rate is adapted, but power isn't, the transmitter choose the rate which corresponding to the capacity at full transmit power. In this case there is not outage capacity, since the transmitter always transmits at the rate supported by the known channel. However, the average rate achieved by adapting the rate based on the known channel is the ergodic capacity and is calculated

$$C = \int_0^\infty B \log_2(1 + \gamma) p(\gamma) d\gamma \quad (4.20)$$

which is identical to the case where the channel is unknown. Thus channel knowledge at the transmitter is not helpful if power adaptation is not used. On the other hand, if power is adapted, the capacity is calculated as

$$C = \max_{P(\gamma): \int_0^\infty P(\gamma) p(\gamma) d\gamma = \bar{P}} \int_0^\infty B \log_2 \left(1 + \frac{P(\gamma)\gamma}{\bar{P}} \right) p(\gamma) d\gamma \quad (4.21)$$

where \bar{P} is the average power available and $P(\gamma)$ is the mapping between the channel SNR and the transmit power. The solution to this is found to be based on the concept of *water-filling* where the power is chosen as

$$\frac{P(\gamma)}{\bar{P}} = \begin{cases} \frac{1}{\gamma_o} - \frac{1}{\gamma} & \gamma \geq \gamma_o \\ 0 & \gamma < \gamma_o \end{cases} \quad (4.22)$$

where γ_o is known as the cut-off value since the transmitter will not transmit for SNR values less than γ_o . The cut-off value must be found numerically using the constraint

$$\int_{\gamma_o}^\infty \left(\frac{1}{\gamma_o} - \frac{1}{\gamma} \right) d\gamma = 1 \quad (4.23)$$

4.5 Random MISO and SIMO Channels

In the case of random MISO and SIMO channels, we can again define either ergodic capacity or outage capacity. The ergodic capacity is defined

$$C_{erg} = E_{\tilde{\mathbf{h}}} \left\{ B \log_2 \left(1 + \gamma \tilde{\mathbf{h}}^H \tilde{\mathbf{h}} \right) \right\} b/s/Hz \quad (4.24)$$

in the case of SIMO (or MISO with channel knowledge at the transmitter) and

$$C_{erg} = E_{\tilde{\mathbf{h}}} \left\{ B \log_2 \left(1 + \frac{\gamma}{N_t} \tilde{\mathbf{h}}^H \tilde{\mathbf{h}} \right) \right\} b/s/Hz \quad (4.25)$$

in the case of MISO in the absence of channel knowledge at the transmitter. The impact of multiple antennas to ergodic capacity with channel information at the receiver can be seen in Figures 4.5 and 4.6. We can see that adding mutliple antennas to either the transmitter or receiver improves ergodic capacity. However, the benefit is much greater when adding them at the receiver, in the absence of transmitter side channel knowledge. Without transmitter side channel knowledge, adding antennas to the transmitter only will provide small increases in ergodic capacity, approaching that of an AWGN channel, but no more. At the receiver, however, we can see that capacity is increased much more from additional antennas, and in fact can exceed that of an AWGN channel even with only two antennas. This is due to the additional received energy available from the additional receive antennas. This same benefit is possible from transmit antennas, but only if

transmitter side channel knowledge is available.

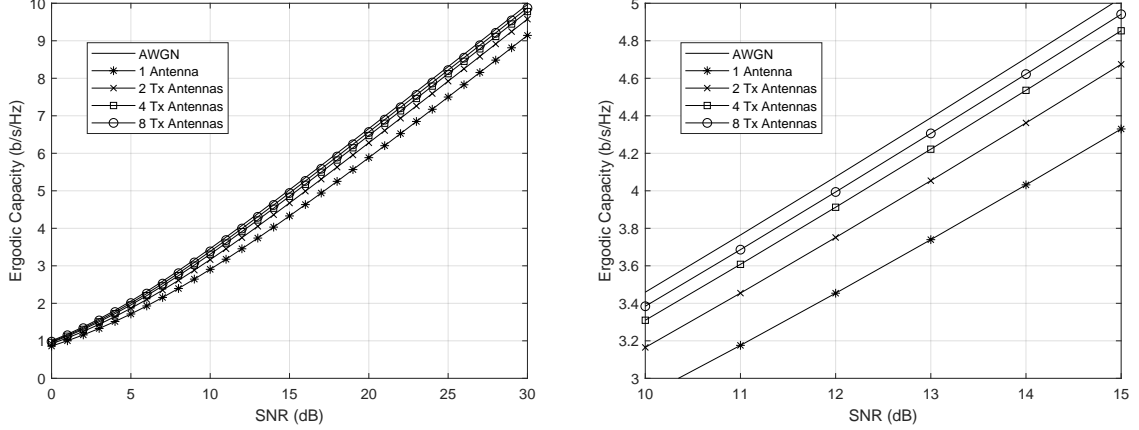


Figure 4.5: Ergodic Capacity (b/s/Hz) versus SNR in MISO Rayleigh (independent) Fading Channel with Channel Information at the Receiver

Mutltiple antennas at the transmitter and receiver can have an even greater impact on outage capacity due to the diversity provided. This can be seen in Figure 4.7 for the MISO case in independent Rayleigh fading and 4.8 for the SIMO case, also independent Rayleigh fading. These figures show the outage probability versus capacity in the case of no transmitter channel knowledge when SNR=15dB. In the case of MISO the outage capacity at 10% outage probability increases from 2.1b/s/Hz with one antenna to 3.2b/s/Hz, 3.9b/s/Hz and 4.3b/s/Hz for 2, 4, and 8 transmit antennas respectively. At 1% outage the gains are even more dramatic going from 0.4b/s/Hz with one antenna to 1.8b/s/Hz, 2.9b/s/Hz and 3.7b/s/Hz using 2, 4, and 8 antennas respectively. Note that AWGN capacity is 5b/s/Hz. Thus, just like in the ergodic capacity case, the outage capacity (regardless of outage probability) is upper-bounded by the capacity of the AWGN channel. This is not true if the transmitter has channel knowledge, since that matches the SIMO case which is not bounded by (single antenna) AWGN capacity due to the average SNR gain.

The gains in outage probability for the SIMO case are even greater due to the natural SNR gain from coherent combining. The outage capacity at 10% outage increases to 4.2b/s/Hz, 5.8b/s/Hz and 7.2b/s/Hz for 2, 4 and 8 receive antennas respectively, while the 1% outage capacity increases to 2.5b/s/Hz, 4.8b/s/Hz and 6.5b/s/Hz for those same numbers of antennas. As mentioned above, the outage capacity for SIMO (like the ergodic capacity) is not bounded by the single antenna AWGN case.

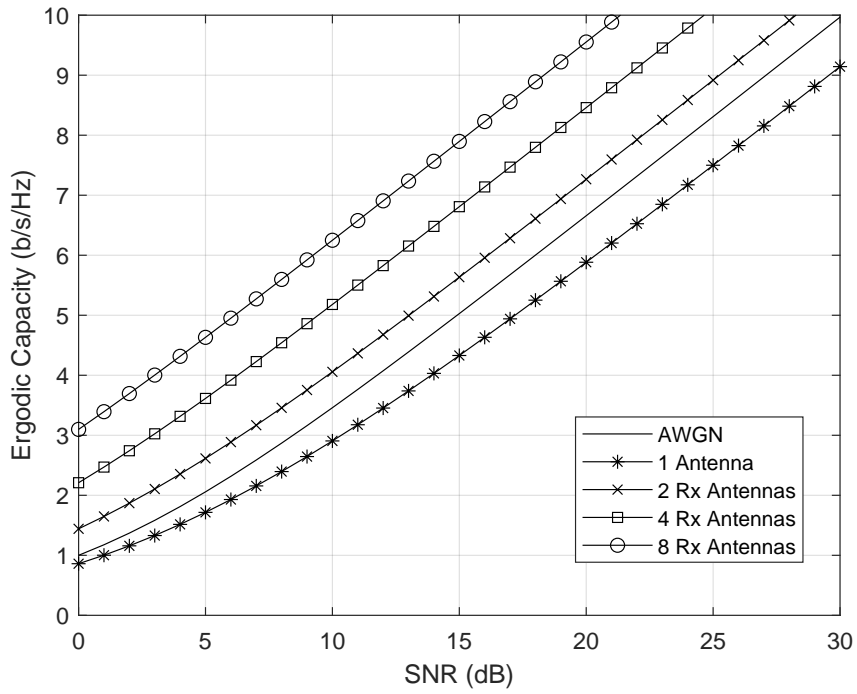


Figure 4.6: Ergodic Capacity (b/s/Hz) versus SNR in SIMO Rayleigh (independent) Fading Channel with Channel Information at the Receiver

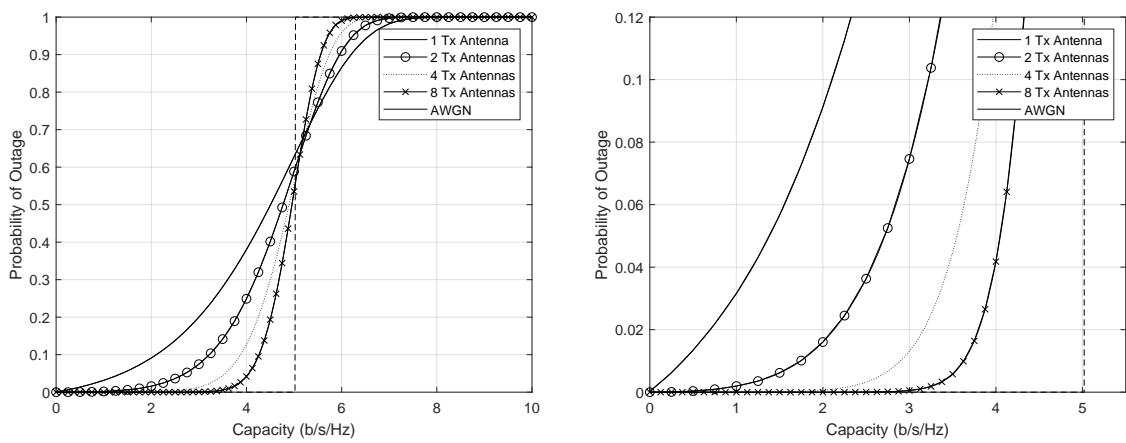


Figure 4.7: Outage Capacity (b/s/Hz) versus SNR in MISO Rayleigh (independent) Fading Channel with Channel Information at the Receiver

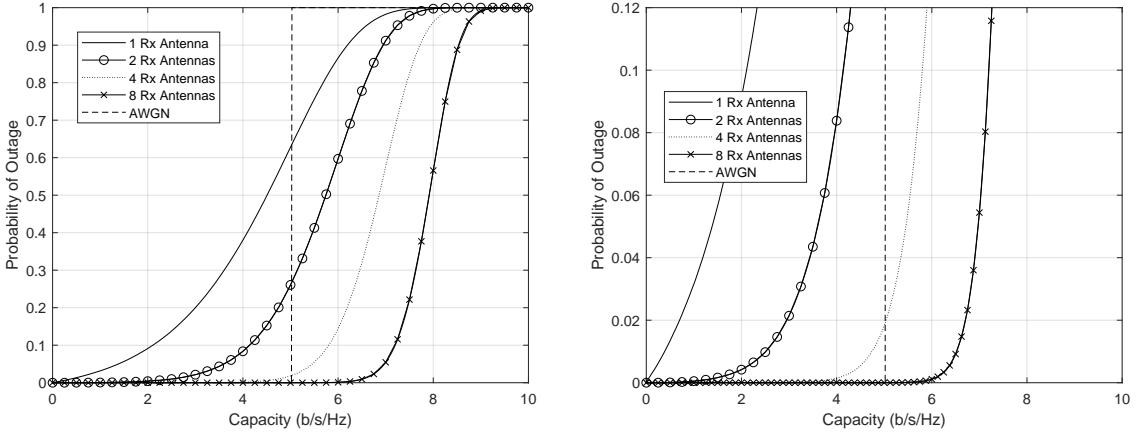


Figure 4.8: Outage Capacity (b/s/Hz) versus SNR in SIMO Rayleigh (independent) Fading Channel with Channel Information at the Receiver

4.6 Matrix Channel

Now let us consider a matrix (i.e., MIMO) channel. Specifically, let

$$\mathbf{y} = \mathbf{H}\mathbf{x} + \mathbf{n} \quad (4.26)$$

where \mathbf{H} is fixed or random and \mathbf{n} is Gaussian circular symmetric noise $\mathbf{n} \sim \text{GRV}(\mathbf{0}, \sigma^2 \mathbf{I})$. For a fixed channel the capacity can be found as

$$C = \max_{f_X(\mathbf{x}): \text{tr}(\Sigma_{\mathbf{x}}) \leq P_t} I(\mathbf{x}, \mathbf{y}) \quad (4.27)$$

where $\Sigma_{\mathbf{x}} = E\{\mathbf{x}\mathbf{x}^T\} - E\{\mathbf{x}\}E\{\mathbf{x}\}^H$. For random channels, we again define ergodic capacity or outage capacity. Ergodic capacity is defined as

$$C_{erg} = E_H \left\{ \max_{f_X(\mathbf{x}): \text{tr}(\Sigma_{\mathbf{x}}) \leq P_t} I(\mathbf{x}, \mathbf{y}) \right\} \quad (4.28)$$

Now,

$$\begin{aligned} I(\mathbf{x}, \mathbf{y}) &= H(\mathbf{y}) - H(\mathbf{y}|\mathbf{x}) \\ &= H(\mathbf{y}) - H(\mathbf{H}\mathbf{x} + \mathbf{n}|\mathbf{x}) \\ &= H(\mathbf{y}) - H(\mathbf{n}) \end{aligned} \quad (4.29)$$

where we have assumed that \mathbf{x} and \mathbf{n} are independent and

$$H(\mathbf{x}) = - \int_{\mathbf{x}} f_X(\mathbf{x}) \log_2 (f_X(\mathbf{x})) d\mathbf{x} \quad (4.30)$$

Now, it is well known that this is maximized when \mathbf{y} and thus \mathbf{x} is Gaussian. Further, for Gaussian random vectors, we can show that

$$H(\mathbf{y}) = \log_2 (\det (\pi e \Sigma_{\mathbf{y}})) \quad (4.31)$$

where $\Sigma_{\mathbf{y}}$ is the covariance matrix of \mathbf{y} . Now, since \mathbf{y} is zero mean

$$\begin{aligned} \Sigma_{\mathbf{y}} &= E \{ \mathbf{y} \mathbf{y}^H \} \\ &= E \{ (\mathbf{H} \mathbf{x} + \mathbf{n})(\mathbf{H} \mathbf{x} + \mathbf{n})^H \} \\ &= E \{ \mathbf{H} \mathbf{x} \mathbf{x}^H \mathbf{H}^H \} + E \{ \mathbf{n} \mathbf{n}^H \} \\ &= \mathbf{H} \Sigma_{\mathbf{x}} \mathbf{H}^H + \sigma^2 \mathbf{I} \end{aligned} \quad (4.32)$$

Thus, we have

$$\begin{aligned} I(\mathbf{x}, \mathbf{y}) &= \log_2 (\det (\pi e (\mathbf{H} \Sigma_{\mathbf{x}} \mathbf{H}^H + \sigma^2 \mathbf{I}))) - \log_2 (\det (\pi e \sigma^2 \mathbf{I})) \\ &= \log_2 \left[\frac{\det (\pi e (\mathbf{H} \Sigma_{\mathbf{x}} \mathbf{H}^H + \sigma^2 \mathbf{I}))}{\det (\pi e \sigma^2 \mathbf{I})} \right] \\ &= \log_2 \left[\det \left((\mathbf{H} \Sigma_{\mathbf{x}} \mathbf{H}^H + \sigma^2 \mathbf{I}) \frac{1}{\sigma^2} \mathbf{I} \right) \right] \\ &= \log_2 \left[\det \left(\left(\frac{1}{\sigma^2} \mathbf{H} \Sigma_{\mathbf{x}} \mathbf{H}^H + \mathbf{I} \right) \right) \right] \end{aligned} \quad (4.33)$$

Thus, the capacity (in b/s/Hz) can be written as

$$\frac{C}{B} = \log_2 \left[\det \left(\left(\frac{1}{\sigma^2} \mathbf{H} \Sigma_{\mathbf{x}} \mathbf{H}^H + \mathbf{I} \right) \right) \right] \quad (4.34)$$

We have already said that $f_X(\mathbf{x})$ is Gaussian. Further, if we have no channel knowledge, it is optimal to choose $\Sigma_{\mathbf{x}} = \frac{P_t}{N_t} \mathbf{I}$, i.e., we put equal power on all transmit antennas. That results in

$$\frac{C}{B} = \log_2 \left[\det \left(\left(\frac{P_t}{N_t \sigma^2} \mathbf{H} \mathbf{H}^H + \mathbf{I} \right) \right) \right] \quad (4.35)$$

Let $\gamma = \frac{P_t}{\sigma^2}$:

$$\frac{C}{B} = \log_2 \left[\det \left(\left(\frac{\gamma}{N_t} \mathbf{H} \mathbf{H}^H + \mathbf{I} \right) \right) \right] \quad (4.36)$$

Further, since $\mathbf{H} \mathbf{H}^H$ is a Hermitian matrix, it has an eigenvalue decomposition

$$\mathbf{H} \mathbf{H}^H = \mathbf{Q} \Lambda \mathbf{Q}^H \quad (4.37)$$

where \mathbf{Q} is a unitary matrix of orthonormal eigenvectors and Λ is a diagonal matrix of eigenvalues. The diagonal of Λ will have r positive eigenvalues and $\min(N_t, M_r) - r$ zeros where $r = \text{rank}(\mathbf{H})$:

$$\Lambda = \begin{bmatrix} \lambda_1 & 0 & \cdots & 0 & 0 & \cdots & 0 \\ 0 & \lambda_2 & \cdots & 0 & 0 & \cdots & 0 \\ 0 & 0 & \ddots & 0 & 0 & \cdots & 0 \\ 0 & 0 & \cdots & \lambda_r & 0 & \cdots & 0 \\ 0 & 0 & \cdots & 0 & 0 & \cdots & 0 \\ 0 & 0 & \cdots & 0 & 0 & \cdots & 0 \\ 0 & 0 & \cdots & 0 & 0 & \cdots & 0 \end{bmatrix} \quad (4.38)$$

Further,

$$\det(\mathbf{Q}\Lambda\mathbf{Q}^H) = \underbrace{\det(\mathbf{Q})}_{=1} \underbrace{\det(\Lambda)}_{=\prod_i \lambda_i} \underbrace{\det(\mathbf{Q}^H)}_{=1} \quad (4.39)$$

NOTE: $\det(\mathbf{Q})\det(\mathbf{Q}^H) = 1$. PROOF: We know that (a) $\det(\mathbf{A}^*) = (\det(\mathbf{A}))^*$, (b) $\det(\mathbf{AB}) = \det(\mathbf{A})\det(\mathbf{B})$ and (c) $\det(\mathbf{I}) = 1$. Thus defining $\det(\mathbf{Q}) = \lambda$ and using $\mathbf{QQ}^H = \mathbf{I}$

$$\begin{aligned} \det(\mathbf{Q})\det(\mathbf{Q}^H) &= \det(\mathbf{I}) \\ \lambda\lambda^* &= 1 \\ |\lambda|^2 &= 1 \end{aligned} \quad (4.40)$$

Thus, we can write:

$$\frac{C}{B} = \log_2 \left(\prod_{i=1}^r \left(1 + \lambda_i \frac{\gamma}{N_t} \right) \right) \quad (4.41)$$

since $\lambda_{r+1}, \lambda_{r+2}, \dots, \lambda_{M_r} = 0$. Thus, the matrix channel \mathbf{H} has r parallel channels where r is the rank of \mathbf{H} . The SNR per channel is $\frac{\gamma}{N_t} \lambda_i$.

For random channels, the ergodic capacity (in b/s) can be written as

$$C_{erg} = E_{\mathbf{H}} \left\{ B \log_2 \left(\prod_{i=1}^r \left(1 + \lambda_i \frac{\gamma}{N_t} \right) \right) \right\} \quad (4.42)$$

and the outage capacity can be defined similar to (4.19)

$$p = \Pr \left\{ B \log_2 \left(\prod_{i=1}^r \left(1 + \lambda_i \frac{\gamma}{N_t} \right) \right) < C_{out} \right\} \quad (4.43)$$

The improvement in capacity for rich scattering can be dramatic. Consider a 4×4 channel (i.e., 4 transmit and 4 receive antennas) where all channels are independent (this is the ideal case). The ergodic capacity is shown in Figure 4.9 for an AWGN channel, a one antenna channel with Rayleigh fading, MISO, SIMO and MIMO (all in independent Rayleigh fading). We can see that Rayleigh fading causes a loss in capacity relative to AWGN, although the losses are small at low SNR. Using four antennas at the transmitter pushes capacity nearly back to the AWGN capacity, while four at the receiver allows for a roughly 35% improvement as compared to AWGN. However, adding antennas to both links (assuming independent channels) results in dramatic improvements, with the improvements increasing for higher SNRs. For example, at SNR = 15dB, four antennas at the

receiver only allows for roughly 6.8b/s/Hz as compared to AWGN which allows for 5b/s/Hz. With four antennas at both ends of the link the capacity increases to 16.3b/s/Hz! Thus, while MISO and SIMO permit modest gains in ergodic capacity, true MIMO offers dramatic improvement.

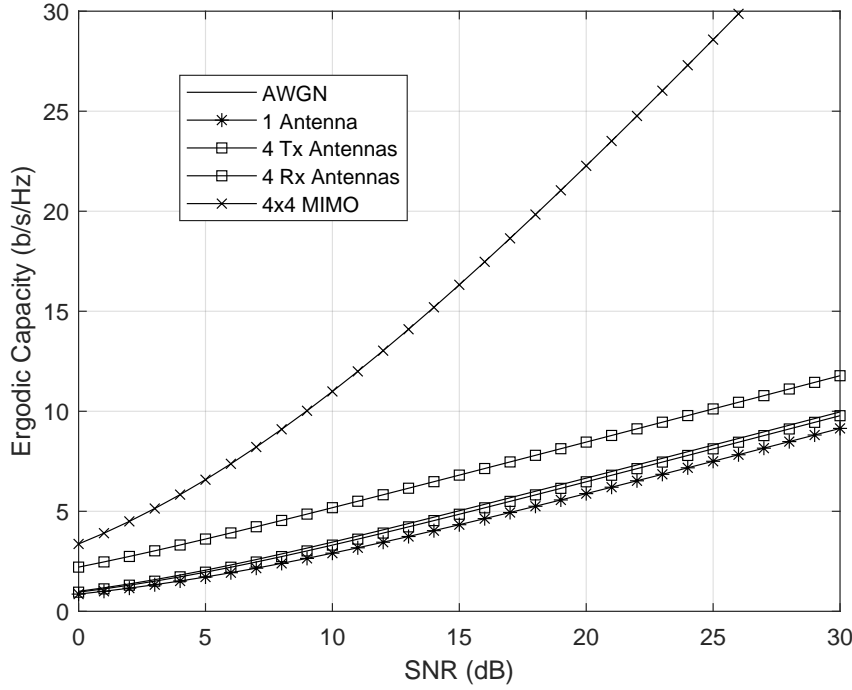


Figure 4.9: Ergodic Capacity (b/s/Hz) versus SNR in Rayleigh (independent) Fading Channel with Channel Information at the Receiver

The capacity improvement can be seen in terms of the outage capacity as well. The outage probability for the same five scenarios is plotted versus outage capacity for SNR=15dB in Figure 4.10. The 1% outage capacity increases from 0.4b/s/Hz to 2.9b/s/Hz or 4.8b/s/Hz for four transmit or four receive antennas respectively. But the 1% outage capacity increases to an amazing 12.6b/s/Hz with four transmit and four receive antennas. Similarly the 10% outage capacity goes from 2.1b/s/Hz to 14.2b/s/Hz when using MIMO as opposed to a single antenna on each end of the link.

4.7 Capacity with Channel Information at the Transmitter: Water-filling

If the channel is known, the transmit vectors \mathbf{x} are still Gaussian, but we choose

$$\Sigma_{\mathbf{x}} = \begin{bmatrix} P_1 & 0 & \cdots & 0 \\ 0 & P_2 & \cdots & 0 \\ 0 & 0 & \ddots & 0 \\ 0 & 0 & \cdots & P_{N_t} \end{bmatrix} \quad (4.44)$$

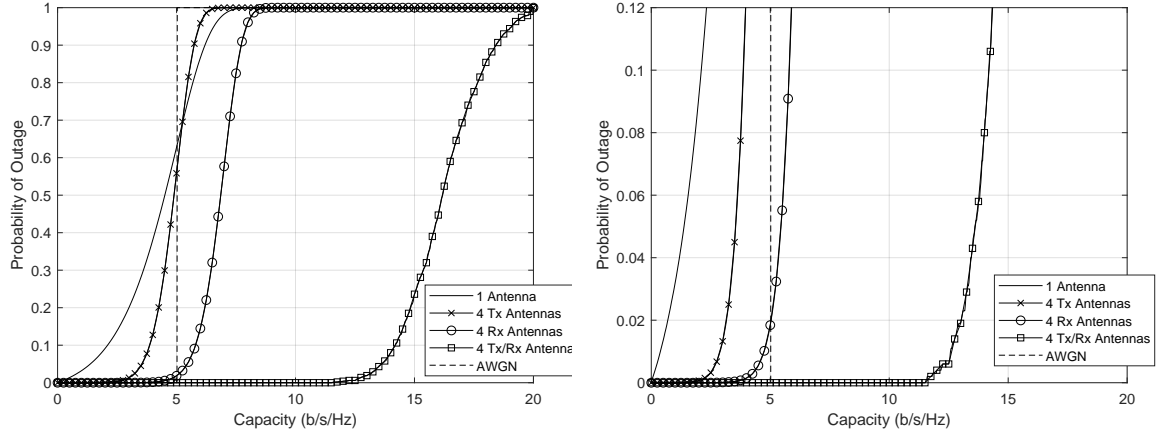


Figure 4.10: Outage Capacity (b/s/Hz) versus SNR in MIMO Rayleigh (independent) Fading Channel with Channel Information at the Receiver

where $P_i = \left(\mu - \frac{1}{\gamma\lambda_i}\right)^+$ and $(x)^+ = \max(x, 0)$. μ is the water-filling level such that $\sum_i P_i = P_t$. Note that for some weak eigenmodes, $P_i = 0$. If we define $\epsilon_i = \frac{P_i}{P_t}$ the resulting capacity is

$$\frac{C}{B} = \sum_{i=1}^r \log_2 (1 + \epsilon_i \gamma \lambda_i) \quad (4.45)$$

The ergodic capacity is

$$\left(\frac{C}{B}\right)_{erg} = E_{\mathbf{H}} \left\{ \sum_{i=1}^r \log_2 (1 + \epsilon_i \gamma \lambda_i) \right\} \quad (4.46)$$

4.7.1 Lagrangian Optimization

We can prove the above statement about the known channel using the method of Lagrange multipliers. Specifically, we wish to maximize $\frac{C}{B}$ over $\epsilon = \frac{P_i}{P_t}$ subject to the constraint that $\sum_i \epsilon_i = 1$ or $\sum_i P_i = P_t$. We can use the method of Lagrange multipliers:

$$F = \sum_{i=1}^r \log_2 (1 + \epsilon_i \gamma \lambda_i) + \eta \left(P_t - P_t \sum_i \epsilon_i \right) \quad (4.47)$$

where η is the Lagrangian multiplier. We can find the optimal ϵ_i by taking the derivative of F with respect to ϵ_i and setting them equal to zero:

$$\begin{aligned} 0 &= \frac{\partial}{\partial \epsilon_i} \{ \log_2 (1 + \epsilon_i \gamma \lambda_i) - \eta P_t \epsilon_i \} \\ &= \frac{1}{\ln(2)} \frac{1}{1 + \gamma \lambda_i \epsilon_i} \gamma \lambda_i - \eta P_t \\ &= \frac{\gamma \lambda_i}{1 + \gamma \lambda_i \epsilon_i} - \eta P_t \ln(2) \\ \epsilon_i &= \frac{1}{\eta \ln(2)} - \frac{1}{\gamma \lambda_i P_t} \\ &= \left[\mu - \frac{1}{\gamma \lambda_i} \right]^+ \end{aligned}$$

where we have set the water level $\mu = \frac{1}{\eta \ln(2) P_t}$ and enforced the condition that $\epsilon_i \geq 0$.

4.7.2 Iterative Algorithm

1. set $i = 1$
2. $\mu = \frac{1}{\nu} = \frac{1}{n-i+1} \left(1 + \sum_{k=1}^{n-i+1} \frac{1}{\gamma \lambda_k} \right)$
3. $p_k(i) = \mu - \frac{1}{\gamma \lambda_k}$ for $k = 1 \dots n-i+1$
4. If all $p_k > 0$ stop; else set $i = i + 1$ and $p_{n-i+1} = 0$ and go to 2.

In general, channel knowledge is only beneficial at low signal to noise ratios. This can be seen in the example shown in Figure 4.11. In the plot we show the capacity of a 4×4 link (independent channels) with and without channel knowledge at the transmitter. As a reference, we also plot the capacity of inverse filling (i.e., attempting to maintain equal SNR). As mentioned, the impact of waterfilling is negligible, with only slight gains at low SNR. Additionally, we see that attempting to maintain constant SNR (and capacity) causes a large reduction in capacity. Thus, we can conclude that equal power transmission is generally an acceptable sub-optimal approach, unless the channel exhibits strong correlation which we examine next.

4.8 Impact of Eigenvalue Distribution

Assume that $N_t = M_r$ and that

$$\sum_{i=1}^{M_r} \lambda_i = N_t M_r \quad (4.48)$$

Let's examine two extreme cases: Extreme #1: $\lambda_1 = N_t M_r$ and $\lambda_2 = \lambda_3 = \dots = \lambda_{M_r} = 0$.

$$\begin{aligned} C &= \log_2(1 + \gamma M_r N_t / N_t) \\ &= \log_2(1 + \gamma M_r) \end{aligned} \quad (4.49)$$

For high SNR

$$C \approx \log_2(\gamma) + \log_2(M_r) \quad (4.50)$$

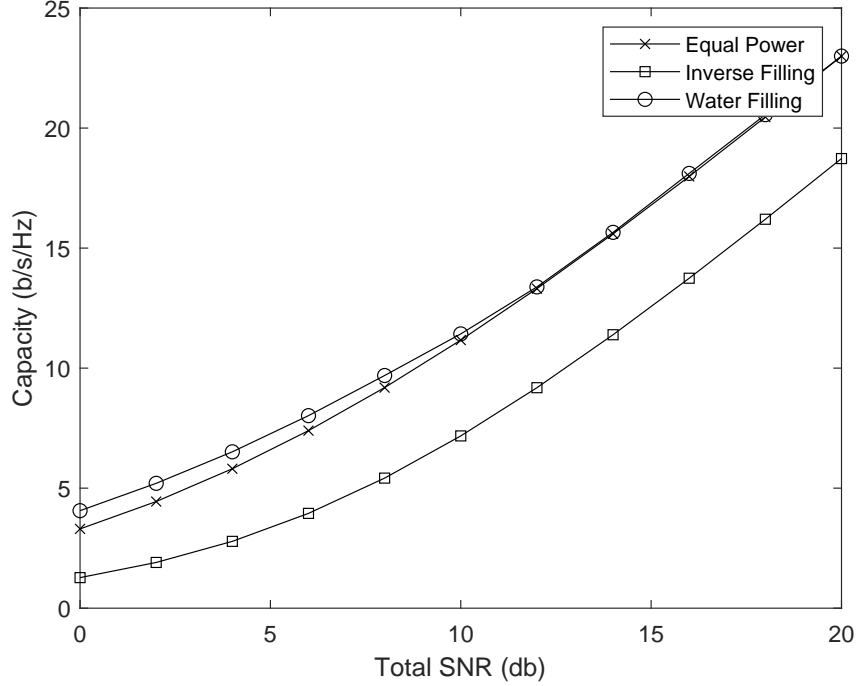


Figure 4.11: Ergodic Capacity (b/s/Hz) versus SNR in Rayleigh (independent) Fading Channel with Channel Information at the Receiver

Thus, we get an *additive effect*.

$$\text{Extreme \#2: } \lambda_1 = \lambda_2 = \lambda_3 = \dots \lambda_{M_r} = \frac{N_t M_r}{M_r} = N_t.$$

$$\begin{aligned} C &= \sum_{i=1}^{M_r} \log_2 \left(1 + \gamma \frac{N_t}{N_t} \right) \\ &= M_r \log_2(1 + \gamma) \end{aligned} \quad (4.51)$$

High SNR

$$C \approx M_r \log_2(\gamma) \quad (4.52)$$

Here we get a *multiplicative effect!*

As another example, consider a 4×4 system with independent Rayleigh fading as compared to a channel with 5° angle spread (and $\lambda/2$ element spacing) on one end of the link. The outage probability versus outage capacity is plotted in Figure 4.12 for the two cases with $\text{SNR} = 15\text{dB}$. The 10% outage capacity drops from 14.2b/s/Hz in independent channels to 5.9b/s/Hz with strong correlation on one end of the link. This again highlights the need for rich scattering to realize the gains promised by MIMO.

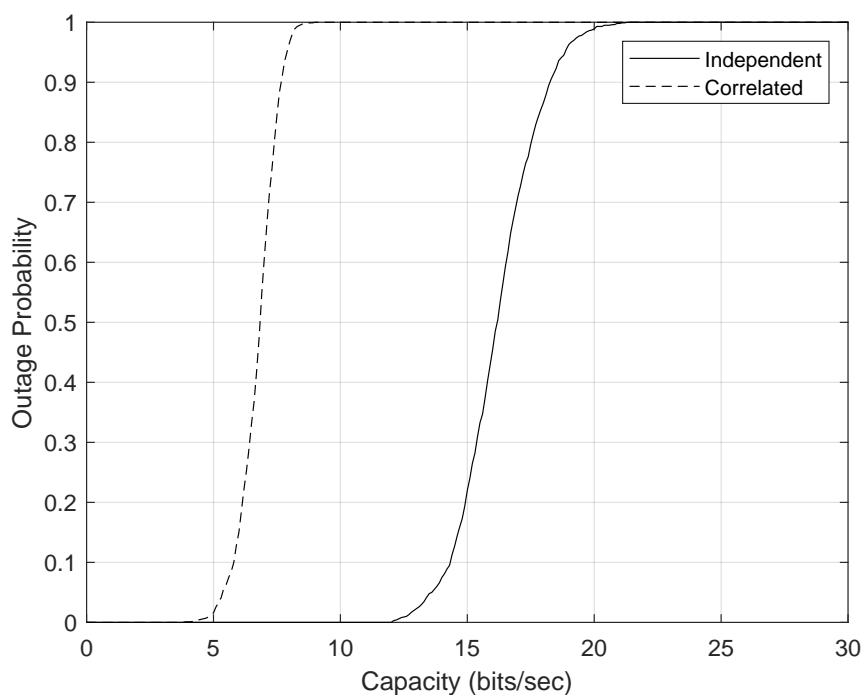


Figure 4.12: Outage Probability versus Capacity (b/s/Hz) SNR in Rayleigh Fading Channel with Channel Information at the Receiver

Chapter 5

Beamforming

The first application of multiple antennas that we will consider is known as beamforming. In the development of beamforming we will assume that the channel is free of multipath at the array. That is, we will make what is known as the plane wave assumption. Note that there are forms of “beamforming” that do not require this assumption, but classical beamforming does. By classical beamforming we simply mean that there exists a meaningful array pattern (“beampattern”) that describes the gain of the array response to signals arriving at various angles (or equivalently the transmit array gain in a particular direction). The primary benefit of beamforming is an SNR gain, sometimes termed “beamforming gain” or equivalently the “array gain”. However, beamforming can also be formulated to mitigate interference as we will see.

5.1 Concept

Consider a linear array at the receiver as shown in Figure 5.1. Let the received signals on each antenna be combined using weights w_i . The received signal in complex baseband after combining can be written as

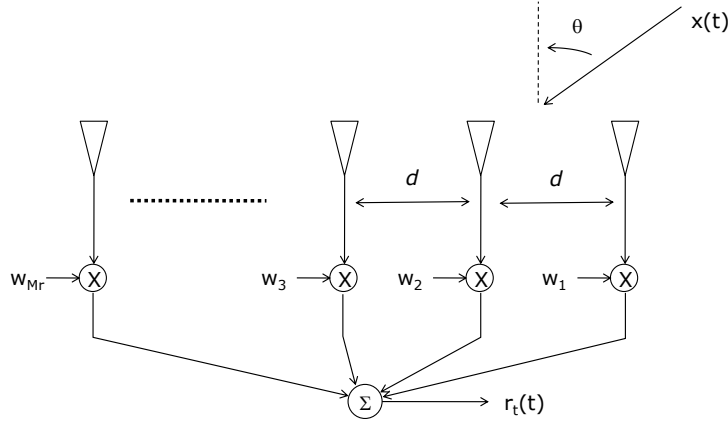
$$r_t(t) = \sum_{i=1}^{M_r} w_i x(t) e^{-j \frac{2\pi d(i-1)}{\lambda} \sin(\theta)} \quad (5.1)$$

where we have ignored noise for the moment, i.e., $r(t) = x(t)$. If we let $w_i = 1$, the received signal becomes:

$$\begin{aligned} r_t(t) &= \sum_{i=1}^{M_r} x(t) e^{-j \frac{2\pi d(i-1)}{\lambda} \sin(\theta)} \\ &= x(t) G(\theta) \end{aligned}$$

where $G(\theta)$ is the beam-pattern as a function of the angle-of-arrival θ :

$$G(\theta) = \sum_{i=1}^{M_r} e^{-j \frac{2\pi d(i-1)}{\lambda} \sin(\theta)} \quad (5.2)$$



5

Figure 5.1: Wavefront impinging on M_r receive antennas in a beamforming array

To get a better understanding of the beampattern created by this array, let's define a new variable $\psi = \frac{2\pi d}{\lambda} \sin(\theta)$ we can write the pattern as a function of ψ :

$$f(\psi) = 1 + e^{-j\psi} + e^{-j2\psi} \dots + e^{-j(M_r-1)\psi} \quad (5.3)$$

To simplify this expression, first define a second relation by multiplying $f(\psi)$ by $e^{-j\psi}$:

$$f(\psi)e^{-j\psi} = e^{-j\psi} + e^{-j2\psi} \dots + e^{-j(M_r)\psi}$$

Now, subtracting the last equation from the previous we obtain:

$$\begin{aligned} f(\psi)(1 - e^{-j\psi}) &= (1 - e^{-jM_r\psi}) \\ f(\psi) &= \frac{1 - e^{-jM_r\psi}}{1 - e^{-j\psi}} \\ &= \frac{e^{-jM_r/2\psi} e^{jM_r/2\psi} - e^{-jM_r/2\psi}}{e^{-j\psi/2} e^{j\psi/2} - e^{-j\psi/2}} \\ &= e^{-j(M_r-1)/2\psi} \frac{\sin(M_r\psi/2)}{\sin(\psi/2)} \end{aligned} \quad (5.4)$$

By making this substitution we have removed the antenna spacing (d/λ) from the pattern expression, which allows us to focus on the impact of the number of elements M_r . From equation (5.4) we can see that (ignoring the leading phase term) with M_r antennas there are $M_r - 1$ lobes in the function $f(\psi)$ over the range of $-\pi \leq \psi \leq \pi$. Since $\psi = \frac{2\pi d}{\lambda} \sin(\theta)$, the number of lobes in the pattern as $-\pi \leq \theta \leq \pi$ depends on the value of $\frac{d}{\lambda}$. For example, if $\frac{d}{\lambda} = \frac{1}{2}$ there are $M_r - 1$ lobes in $G(\theta)$, $M_r - 2$ sidelobes and one main lobe. More specifically, the value of $\frac{d}{\lambda}$ dictates the range of the generic pattern $f(\psi)$ that appears in the array pattern $G(\theta)$, which we explore in a moment.

Example patterns for two, four, six and eight elements are shown in Figure 5.2. We can clearly see that for M_r elements, there are $M_r - 1$ lobes. The width of the sidelobes in ψ is $\frac{2\pi}{M_r}$ and the width of the main beam is $\frac{4\pi}{M_r}$. As expected,

$$(M_r - 2) \frac{2\pi}{M_r} + \frac{4\pi}{M_r} = 2\pi \quad (5.5)$$

Now, since 2π in ψ is mapped to $\frac{2\pi d}{\lambda} \sin(\theta)$, $-\frac{\pi}{2} \leq \theta \leq \frac{\pi}{2}$, the beamwidth will also decrease with M_r and central AOA. If $\frac{d}{\lambda} = \frac{1}{2}$, the beamwidth in θ is $\frac{2\pi}{M_r}$ when the AOA is 0 degrees.

We now consider some important implications of this relationship. First, we can see from (5.4) that $f(\psi)$ repeats when ψ is a multiple of 2π . In other words, the pattern has a periodicity of 2π . Since $\psi = \frac{2\pi d}{\lambda} \sin(\theta)$, for the range of arrival angles $-\pi \leq \theta \leq \pi$ we have $-\frac{2\pi d}{\lambda} \leq \psi \leq \frac{2\pi d}{\lambda}$. Thus, the value of $\frac{d}{\lambda}$ will dictate the amount of the pattern $f(\psi)$ seen by the array. For example consider the following scenarios for $-\frac{\pi}{2} \leq \theta \leq \frac{\pi}{2}$:

- * If $\frac{d}{\lambda} = \frac{1}{4}$, then $-\frac{\pi}{2} \leq \psi \leq \frac{\pi}{2}$
- * If $\frac{d}{\lambda} = \frac{1}{2}$, then $-\pi \leq \psi \leq \pi$
- * If $\frac{d}{\lambda} = \frac{3}{4}$, then $-\frac{3\pi}{2} \leq \psi \leq \frac{3\pi}{2}$.
- * If $\frac{d}{\lambda} = 1$, then $-2\pi \leq \psi \leq 2\pi$.

The gain patterns $g(\theta)$ for these four cases are plotted in Figure 5.3 for $M_r = 8$. In the first case, a spacing of one quarter of a wavelength results in a gain pattern that corresponds to a fraction of the overall pattern $f(\psi)$. This means that the main beamwidth is wider than it could be based on the number of antenna elements. On the other hand, a spacing of one-half a wavelength allows the gain pattern to correspond to the entire pattern $f(\psi)$ and provides a main beamwidth commensurate with the number of antenna elements (i.e., 45°). Third, using a spacing of three-quarters of a wavelength causes the pattern repeat, although the beamwidth continues to narrow. Finally, using a spacing of λ causes sufficient repetition that what are known as “grating lobes” appear, since ψ spans more than 2π .

Finally, it should be noted that θ and $\pi - \theta$ give the same value of ψ . This results from the fact that for a linear array, there is an ambiguity between signals arriving from the angle θ and the angle $\pi - \theta$. This means that the array cannot distinguish whether a signal is arriving from the angle θ or $\pi - \theta$ and the gain pattern repeats on both sides of the array.

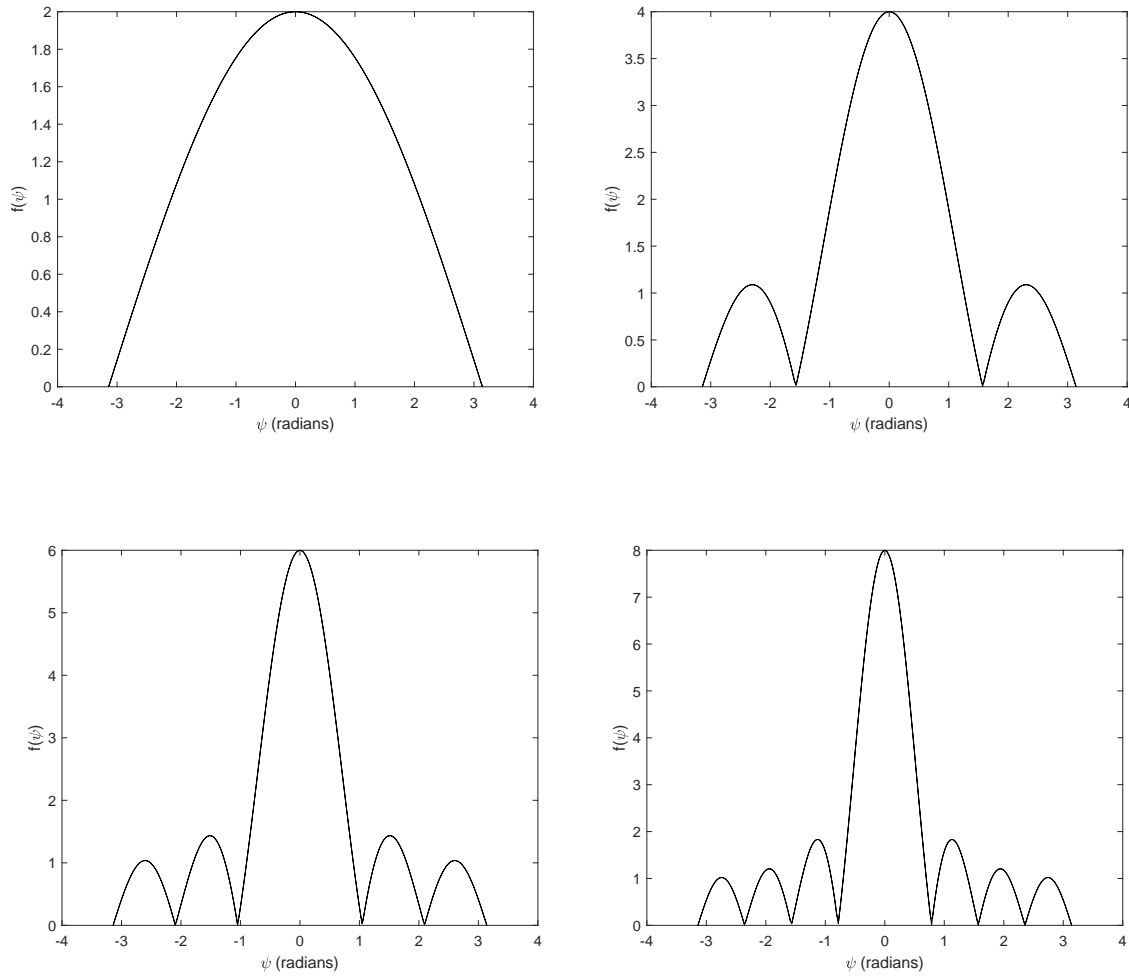


Figure 5.2: The Universal Pattern $f(\psi)$ for Two, Four, Six and Eight Antenna Elements

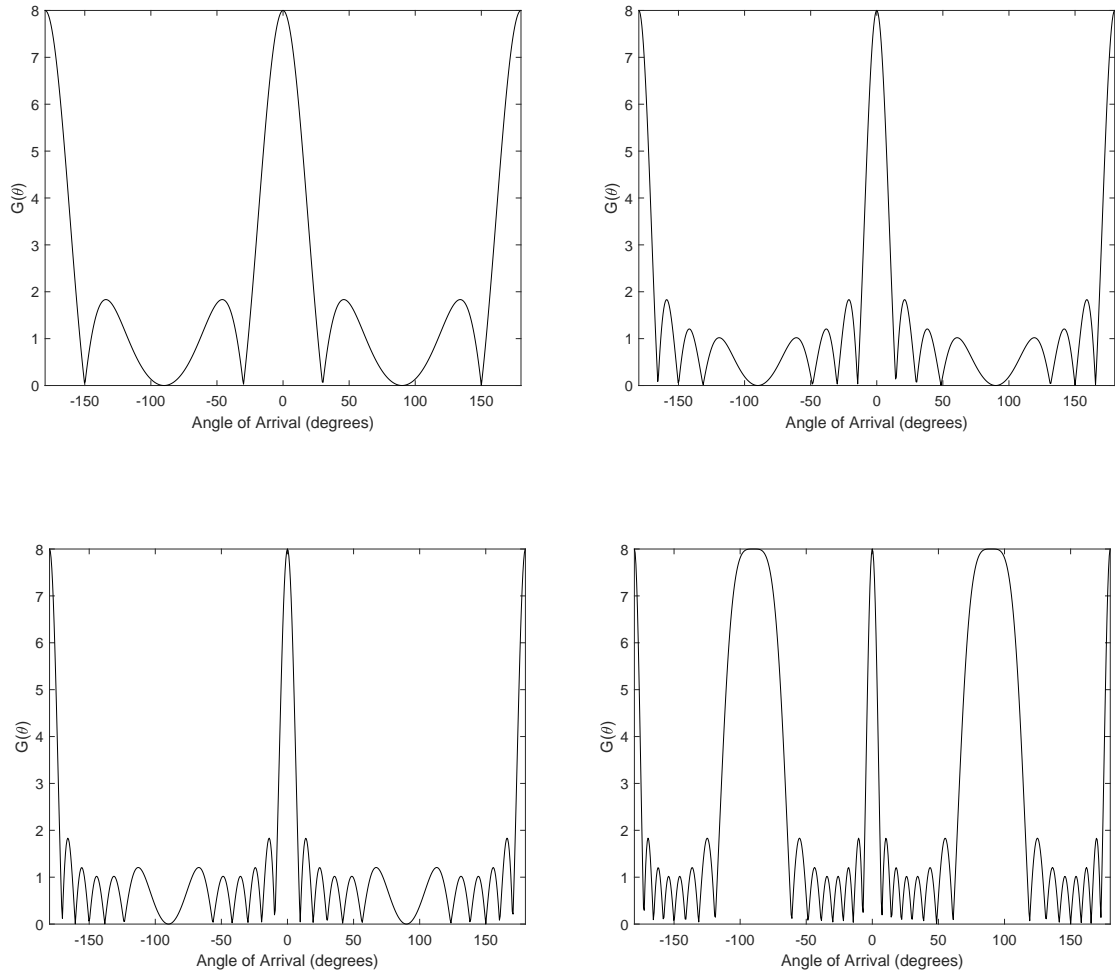


Figure 5.3: The Gain Pattern $g(\theta)$ for Eight Antenna Elements with $\frac{d}{\lambda} = \frac{1}{4}, \frac{d}{\lambda} = \frac{1}{2}, \frac{d}{\lambda} = \frac{3}{4}$, and $\frac{d}{\lambda} = 1$

5.2 Beam-steering

In the previous discussion, we assumed that the weights were all ones. This is helpful if the signal is arriving from boresight (broad-side or $\theta = 0$). If we wish to maximize the array gain in a direction θ_o other than 0° , we must consider the the channel resulting from that particular angle. To see this, the received signal can be written (ignoring any Rayleigh fading and assuming that the channel is constant across antennas except for a phase shift - i.e., the plane wave assumption) as

$$\mathbf{r}(t) = \mathbf{a}(\theta_o)x(t) + \mathbf{n}(t) \quad (5.6)$$

where we shall define $\mathbf{a}(\theta_o) = \begin{bmatrix} 1 \\ e^{-j\psi_o} \\ e^{-j2\psi_o} \\ e^{-j3\psi_o} \\ \vdots \\ e^{-j(M_r-1)\psi_o} \end{bmatrix}$ as the array factor (or array manifold vector) for our uniform linear array, $\psi_o = \frac{2\pi d}{\lambda} \sin(\theta_o)$ and θ_o is the angle of arrival. After combining we have (ignoring noise)

$$\begin{aligned} r_t(t) &= \sum_{i=1}^{M_r} w_i^* a_i(\theta_o) x(t) \\ &= \underbrace{\mathbf{w}^H \mathbf{a}(\theta_o)}_{=\eta} x(t) \end{aligned} \quad (5.7)$$

The array factor is equivalent to the channel experienced by the signal across the array. Note that the gain η is maximized when $\mathbf{w} = \mathbf{a}(\theta_o)$. In this case

$$r_t(t) = M_r x(t) \quad (5.8)$$

where M_r is our *array gain* and is the gain in SNR we will observe (as we will shown in Section 5.5.1).

5.2.1 Beam pattern

For an array tuned to θ_o , we can write the expression for the gain as function of θ , i.e., the beampattern as

$$G(\theta) = \mathbf{w}^H(\theta_o) \mathbf{a}(\theta) \quad (5.9)$$

By choosing the appropriate weight vector we can steer (tune) the beam to any direction θ_o . This is often termed the “steering vector”. For example, but choosing

$$\mathbf{w} = \mathbf{a}(\theta) \quad (5.10)$$

for different values of θ , we can move the gain of the array to different locations. This can be seen in the three examples of Figure 5.4 with $\theta = 0, \frac{\pi}{4}, \frac{\pi}{2}$. We can see that changing the value of θ steers the gain to the location of θ . Additionally, steering the gain away from 0 towards $\frac{\pi}{2}$ (i.e., from broadside to endfire) broadens the beam.

5.2.2 Ambiguity with a linear array

Note that we hinted at earlier,

$$\begin{aligned}
 \mathbf{a}(\pi - \theta_o) &= \begin{bmatrix} 1 \\ e^{-j\frac{2\pi d}{\lambda} \sin(\pi - \theta_o)} \\ e^{-j\frac{4\pi d}{\lambda} \sin(\pi - \theta_o)} \\ e^{-j\frac{6\pi d}{\lambda} \sin(\pi - \theta_o)} \\ \vdots \\ e^{-j\frac{2(M_r-1)\pi d}{\lambda} \sin(\pi - \theta_o)} \end{bmatrix} \\
 &= \begin{bmatrix} 1 \\ e^{-j\frac{2\pi d}{\lambda} \sin(\theta_o)} \\ e^{-j\frac{4\pi d}{\lambda} \sin(\theta_o)} \\ e^{-j\frac{6\pi d}{\lambda} \sin(\theta_o)} \\ \vdots \\ e^{-j\frac{2(M_r-1)\pi d}{\lambda} \sin(\theta_o)} \end{bmatrix} \tag{5.11}
 \end{aligned}$$

where we have used the fact that $\sin(\pi - \theta_o) = \cos(\pi) \sin(-\theta_o) + \cos(\theta_o) \sin(\pi) = \sin(\theta_o)$. Thus, the array cannot differentiate between a signal arriving from θ_o and $\pi - \theta_o$. Thus, the gain pattern repeats as seen in Figure 5.4. Finally, it should be noted that this array is often termed a *phased array* since the array weights are simple phase shifts.

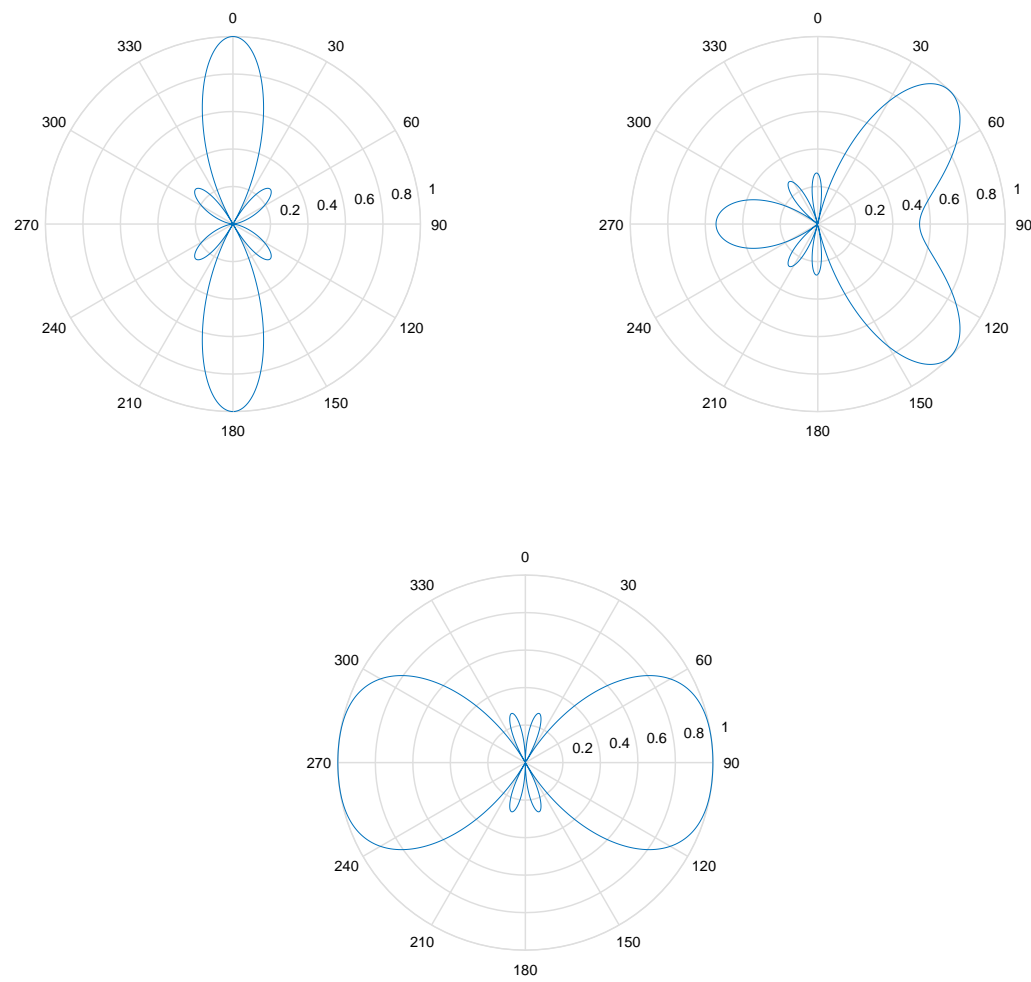


Figure 5.4: The Gain Pattern $g(\theta)$ for Four Antenna Elements with $\frac{d}{\lambda} = \frac{1}{2}$ and steering angles $\theta = 0$ (top, left), $\theta = \frac{\pi}{4}$ (top, right), and $\theta = \frac{\pi}{2}$ (bottom)

5.3 Directivity

Directivity is a measure of an antenna's ability to direct energy in a desired direction relative to a point source. It is defined as

$$D = \frac{4\pi}{\Omega_A} \quad (5.12)$$

where Ω_A is the solid beam angle defined as

$$\Omega_A = \iint_{\text{antenna pattern}} \underbrace{|g_a(\theta, \phi)|^2}_{\text{normalized array factor}} \underbrace{\left| \hat{f}(\theta) \right|^2}_{\cos(\theta)} \underbrace{d\Omega}_{\cos(\theta)d\theta d\phi} \quad (5.13)$$

Assumes that the antenna elements are point sources which is an OK assumption if the element pattern is much more broad than the array factor ($g_A(\theta, \phi) = 1$). Further, we know that

$$\begin{aligned} \left| \hat{f}(\psi) \right|^2 &= \left| \frac{\sin(M_r \psi / 2)}{M_r \sin(\psi / 2)} \right|^2 \\ &= \frac{1}{M_r} + \frac{2}{M_r^2} \sum_{i=1}^{M_r} (M_r - i) \cos(i\psi) \end{aligned}$$

Let the pointing angle of the array weights be θ_o . Then

$$\psi = \frac{2\pi d}{\lambda} \sin(\theta) + \psi_o \quad (5.14)$$

where $\psi_o = \frac{2\pi d}{\lambda} \sin(\theta_o)$. Now $\cos(\theta) d\theta = \frac{\lambda}{2\pi d} d\psi$. Thus,

$$\begin{aligned} \Omega_A &= \int_0^{2\pi} d\phi \int_{-\pi/2}^{\pi/2} |f(\theta)|^2 \cos(\theta) d\theta \\ &= 2\pi \int_{-\frac{2\pi d}{\lambda} + \psi_o}^{\frac{2\pi d}{\lambda} + \psi_o} |f(\psi)|^2 \left(\frac{\lambda}{2\pi d} \right) d\psi \\ &= \frac{\lambda}{d} \int_{-\frac{2\pi d}{\lambda} + \psi_o}^{\frac{2\pi d}{\lambda} + \psi_o} |f(\psi)|^2 d\psi \\ &= \frac{\lambda}{d} \left[\frac{1}{M_r} \int_{-\frac{2\pi d}{\lambda} + \psi_o}^{\frac{2\pi d}{\lambda} + \psi_o} d\psi + \frac{2}{M_r^2} \sum_{i=1}^{M_r-1} (M_r - i) \int_{-\frac{2\pi d}{\lambda} + \psi_o}^{\frac{2\pi d}{\lambda} + \psi_o} \cos(i\psi) d\psi \right] \\ &= \frac{\lambda}{d} \left[\frac{\psi}{M_r} \Big|_{-\frac{2\pi d}{\lambda} + \psi_o}^{\frac{2\pi d}{\lambda} + \psi_o} + \frac{2}{M_r^2} \sum_{i=1}^{M_r-1} (M_r - i) \frac{\sin(i\psi)}{i} \Big|_{-\frac{2\pi d}{\lambda} + \psi_o}^{\frac{2\pi d}{\lambda} + \psi_o} \right] \\ &= \frac{4\pi}{M_r} + \frac{4\pi}{M_r^2} \sum_{i=1}^{M_r-1} \frac{M_r - i}{i 2\pi d / \lambda} 2 \cos(i\psi_o) \sin\left(\frac{2\pi di}{\lambda}\right) \end{aligned} \quad (5.15)$$

And thus we have the directivity is equal to

$$D = \frac{1}{\frac{1}{M_r} + \frac{1}{M_r^2} \sum_{i=1}^{M_r-1} \frac{M_r - i}{i 2\pi d / \lambda} 2 \cos(i\psi_o) \sin\left(\frac{2\pi di}{\lambda}\right)} \quad (5.16)$$

Note that if $d = \frac{\lambda}{2}$ then $D = M_r$ irrespective of θ_o . This is because $\sin\left(\frac{2\pi di}{\lambda}\right) = \sin(i\pi) = 0$

5.4 Circular Array

For a any array we can define the received signal as $\mathbf{r}(t) = \mathbf{a}(\theta)r(t)$ where $\mathbf{a}(\theta)$ is the array factor (also called the array manifold vector). For a linear array we have

$$\mathbf{a}(\theta) = \begin{bmatrix} 1 \\ e^{-j\frac{2\pi d}{\lambda}\sin(\theta)} \\ e^{-j2\frac{2\pi d}{\lambda}\sin(\theta)} \\ e^{-j3\frac{2\pi d}{\lambda}\sin(\theta)} \\ \vdots \\ e^{-j(M_r-1)\frac{2\pi d}{\lambda}\sin(\theta)} \end{bmatrix} \quad (5.17)$$

where the first element is the phase reference. For a uniformly space circular array, we define the phase reference (phase center) to be the center of the array. Further, let R be the radius of the array. The new array factor is then:

$$\mathbf{a}(\theta) = \begin{bmatrix} e^{-j\frac{2\pi R}{\lambda}\sin(\theta-\zeta_1)} \\ e^{-j\frac{2\pi R}{\lambda}\sin(\theta-\zeta_2)} \\ e^{-j\frac{2\pi R}{\lambda}\sin(\theta-\zeta_3)} \\ e^{-j\frac{2\pi R}{\lambda}\sin(\theta-\zeta_4)} \\ \vdots \\ e^{-j\frac{2\pi R}{\lambda}\sin(\theta-\zeta_{M_r})} \end{bmatrix} \quad (5.18)$$

where $\zeta_i = \left(\frac{i-1}{M_r}\right)2\pi$ is the location (in angle) of the i th antenna element on the array. As with a linear array, we can maximize the gain when we set $\mathbf{w} = \mathbf{a}^*(\theta_o)$ in which case the gain is M_r .

As an example, consider an eight element circular array with $R = \frac{\lambda}{2}$. The beampatterns for this array when the steering angle is $\theta = 0$ and $\theta = \frac{\pi}{4}$ are shown in Figure 5.5. We can see that the pattern does not repeat on the backside of the array, and thus there is no ambiguity for angles greater than $\pi/2$ or less than $-\pi/2$. Further, we see that in this example the beampattern doesn't fundamentally change, but simply rotates.

5.5 Optimal Beamforming

In the previous section we examined the antenna weights that steered a beam in a particular direction. This can also be thought of as maximizing the gain in a particular direction. We will also show in this section that these are the weights which maximize the SNR of the signal post-combining, when the signal is arriving from the direction of the maximum pattern gain. In other words, setting $\mathbf{w} = \mathbf{a}$ maximizes SNR. However, what if there are other signals in the environment? Does maximizing SNR still provide the best results? It is unlikely that maximizing SNR will be the best option. Thus, we can also set the weights to eliminate the interference (known as “zero-forcing”), maximize SINR or minimize the mean square error between a desired signal and the output of the array. We will examine each of these different optimality criteria in the following subsections.

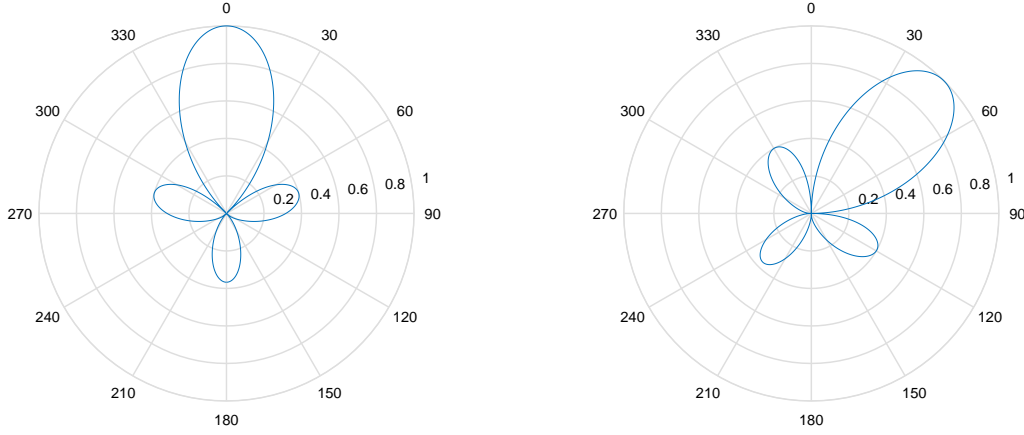


Figure 5.5: The Gain Pattern $g(\theta)$ for an Eight Element Circular Array with $\frac{R}{\lambda} = \frac{1}{2}$ and steering angles $\theta = 0$ (left) and $\theta = \frac{\pi}{4}$ (right)

5.5.1 Maximum SNR

Consider the received signal vector in complex baseband

$$\tilde{\mathbf{r}}(t) = \mathbf{a}x(t) + \mathbf{n}(t) \quad (5.19)$$

where $\mathbf{a} = \mathbf{a}(\theta)$ (we have dropped the function of θ for notational simplicity), $\mathbf{n}(t)$ is a Gaussian random process with $E\{\mathbf{n}(t)\} = \bar{\mathbf{0}}$ and $E\{\mathbf{n}(t)\mathbf{n}^H(t)\} = \sigma_n^2 \mathbf{I}^{M_r \times M_r}$. Assume that the desired signal is assumed to be a modulated pulse stream: $x(t) = \sum_{i=-\infty}^{\infty} s_i p(t - iT)$. After pulse matched filtering and sampling, we have for an arbitrary symbol the vector

$$\tilde{\mathbf{r}} = \mathbf{a}s + \mathbf{n} \quad (5.20)$$

where $E\{|s|^2\} = E_s$ (the energy per symbol). At the output of a combiner using weights \mathbf{w} we have the decision variable

$$z = \mathbf{w}^H \tilde{\mathbf{r}} \quad (5.21)$$

The question is, how do we choose \mathbf{a} to maximize the SNR of z ? First, we write z in terms of the desired and undesired components (z_s and z_n respectively):

$$\begin{aligned} z &= \mathbf{w}^H \tilde{\mathbf{r}} \\ &= z_s + z_n \\ &= \mathbf{w}^H \mathbf{a} s + \mathbf{w}^H \mathbf{n} \end{aligned}$$

Now the signal to noise ratio can be written as

$$\begin{aligned}\gamma &= \frac{\mathbb{E} \{ |z_s|^2 \}}{\mathbb{E} \{ |z_n|^2 \}} \\ &= \frac{\mathbb{E} \{ |\mathbf{w}^H \mathbf{a} s|^2 \}}{\mathbb{E} \{ |\mathbf{w}^H \mathbf{n}|^2 \}} \\ &= \frac{\mathbf{w}^H \mathbf{a} \mathbf{a}^H \mathbf{w} E_s}{\mathbf{w}^H \mathbf{R}_{nn} \mathbf{w}}\end{aligned}$$

Since $\mathbf{R}_{nn} = \sigma_n^2 \mathbf{I}$ we have

$$\gamma = \underbrace{\frac{\mathbf{w}^H \mathbf{R}_{aa} \mathbf{w}}{\mathbf{w}^H \mathbf{w}}}_{\text{Rayleigh Quotient}} \frac{E_s}{\sigma_n^2}$$

Note that $\mathbf{R}_{aa} = \mathbf{a} \mathbf{a}^H$ is Hermitian and positive semidefinite. Thus, γ is the well-known Rayleigh quotient which is maximized when \mathbf{w} is the maximum eigenvector of \mathbf{R}_{aa} . Since \mathbf{R}_{aa} is just the outer product of \mathbf{a} , there is only one eigenvector that has a non-zero eigenvalue, which is \mathbf{a} . Thus, $\mathbf{w}_{opt} = \mathbf{a}$ and the maximum SNR is

$$\begin{aligned}\gamma_{opt} &= \frac{E_s |\mathbf{a}^H \mathbf{a}|^2}{\sigma_n^2 |\mathbf{a}^H \mathbf{a}|} \\ &= \mathbf{a}^H \mathbf{a} \frac{E_s}{\sigma_n^2} \\ &= M_r \frac{E_s}{\sigma_n^2}\end{aligned}$$

and M_r is the beamforming gain, meaning that there is an M_r -fold improvement in SNR in the optimal case. Note that this is the same analysis that we would apply to a diversity array. Thus **optimal SNR weights are the same as Maximal Ratio Combining** as we will show in the next chapter.

5.5.2 Zero-Forcing

Consider the received signal on $M_r = 4$ antennas where there are $N_I = 3$ interferers. Let's assume that the signals are all synchronous in time and ignore the fading channel and noise. Let the array factor (response) to the desired signal be \mathbf{a}_0 and the array response to the interfering signals be \mathbf{a}_k for $k = 1, 2, 3$. The vector of received signals (after matched filtering) can be written as

$$\begin{aligned}r_1 &= a_{0,1}s + a_{1,1}i_1 + a_{2,1}i_2 + a_{3,1}i_3 \\ r_2 &= a_{0,2}s + a_{1,2}i_1 + a_{2,2}i_2 + a_{3,2}i_3 \\ r_3 &= a_{0,3}s + a_{1,3}i_1 + a_{2,3}i_2 + a_{3,3}i_3 \\ r_4 &= a_{0,4}s + a_{1,4}i_1 + a_{2,4}i_2 + a_{3,4}i_3\end{aligned} \tag{5.22}$$

or in vector form

$$\mathbf{r} = \mathbf{As} \tag{5.23}$$

where $\mathbf{A} = [\mathbf{a}_0, \mathbf{a}_1, \mathbf{a}_2, \mathbf{a}_3]$ and $\mathbf{s} = [s, i_1, i_2, i_3]^T$. We wish to create weights \mathbf{w} such that $\mathbf{w}^T \tilde{\mathbf{r}} = \kappa s$ for arbitrary constant κ . In other words, for four antennas we desire

$$\begin{aligned} w_1 a_{0,1} + w_2 a_{0,2} + w_3 a_{0,3} + w_4 a_{0,4} &= \kappa \\ w_1 a_{1,1} + w_2 a_{1,2} + w_3 a_{1,3} + w_4 a_{1,4} &= 0 \\ w_1 a_{2,1} + w_2 a_{2,2} + w_3 a_{2,3} + w_4 a_{2,4} &= 0 \\ w_1 a_{3,1} + w_2 a_{3,2} + w_3 a_{3,3} + w_4 a_{3,4} &= 0 \end{aligned} \tag{5.24}$$

or in vector form we desire

$$\mathbf{A}^T \mathbf{w} = \kappa \bar{\delta} \tag{5.25}$$

where $\bar{\delta} = [1, 0, 0, 0]^T$. Thus, we need to set

$$\mathbf{w} = (\mathbf{A}^T)^{-1} \kappa \bar{\delta} \tag{5.26}$$

This solution is termed the “zero-forcing” solution since it forces the interference to zero. Note that the zero-forcing weights are the first column of $(\mathbf{A}^T)^{-1}$. In this case (3 interferers and 1 desired user with 4 antennas), $\text{rank}(\mathbf{A}) = N_I + 1 = M_r$. However, if $\text{rank}(\mathbf{A}) < M_r$ (i.e., $N_I < M_r - 1$) we have

$$\mathbf{w} = \mathbf{A}(\mathbf{A}^T \mathbf{A})^{-1} \kappa \bar{\delta} = (\mathbf{A}^T)^\dagger \kappa \bar{\delta} \tag{5.27}$$

while if $N_I \geq M_r$ we have

$$\mathbf{w} = \mathbf{A}^\dagger \kappa \bar{\delta} \tag{5.28}$$

Note that this does not eliminate all interferers, but instead is the least squares (LS) solution. Note that although this weight vector eliminates interference, it does not necessarily maximize SNR. In fact, it is very likely that the SNR will be decidedly sub-optimal. From a beampattern perspective, we find that forcing nulls in the directions of all interferers means that a peak gain cannot be guaranteed in the direction of the desired signal, thus resulting in a loss in SNR relative to the optimal SNR case. This can be seen in the examples plotted in Figure 5.6. The first plot shows the beampattern with a four antenna element linear array (half wavelength spacing) and maximum SNR weights. The desired signal is coming from $\theta = \frac{\pi}{4}$. Clearly, the peak gain is in the direction of the desired user. The second plot shows the beampattern formed using zero-forcing weights when the desired signal is coming from $\theta = \frac{\pi}{4}$ and a single interferer is coming from $\theta = \frac{\pi}{2}$. We can see that a null is now placed in the direction of the interferer, but the gain in the direction of the desired user is no longer maximum. As a result, the SNR will suffer. IN the third plot, we add an interferer at $\theta = -\frac{\pi}{4}$ causing a second null and reducing the gain in the direction of the desired signal slightly more. In general, we can use the degrees of freedom in the array weights to either eliminate interference or maximize SNR, but not both.

5.5.3 Max SINR

In the previous two sections we examined the weights which maximized either the SNR or the SIR. However, in the presence of both noise and interference, neither choice may be ideal. Thus, we wish to determine weights which maximize SINR. Consider the following received signal (again

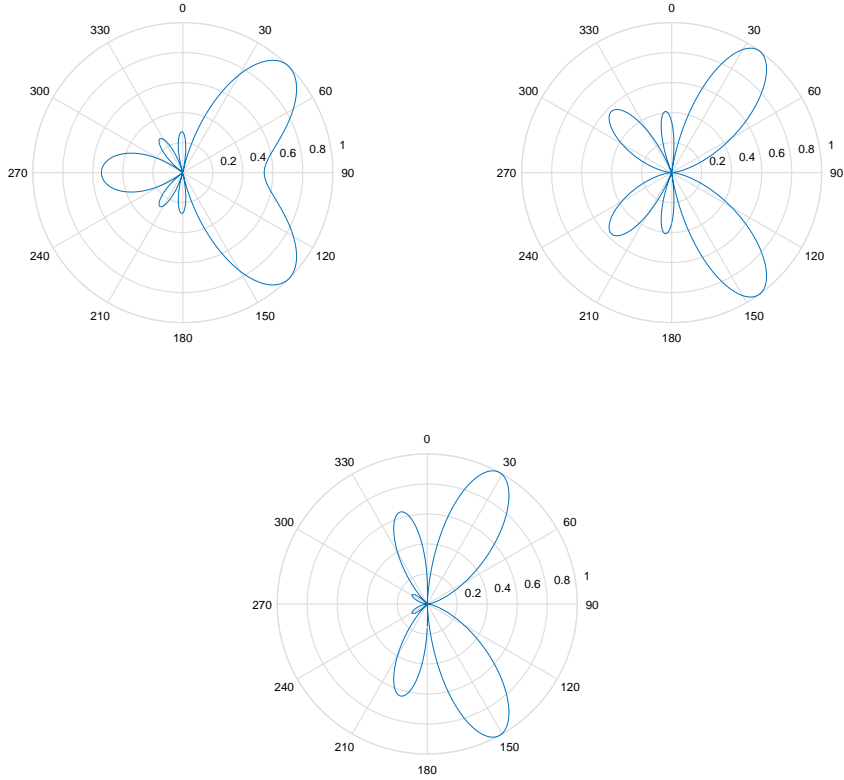


Figure 5.6: The Gain Pattern $g(\theta)$ for Four Antenna Elements with $\frac{d}{\lambda} = \frac{1}{2}$ using Maximum SNR Weights with desired signal at $\theta = \frac{\pi}{4}$ (top, left), Zero-Forcing Weights with One Interferer at $\theta = \frac{\pi}{2}$ (top, right) and Zero-Forcing Weights with Two Interferers at $\theta = \frac{\pi}{2}$ and $\theta = -\frac{\pi}{4}$ (bottom)

in complex baseband) on a set of M_r antennas

$$\mathbf{r}(t) = \mathbf{a}_0 x(t) + \sum_{k=1}^{N_I} \mathbf{a}_k i_k(t) + \mathbf{n}(t) \quad (5.29)$$

After matched filtering we obtain a vector $\tilde{\mathbf{r}}$ which is combined using a weight vector \mathbf{w} to obtain a decision variable z :

$$\begin{aligned} z &= \mathbf{w}^H \mathbf{r} \\ &= \underbrace{\mathbf{w}^H \mathbf{a}_0 s}_{z_s} + \underbrace{\mathbf{w}^H \left(\sum_{k=1}^{N_I} \mathbf{a}_k i_k + \mathbf{n} \right)}_{z_n} \end{aligned} \quad (5.30)$$

The SINR can be shown to be

$$\begin{aligned}\gamma &= \frac{\mathbb{E}\{|z_s|^2\}}{\mathbb{E}\{|z_n|^2\}} \\ &= \frac{\mathbb{E}\{|\mathbf{w}^H \mathbf{a}_0 s|^2\}}{\mathbb{E}\{|\mathbf{w}^H \bar{\nu}|^2\}} \\ &= \frac{\mathbf{w}^H \mathbf{a}_0 \mathbf{a}_0^H \mathbf{w} E_s}{\mathbf{w}^H \mathbf{R}_{\nu\nu} \mathbf{w}}\end{aligned}$$

where $\bar{\nu} = \sum_{k=1}^{N_I} \mathbf{a}_k i_k + \mathbf{n}$. $\mathbf{R}_{\nu\nu}$ is found to be

$$\begin{aligned}\mathbf{R}_{\nu\nu} &= \mathbb{E}\{\bar{\nu} \bar{\nu}^H\} \\ &= \mathbf{R}_{ii} + \sigma_n^2 \mathbf{I}\end{aligned}\tag{5.31}$$

The interference covariance matrix is equal to

$$\begin{aligned}\mathbf{R}_{ii} &= \mathbb{E}\left\{\left(\sum_{k=1}^{N_I} \mathbf{a}_k i_k\right) \left(\sum_{k=1}^{N_I} \mathbf{a}_k i_k\right)^H\right\} \\ &= \sum_{k=1}^{N_I} \mathbf{a}_k \mathbf{a}_k^H\end{aligned}$$

and we have assumed that $\mathbb{E}\{i_k i_j\} = \begin{cases} 0 & j \neq k \\ 1 & j = k \end{cases}$ (i.e., the interference signals are uncorrelated).

Now we can write the SINR as

$$\gamma = \frac{\mathbf{w}^H \mathbf{R}_{aa} \mathbf{w}}{\mathbf{w}^H \mathbf{R}_{\nu\nu} \mathbf{w}} E_s\tag{5.32}$$

where $\mathbf{R}_{aa} = E\{\mathbf{a}_0 \mathbf{a}_0^H\}$. Let's define $\mathbf{z} \triangleq \mathbf{R}_{\nu\nu}^{1/2} \mathbf{w}$. We can then rewrite the SINR as

$$\gamma = \frac{\mathbf{z}^H \mathbf{R}_{\nu\nu}^{-1/2} \mathbf{R}_{aa} \mathbf{R}_{\nu\nu}^{-1/2} \mathbf{z}}{\mathbf{z}^H \mathbf{z}} E_s\tag{5.33}$$

where we have used the fact that $\mathbf{R}_{\nu\nu}^{1/2}$ is Hermitian. Thus, we again have a Rayleigh quotient and the SINR is maximized when \mathbf{z} is the maximum eigenvector of $\mathbf{R}_{\nu\nu}^{-1/2} \mathbf{R}_{aa} \mathbf{R}_{\nu\nu}^{-1/2}$. Alternatively, we seek the maximum eigenvector which solves

$$\mathbf{R}_{aa} \mathbf{w} = \gamma_{max} \mathbf{R}_{\nu\nu} \mathbf{w}\tag{5.34}$$

Now, we know that (assuming $E_s = 1$ for simplicity of notation)

$$\gamma_{max} = \frac{\mathbf{w}_{opt}^H \mathbf{R}_{aa} \mathbf{w}_{opt}}{\mathbf{w}_{opt}^H \mathbf{R}_{\nu\nu} \mathbf{w}_{opt}}\tag{5.35}$$

$$\begin{aligned}\mathbf{R}_{aa} \mathbf{w}_{opt} &= \frac{\mathbf{w}_{opt}^H \mathbf{R}_{aa} \mathbf{w}_{opt}}{\mathbf{w}_{opt}^H \mathbf{R}_{\nu\nu} \mathbf{w}_{opt}} \mathbf{R}_{\nu\nu} \mathbf{w}_{opt} \\ \mathbf{a}_0 \mathbf{a}_0^H \mathbf{w}_{opt} &= \frac{\mathbf{w}_{opt}^H \mathbf{a}_0 \mathbf{a}_0^H \mathbf{w}_{opt}}{\mathbf{w}_{opt}^H \mathbf{R}_{\nu\nu} \mathbf{w}_{opt}} \mathbf{R}_{\nu\nu} \mathbf{w}_{opt}\end{aligned}\tag{5.36}$$

Since $\mathbf{a}_0^H \mathbf{w}_{opt}$ is a scalar, we can cancel it from both sides giving

$$\begin{aligned}\mathbf{a}_0 &= \frac{\mathbf{w}_{opt}^H \mathbf{a}_0}{\underbrace{\mathbf{w}_{opt}^H \mathbf{R}_{\nu\nu} \mathbf{w}_{opt}}_{\text{constant } \kappa}} \mathbf{R}_{\nu\nu} \mathbf{w}_{opt} \\ &= \kappa \mathbf{R}_{\nu\nu} \mathbf{w}_{opt}\end{aligned}$$

Thus,

$$\boxed{\mathbf{w}_{opt} = \frac{1}{\kappa} \mathbf{R}_{\nu\nu}^{-1} \mathbf{a}_0} \quad (5.37)$$

where κ can be dropped since it will not affect the final SINR. Further, the maximum SINR can be found as

$$\begin{aligned}\gamma_{max} &= \frac{\mathbf{w}_{opt}^H \mathbf{R}_{aa} \mathbf{w}_{opt}}{\mathbf{w}_{opt}^H \mathbf{R}_{\nu\nu} \mathbf{w}_{opt}} \\ &= \frac{(\frac{1}{\kappa} \mathbf{R}_{\nu\nu}^{-1} \mathbf{a}_0)^H \mathbf{R}_{aa} (\frac{1}{\kappa} \mathbf{R}_{\nu\nu}^{-1} \mathbf{a}_0)}{(\frac{1}{\kappa} \mathbf{R}_{\nu\nu}^{-1} \mathbf{a}_0)^H \mathbf{R}_{\nu\nu} (\frac{1}{\kappa} \mathbf{R}_{\nu\nu}^{-1} \mathbf{a}_0)} \\ &= \frac{(\mathbf{R}_{\nu\nu}^{-1} \mathbf{a}_0)^H \mathbf{a}_0 \mathbf{a}_0^H (\mathbf{R}_{\nu\nu}^{-1} \mathbf{a}_0)}{(\mathbf{R}_{\nu\nu}^{-1} \mathbf{a}_0)^H \mathbf{a}_0} \\ &= \mathbf{a}_0^H \mathbf{R}_{\nu\nu}^{-1} \mathbf{a}_0\end{aligned}$$

Example gain patterns are shown in Figure 5.7. Three plots are provided: (a) desired signal only at $\theta = \frac{\pi}{4}$; (b) desired signal at $\theta = \frac{\pi}{4}$ and an interferer at $\theta = \frac{\pi}{2}$; (c) desired signal at $\theta = \frac{\pi}{4}$ and Two Interferers at $\theta = \frac{\pi}{2}$ and $\theta = -\frac{\pi}{4}$. The INR assumed is 0dB. As one would expect, the first case corresponds to the maximum SNR pattern (and weights). This is to be expected since $R_{\nu\nu} = \sigma^2 \mathbf{I}$ and thus the weights correspond to the maximum SNR solution. This can also be seen by comparing with the patterns shown in Figure 5.6. Examining the other two patterns we see that the maximum SINR weights do not necessarily place a null in the direction of the interferers since it also attempts to maintain a strong gain in the direction of the desired signal.

5.5.4 MMSE

Another way to balance noise and interference is to minimize the error between the received signal and the desired signal. A common way to accomplish this is to minimize the mean square error. Consider the received signal

$$\mathbf{r}(t) = \mathbf{a}_0 x(t) + \sum_{k=1}^{N_I} \mathbf{a}_k i_k(t) + \mathbf{n}(t) \quad (5.38)$$

which after pulse matched filtering on each antenna gives the vector

$$\mathbf{r} = \mathbf{a}_0 s + \sum_{k=1}^{N_I} \mathbf{a}_k i_k + \mathbf{n} \quad (5.39)$$

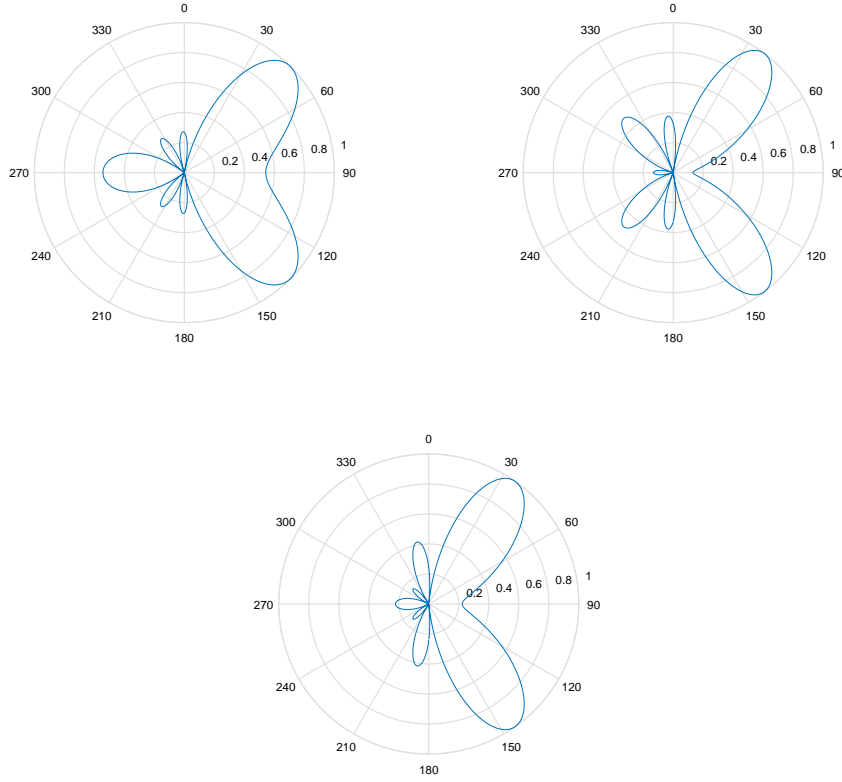


Figure 5.7: The Gain Pattern $g(\theta)$ for Four Antenna Elements with $\frac{d}{\lambda} = \frac{1}{2}$ using Maximum SINR Weights with only a desired signal at $\theta = \frac{\pi}{4}$ (top, left), One Interferer at $\theta = \frac{\pi}{2}$ (top, right) and Two Interferers at $\theta = \frac{\pi}{2}$ and $\theta = -\frac{\pi}{4}$ (bottom)

The decision variable is $z = \mathbf{w}^H \mathbf{r}$. We would like to find the weights \mathbf{w} that minimize the mean squared error:

$$\begin{aligned} J(\mathbf{w}) &= E \left\{ |\mathbf{w}^H \mathbf{r} - s|^2 \right\} \\ &= \mathbf{w}^H E \left\{ \tilde{\mathbf{r}} \tilde{\mathbf{r}}^H \right\} \mathbf{w} - E \left\{ s^* \tilde{\mathbf{r}}^H \right\} \mathbf{w} - \mathbf{w}^H E \left\{ \tilde{\mathbf{r}} s^* \right\} + E \left\{ s s^* \right\} \end{aligned} \quad (5.40)$$

In order to minimize this function, we need to find the point where the gradient $\nabla J(\mathbf{w}) = \mathbf{0}$. The gradient is

$$\nabla J(\mathbf{w}) = \begin{bmatrix} \frac{\partial J(\mathbf{w})}{\partial w_{1I}} \\ \frac{\partial J(\mathbf{w})}{\partial w_{2I}} \\ \vdots \\ \frac{\partial J(\mathbf{w})}{\partial w_{M_I}} \end{bmatrix} + j \begin{bmatrix} \frac{\partial J(\mathbf{w})}{\partial w_{1Q}} \\ \frac{\partial J(\mathbf{w})}{\partial w_{2Q}} \\ \vdots \\ \frac{\partial J(\mathbf{w})}{\partial w_{M_Q}} \end{bmatrix} \quad (5.41)$$

where $w_i = w_{iI} + jw_{iQ}$. In general, the following rules apply to gradients:

$$\begin{aligned}\nabla(\mathbf{w}^H \mathbf{A} \mathbf{w}) &= 2\mathbf{A} \mathbf{w}^* \\ \nabla(\mathbf{w}^H \mathbf{c}) &= \mathbf{c} \\ \nabla(\mathbf{c}^H \mathbf{w}) &= \mathbf{c}\end{aligned}\tag{5.42}$$

Thus,

$$\begin{aligned}\nabla J(\mathbf{w}) &= 2E\{\tilde{\mathbf{r}}\tilde{\mathbf{r}}^H\}\mathbf{w} - 2E\{\tilde{\mathbf{r}}s^*\} \\ &= 2\mathbf{R}_{\mathbf{rr}}\mathbf{w} - 2\mathbf{a}\end{aligned}\tag{5.43}$$

assuming that $E\{s_i k\} = 0, \forall k$. Setting the gradient equal to zero gives

$$\boxed{\mathbf{w}_{mmse} = \mathbf{R}_{\mathbf{rr}}^{-1}\mathbf{a}}\tag{5.44}$$

which is very similar to the maximum SINR weights. In fact, we will show in the next section that the two weight vectors are equivalent in terms of SINR. In practice we can estimate $\mathbf{R}_{\mathbf{rr}}$ directly from the received signal. The vector \mathbf{a} must be estimated using known symbols s , i.e., pilot symbols. Alternatively, we can use known symbols to drive an adaptive algorithm as we will discuss in the next section.

5.5.5 Equivalence of Max SINR and MMSE Weights

The two formulations which seek to balance the impact of noise and interference turn out to be very similar. In fact, we can show that from an SINR perspective, the two weight vectors are equivalent. To see this consider the inverse of the signal covariance matrix $\mathbf{R}_{\mathbf{rr}}^{-1}$. Using the matrix inversion lemma we can show that it is related to the inverse of the interference plus noise covariance matrix $\mathbf{R}_{\nu\nu}$:

$$\begin{aligned}\mathbf{R}_{\mathbf{rr}}^{-1} &= [\mathbf{R}_{\nu\nu} + \mathbf{a}_0 \mathbf{a}_0^H]^{-1} \\ &= \mathbf{R}_{\nu\nu}^{-1} - \frac{\mathbf{R}_{\nu\nu}^{-1} \mathbf{a}_0 \mathbf{a}_0^H \mathbf{R}_{\nu\nu}^{-1}}{\mathbf{a}_0^H \mathbf{R}_{\nu\nu}^{-1} \mathbf{a}_0 + 1}\end{aligned}\tag{5.45}$$

Now if we multiply $\mathbf{R}_{\mathbf{rr}}^{-1}$ by \mathbf{a}_0 to obtain the MMSE weights we obtain

$$\begin{aligned}\mathbf{R}_{\mathbf{rr}}^{-1} \mathbf{a}_0 &= \mathbf{R}_{\nu\nu}^{-1} \mathbf{a}_0 - \frac{\mathbf{R}_{\nu\nu}^{-1} \mathbf{a}_0 \mathbf{a}_0^H \mathbf{R}_{\nu\nu}^{-1} \mathbf{a}_0}{\mathbf{a}_0^H \mathbf{R}_{\nu\nu}^{-1} \mathbf{a}_0 + 1} \\ &= \left(1 - \frac{\mathbf{a}_0^H \mathbf{R}_{\nu\nu}^{-1} \mathbf{a}_0}{\mathbf{a}_0^H \mathbf{R}_{\nu\nu}^{-1} \mathbf{a}_0 + 1}\right) \mathbf{R}_{\nu\nu}^{-1} \mathbf{a}_0 \\ &= \left(\frac{1}{\mathbf{a}_0^H \mathbf{R}_{\nu\nu}^{-1} \mathbf{a}_0 + 1}\right) \mathbf{R}_{\nu\nu}^{-1} \mathbf{a}_0 \\ &= c \mathbf{R}_{\nu\nu}^{-1} \mathbf{a}_0\end{aligned}\tag{5.46}$$

where c is a scaling constant that does not affect SINR or the weight vector direction. Thus, the MMSE weights are equivalent to the max SINR weights and we can state that the SINR of the

MMSE solution is identical to the maximum SINR:

$$\gamma_{mmse} = \gamma_{max} = \mathbf{a}_0^H \mathbf{R}_{\nu\nu}^{-1} \mathbf{a}_0 \quad (5.47)$$

5.6 Adaptive Algorithms

5.6.1 Least Mean Squares Algorithm

Each of the choices for optimal weights discussed previously assumes knowledge of the array vectors of the desired signal *and the interference*. Typically, this information is not available *a priori*. Thus, we seek adaptive algorithms that can essentially learn this information (indirectly).

The classic approach is the Least Mean Squares (LMS) Algorithm which is based on the method of *steepest descent*, which is a stochastic approach to find the vector which minimizes an objective function. The approach assumes the availability of a data training sequence (decision-directed approaches can be used after initial convergence).

The iterative technique adapts the weights according to the recursion

$$\mathbf{w}(k+1) = \mathbf{w}(k) + \delta_s \hat{\nabla}(k) \quad (5.48)$$

where δ_s is a *negative* scaling factor which controls convergence and $\hat{\nabla}$ is the estimated gradient of the squared error ϵ^2 with respect to \mathbf{w} . Specifically, if the error is defined as

$$\epsilon(k) = s(k) - \mathbf{w}^H(k) \tilde{\mathbf{r}}(k) \quad (5.49)$$

then we have

$$\begin{aligned} \hat{\nabla}(k) &= \nabla [\epsilon^2(k)] \\ &= 2\epsilon^*(k) \nabla[\epsilon(k)] \\ &= -2\epsilon^*(k) \mathbf{r}(k) \end{aligned} \quad (5.50)$$

Does this get us what we want? Let's look at the average value of the estimated gradient:

$$\begin{aligned} \mathbb{E}\left\{\hat{\nabla}(k)\right\} &= \mathbb{E}\{-2\epsilon^*(k) \mathbf{r}(k)\} \\ &= \mathbb{E}\{-2(s(k) - \mathbf{w}^H(k) \tilde{\mathbf{r}}(k))^* \mathbf{r}(k)\} \\ &= -2\mathbb{E}\{s^*(k) \mathbf{r}(k)\} - 2\mathbb{E}\{\mathbf{w}^H(k) \tilde{\mathbf{r}}^*(k) \tilde{\mathbf{r}}(k)\} \\ &= -2\mathbf{a} + 2\mathbf{R}_{\mathbf{r}\mathbf{r}} \mathbf{w} \end{aligned}$$

Thus, the expected value of the gradient estimate is in fact the gradient of the MSE. The LMS update is then defined as

$$\boxed{\mathbf{w}(k+1) = \mathbf{w}(k) - 2\delta_s \epsilon^*(k) \mathbf{r}(k)} \quad (5.51)$$

where δ_s is a *negative* scaling factor that controls the speed of convergence. For convergence we require that

$$-\frac{1}{\lambda_{max}} < \delta_s < 0 \quad (5.52)$$

where $\lambda_{max} = \max eig(\mathbf{R}_{rr})$. Note that smaller $|\delta_s|$ results in slower convergence but less final error.

5.6.2 Recursive Least Squares

Recursive Least Squares is an approach that recursively estimates the weights that minimize the weighted square error. Let us define a weighted square cost function as follows:

$$J(k) = \sum_{i=1}^k \beta(k, i) |\epsilon(i)|^2 \quad (5.53)$$

where $\epsilon(i)$ is the error in the i th estimate:

$$\epsilon(i) = s(i) - \mathbf{w}^H(i) \tilde{\mathbf{r}}(i) \quad (5.54)$$

where $\tilde{\mathbf{r}}(i)$ is the received signal vector (after pulse matched filtering) at time step i , $s(i)$ is the desired (known) signal at time step i , and $\mathbf{w}(i)$ is the weight vector at time step i . The term $\beta(k, i)$ is a forgetting factor that forgets old data. Note that

$$0 \leq \beta(k, i) \leq 1 \quad (5.55)$$

We shall choose $\beta(k, i) = \chi^{k-i}$ for $0 \leq \chi \leq 1$. Thus, we have

$$J(k) = \sum_{i=1}^k \chi^{k-i} |\epsilon(i)|^2 \quad (5.56)$$

It can be shown that this squared error is minimized by the least squared solution:

$$\begin{aligned} \mathbf{w}(k) &= \tilde{\mathbf{R}}_{rr}^{-1}(k) \tilde{\mathbf{x}}(k) \\ \tilde{\mathbf{R}}_{rr}(k) &= \sum_{i=1}^k \chi^{k-i} \tilde{\mathbf{r}}(i) \tilde{\mathbf{r}}^H(i) \\ \tilde{\mathbf{x}}(k) &= \sum_{i=1}^k \chi^{k-i} \mathbf{r}(i) s^*(i) \end{aligned}$$

The RLS method provides an efficient recursive approach to determine $\mathbf{w}(k)$. First, let us rewrite the expression for $\tilde{\mathbf{R}}_{rr}(k)$:

$$\begin{aligned} \tilde{\mathbf{R}}_{rr}(k) &= \sum_{i=1}^k \chi^{k-i} \tilde{\mathbf{r}}(i) \tilde{\mathbf{r}}^H(i) \\ &= \chi \underbrace{\left[\sum_{i=1}^{k-1} \chi^{k-i-1} \tilde{\mathbf{r}}(i) \tilde{\mathbf{r}}^H(i) \right]}_{\tilde{\mathbf{R}}_{rr}(k-1)} + \tilde{\mathbf{r}}(k) \tilde{\mathbf{r}}(k)^H \\ &= \chi \tilde{\mathbf{R}}_{rr}(k-1) + \tilde{\mathbf{r}}(k) \tilde{\mathbf{r}}(k)^H \end{aligned}$$

Similarly, we can write

$$\tilde{\mathbf{x}}(k) = \chi \tilde{\mathbf{x}}(k-1) + \tilde{\mathbf{r}}(k) s^*(k) \quad (5.57)$$

Now, according to the matrix inversion lemma:

$$(\mathbf{A} + \mathbf{u}\mathbf{v}^H)^{-1} = \mathbf{A}^{-1} - \frac{\mathbf{A}^{-1}\mathbf{u}\mathbf{v}^H\mathbf{A}^{-1}}{1 + \mathbf{v}^H\mathbf{A}^{-1}\mathbf{u}} \quad (5.58)$$

Thus, we can update the inverse as

$$\left(\chi \tilde{\mathbf{R}}_{\mathbf{rr}}(k-1) + \tilde{\mathbf{r}}(k)\tilde{\mathbf{r}}(k)^H \right)^{-1} = \chi^{-1} \tilde{\mathbf{R}}_{\mathbf{rr}}^{-1}(k-1) - \frac{\chi^{-1} \tilde{\mathbf{R}}_{\mathbf{rr}}^{-1}(k-1) \tilde{\mathbf{r}}(k) \tilde{\mathbf{r}}^H(k) \chi^{-1} \tilde{\mathbf{R}}_{\mathbf{rr}}^{-1}(k-1)}{1 + \tilde{\mathbf{r}}^H(k) \chi^{-1} \tilde{\mathbf{R}}_{\mathbf{rr}}^{-1}(k-1) \tilde{\mathbf{r}}(k)} \quad (5.59)$$

For ease of notation we define

$$\begin{aligned} \mathbf{P}(k) &= \tilde{\mathbf{R}}_{\mathbf{rr}}^{-1}(k) \\ \mathbf{K}(k) &= \frac{\chi^{-1}}{1 + \chi^{-1} \tilde{\mathbf{r}}^H(k) \mathbf{P}(k-1) \tilde{\mathbf{r}}(k)} \mathbf{P}(k-1) \tilde{\mathbf{r}}(k) \end{aligned} \quad (5.60)$$

Thus, the matrix inversion update can be written as

$$\mathbf{P}(k) = \chi^{-1} \mathbf{P}(k-1) - \chi^{-1} \mathbf{K}(k) \tilde{\mathbf{r}}^H(k) \mathbf{P}(k-1) \quad (5.61)$$

Now, rearranging the equation above we have

$$\begin{aligned} \mathbf{K}(k)(1 + \chi^{-1} \tilde{\mathbf{r}}^H(k) \mathbf{P}(k-1) \tilde{\mathbf{r}}(k)) &= \chi^{-1} \mathbf{P}(k-1) \tilde{\mathbf{r}}(k) \\ \mathbf{K}(k) &= \underbrace{[\chi^{-1} \mathbf{P}(k-1) - \chi^{-1} \mathbf{K}(k) \tilde{\mathbf{r}}^H(k) \mathbf{P}(k-1)]}_{\mathbf{P}(k)} \tilde{\mathbf{r}}(k) \\ &= \mathbf{P}(k) \tilde{\mathbf{r}}(k) \end{aligned} \quad (5.62)$$

Now, examining the weights:

$$\begin{aligned} \mathbf{w}(k) &= \mathbf{R}_{\mathbf{rr}}^{-1}(k) \tilde{\mathbf{x}}(k) \\ &= \mathbf{P}(k) \tilde{\mathbf{x}}(k) \\ &= \chi \mathbf{P}(k) \tilde{\mathbf{x}}(k-1) + \mathbf{P}(k) \tilde{\mathbf{r}}(k) s^*(k) \\ &= \mathbf{P}(k-1) \tilde{\mathbf{x}}(k-1) - \mathbf{K}(k) \tilde{\mathbf{r}}^H(k) \mathbf{P}(k-1) \tilde{\mathbf{x}}(k-1) + \mathbf{P}(k) \tilde{\mathbf{r}}(k) s^*(k) \\ &= \mathbf{w}(k-1) - \mathbf{K}(k) \tilde{\mathbf{r}}^H(k) \mathbf{w}(k-1) + \underbrace{\mathbf{P}(k) \tilde{\mathbf{r}}(k)}_{\mathbf{K}(k)} s^*(k) \\ &= \mathbf{w}(k-1) - \mathbf{K}(k) \tilde{\mathbf{r}}^H(k) \mathbf{w}(k-1) + \mathbf{K}(k) s^*(k) \\ &= \mathbf{w}(k-1) + \mathbf{K}(k) \epsilon^*(k) \end{aligned} \quad (5.63)$$

where $\epsilon(k) = s(k) - \mathbf{w}^H(k-1) \tilde{\mathbf{r}}(k)$.

Thus we can define the RLS recursion as

$$1. \quad \mathbf{K}(k) = \frac{\chi^{-1} \mathbf{P}(k-1) \tilde{\mathbf{r}}(k)}{1 + \chi^{-1} \tilde{\mathbf{r}}^H(k) \mathbf{P}(k-1) \tilde{\mathbf{r}}(k)}$$

$$2. \quad \epsilon(k) = s(k) - \mathbf{w}^H(k-1) \tilde{\mathbf{r}}(k)$$

$$3. \quad \mathbf{w}(k) = \mathbf{w}(k-1) + \mathbf{K}(k) \epsilon^*(k)$$

$$4. \quad \mathbf{P}(k) = \chi^{-1} \mathbf{P}(k-1) - \chi^{-1} \mathbf{K}(k) \tilde{\mathbf{r}}^H(k) \mathbf{P}(k-1)$$

with initial conditions $\mathbf{P}(0) = \kappa \mathbf{I}$ and $\mathbf{w}(0) = \mathbf{0}^{M_r \times 1}$ for positive constant κ .

5.7 Direction Finding

A common use of beamforming (coherent) arrays is direction finding - i.e., the estimation of the angles-of-arrival θ_i if one or more signals arriving at the array.

$$\tilde{\mathbf{r}}(t) = \sum_{i=1}^{N_s} \mathbf{a}_i x_i(t) + \mathbf{n}(t) \quad (5.64)$$

where N_s is the total number of signals present each with array response \mathbf{a}_i and signal $x_i(t)$. We shall assume that $E\{|x_i(t)|^2\} = 1$ and $E\{\mathbf{n}(t)\mathbf{n}^H(t)\} = \sigma_n^2 \mathbf{I}$. If we filter and sample the received signal, we can write one sample vector as

$$\tilde{\mathbf{r}} = \mathbf{A}(\bar{\theta}) \mathbf{x} + \mathbf{n} \quad (5.65)$$

where $\mathbf{A}(\bar{\theta}) = [\mathbf{a}(\theta_1), \mathbf{a}(\theta_2), \dots, \mathbf{a}(\theta_{N_s})]$, \mathbf{x} is a vector of sampled signals and \mathbf{n} is a vector of noise samples. Note that we have used $\mathbf{a}_i = \mathbf{a}(\theta_i)$ to explicitly show the dependence of \mathbf{a}_i on θ_i . Also, we have defined $\bar{\theta} = [\theta_1, \theta_2, \dots, \theta_{N_s}]^T$. If we consider the vector $\tilde{\mathbf{r}}$ as our observables, and we assume Gaussian noise and Gaussian distributed signals, we can write the distribution of $\tilde{\mathbf{r}}$ as

$$f(\tilde{\mathbf{r}}) = \frac{1}{\sqrt{(2\pi)^{M_r} |\mathbf{R}_{rr}|}} \exp\left(-\frac{1}{2} \tilde{\mathbf{r}}^H \mathbf{R}_{rr}^{-1} \tilde{\mathbf{r}}\right) \quad (5.66)$$

where $|\mathbf{R}|$ is the determinant of \mathbf{R} , $\mathbf{R}_{rr} = \mathbf{A}(\bar{\theta}) \mathbf{A}^H(\bar{\theta}) + \sigma_n^2 \mathbf{I}$ and we have assumed that $R_{xx} = \mathbf{I}$. Further, if we assume a series of K observed vectors separated in time such that the transmit signals and noise processes are independent from one sample to the next, we can write the distribution of the observed sequences of vectors as:

$$f(\tilde{\mathbf{r}}_1, \tilde{\mathbf{r}}_2, \dots, \tilde{\mathbf{r}}_K) = \prod_{k=1}^K \frac{1}{\sqrt{(2\pi)^{M_r} |\mathbf{R}_{rr}|}} \exp\left(-\frac{1}{2} \tilde{\mathbf{r}}_k^H \mathbf{R}_{rr}^{-1} \tilde{\mathbf{r}}_k\right) \quad (5.67)$$

For an observed set of $\{\tilde{\mathbf{r}}_k\}$ with fixed but unknown $\bar{\theta}$, we can view (5.67) as a likelihood function. The Maximum Likelihood estimate of $\bar{\theta}$ can then be found by maximizing the log likelihood function:

$$\hat{\bar{\theta}}_{ML} = \max_{\bar{\theta}} -K \log |\mathbf{R}_{rr}| - \sum_{k=1}^K \tilde{\mathbf{r}}_k^H \mathbf{R}_{rr}^{-1} \tilde{\mathbf{r}}_k \quad (5.68)$$

The maximum likelihood estimate of $\bar{\theta}$ is straightforward to compute, albeit computationally intensive. Assuming a grid search over N values of θ , the overall estimation process requires calculating the argument of the maximization in (eq:MLAOA) N^{N_s} times. In other words, for a 1 degree granularity over unambiguous angles of a linear array with four signals we would require calculating the metric above $180^4 \approx 10^9$ times. Thus, ML estimation is in general too computationally intensive. Thus, we seek alternative, less complex suboptimal methods.

5.7.1 The Fourier Method

This method is also known as the “Delay-and-Sum Method” or “Classical Beamformer Method”. Again, if we let

$$\tilde{\mathbf{r}}(t) = \sum_{i=1}^{N_t} \mathbf{a}_i x_i(t) + \mathbf{n}(t) \quad (5.69)$$

where N_t is the total number of signals present each with array response \mathbf{a}_i and signal $x_i(t)$. We shall assume that $E\{|x_i(t)|^2\} = 1$ and $E\{\mathbf{n}(t)\mathbf{n}^H(t)\} = \sigma_n^2 \mathbf{I}$. If we know that there are N_t signals and we look for N_t peaks in the angle spectrum

$$P(\theta) = E\{|\mathbf{w}^H(\theta)\tilde{\mathbf{r}}(t)|^2\} \quad (5.70)$$

where the peaks will occur at $\mathbf{w}(\theta) = \mathbf{a}_i(\theta)$. Thus, assuming that we know the array response we set the weights to $\mathbf{a}(\theta)$ and vary θ the angle spectrum is

$$\begin{aligned} P(\theta) &= \mathbf{a}^H(\theta) E\{\tilde{\mathbf{r}}(t)\tilde{\mathbf{r}}^H(t)\} \mathbf{a}(\theta) \\ &= \mathbf{a}^H(\theta) \mathbf{R}_{rr} \mathbf{a}(\theta) \end{aligned} \quad (5.71)$$

where \mathbf{R}_{rr} is the covariance of the received signal. If there is only one signal in the environment with array response $\mathbf{a}_o = \mathbf{a}(\theta_o)$, the covariance matrix is

$$\mathbf{R}_{rr} = P_o \mathbf{a}_o \mathbf{a}_o^H + \sigma_n^2 \mathbf{I} \quad (5.72)$$

Thus, the resulting angle spectrum is

$$P(\theta) = P_o \mathbf{a}^H(\theta) \mathbf{a}_o \mathbf{a}_o^H \mathbf{a}(\theta) + \sigma_n^2 \mathbf{a}^H(\theta) \mathbf{I} \mathbf{a}(\theta) \quad (5.73)$$

Clearly, $P(\theta)$ will be maximized at $\mathbf{a}(\theta) = \mathbf{a}(\theta_o)$, i.e., when $\theta = \theta_o$. If there are multiple (N) signals in the environment,

$$P(\theta) = \sum_{i=1}^N P_i \mathbf{a}^H(\theta) \mathbf{a}_i \mathbf{a}_i^H \mathbf{a}(\theta) + \sigma_n^2 M_r \quad (5.74)$$

Now there can be up to N peaks although the number of peaks may be less if the \mathbf{a}_i are not spatially resolvable.

Notes:

- * We have not made any assumptions about the kind of array we have. It can be linear, circular, planar, etc. However, we **must know** the array manifold $\mathbf{a}(\theta)$ for the array.
- * Due to imperfections in the array, typically the array manifold is determined via calibration.
- * If the array is linear, there will always be an ambiguity in θ of 180° since the array cannot distinguish between θ and $\pi - \theta$.

5.7.2 Capon's Minimum Variance Approach

The Fourier method can be ineffective when there are multiple signals in the environment. Fundamentally, the Fourier method uses all M_r degrees of freedom (DOF) to form a beam in the desired direction but is not concerned with signals in the environment coming from other directions. Capon's technique (also known as Minimum Variance Distortionless Response) uses some of the DOF to form a beam in the desired direction and some to null the other signals. The technique minimizes output power subject to the constraint that the gain in the desired direction is unity.

Formulation

Again, we wish to create a power spectrum $P(\theta)$ but now with weights chosen to minimize the impact of signals coming from directions other than θ . More specifically, the weights are chosen as

$$\begin{aligned}\mathbf{w}_{opt}(\theta) &= \min_{\mathbf{w}} \mathbb{E} \{ |P(\theta)|^2 \} \quad s.t. \quad \mathbf{a}^H(\theta)\mathbf{a}(\theta) = 1 \\ &= \min_{\mathbf{w}} \mathbf{w}^H \mathbf{R}_{rr} \mathbf{w} \quad s.t. \quad \mathbf{a}^H(\theta)\mathbf{a}(\theta) = 1\end{aligned}\tag{5.75}$$

Using the technique of Lagrange multipliers the solution is found to be

$$\mathbf{w}_{opt}(\theta) = \frac{\mathbf{R}_{rr}^{-1} \mathbf{a}(\theta)}{\mathbf{a}^H(\theta) \mathbf{R}_{rr}^{-1} \mathbf{a}(\theta)}\tag{5.76}$$

Further, the minimum output is

$$J_{min} = \frac{1}{\mathbf{a}^H(\theta) \mathbf{R}_{rr}^{-1} \mathbf{a}(\theta)}\tag{5.77}$$

In general, the output angle spectrum

$$P(\theta) = \frac{1}{\mathbf{a}^H(\theta) \mathbf{R}_{rr}^{-1} \mathbf{a}(\theta)}\tag{5.78}$$

This is also known as the **Minimum Variance Distortionless Response** (MVDR).

NOTE: This solution will minimize the output power and be distortionless at the desired angle.

5.7.3 MUSIC

Let

$$\tilde{\mathbf{r}}(t) = \sum_{i=0}^{N_t-1} \mathbf{a}_i x_i(t) + \mathbf{n}(t)\tag{5.79}$$

where N_t is the total number of signals present each with array response \mathbf{a}_i and signal $x_i(t)$. We shall assume that $\mathbb{E} \{ |x_i(t)|^2 \} = 1$ and $\mathbb{E} \{ \mathbf{n}(t) \mathbf{n}^H(t) \} = \sigma_n^2 \mathbf{I}$. Dropping the dependence on time,

after matched filtering and sampling, we can re-write this as

$$\begin{aligned}\tilde{\mathbf{r}} &= [\mathbf{a}_0, \mathbf{a}_1, \dots, \mathbf{a}_{N_t-1}] \begin{bmatrix} s_0 \\ s_1 \\ \vdots \\ s_{N_t-1} \end{bmatrix} + \mathbf{n} \\ &= \mathbf{As} + \mathbf{n}\end{aligned}\quad (5.80)$$

Note that \mathbf{a}_i vectors are vectors in M_r -dimensional space and $\tilde{\mathbf{r}}$ is a linear combination of these vectors. The input covariance matrix \mathbf{R}_{rr} can be written as

$$\begin{aligned}\mathbf{R}_{rr} &= E\{\tilde{\mathbf{r}}\tilde{\mathbf{r}}^H\} \\ &= \mathbf{A}E\{\mathbf{s}\mathbf{s}^H\}\mathbf{A}^H + E\{\mathbf{n}\mathbf{n}^H\} \\ &= \mathbf{A}\mathbf{R}_{ss}\mathbf{A}^H + \sigma_n^2\mathbf{I}\end{aligned}\quad (5.81)$$

Now, the eigenvalues of \mathbf{R}_{rr} are such that

$$\begin{aligned}|\mathbf{R}_{rr} - \lambda_i \mathbf{I}| &= 0 \\ |\mathbf{A}\mathbf{R}_{ss}\mathbf{A}^H + \sigma_n^2\mathbf{I} - \lambda_i \mathbf{I}| &= 0 \\ |\mathbf{A}\mathbf{R}_{ss}\mathbf{A}^H - (\lambda_i - \sigma_n^2)\mathbf{I}| &= 0\end{aligned}\quad (5.82)$$

Thus, we can define $v_i = \lambda_i - \sigma_n^2$ as the eigenvalues of $\mathbf{A}\mathbf{R}_{ss}\mathbf{A}^H$. Now, since \mathbf{a}_i are linearly independent steering vectors, \mathbf{A} has full rank. Assuming that \mathbf{R}_{ss} is non-singular, provided that the number of signals $N_t < M_r$ the $M_r \times M_r$ matrix $\mathbf{A}\mathbf{R}_{ss}\mathbf{A}^H$ is positive semi-definite with rank N_t . Thus, $M_r - N_t$ eigenvalues v_i of $\mathbf{A}\mathbf{R}_{ss}\mathbf{A}^H$ are zero.

Thus, $M_r - N_t$ eigenvalues λ_i of \mathbf{R}_{rr} are equal to σ_n^2 . Sorting the eigenvalues such that

$$\lambda_0 < \lambda_1 < \dots < \lambda_{M_r-1} \quad (5.83)$$

we can say that $\lambda_0 = \lambda_1 = \dots = \lambda_{M_r-N_t-1} = \sigma_n^2$.

In a real application, since \mathbf{R}_{rr} is estimated, $M_r - N_t$ eigenvalues will not be *exactly* σ_n^2 , but will be close. Using this fact we can determine the number of signals in the environment.

Now, let us define \mathbf{q}_i $0 \leq i \leq M_r - N_t - 1$ as the eigenvectors of \mathbf{R}_{rr} associated with the $M_r - N_t$ eigenvalues corresponding to the noise subspace. Since the steering vectors \mathbf{a}_i do not correspond to the noise we are guaranteed that $\mathbf{A}^H \mathbf{q}_i = \mathbf{0}$ and $\mathbf{a}_i^H \mathbf{q}_i = 0$.

Proof:

From the definition of eigenvectors

$$(\mathbf{R}_{rr} - \lambda_i \mathbf{I}) \mathbf{q}_i = \mathbf{0} \quad (5.84)$$

However, for \mathbf{q}_i , the associated eigenvalues $\lambda_i = \sigma_n^2$. Thus,

$$\begin{aligned} (\mathbf{R}_{rr} - \sigma_n^2 \mathbf{I}) \mathbf{q}_i &= \mathbf{0} \\ (\mathbf{A} \mathbf{R}_{ss} \mathbf{A}^H + \sigma_n^2 \mathbf{I} - \sigma_n^2 \mathbf{I}) \mathbf{q}_i &= \mathbf{0} \\ \mathbf{A} \mathbf{R}_{ss} \mathbf{A}^H \mathbf{q}_i &= \mathbf{0} \end{aligned} \quad (5.85)$$

Since \mathbf{A} is full rank and \mathbf{R}_{ss} is non-singular we have

$$\mathbf{A}^H \mathbf{q}_i = \mathbf{0} \quad (5.86)$$

Since all of the steering vectors are orthogonal to the noise subspace, the MUSIC algorithm (MULTiple SIgnal Classification) is

1. Find the eigen-decomposition $\mathbf{R}_{rr} = \mathbf{Q} \Lambda \mathbf{Q}^H$
2. Identify the noise subspace as the $M_r - N$ eigenvectors associated with the weakest eigenvalues:

$$\mathbf{Q} = \left[\underbrace{\mathbf{q}_0 \mathbf{q}_1 \dots \mathbf{q}_{M_r - N_t - 1}}_{M_r \times (M_r - N_t) \text{ noise subspace } \mathbf{V}} \dots \mathbf{q}_{M_r - 1} \right] \quad (5.87)$$

3. Calculate the MUSIC angle spectrum as

$$P(\theta) = \frac{\mathbf{a}^H(\theta) \mathbf{a}(\theta)}{\mathbf{a}^H(\theta) \mathbf{V} \mathbf{V}^H \mathbf{a}(\theta)} \quad (5.88)$$

Note that we are guaranteed that \mathbf{a}_i is perpendicular to \mathbf{V} . Thus, when $\mathbf{a}(\theta) = \mathbf{a}_i$ the spectrum $P(\theta)$ will have a sharp peak. There are then peaks in the MUSIC spectrum corresponding to the AOA's of the signals in the environment.

5.7.4 ESPRIT

Estimation of Signal Parameters using Rotational Invariance Techniques (ESPRIT) is another DoA estimation technique which is based on the fact that for a linear array each element in the steering vector is a constant phase shift from the neighboring element. More specifically, defining the $M_r \times K$ matrix of K steering vectors \mathbf{A} :

$$\begin{aligned} \mathbf{A} &= [\mathbf{a}_0, \mathbf{a}_1, \dots, \mathbf{a}_{K-1}] \\ &= \begin{bmatrix} 1 & \dots & 1 \\ e^{-\frac{j2\pi d}{\lambda} \sin(\theta_0)} & \dots & e^{-\frac{j2\pi d}{\lambda} \sin(\theta_{K-1})} \\ \vdots & \dots & \vdots \\ e^{-\frac{j2\pi d(M_r-1)}{\lambda} \sin(\theta_0)} & \dots & e^{-\frac{j2\pi d(M_r-1)}{\lambda} \sin(\theta_{K-1})} \end{bmatrix} \end{aligned} \quad (5.89)$$

we can define two new vectors corresponding to the first $M_r - 1$ rows and the last $M_r - 1$ rows:

$$\mathbf{A}_0 = \begin{bmatrix} 1 & \dots & 1 \\ e^{-\frac{j2\pi d}{\lambda} \sin(\theta_0)} & \dots & e^{-\frac{j2\pi d}{\lambda} \sin(\theta_{K-1})} \\ \vdots & \dots & \vdots \\ e^{-\frac{j2\pi d(M_r-2)}{\lambda} \sin(\theta_0)} & \dots & e^{-\frac{j2\pi d(M_r-2)}{\lambda} \sin(\theta_{K-1})} \end{bmatrix} \quad (5.90)$$

$$\mathbf{A}_1 = \begin{bmatrix} e^{-\frac{j2\pi d}{\lambda} \sin(\theta_0)} & \dots & e^{-\frac{j2\pi d}{\lambda} \sin(\theta_{K-1})} \\ \vdots & \dots & \vdots \\ e^{-\frac{j2\pi d(M_r-1)}{\lambda} \sin(\theta_0)} & \dots & e^{-\frac{j2\pi d(M_r-1)}{\lambda} \sin(\theta_{K-1})} \end{bmatrix} \quad (5.91)$$

Note that

$$\mathbf{A}_1 = \mathbf{A}_0 \Phi \quad (5.92)$$

where

$$\Phi = \begin{bmatrix} e^{-\frac{j2\pi d}{\lambda} \sin(\theta_0)} & 0 & \dots & 0 \\ 0 & \ddots & & 0 \\ 0 & 0 & \ddots & 0 \\ 0 & 0 & & e^{-\frac{j2\pi d}{\lambda} \sin(\theta_{K-1})} \end{bmatrix} \quad (5.93)$$

Thus, the diagonal values of Φ correspond to the constant phase shift across the array due to each signal. If we can determine Φ , we can find the DoAs. Unfortunately, the matrix of steering vectors is not available. However, we can find the signal subspace which spans the same subspace as the steering vectors. If we define the matrix \mathbf{Q} as the matrix of eigenvectors, we can partition \mathbf{Q} the same way we did with the steering vector matrix to obtain \mathbf{Q}_0 and \mathbf{Q}_1 , we know that

$$\mathbf{Q}_0 = \mathbf{A}_0 \mathbf{C} \quad (5.94)$$

$$\mathbf{Q}_1 = \mathbf{A}_1 \mathbf{C} \quad (5.95)$$

$$(5.96)$$

for some unknown matrix \mathbf{C} . Further, this implies that

$$\mathbf{Q}_1 = \mathbf{Q}_0 \Psi \quad (5.97)$$

for some matrix Ψ . Now, using the relationships above we can easily show that

$$\Psi = \mathbf{C}^{-1} \Phi \mathbf{C} \quad (5.98)$$

which implies that Φ corresponds to the eigenvalues of Ψ . This suggests the following algorithm:

1. Estimate the covariance matrix of the received signal \mathbf{R} .
2. Determine the eigenvalue decomposition of $\mathbf{R} = \mathbf{Q} \Lambda \mathbf{Q}^H$.

3. Divide the eigenvectors into the signal subspace \mathbf{Q}_s and the noise subspace \mathbf{Q}_n .
4. Create two new matrices \mathbf{Q}_0 and \mathbf{Q}_1 as the first and last $M_r - 1$ rows of \mathbf{Q}_s respectively.
5. Using equation (5.97) find the least squares estimate of Ψ . This can be found as $\mathbf{Q}_0^\dagger \mathbf{Q}_1$.
6. Determine the eigenvalues of $\hat{\Psi}$, λ_i , $1 \leq i \leq K$.
7. Noting that $\lambda_i = e^{-\frac{j2\pi d}{\lambda} \sin(\theta_i)}$, solve for $\hat{\theta}_i$.

Note that the least squares estimate of $\hat{\Psi}$ assumes that \mathbf{Q}_0 is noisy, but that \mathbf{Q}_1 is not. Since in reality, both are noisy estimates, a total least squares solution is more appropriate. In that case we can solve for Ψ by first creating the singular value decomposition of the $(M_r - 1) \times 2K$ matrix $[\mathbf{Q}_0 \mathbf{Q}_1]$:

$$[\mathbf{Q}_0 \mathbf{Q}_1] = \mathbf{U} \Sigma \mathbf{V}^H \quad (5.99)$$

Then, defining the four $M \times M$ sub-matrices of \mathbf{V} as

$$\begin{bmatrix} \mathbf{V}_{11} & \mathbf{V}_{12} \\ \mathbf{V}_{21} & \mathbf{V}_{22} \end{bmatrix} \quad (5.100)$$

we finally have

$$\hat{\Psi} = -\mathbf{V}_{12} \mathbf{V}_{22}^{-1} \quad (5.101)$$

The advantage of this algorithm over MUSIC is that there is no requirement to search for peaks which can be fraught with difficulty, and no requirement for choosing a resolution (i.e., number of candidate steering vectors). Example performance of ESPRIT for one signal ($\theta = 0$) with $N_s = 100$ samples and $M_r = 4$ is plotted in Figure 5.8. We can see that for SNR greater than 0dB, ESPRIT approaches the CRLB.

Appendix: Cramer Rao Lower Bound

Consider N_s samples of the receive vector $\tilde{\mathbf{r}}(t)$

$$\tilde{\mathbf{r}}(t) = \mathbf{a}(\theta) + \mathbf{n}(t) \quad (5.102)$$

for $t = 1, 2, \dots, N_s$. The conditional probability function is written as

$$f_r(\tilde{\mathbf{r}}|\theta) = \frac{1}{(2\pi\sigma^2)^{M_r N_s}} e^{-\sum_{t=1}^{N_s} (\tilde{\mathbf{r}}(t) - \mathbf{a})^H \mathbf{R}^{-1} (\tilde{\mathbf{r}}(t) - \mathbf{a})} \quad (5.103)$$

where the covariance matrix $\mathbf{R} = \sigma^2 \mathbf{I}$. Taking the log of $f_r(\tilde{\mathbf{r}}|\theta)$ we obtain

$$\log f_r(\tilde{\mathbf{r}}|\theta) = -\log [(2\pi\sigma^2)^{M_r N_s}] - \frac{1}{\sigma^2} \sum_{t=1}^{N_s} (\tilde{\mathbf{r}}(t) - \mathbf{a})^H (\tilde{\mathbf{r}}(t) - \mathbf{a}) \quad (5.104)$$

$$= -\log [(2\pi\sigma^2)^{M_r N_s}] - \frac{1}{\sigma^2} \sum_{t=1}^{N_s} \{ \tilde{\mathbf{r}}^H(t) \tilde{\mathbf{r}}(t) - \tilde{\mathbf{r}}^H(t) \mathbf{a} - \mathbf{a}^H \tilde{\mathbf{r}}(t) + \mathbf{a}^H \mathbf{a} \} \quad (5.105)$$

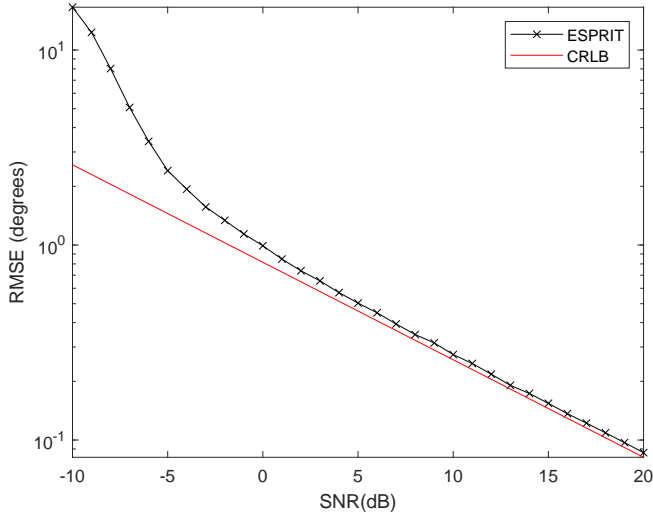


Figure 5.8: Performance of ESPRIT with $M_r = 4$, $N_s = 100$ and $\theta = 0$

Dropping the terms that don't depend on θ we obtain

$$g(\theta) = \frac{1}{\sigma^2} \sum_{t=1}^{N_s} \{ \tilde{\mathbf{r}}^H(t) \mathbf{a} + \mathbf{a}^H \tilde{\mathbf{r}}(t) - \mathbf{a}^H \mathbf{a} \} \quad (5.106)$$

The Cramer-Rao Lower Bound on the estimation variance is then

$$CRLB(\theta) \geq \mathbf{J}^{-1} \quad (5.107)$$

where

$$\mathbf{J} = E \left\{ \frac{\partial^2 g(\theta)}{\partial \theta^2} \right\} \quad (5.108)$$

Now,

$$\frac{\partial g(\theta)}{\partial \theta} = \frac{1}{\sigma^2} \sum_{t=1}^{N_s} \left\{ \tilde{\mathbf{r}}^H(t) \frac{\partial \mathbf{a}}{\partial \theta} + \frac{\partial \mathbf{a}^H}{\partial \theta} \tilde{\mathbf{r}}(t) - \mathbf{a}^H \frac{\partial \mathbf{a}}{\partial \theta} - \frac{\partial \mathbf{a}^H}{\partial \theta} \mathbf{a} \right\} \quad (5.109)$$

Further,

$$\frac{\partial^2 g(\theta)}{\partial \theta^2} = \frac{1}{\sigma^2} \sum_{t=1}^{N_s} \left\{ \tilde{\mathbf{r}}^H(t) \frac{\partial^2 \mathbf{a}}{\partial \theta^2} + \frac{\partial^2 \mathbf{a}^H}{\partial \theta^2} \tilde{\mathbf{r}}(t) - \mathbf{a}^H \frac{\partial^2 \mathbf{a}}{\partial \theta^2} - \frac{\partial \mathbf{a}^H}{\partial \theta} \frac{\partial \mathbf{a}}{\partial \theta} - \frac{\partial^2 \mathbf{a}^H}{\partial \theta^2} \mathbf{a} - \frac{\partial \mathbf{a}^H}{\partial \theta} \frac{\partial \mathbf{a}}{\partial \theta} \right\} \quad (5.110)$$

Now taking the expectation and realizing that $E\{\tilde{\mathbf{r}}(t)\} = \mathbf{a}$:

$$E\left\{\frac{\partial^2 g(\theta)}{\partial \theta^2}\right\} = -\frac{2N_s}{\sigma^2} \frac{\partial \mathbf{a}^H}{\partial \theta} \frac{\partial \mathbf{a}}{\partial \theta} \quad (5.111)$$

$$= -\frac{2N_s}{\sigma^2} \left(\frac{2\pi d}{\lambda}\right)^2 \frac{M_r(M_r - 1)^2}{12} (\cos(\theta))^2 \quad (5.112)$$

And thus

$$CRLB(\theta) \geq \frac{6}{N_s \gamma \left(\frac{2\pi d}{\lambda}\right)^2 M_r(M_r - 1)^2 (\cos(\theta))^2} \quad (5.113)$$

Chapter 6

Fading and Diversity

6.1 Introduction

In this chapter we examine a fundamental use of multiple antennas - diversity. As we will show shortly, fading is a highly detrimental factor in wireless communications. The primary tool to combat fading is diversity (typically combined with error correction coding). While diversity can be achieved in time and/or frequency, we are focused in this chapter on spatial diversity. However, much of what is developed can be applied to time/frequency with appropriate adjustments.

6.2 Preliminaries

In this section, we provide a few useful mathematical basics that are useful in our study of diversity.

6.2.1 Transformation of Random Variables

Let the random variable X have probability density function (pdf) and cumulative distribution function (cdf) defined as $f_X(x)$ and $F_X(x)$ respectively. Assume further that we have a random variable $Y = g(X)$ where $g(x)$ is a one-to-one transformation and is increasing on the range of X . This implies that g^{-1} is also an increasing function. Now the cdf of Y is

$$\begin{aligned} F_Y(y) &= \Pr\{Y \leq y\} \\ &= \Pr\{g(X) \leq y\} \\ &= \Pr\{X \leq g^{-1}(y)\} \\ &= F_X(g^{-1}(y)) \end{aligned} \tag{6.1}$$

The pdf can then be found using the chain rule

$$\begin{aligned} f_Y(y) &= \frac{d}{dy} F_Y(y) \\ &= \frac{d}{dy} F_X(g^{-1}(y)) \\ &= f_X(g^{-1}(y)) \frac{d}{dy} g^{-1}(y) \end{aligned} \quad (6.2)$$

Similarly if $g(X)$ is a decreasing function of X we get

$$f_Y(y) = -f_X(g^{-1}(y)) \frac{d}{dy} g^{-1}(y) \quad (6.3)$$

Combining the two, we arrive at a general rule for one-to-one transformations:

$$f_Y(y) = f_X(g^{-1}(y)) \left| \frac{d}{dy} g^{-1}(y) \right| \quad (6.4)$$

For transformations that are not one-to-one, we have to be a bit more careful. For example, we are interested in the following transformation:

$$Y = aX^2 \quad (6.5)$$

and wish to find $f_Y(y)$. Again, we shall start by finding an expression for $F_Y(y)$, the cdf of Y . Specifically, using Figure 6.1 we have

$$\begin{aligned} F_Y(y) &= \Pr\{Y \leq y\} \\ &= \Pr\left\{|X| \leq \sqrt{\frac{y}{a}}\right\} \\ &= F_X\left(\sqrt{\frac{y}{a}}\right) - F_X\left(-\sqrt{\frac{y}{a}}\right) \end{aligned}$$

Taking the derivative to get the pdf:

$$\begin{aligned} f_Y(y) &= \frac{d}{dy} F_Y(y) \\ &= \frac{1}{2} \sqrt{\frac{a}{y}} \frac{1}{a} f_X\left(\sqrt{\frac{y}{a}}\right) + \frac{1}{2} \sqrt{\frac{a}{y}} \frac{1}{a} f_X\left(-\sqrt{\frac{y}{a}}\right) \\ &= \frac{1}{2a\sqrt{y/a}} f_X\left(\sqrt{\frac{y}{a}}\right) + \frac{1}{2a\sqrt{y/a}} f_X\left(-\sqrt{\frac{y}{a}}\right) \end{aligned}$$

Now, since $f_X(x) = 0$ for $x < 0$ we have finally:

$$\boxed{f_Y(y) = \frac{1}{2a\sqrt{y/a}} f_X\left(\sqrt{\frac{y}{a}}\right)} \quad (6.6)$$

This particular transformation will be useful for converting the distribution of signal amplitude

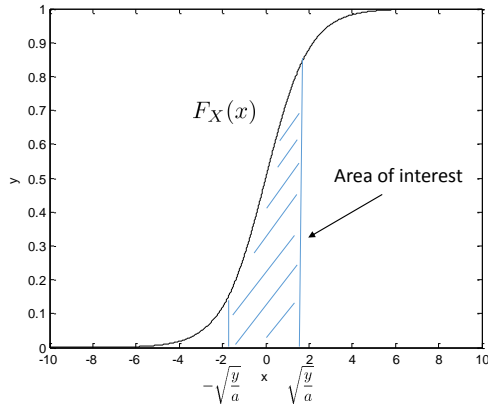


Figure 6.1: Determining the Integration region for the transformation of random variables

(e.g., Rayleigh fading) to the distribution of received signal power (and thus SNR).

6.2.2 Order Statistics

Let X_1, X_2, \dots, X_N be i.i.d. random variables. For any sample of N values let's reorder them as

$$Y_1 < Y_2 < \dots < Y_N \quad (6.7)$$

where $Y_N = \max_j \{X_j\}$ and $Y_1 = \min_j \{X_j\}$. The study of the statistics of Y_r is known as *order statistics*. As an example, the distribution of Y_r is

$$f_{Y_r}(y) = \frac{N!}{(r-1)!(N-r)!} [F_X(y)]^{r-1} [1 - F_X(y)]^{N-r} f_X(y) \quad (6.8)$$

Thus, for the maximum value we have

$$f_{\max}(y) = f_{Y_N}(y) = N [F_X(y)]^{N-1} f_X(y) \quad (6.9)$$

and for the minimum value

$$f_{\min}(y) = f_{Y_1}(y) = N [1 - F_X(y)]^{N-1} f_X(y) \quad (6.10)$$

6.2.3 The Moment Generating Function

When considering sums of random variables, we often use the property that the distribution of the sum of independent random variables is the convolution of the individual distributions. In general, this convolution is not mathematically convenient. However, an equivalent property is that the moment generating function of a sum of independent random variables is the product of the individual moment generating functions. The same is also true of the characteristic function. We will use a slightly modified definition of the moment generating function (in order to exploit

the Laplace Transform). Specifically, we will define it as

$$\Phi_X(s) = \mathbb{E} \{ e^{-sx} \} = \int_{-\infty}^{\infty} e^{sx} f_X(x) dx \quad (6.11)$$

Note that

$$\Phi'_X(s) = -\mathbb{E} \{ xe^{-sx} \} \quad (6.12)$$

and thus

$$\Phi'_X(0) = -\mathbb{E} \{ x \} \quad (6.13)$$

Thus, the k th moment about zero is simply

$$\mu_k = (-1)^k \Phi_X^{(k)}(0) \quad (6.14)$$

The moment generating function is similar to the Laplace transform but replaces s with $-s$. Note that the moment generating function of $\frac{1}{\gamma}e^{-\gamma/\bar{\gamma}}$ can be found as

$$\begin{aligned} \Phi_\gamma(s) &= \mathbb{E} \{ e^{s\gamma} \} \\ &= \int_0^\infty e^{s\gamma} \frac{1}{\bar{\gamma}} e^{-\gamma/\bar{\gamma}} \\ &= \frac{1}{1 + s\bar{\gamma}} \end{aligned} \quad (6.15)$$

As stated above, an important aspect of the moment generating function is that the moment generating function of the sum of two independent random variables is the product of the individual moment generating functions. To see this, let's assume that we have a random variable $z = x + y$ where x and y are independent random variables. The moment generating function of z is

$$\begin{aligned} \Phi_z(s) &= \mathbb{E} \{ e^{sz} \} \\ &= \int_{-\infty}^{\infty} \int_{-\infty}^{\infty} e^{(x+y)s} f_X(x) f_Y(y) dx dy \\ &= \int_{-\infty}^{\infty} e^{xs} f_X(x) dx \int_{-\infty}^{\infty} e^{ys} f_Y(y) dy \\ &= \Phi_x(s) \Phi_y(s) \end{aligned} \quad (6.16)$$

6.2.4 The Complex Sinusoid

We have already used the complex sinusoid extensively in the study of complex baseband. However, we will formally introduce it here. The complex sinusoid is defined as

$$\begin{aligned} e^{jx} &= \cos(x) + j\sin(x) \\ &= \sum_{i=0}^{\infty} \frac{(jx)^i}{i!} \end{aligned} \quad (6.17)$$

$$\begin{aligned}
E \{ e^{jx} \} &= \int_{-\infty}^{\infty} \sum_{i=0}^{\infty} \frac{(jx)^i}{i!} f(x) dx \\
&= \sum_{i=0}^{\infty} \int_{-\infty}^{\infty} \frac{(jx)^i}{i!} f(x) dx \\
&= \sum_{i=0}^{\infty} \frac{j^i}{i!} \underbrace{\int_{-\infty}^{\infty} x^i f(x) dx}_{i\text{th moment about zero}} \\
&= \sum_{i=0}^{\infty} \frac{j^i}{i!} \mu_i
\end{aligned} \tag{6.18}$$

6.2.5 The Characteristic Function

Similar to the moment generator function, the characteristic function is defined as

$$\begin{aligned}
E \{ e^{jx\omega} \} &= \int_{-\infty}^{\infty} e^{jx\omega} f_X(x) dx \\
&\triangleq \phi(\omega)
\end{aligned}$$

This is essentially the Fourier Transform (with $-\omega$ replaced by ω) of the pdf of X and is analogous to the relationship between the Moment Generating Function and the Laplace Transform. This function can be used to generate either the moments or the cumulants. Specifically for the moments:

$$\left[\frac{d^n}{d\omega^n} \phi(\omega) \right]_{\omega=0} = j^n \mu_n \tag{6.19}$$

and for the Cumulants (κ_n is the n th cumulant)

$$c(\omega) = \ln(\phi(\omega)) = \sum_{k=0}^{\infty} \kappa_k \frac{(j\omega)^k}{k!} \tag{6.20}$$

Thus,

$$\kappa_n = j^{-n} \left[\frac{d^n}{d\omega^n} c(\omega) \right]_{\omega=0} \tag{6.21}$$

6.2.6 Gamma Distribution

In the study of the SNR in fading channels, the Gamma distribution is very useful. The Gamma distribution is defined by two parameters a and b :

$$f_X(x) = \frac{a^b x^{b-1} e^{-ax}}{\Gamma(b)} \tag{6.22}$$

for $x > 0$, $a > 0$, $b > 0$. The moment generating function of the Gamma distribution is easily shown to be

$$\Phi(s) = \left(\frac{a}{a-s} \right)^b \tag{6.23}$$

The cumulative distribution function (CDF) is

$$\begin{aligned} F_X(x) &= \int_0^x \frac{a^b y^{b-1} e^{-ay}}{\Gamma(b)} dy \\ &= \frac{1}{\Gamma(b)} \int_0^{ax} z^{b-1} e^{-z} dz \\ &= \frac{\tilde{\gamma}(b, ax)}{\Gamma(b)} \end{aligned} \quad (6.24)$$

where $\tilde{\gamma}(\alpha, \beta)$ is the incomplete gamma function defined as

$$\tilde{\gamma}(\alpha, \beta) = \int_0^\beta \eta^{\alpha-1} e^{-\eta} d\eta \quad (6.25)$$

6.2.7 Chi-Square Distribution

A Gamma distribution where the $a = \frac{1}{2}$ and $b = \frac{k}{2}$ for integer values k is a special case known as the Chi-Square Distribution (or χ^2 Distribution). The pdf and cdf are written as

$$\begin{aligned} f_X(x) &= \frac{1}{2^{k/2} \Gamma(k/2)} x^{k/2-1} e^{-x/2} \\ F_X(x) &= \frac{\tilde{\gamma}(k/2, x/2)}{\Gamma(k/2)} \end{aligned} \quad (6.26)$$

and k is termed the *degrees of freedom*.

6.2.8 The Cauchy-Schwarz Inequality

The Cauchy-Schwarz Inequality is an incredibly important theorem in mathematics. Sometimes also called simply the Schwarz Inequality, the theorem states that for two real length- L vectors \mathbf{x} and \mathbf{y}

$$\begin{aligned} |<\mathbf{x}, \mathbf{y}>|^2 &\leq \langle \mathbf{x}, \mathbf{x} \rangle \langle \mathbf{y}, \mathbf{y} \rangle \\ \left(\sum_{i=1}^L x_i y_i \right)^2 &\leq \left(\sum_{i=1}^L x_i^2 \right) \left(\sum_{i=1}^L y_i^2 \right) \end{aligned} \quad (6.27)$$

with equality holding if and only if $ax_i = by_i$ for arbitrary a and b . The complex version states that

$$\left| \sum_{i=1}^L x_i y_i^* \right|^2 \leq \left(\sum_{i=1}^L |x_i|^2 \right) \left(\sum_{i=1}^L |y_i|^2 \right) \quad (6.28)$$

with equality occurring when $ax_i = by_i$ for arbitrary real values a and b .

6.3 SNR Distribution in Rayleigh Fading

As discussed in Chapter 2, a common model for the wireless channel when there is no line-of-sight component is Rayleigh fading. Rayleigh fading results from the superposition of a large number of phase shifted received signals of roughly equal power. This complex sum results in Gaussian distributed signal voltages in the real and imaginary components and thus a Rayleigh

distributed amplitude. Here we would like to determine the resulting distribution of received signal power (and consequently SNR). Let α be the absolute value (i.e., amplitude) of the channel, i.e., $\alpha = |\tilde{\alpha}| = |\alpha e^{j\phi}|$. For a Rayleigh fading channel the real and imaginary parts of the complex channel are Gaussian distributed and the amplitude distribution is Rayleigh:

$$f_\alpha(a) = \frac{a}{\sigma^2} e^{-\frac{a^2}{2\sigma^2}} \quad 0 \leq a \leq \infty \quad (6.29)$$

where σ is the standard deviation of either of the two i.i.d. Gaussian random variables (i.e., real or imaginary components). Further, $E\{\alpha^2\} = 2\sigma^2$. When we normalize the channel such that $E\{\alpha^2\} = 1$, we have $\sigma^2 = \frac{1}{2}$. If the received signal (during one symbol interval) is written as

$$\tilde{r}(t) = \tilde{\alpha} \sqrt{P_r} x(t) + \tilde{n}(t) \quad (6.30)$$

where P_r is the *average* received power and $\tilde{\alpha} = \alpha e^{j\phi}$ is the normalized complex channel, then at the output of a pulse-matched filter (assuming pulse-amplitude modulated signaling with unit energy symbols s_ν) we have at the ν th symbol

$$r[\nu] = \tilde{\alpha} E_s s_\nu + \tilde{n}[\nu] \quad (6.31)$$

where $\tilde{n}[\nu]$ is $\mathcal{N}(0, N_o E_s)$ and E_s is the energy per symbol. The average SNR per symbol can be written as

$$\gamma = \alpha^2 \frac{E_s}{N_o} \quad (6.32)$$

What is the distribution of the SNR given that α represents the channel amplitude? We know that the transformation of random variables $Y = aX^2$ is accomplished as

$$f_Y(y) = \frac{1}{2a\sqrt{y/a}} f_X\left(\sqrt{\frac{y}{a}}\right) \quad (6.33)$$

Thus, we have

$$\begin{aligned} f_\gamma(\gamma) &= \frac{1}{2\frac{E_s}{N_o}\sqrt{\frac{\gamma}{E_s/N_o}}} f_\alpha\left(\sqrt{\frac{\gamma}{E_s/N_o}}\right) \\ &= \frac{1}{2\frac{E_s}{N_o}\sqrt{\frac{\gamma}{E_s/N_o}}} \frac{\sqrt{\frac{\gamma}{E_s/N_o}}}{\sigma^2} e^{-\frac{\gamma}{2\sigma^2 E_s/N_o}} \\ &= \frac{1}{\bar{\gamma}} e^{-\frac{\gamma}{\bar{\gamma}}} \end{aligned} \quad (6.34)$$

where the average SNR $\bar{\gamma} = 2\sigma^2 \frac{E_s}{N_o} = \frac{E_s}{N_o}$ since $\sigma^2 = \frac{1}{2}$.

The CDF of SNR is then

$$\begin{aligned} F_\gamma(\gamma) &= \int_0^\gamma f_\gamma(x) dx \\ &= \int_0^\gamma \frac{1}{\bar{\gamma}} e^{-\frac{x}{\bar{\gamma}}} dx \\ &= 1 - e^{-\frac{\gamma}{\bar{\gamma}}} \end{aligned}$$

Note that the probability of outage $P_{out}(\gamma_{th}) = F_\gamma(\gamma_{th})$.

6.4 Probability of Bit Error of BPSK in a Rayleigh Fading Channel

It is well known that the probability of error for BPSK in an AWGN channel can be written as

$$P_b^{awgn} = Q\left(\sqrt{2\frac{E_b}{N_o}}\right) \quad (6.35)$$

where

$$Q(x) = \frac{1}{\sqrt{2\pi}} \int_x^\infty e^{-\frac{y^2}{2}} dy \quad (6.36)$$

If we assume that the channel in a Rayleigh fading environment is constant over one symbol, the *average* probability of error for BPSK in Rayleigh fading can be written as

$$\begin{aligned} P_b &= \int_0^\infty f_\gamma(\gamma) Q(\sqrt{2\gamma}) d\gamma \\ &= \int_0^\infty \frac{1}{\gamma} e^{-\frac{\gamma}{2}} Q(\sqrt{2\gamma}) d\gamma \end{aligned} \quad (6.37)$$

where we have set γ as the SNR per bit which is equivalent to the SNR per symbol for BPSK.

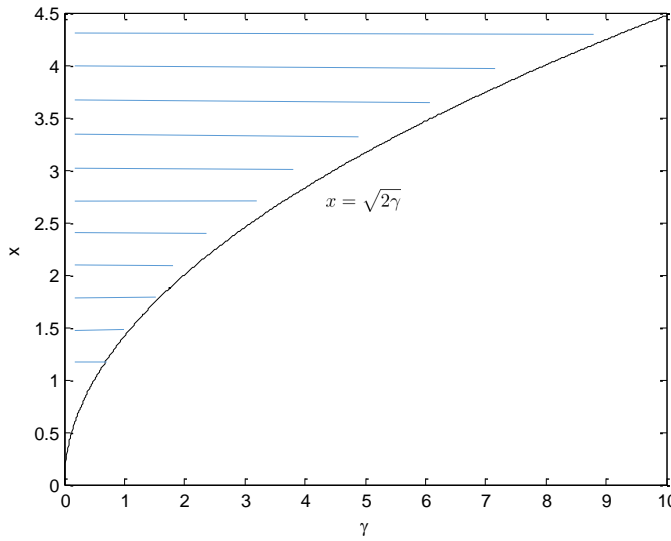


Figure 6.2: Understanding the change in integration limits when reversing the order of integration

Thus, we have (substituting (6.36) for $Q(x)$):

$$P_b = \int_0^\infty \frac{1}{\gamma} e^{-\frac{\gamma}{2}} \frac{1}{\sqrt{2\pi}} \int_{\sqrt{2\gamma}}^\infty e^{-\frac{x^2}{2}} dx d\gamma$$

Now, to proceed we interchange the order of integration. To understand the new limits see Figure

6.2. This results in

$$\begin{aligned}
P_b &= \int_0^\infty \int_0^{x^2/2} \frac{1}{\bar{\gamma}} e^{-\frac{\gamma}{\bar{\gamma}}} \frac{1}{\sqrt{2\pi}} e^{-\frac{x^2}{2}} d\gamma dx \\
&= \int_0^\infty \frac{1}{\sqrt{2\pi}} e^{-\frac{x^2}{2}} \underbrace{\int_0^{x^2/2} \frac{1}{\bar{\gamma}} e^{-\frac{\gamma}{\bar{\gamma}}} d\gamma}_{=1-e^{-x^2/(2\bar{\gamma})}} dx \\
&= \int_0^\infty \frac{1}{\sqrt{2\pi}} e^{-\frac{x^2}{2}} \left(1 - e^{-x^2/(2\bar{\gamma})}\right) dx \\
&= \underbrace{\int_0^\infty \frac{1}{\sqrt{2\pi}} e^{-\frac{x^2}{2}} dx}_{=\frac{1}{2}} - \int_0^\infty \frac{1}{\sqrt{2\pi}} e^{-\frac{x^2}{2} - \frac{x^2}{2\bar{\gamma}}} dx \\
&= \frac{1}{2} - \int_0^\infty \frac{1}{\sqrt{2\pi}} e^{-\frac{x^2}{2} - \frac{x^2}{2\bar{\gamma}}} dx
\end{aligned}$$

Now, let $z = x\sqrt{1 + \frac{1}{\bar{\gamma}}} = x\sqrt{\frac{1+\bar{\gamma}}{\bar{\gamma}}}$ and $dz = dx\sqrt{\frac{1+\bar{\gamma}}{\bar{\gamma}}}$. This provides

$$\begin{aligned}
P_b &= \frac{1}{2} - \int_0^\infty \frac{1}{\sqrt{2\pi}} e^{-\frac{z^2}{2}} \left(\sqrt{\frac{1+\bar{\gamma}}{\bar{\gamma}}}\right)^{-1} dz \\
&= \frac{1}{2} - \sqrt{\frac{\bar{\gamma}}{1+\bar{\gamma}}} \underbrace{\int_0^\infty \frac{1}{\sqrt{2\pi}} e^{-\frac{z^2}{2}} dz}_{=\frac{1}{2}} \\
&= \frac{1}{2} \left(1 - \sqrt{\frac{\bar{\gamma}}{1+\bar{\gamma}}}\right)
\end{aligned} \tag{6.38}$$

For large average SNR $\bar{\gamma} \gg 1$ we have the approximation

$$P_b \approx \frac{1}{4\bar{\gamma}} \tag{6.39}$$

To see this, consider the Taylor Series expansion

$$\sqrt{\frac{1}{1+1/\bar{\gamma}}} \approx 1 - \frac{1}{2\bar{\gamma}} \tag{6.40}$$

Thus,

$$\begin{aligned}
P_b &= \frac{1}{2} \left(1 - \sqrt{\frac{\bar{\gamma}}{1+\bar{\gamma}}}\right) \\
&\approx \frac{1}{2} \left(1 - \left(1 - \frac{1}{2\bar{\gamma}}\right)\right) \\
&= \frac{1}{4\bar{\gamma}}
\end{aligned} \tag{6.41}$$

The impact of Rayleigh fading can be seen in Figure 6.3. The probability of bit error (bit error rate or BER) is plotted for both AWGN and Rayleigh fading for BPSK versus the average SNR per bit $\gamma_b = \frac{E_b}{N_o} = \bar{\gamma}$. We can see two things from the plot. First, we can see that the simple approximation in (6.39) matches well for $E_b/N_o > 10\text{dB}$. Second, and more importantly, Rayleigh fading has a major impact on performance. For example, if a BER of 1% is desired, approximately 9dB of additional received energy is needed (on average) in the case of Rayleigh fading. For higher

BER values, the needed additional energy is even higher. Thus, combating the impact of fading is major design requirement for wireless communications.

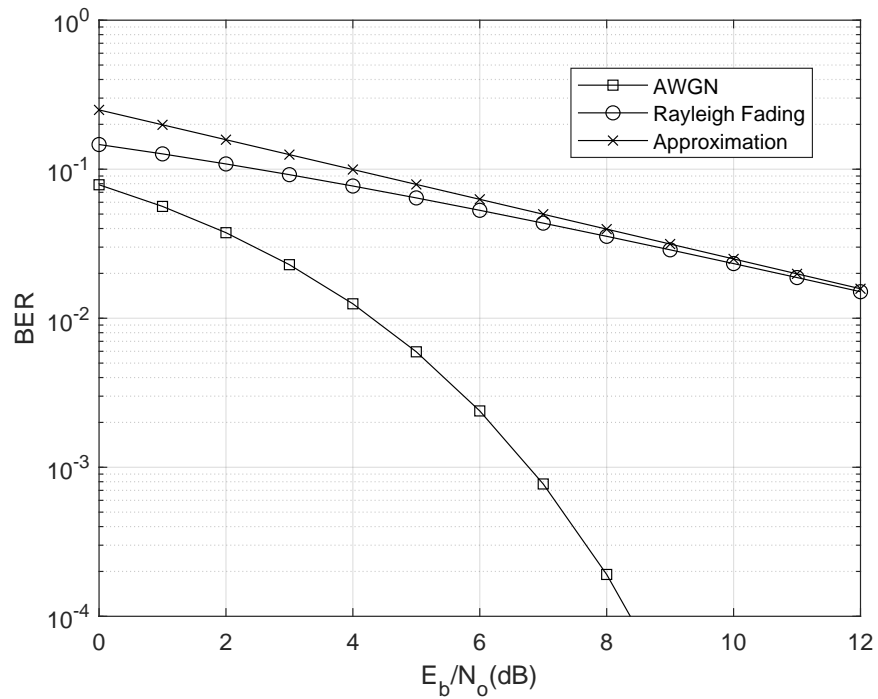


Figure 6.3: Probability of Bit Error for BPSK in AWGN and Rayleigh Fading

6.5 Selection Diversity

In the previous section we saw that Rayleigh fading has a strong negative impact on the bit error rate of wireless communications links. The primary means of mitigating the impact of fading is *diversity*. Diversity is based on the properties of spatial, temporal and/or frequency coherence of the wireless channel. A simple means of achieving diversity is by exploiting the spatial coherence of the wireless channel and using antennas that are spaced greater than that spatial coherence. This is called *spatial diversity*. The simplest form of spatial diversity is known as *selection diversity*. With selection diversity, the receiver uses M_r receive antennas, but only a single receiver preceded by a switch and a simple form of energy measurement. The switch simply chooses the antenna with the largest received energy.

To understand the impact of selection diversity, assume that we observe L i.i.d. channels (frequency, time or antennas). Let γ_i be the SNR seen on the i th channel. The selection diversity mechanism chooses the SNR with the highest SNR (typically by choosing the largest received signal) so that the SNR at the output of the detector is

$$\gamma_{sel} = \max \{\gamma_1, \gamma_2, \dots, \gamma_L\} \quad (6.42)$$

From order statistics we know that for i.i.d. random variables the pdf of the maximum is

$$\begin{aligned} f_{\gamma_{\max}}(\gamma) &= L f_\gamma(\gamma) \left(\int_0^\gamma f_\gamma(x) dx \right)^{L-1} \\ &= L f_\gamma(\gamma) (F_\gamma(\gamma))^{L-1} \end{aligned}$$

where $f_\gamma(\gamma)$ is the pdf of the SNR for all channels (since iid). For Rayleigh fading γ is exponentially distributed thus

$$f_\gamma(\gamma) = \frac{1}{\bar{\gamma}} e^{-\frac{\gamma}{\bar{\gamma}}} \quad \gamma > 0 \quad (6.43)$$

where $\bar{\gamma}$ is the average SNR per channel. Further,

$$F_\gamma(\gamma) = 1 - e^{-\frac{\gamma}{\bar{\gamma}}} \quad (6.44)$$

Thus, we have

$$f_{\gamma_{\max}}(\gamma) = \frac{L}{\bar{\gamma}} e^{-\frac{\gamma}{\bar{\gamma}}} \left(1 - e^{-\frac{\gamma}{\bar{\gamma}}} \right)^{L-1} \quad (6.45)$$

Now, using the binomial expansion

$$(1-x)^n = 1 - nx + \frac{n(n-1)x^2}{2!} - \frac{n(n-1)(n-2)x^3}{3!} + \dots + \frac{n(n-1)(n-2)\dots(n-(n-1))x^n}{n!} \quad (6.46)$$

we can write

$$\begin{aligned}
f_{\gamma_{\max}}(\gamma) &= \frac{L}{\bar{\gamma}} e^{-\frac{\gamma}{\bar{\gamma}}} \left\{ 1 - (L-1)e^{-\frac{\gamma}{\bar{\gamma}}} + \frac{(L-1)(L-2)}{2} e^{-\frac{2\gamma}{\bar{\gamma}}} \dots \right\} \\
&= \frac{1}{\bar{\gamma}} \left\{ L e^{-\frac{\gamma}{\bar{\gamma}}} - L(L-1)e^{-\frac{2\gamma}{\bar{\gamma}}} + \frac{L(L-1)(L-2)}{2} e^{-\frac{3\gamma}{\bar{\gamma}}} \dots + \frac{L(L-1)(L-2)\dots(2)(1)}{(L-1)!} e^{-\frac{L\gamma}{\bar{\gamma}}} \right\} \\
&= \sum_{k=1}^L \binom{L}{k} \frac{k}{\bar{\gamma}} (-1)^{k-1} e^{-\frac{k\gamma}{\bar{\gamma}}}
\end{aligned} \tag{6.47}$$

6.5.1 Probability of Outage

Bit errors in fading channels are dominated by outages, i.e., drops in SNR. Thus, we are interested in the probability that the SNR drops below a specific threshold. That can be found from the cumulative distribution function (CDF). That is

$$\begin{aligned}
P_{out} &= Pr(\gamma \leq \gamma_{th}) \\
&= F_{\gamma_{\max}}(\gamma_{th}) \\
&= (1 - e^{-\frac{\gamma_{th}}{\bar{\gamma}}})^L
\end{aligned} \tag{6.48}$$

For large values of $\bar{\gamma}$

$$(1 - e^{-\frac{\gamma_{th}}{\bar{\gamma}}})^L \approx 1 - L e^{-\frac{\gamma_{th}}{\bar{\gamma}}} \tag{6.49}$$

We say that the diversity order is L since on a log plot, the slope will be related to L . The benefit of selection diversity can be seen in Figure 6.4. We see that even though only a single receiver is ultimately used, the diversity benefit is substantial as large improvements in the outage probability are obtained.

6.5.2 Mean SNR

In addition to improving the probability of outage, diversity can improve the average SNR. This is true of selection diversity even though only one receiver is used. To see this, consider the mean of the maximum SNR:

$$\begin{aligned}
\bar{\gamma}_{\max} &= \int_0^\infty x f_{\gamma_{\max}}(x) dx \\
&= \sum_{k=1}^L \binom{L}{k} \frac{k}{\bar{\gamma}} (-1)^{k-1} \int_0^\infty x e^{-\frac{kx}{\bar{\gamma}}} dx
\end{aligned}$$

Now

$$\begin{aligned}
\int_0^\infty x e^{-\frac{kx}{\bar{\gamma}}} dx &= e^{-\frac{kx}{\bar{\gamma}}} \left[\frac{x}{-k/\bar{\gamma}} - \frac{1}{k^2/\bar{\gamma}^2} \right]_0^\infty \\
&= \frac{\bar{\gamma}^2}{k^2}
\end{aligned}$$

Thus,

$$\begin{aligned}\bar{\gamma}_{max} &= \sum_{k=1}^L \binom{L}{k} \frac{k}{\bar{\gamma}} (-1)^{k-1} \frac{\bar{\gamma}^2}{k^2} \\ &= \bar{\gamma} \sum_{k=1}^L \frac{1}{k}\end{aligned}\quad (6.50)$$

Clearly, selection diversity provides a gain in the average SNR of $\sum_{k=1}^L \frac{1}{k}$.

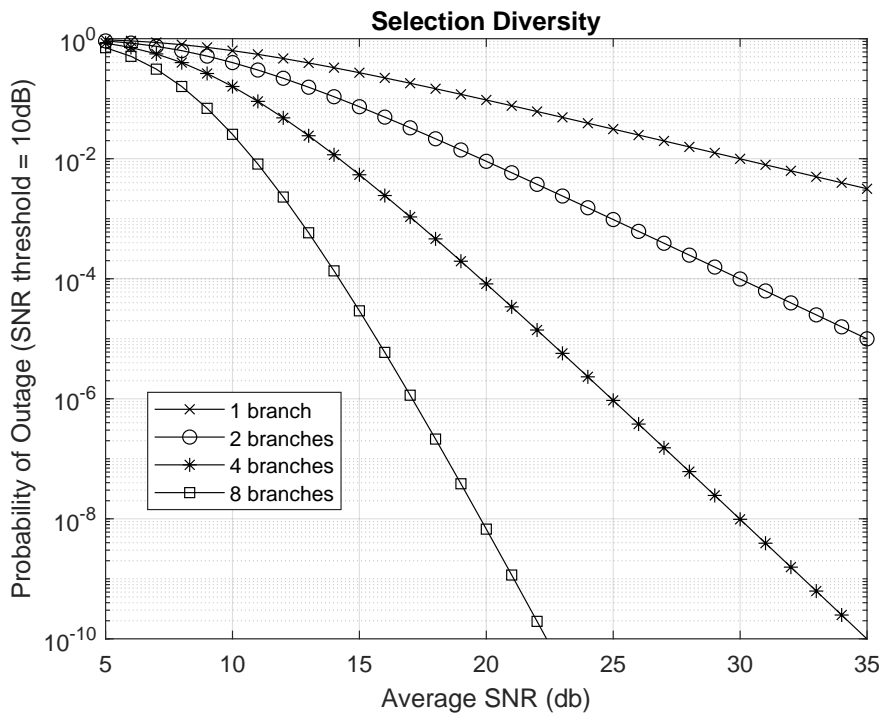


Figure 6.4: Probability of Outage for a Threshold SNR of $\gamma_{th} = 10dB$ in Rayleigh Fading with Selection Diversity

6.5.3 Probability of Bit Error

The probability of bit error can be calculated as

$$P_b = \int_0^\infty f(\gamma)Q(\sqrt{2\gamma})d\gamma \quad (6.51)$$

Using (6.47):

$$\begin{aligned} P_b &= \int_0^\infty \sum_{k=1}^L \binom{L}{k} \frac{k}{\bar{\gamma}} (-1)^{k-1} e^{-\frac{k\gamma}{\bar{\gamma}}} Q(\sqrt{2\gamma}) d\gamma \\ &= \sum_{k=1}^L \binom{L}{k} (-1)^{k-1} \int_0^\infty \frac{k}{\bar{\gamma}} e^{-\frac{k\gamma}{\bar{\gamma}}} Q(\sqrt{2\gamma}) d\gamma \end{aligned} \quad (6.52)$$

Using our result from the probability of bit error for Rayleigh fading without diversity, we obtain the final probability of bit error

$$P_b = \frac{1}{2} \sum_{k=1}^L \binom{L}{k} (-1)^{k-1} \left(1 - \sqrt{\frac{\bar{\gamma}}{k + \bar{\gamma}}} \right) \quad (6.53)$$

The probability of bit error for $L = 1, 2, 4$ is plotted in Figure 6.5. Note that the probability of error is plotted versus the average SNR per bit $\gamma_b = \frac{E_b}{N_o} = \frac{\bar{\gamma}}{\sum_{k=1}^L \frac{1}{k}}$. As with the outage probability, the probability of bit error improves substantially with two or four diversity branches.

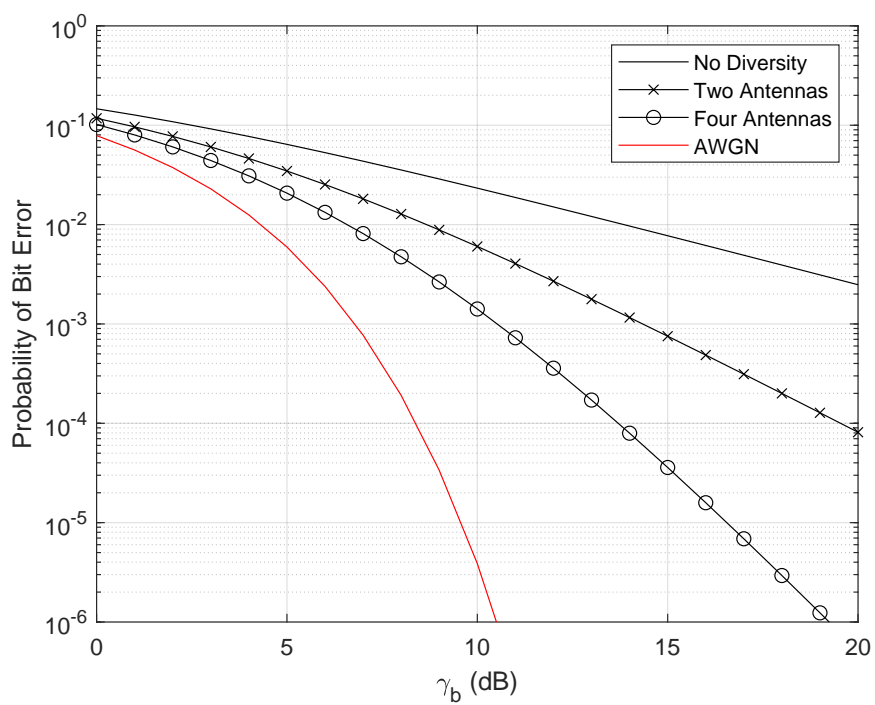


Figure 6.5: Probability of Bit Error (BPSK) in Rayleigh Fading with Selection Diversity

6.6 Equal Gain Combining

Instead of simply selecting the largest SNR, we can improve performance by combining signals. Specifically, we consider coherently combining the signals on L diversity channels. The desired signal adds up coherently while the noise adds up incoherently. If the channel on the i th channel is $\tilde{\alpha}_i = \alpha_i e^{j\phi_i}$, the decision variable is created as

$$z[\nu] = \sum_{i=1}^L r_i[\nu] e^{-j\phi_i} \quad (6.54)$$

The SNR per channel is $\gamma_i = \alpha_i^2 \frac{E_s}{N_o}$. The total SNR is then

$$\gamma_{egc} = \frac{1}{L} \frac{E_s}{N_o} \left(\sum_{i=1}^L \alpha_i^2 \right)^2 \quad (6.55)$$

If we normalize the channel such that $E\{\alpha^2\} = 1$ and $\bar{\gamma}_i = \frac{E_s}{N_o}$. Further, assuming iid channels, we can show that in the case of Rayleigh fading we can approximate the SNR of equal gain combining as

$$f_{\gamma_{egc}}(\gamma) \approx \frac{1}{(L-1)!} \frac{\eta^L}{\bar{\gamma}^L} \gamma^{L-1} e^{-\eta \frac{\gamma}{\bar{\gamma}}} \quad (6.56)$$

where

$$\eta = \frac{L}{2} \left(\frac{(2L-1)!}{(L-1)! 2^{2L-1}} \right)^{-\frac{1}{L}} \quad (6.57)$$

Note that this is a Chi-Square distribution. Further, we can write the average SNR as

$$\bar{\gamma}_{egc} = L \frac{\bar{\gamma}}{\eta} \quad (6.58)$$

The probability of outage is simply

$$\begin{aligned} P_{out}^{egc}(\gamma) &= F_{\gamma_{egc}}(\gamma) \\ &= 1 - e^{-\gamma \frac{\eta}{\bar{\gamma}}} \sum_{k=0}^{L-1} \frac{1}{k!} \left(-\gamma \frac{\eta}{\bar{\gamma}} \right)^k \end{aligned} \quad (6.59)$$

Recalling the series expansion $e^x = \sum_{k=0}^{\infty} \frac{x^k}{k!}$

$$\begin{aligned} P_{out}^{egc}(\gamma) &= 1 - e^{-\gamma \frac{\eta}{\bar{\gamma}}} \left(e^{-\gamma \frac{\eta}{\bar{\gamma}}} - \sum_{k=L}^{\infty} \frac{1}{k!} \left(-\gamma \frac{\eta}{\bar{\gamma}} \right)^k \right) \\ &= e^{-\gamma \frac{\eta}{\bar{\gamma}}} \sum_{k=L}^{\infty} \frac{1}{k!} \left(-\gamma \frac{\eta}{\bar{\gamma}} \right)^k \\ &\approx e^{-\gamma \frac{\eta}{\bar{\gamma}}} \frac{1}{L!} \left(-\gamma \frac{\eta}{\bar{\gamma}} \right)^L \end{aligned} \quad (6.60)$$

where we can see that the outage probability drops to the L th power (or has a slope of L in the log domain). We can this the diversity order or diversity gain. An example for a threshold of 10dB is plotted in Figure 6.6. Note that this is somewhat better than selection diversity due to the increase in average SNR, since both have the same diversity gain.

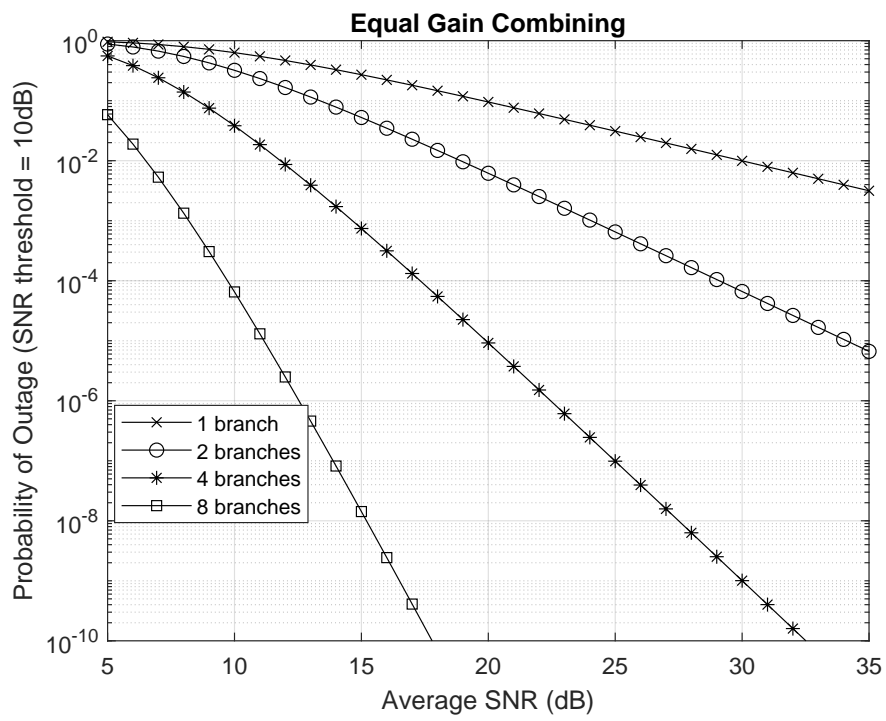


Figure 6.6: Probability of Outage for a Threshold SNR of $\gamma_{th} = 10dB$ in Rayleigh Fading with Equal Gain Combining

6.7 Optimal Combining

It is intuitive that equal gain combining cannot be optimal, since it includes low SNR signals and high SNR signals with equal weight. We would like to determine the optimal weights for combining. To do this, let the received signal on the i th antenna be (assuming all real signals for ease of notation)

$$r_i(t) = \tilde{\alpha}_i(t)x(t) + n_i(t) \quad (6.61)$$

with AWGN $n_i(t)$ having variance σ_n^2 . Further, the instantaneous SNR per channel is

$$\gamma_i = \frac{\alpha_i^2}{\sigma^2} \quad (6.62)$$

After matched filtering we have

$$r_i[\nu] = \tilde{\alpha}_i s_\nu + n_i[\nu] \quad (6.63)$$

or dropping dependence on time

$$r_i = \tilde{\alpha}_i s + n_i \quad (6.64)$$

The decision statistic is formed as

$$\begin{aligned} z &= \sum_{i=1}^L w_i^* r_i \\ &= \sum_{i=1}^L (w_i^* \tilde{\alpha}_i s + w_i^* n_i) \\ &= \underbrace{\sum_{i=1}^L w_i^* \tilde{\alpha}_i s}_{\text{desiredterm}} + \underbrace{\sum_{i=1}^L w_i^* n_i}_{\text{undesiredterm}} \end{aligned}$$

The resulting SNR (for fixed channels $\tilde{\alpha}_i$) is

$$\begin{aligned} \gamma &= \frac{\mathbb{E} \left\{ \left| \sum_{i=1}^L w_i^* \tilde{\alpha}_i s_i \right|^2 \right\}}{\mathbb{E} \left\{ \left| \sum_{i=1}^L w_i^* n_i \right|^2 \right\}} \\ &= \frac{\left| \sum_{i=1}^L w_i^* \tilde{\alpha}_i \right|^2}{\sum_{i=1}^L |w_i|^2 \sigma_n^2} \end{aligned} \quad (6.65)$$

Now, define $x_i = \frac{\tilde{\alpha}_i}{\sigma_n}$ and $y_i = w_i \sigma_n$. From the complex version of Schwarz' Inequality

$$\left| \sum_{i=1}^L w_i^* \tilde{\alpha}_i \right|^2 \leq \sum_{i=1}^L |w_i|^2 \sigma_n^2 \sum_{i=1}^L \underbrace{\frac{|\tilde{\alpha}_i|^2}{\sigma_n^2}}_{\gamma_i} \quad (6.66)$$

Or in other words

$$\gamma = \frac{\left(\sum_{i=1}^L w_i^* \tilde{\alpha}_i \right)^2}{\sum_{i=1}^L |w_i|^2 \sigma_n^2} \leq \sum_{i=1}^L \gamma_i \quad (6.67)$$

with equality occurring iff $a w_i \sigma_n = b \tilde{\alpha}_i / \sigma_n$ or in other words $w_i = c \frac{\tilde{\alpha}_i}{\sigma_n^2}$ since $c = b/a$ is arbitrary, we choose it to be $c = \sigma_n^2$ and thus,

$$w_i = \tilde{\alpha}_i \quad (6.68)$$

We term this **Maximal Ratio Combining**. Further, we see that the optimal SNR as

$$\gamma_{mrc} = \sum_{i=1}^L \gamma_i \quad (6.69)$$

6.7.1 SNR Distribution

For a Rayleigh channel with iid channels (each having average SNR $\bar{\gamma}$), we know that the SNR is the sum of the SNRs per channel. The moment generating function can be written as:

$$\begin{aligned} \Phi_{\gamma_{mrc}}(s) &= \prod_{i=1}^L \Phi_{\gamma_i}(s) \\ &= \prod_{i=1}^L \frac{1}{1 + s\bar{\gamma}} \\ &= \frac{1}{(1 + s\bar{\gamma})^L} \end{aligned} \quad (6.70)$$

Taking the inverse Laplace Transform we have

$$f_{\gamma_{mrc}}(\gamma) = \frac{1}{(L-1)!} \frac{\gamma^{L-1}}{\bar{\gamma}^L} e^{-\frac{\gamma}{\bar{\gamma}}} \quad \gamma > 0 \quad (6.71)$$

Note, that this is a Chi-Square distribution with $2L$ degrees of freedom. Further, the mean SNR is

$$\bar{\gamma}_{mrc} = L\bar{\gamma} \quad (6.72)$$

6.7.2 Probability of Outage

For Rayleigh fading channels, the probability of outage is

$$\begin{aligned} P_{out}^{mrc}(\gamma_{th}) &= F_{\gamma_{mrc}}(\gamma_{th}) = 1 - e^{-\frac{\gamma_{th}}{\bar{\gamma}}} \sum_{k=0}^{L-1} \frac{1}{k!} \left(\frac{\gamma_{th}}{\bar{\gamma}} \right)^k \\ &\approx e^{-\frac{\gamma_{th}}{\bar{\gamma}}} \frac{1}{L!} \left(\frac{\gamma_{th}}{\bar{\gamma}} \right)^L \end{aligned} \quad (6.73)$$

for large values of $\bar{\gamma}$. The probability of outage is plotted in Figure fig:mrc for $L = 1, 2, 4$. We can see that MRC provides a tremendous improvement over no diversity, especially in terms of the average SNR improvement.

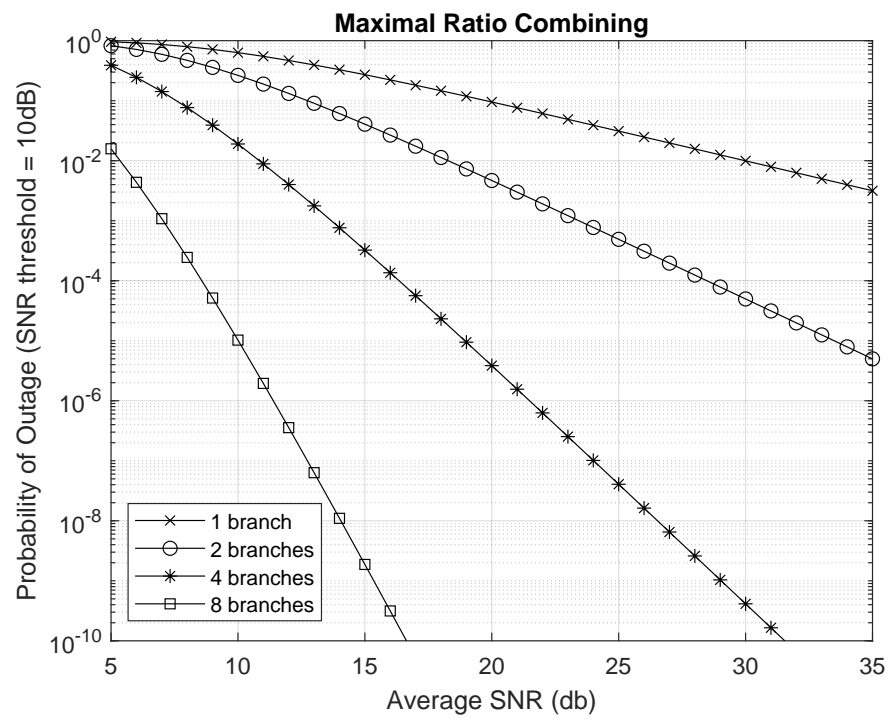


Figure 6.7: Probability of Outage for a Threshold SNR of $\gamma_{th} = 10dB$ in Rayleigh Fading with Maximal Ratio Combining

6.7.3 Bit Error Rate for BPSK

We can find the probability of bit error for BPSK by using (6.71) in (6.37) which gives

$$P_b = \int_0^\infty \frac{1}{(L-1)!} \frac{\gamma^{L-1}}{\bar{\gamma}^L} e^{-\gamma/\bar{\gamma}} Q\left(\sqrt{2\gamma}\right) d\gamma \quad (6.74)$$

Now, we can integrate this as we did previously, but the integration is a bit more difficult. Again, replacing $Q(x)$ with its integral definition:

$$\begin{aligned} P_b &= \int_0^\infty \int_{-\infty}^{\sqrt{2\gamma}} \frac{1}{\sqrt{2\pi}} e^{-x^2/2} \frac{1}{(L-1)!} \frac{\gamma^{L-1}}{\bar{\gamma}^L} e^{-\gamma/\bar{\gamma}} dx d\gamma \\ &= \int_0^\infty \left\{ \int_0^{x^2/2} \frac{1}{(L-1)!} \frac{\gamma^{L-1}}{\bar{\gamma}^L} e^{-\gamma/\bar{\gamma}} d\gamma \right\} \frac{1}{\sqrt{2\pi}} e^{-x^2/2} dx \\ &= \frac{1}{(L-1)!} \frac{1}{\bar{\gamma}^L} \int_0^\infty \left\{ \int_0^{x^2/2} \gamma^{L-1} e^{-\gamma/\bar{\gamma}} d\gamma \right\} \frac{1}{\sqrt{2\pi}} e^{-x^2/2} dx \end{aligned} \quad (6.75)$$

The inner integral can be solved using integration by parts:

$$\int \gamma^{L-1} e^{-\gamma/\bar{\gamma}} d\gamma = -e^{-\gamma/\bar{\gamma}} \sum_{i=0}^{L-1} \bar{\gamma}^{L-i} \gamma^i \frac{(L-1)!}{i!} \quad (6.76)$$

Applying the limits we get for the inner integral

$$\bar{\gamma}^L (L-1)! - e^{-x^2/(2\bar{\gamma})} \sum_{i=0}^{L-1} \bar{\gamma}^{L-i} \left(\frac{x^2}{2}\right)^i \frac{(L-1)!}{i!} \quad (6.77)$$

Using this in (6.75) gives

$$P_b = \frac{1}{(L-1)!} \frac{1}{\bar{\gamma}^L} \left\{ \int_0^\infty \frac{1}{\sqrt{2\pi}} e^{-x^2/2} \bar{\gamma}^L (L-1)! dx - \int_0^\infty \frac{1}{\sqrt{2\pi}} e^{-x^2/2} e^{-x^2/(2\bar{\gamma})} \sum_{i=0}^{L-1} \bar{\gamma}^{L-i} \left(\frac{x^2}{2}\right)^i \frac{(L-1)!}{i!} dx \right\} \quad (6.78)$$

Simplifying,

$$P_b = \frac{1}{2} - \int_0^\infty \frac{1}{\sqrt{2\pi}} e^{-(x^2/2+x^2/(2\bar{\gamma}))} \sum_{i=0}^{L-1} \frac{1}{\bar{\gamma}^i} \left(\frac{x^2}{2}\right)^i \frac{1}{i!} dx \quad (6.79)$$

$$= \frac{1}{2} - \sum_{i=0}^{L-1} \frac{1}{\bar{\gamma}^i} \frac{1}{i!} \frac{1}{2^i} \int_0^\infty \frac{x^{2i}}{\sqrt{2\pi}} e^{-(x^2/2)(1+1/\bar{\gamma})} dx \quad (6.80)$$

Now, using integration tables we can find

$$\int_0^\infty x^{2i} e^{-kx^2} dx = \frac{(2i-1)!!}{2^{i+1} k^i} \sqrt{\frac{\pi}{k}} \quad (6.81)$$

Thus,

$$P_b = \frac{1}{2} - \sum_{i=0}^{L-1} \frac{1}{\bar{\gamma}^i} \frac{1}{i!} \frac{1}{2^i} \frac{1}{\sqrt{2\pi}} \frac{(2i-1)!!}{2^{i+1} \left(\frac{1}{2} \left(1 + \frac{1}{\bar{\gamma}}\right)\right)^i} \sqrt{\frac{2\pi}{1 + \frac{1}{\bar{\gamma}}}} \quad (6.82)$$

Using $(2i - 1)!! = \frac{(2i)!}{2^i i!}$ we obtain

$$P_b = \frac{1}{2} - \frac{1}{2} \sqrt{\frac{\bar{\gamma}}{1 + \bar{\gamma}}} \sum_{i=0}^{L-1} \binom{2i}{i} \left(\frac{1}{4} \frac{1}{1 + \bar{\gamma}} \right)^i \quad (6.83)$$

Alternate Derivation

Another way of solving the problem is as follows. First, Alouini and Simon show that the following integral can be used for the Q -function[8]:

$$Q(x) = \frac{1}{\pi} \int_0^{\pi/2} \exp \left(-\frac{x^2}{2 \sin^2(\theta)} \right) d\theta \quad (6.84)$$

Thus, we can write the probability of error as

$$\begin{aligned} P_b &= \int_0^\infty \frac{1}{\pi} \int_0^{\pi/2} \exp \left(-\frac{\gamma}{\sin^2(\theta)} \right) f_\gamma(\gamma) d\theta d\gamma \\ &= \frac{1}{\pi} \int_0^{\pi/2} \int_0^\infty \exp \left(-\frac{\gamma}{\sin^2(\theta)} \right) f_\gamma(\gamma) d\gamma d\theta \end{aligned}$$

However, the definition of the moment-generating function

$$\Phi(s) = \int_{-\infty}^{\infty} e^{s\gamma} f_\gamma(\gamma) d\gamma \quad (6.85)$$

Thus,

$$\int_0^\infty \exp \left(-\frac{\gamma}{\sin^2(\theta)} \right) f_\gamma(\gamma) d\gamma = \Phi \left(-\frac{1}{\sin^2(\theta)} \right) \quad (6.86)$$

and

$$P_b = \frac{1}{\pi} \int_0^{\pi/2} \Phi \left(-\frac{1}{\sin^2(\theta)} \right) d\theta \quad (6.87)$$

Now, we know that for MRC

$$\Phi(s) = \left(\frac{1}{1 - s\bar{\gamma}} \right)^L \quad (6.88)$$

Thus,

$$P_b = \frac{1}{\pi} \int_0^{\pi/2} \left(\frac{1}{1 + \frac{\bar{\gamma}}{\sin^2(\theta)}} \right)^L d\theta \quad (6.89)$$

$$= \frac{1}{\pi} \int_0^{\pi/2} \left(\frac{\sin^2(\theta)}{\sin^2(\theta) + \bar{\gamma}} \right)^L d\theta \quad (6.90)$$

It is shown in [8] that

$$\frac{1}{\pi} \int_0^{\pi/2} \left(\frac{\sin^2(\theta)}{\sin^2(\theta) + a} \right)^m d\theta = \frac{1}{2} \left[1 - \mu(a) \sum_{k=0}^{m-1} \binom{2k}{k} \left(\frac{1 - \mu^2(a)}{4} \right)^k \right] \quad (6.91)$$

where

$$\mu(a) = \sqrt{\frac{a}{1+a}} \quad (6.92)$$

Further, it is also shown in [8] the integral can also be written as

$$\frac{1}{\pi} \int_0^{\pi/2} \left(\frac{\sin^2(\theta)}{\sin^2(\theta) + a} \right)^m d\theta = \left(\frac{1 - \mu(a)}{2} \right)^m \sum_{k=0}^{m-1} \binom{m-1+k}{k} \left(\frac{1 + \mu(a)}{2} \right)^k \quad (6.93)$$

Using the first solution of (6.91) in (6.90) results in,

$$P_b = \frac{1}{\pi} \int_0^{\pi/2} \left(\frac{\sin^2(\theta)}{\sin^2(\theta) + \bar{\gamma}} \right)^L d\theta \quad (6.94)$$

$$= \frac{1}{2} \left[1 - \sqrt{\frac{\bar{\gamma}}{1+\bar{\gamma}}} \sum_{k=0}^{L-1} \binom{2k}{k} \left(\frac{1 - \frac{\bar{\gamma}}{1+\bar{\gamma}}}{4} \right)^k \right] \quad (6.95)$$

$$= \frac{1}{2} \left[1 - \sqrt{\frac{\bar{\gamma}}{1+\bar{\gamma}}} \sum_{k=0}^{L-1} \binom{2k}{k} \left(\frac{1}{4} \frac{1}{1+\bar{\gamma}} \right)^k \right] \quad (6.96)$$

which is equivalent to our previous result.

Using the second integral solution from (6.93) in (6.90) results in

$$P_b = \left[\frac{1}{2} \left(1 - \sqrt{\frac{\bar{\gamma}}{1+\bar{\gamma}}} \right) \right]^L \sum_{k=0}^{L-1} \binom{L-1+k}{k} \left[\frac{1}{2} \left(1 + \sqrt{\frac{\bar{\gamma}}{1+\bar{\gamma}}} \right) \right]^k \quad (6.97)$$

The performance for $L = 1, 2, 4$ branches is plotted in Figure and 6.8. We can see that on an *SNR per bit* basis, the difference between MRC and selection diversity is very small. This tells us that the *diversity gain* is essentially the same. Note that even with four branches, there is still a large difference between the fading case and AWGN (no fading). Comparing the performance from an SNR per branch perspective, we can see more difference between MRC and selection diversity due to the better average SNR improvement from coherent combining. There is also a larger improvement when adding more antennas.

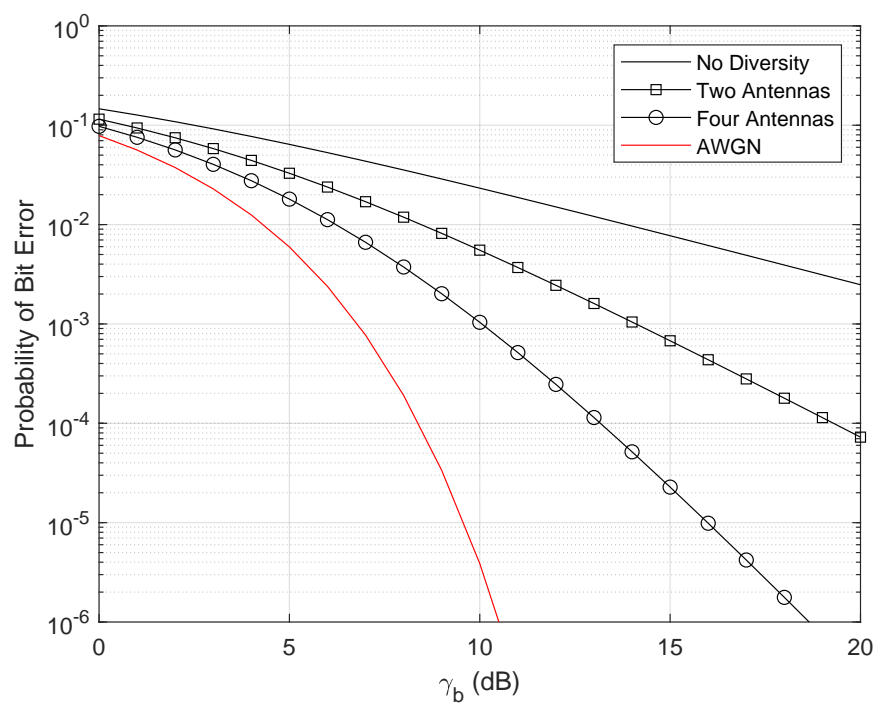


Figure 6.8: Probability of Bit Error (BPSK) in Rayleigh Fading with Maximal Ratio Combining

6.7.4 Impact of Unequal Powers on MRC

To this point we have assumed that each branch has equal average power and thus equal average SNR $\bar{\gamma}$. What if the average SNRs are different? We will show that this does have an effect on overall performance. To see this recall that the SNR of MRC is

$$\gamma_{mrc} = \sum_{i=1}^L \gamma_i \quad (6.98)$$

where $\gamma_i = \frac{\alpha_i^2}{\sigma_n^2}$. The SNR per channel (Rayleigh fading):

$$f_{\gamma_i}(\gamma) = \frac{1}{\bar{\gamma}_i} e^{-\frac{\gamma}{\bar{\gamma}_i}} \quad \gamma > 0 \quad (6.99)$$

The Moment-Generating Function for the SNR per channel is defined as

$$\begin{aligned} \Phi(s) &= \text{E}_{\gamma} \{e^{-s\gamma}\} \\ &= \int_0^\infty e^{-s\gamma} \frac{1}{\bar{\gamma}_i} e^{-\frac{\gamma}{\bar{\gamma}_i}} d\gamma \\ &= \frac{1}{1 + s\bar{\gamma}_i} \end{aligned} \quad (6.100)$$

The Moment Generating Function of γ_{mrc} is the product of L moment generating functions

$$\begin{aligned} \Phi(s) &= \frac{1}{\prod_{i=1}^L (1 + s\bar{\gamma}_i)} \\ &= \sum_{i=1}^L \frac{\eta_i}{1 + s\bar{\gamma}_i} \\ &= \sum_{i=1}^L \frac{\bar{\gamma}_i^{L-1}}{\prod_{k \neq i} (\bar{\gamma}_i - \bar{\gamma}_k)} \frac{1}{1 + s\bar{\gamma}_i} \end{aligned} \quad (6.101)$$

Taking the inverse Laplace Transform:

$$f_{\gamma}(\gamma) = \sum_{i=1}^L \frac{\bar{\gamma}_i^{L-2}}{\prod_{k \neq i} (\bar{\gamma}_i - \bar{\gamma}_k)} e^{-\frac{\gamma}{\bar{\gamma}_i}} \quad (6.102)$$

The outage probability (cdf) is

$$P_{out} = F_{\gamma}(\gamma_{th}) = \sum_{i=1}^L \frac{\bar{\gamma}_i^{L-1}}{\prod_{k \neq i} (\bar{\gamma}_i - \bar{\gamma}_k)} \left(1 - e^{-\frac{\gamma_{th}}{\bar{\gamma}_i}}\right) \quad (6.103)$$

The mean SNR is

$$\begin{aligned}
\bar{\gamma}_{mrc} &= \int_0^\infty \gamma \left(\sum_{i=1}^L \frac{\bar{\gamma}_i^{L-2}}{\prod_{k \neq i} (\bar{\gamma}_i - \bar{\gamma}_k)} e^{-\frac{\gamma}{\bar{\gamma}_i}} \right) d\gamma \\
&= \sum_{i=1}^L \frac{\bar{\gamma}_i^{L-2}}{\prod_{k \neq i} (\bar{\gamma}_i - \bar{\gamma}_k)} \int_0^\infty \gamma e^{-\frac{\gamma}{\bar{\gamma}_i}} d\gamma \\
&= \sum_{i=1}^L \frac{\bar{\gamma}_i^{L-1}}{\prod_{k \neq i} (\bar{\gamma}_i - \bar{\gamma}_k)} \underbrace{\int_0^\infty \frac{\gamma}{\bar{\gamma}_i} e^{-\frac{\gamma}{\bar{\gamma}_i}} d\gamma}_{=\bar{\gamma}_i} \\
&= \sum_{i=1}^L \frac{\bar{\gamma}_i^L}{\prod_{k \neq i} (\bar{\gamma}_i - \bar{\gamma}_k)}
\end{aligned} \tag{6.104}$$

The probability of bit error for BPSK can be found as

$$\begin{aligned}
P_b &= \int_0^\infty f_\gamma(\gamma) Q(\sqrt{(2\gamma)}) d\gamma \\
&= \int_0^\infty \sum_{i=1}^L \frac{\bar{\gamma}_i^{L-2}}{\prod_{k \neq i} (\bar{\gamma}_i - \bar{\gamma}_k)} e^{-\frac{\gamma}{\bar{\gamma}_i}} Q(\sqrt{(2\gamma)}) d\gamma \\
&= \sum_{i=1}^L \frac{\bar{\gamma}_i^{L-2}}{\prod_{k \neq i} (\bar{\gamma}_i - \bar{\gamma}_k)} \int_0^\infty e^{-\frac{\gamma}{\bar{\gamma}_i}} Q(\sqrt{(2\gamma)}) d\gamma \\
&= \sum_{i=1}^L \frac{\bar{\gamma}_i^{L-1}}{\prod_{k \neq i} (\bar{\gamma}_i - \bar{\gamma}_k)} \underbrace{\int_0^\infty \frac{1}{\bar{\gamma}_i} e^{-\frac{\gamma}{\bar{\gamma}_i}} Q(\sqrt{(2\gamma)}) d\gamma}_{\frac{1}{2}(1-\sqrt{\frac{\bar{\gamma}_i}{1+\bar{\gamma}_i}})} \\
&= \frac{1}{2} \sum_{i=1}^L \frac{\bar{\gamma}_i^{L-1}}{\prod_{k \neq i} (\bar{\gamma}_i - \bar{\gamma}_k)} \left(1 - \sqrt{\frac{\bar{\gamma}_i}{1+\bar{\gamma}_i}} \right)
\end{aligned} \tag{6.105}$$

6.8 Diversity Schemes Compared

In the previous section we compared three different diversity combining techniques: selection, equal gain combining, and maximal ratio combining. All three are fairly similar in terms of the SNR improvement. More specifically, as shown in Tables 6.1 and 6.2, all three combining techniques achieve the same diversity gain and thus show the same slope in log-log plot of BER vs SNR per bit. On the other hand, the three techniques do differ in terms of the mean SNR improvement. Selection combining provides the least improvement followed by equal gain combining with MRC providing the largest improvement. For a small number of antennas, the difference is relatively minor, but as the number of antennas (more generally diversity branches) grows, the difference becomes much larger as seen in Figure 6.9. The resulting benefit in terms of the bit error rate is shown in Figure 6.10. Note that the BER is plotted versus SNR per bit $\gamma_b = \frac{E_b}{N_o}$ as opposed to SNR per branch γ_c . If the results were plotted versus SNR per branch (which includes the average SNR improvement), the benefits of MRC would have been larger. Also, note that the performance of equal gain combining falls between the other two techniques.

Table 6.1: General Relationship between Diversity Schemes

	Average SNR Gain	Diversity Order
Selection Combining	$\sum_{k=1}^L \frac{1}{k}$	L
Equal Gain Combining	$2 \left(\frac{(2L-1)!}{(L-1)! 2^{2L-1}} \right)^{\frac{1}{L}}$	L
Maximal Ratio Combining	L	L

Table 6.2: Example with $L = 4$

	Average SNR Gain	Diversity Order
Selection Combining	2.08	4
Equal Gain Combining	3.2	4
Maximal Ratio Combining	4	4

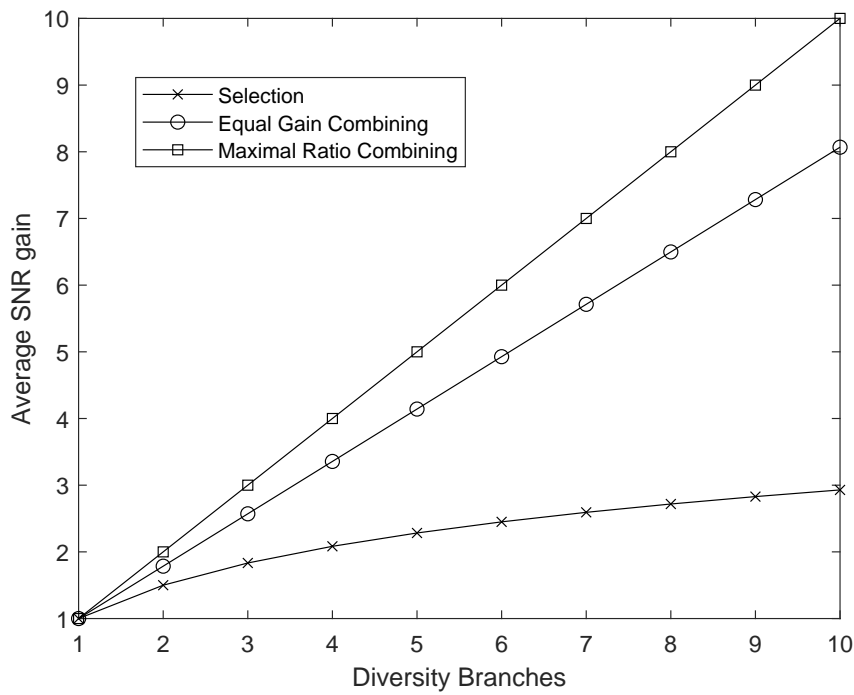


Figure 6.9: Comparison of the Average SNR Gains for Different Diversity Combining Techniques

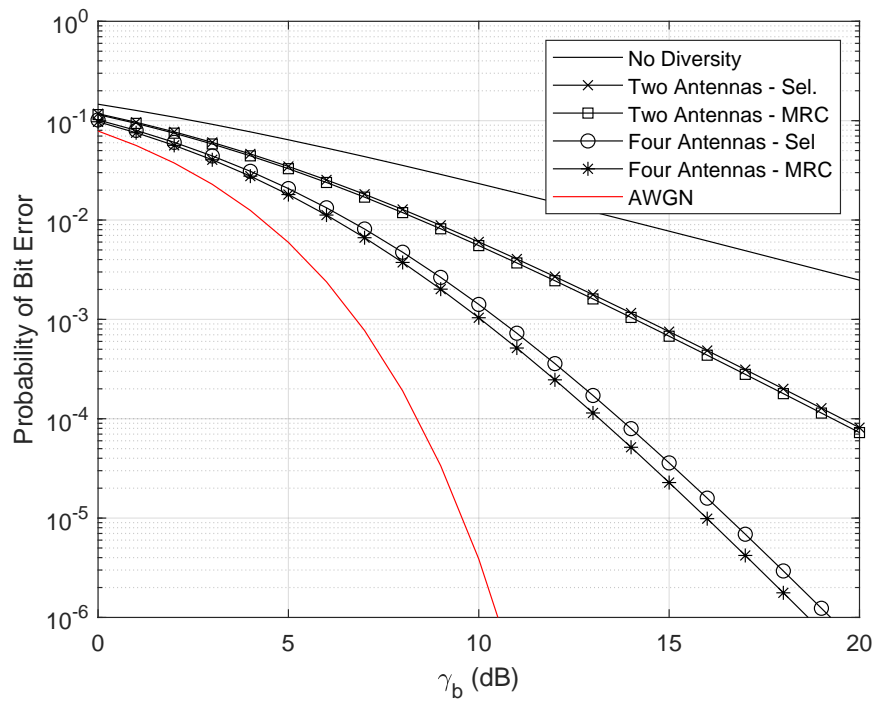


Figure 6.10: Comparison of the Probability of Bit Error (BPSK) in Rayleigh Fading with Selection Diversity and Maximal Ratio Combining

6.9 Generalized Selection Combining

Let $\gamma_1, \gamma_2, \dots, \gamma_L$ be the SNR on L channels. For any instantiation let's redefine them as g_1, g_2, \dots, g_L such that $g_1 > g_2 > \dots > g_L$. Now further, we select the first L_c values: g_1, g_2, \dots, g_{L_c} . If we combine these via MRC, we have an SNR

$$\gamma_{gsc} = \sum_{i=1}^{L_c} g_i \quad (6.106)$$

It can be shown that for iid γ_i , the joint pdf can be written as

$$f_{g_1, g_2, \dots, g_{L_c}}(g_1, g_2, \dots, g_{L_c}) = L_c! \begin{pmatrix} L \\ L_c \end{pmatrix} [F_\gamma(g_{L_c})]^{L-L_c} \prod_{i=1}^{L_c} f_\gamma(g_i) \quad (6.107)$$

where $f_\gamma(\gamma)$ and $F_\gamma(\gamma)$ are the pdf and cdf of the SNR per branch. Now, to find the pdf of γ_{gsc} we can use the moment generating function approach (as before):

$$\begin{aligned} \Phi(s) &= E_{\gamma_{gsc}} \{ e^{s\gamma_{gsc}} \} \\ &= E_{\gamma_1, \gamma_2, \dots, \gamma_L} \left\{ e^{s \sum_{i=1}^{L_c} g_i} \right\} \\ &= \underbrace{\int_0^\infty \int_{g_{L_c}}^\infty \int_{g_{L_c-1}}^\infty \dots \int_{g_2}^\infty}_{L_c-fold} f_{g_1, g_2, \dots, g_{L_c}}(g_1, g_2, \dots, g_{L_c}) e^{s \sum_{i=1}^{L_c} g_i} dg_1 dg_2 \dots dg_{L_c} \end{aligned}$$

Unfortunately, this isn't separable as in the case of MRC (since g_i are not independent). Trick: we will define

$$\begin{aligned} x_k &\stackrel{\triangle}{=} g_k - g_{k+1} \\ x_L &\stackrel{\triangle}{=} g_L \end{aligned}$$

It can be shown that the x_i are independent with exponential distribution:

$$f_{x_i}(x) = \frac{1}{\bar{\gamma}} e^{-\frac{ix}{\bar{\gamma}}} \quad x > 0 \quad i = 1, 2, \dots, L \quad (6.108)$$

Now,

$$\begin{aligned} \gamma_{gsc} &= \sum_{i=1}^{L_c} g_i \\ &= \sum_{i=1}^{L_c} \sum_{k=i}^L x_k \end{aligned}$$

Thus,

$$\begin{aligned} \Phi_{\gamma_{gsc}}(s) &= \underbrace{\int_0^\infty \int_0^\infty \int_0^\infty \dots \int_0^\infty}_{L-fold} f_{x_1, x_2, \dots, x_L}(x_1, x_2, \dots, x_L) e^{s \sum_{i=1}^{L_c} \sum_{k=i}^L x_i} dx_1 dx_2 \dots dx_L \\ &= \underbrace{\int_0^\infty \int_0^\infty \int_0^\infty \dots \int_0^\infty}_{L-fold} \prod_{i=1}^L \frac{1}{\bar{\gamma}} e^{-\frac{ix_i}{\bar{\gamma}}} e^{s \sum_{i=1}^{L_c} \sum_{k=i}^L x_i} dx_1 dx_2 \dots dx_L \end{aligned}$$

We can write

$$\sum_{i=1}^{L_c} \sum_{k=i}^L x_i = x_1 + 2x_2 + 3x_3 + \dots L_c x_{L_c} + L_c x_{L_c+1} + L_c x_{L_c+2} + \dots L_c x_L \quad (6.109)$$

Thus, we have

$$\begin{aligned} \Phi_{\gamma_{gsc}}(s) &= \int_0^\infty e^{sx_1} \frac{1}{\bar{\gamma}} e^{-\frac{x_1}{\bar{\gamma}}} dx_1 \int_0^\infty e^{2sx_2} \frac{1}{\bar{\gamma}} e^{-\frac{2x_2}{\bar{\gamma}}} dx_2 + \dots \int_0^\infty e^{L_c s x_L} \frac{1}{\bar{\gamma}} e^{-L_c \frac{x_L}{\bar{\gamma}}} dx_L \\ &= (1 - s\bar{\gamma})^{-L_c+1} \prod_{k=L_c}^L (1 - s\bar{\gamma} L_c/k)^{-1} \end{aligned}$$

Through partial fraction expansion,

$$\Phi_{\gamma_{gsc}}(s) = (1 - s\bar{\gamma})^{-L_c+1} \sum_{k=0}^{L-L_c} (-1)^k \binom{L}{L_c} \binom{L-L_c}{k} \frac{1}{1 + k/L_c - s\bar{\gamma}} \quad (6.110)$$

Using inverse Laplace Transform identities we arrive at

$$\begin{aligned} f_{\gamma_{gsc}}(\gamma) &= \binom{L}{L_c} \left[\frac{\gamma^{L_c-1} e^{-\gamma/\bar{\gamma}}}{\bar{\gamma}^{L_c} (L_c-1)!} + \dots \right. \\ &\quad \left. \frac{1}{\bar{\gamma}} \sum_{k=1}^{L-L_c} (-1)^{L_c+k-1} \binom{L-L_c}{k} \left(\frac{L_c}{k} \right)^{L_c-1} e^{-\gamma/\bar{\gamma}} \left(e^{-k\gamma/L_c\bar{\gamma}} - \sum_{m=0}^{L_c-2} \frac{1}{m!} \left(-\frac{k\gamma}{L_c\bar{\gamma}} \right)^m \right) \right] \end{aligned}$$

We can check this and show that it reduces properly for the cases of $L_c = L$ or $L_c = 1$.

6.9.1 Outage Probability

$$\begin{aligned} F_{\gamma_{gsc}}(\gamma) &= \binom{L}{L_c} \left[1 - e^{-\gamma/\bar{\gamma}} \sum_{k=0}^{L_c-1} \frac{1}{k!} \left(\frac{\gamma_{th}}{\bar{\gamma}} \right)^k + \sum_{k=1}^{L-L_c} (-1)^{L_c+k-1} \binom{L-L_c}{k} \left(\frac{L_c}{k} \right)^{L_c-1} \right. \\ &\quad \times \left. \left(\frac{1 - e^{-(1+k/L_c)(\gamma_{th}/\bar{\gamma})}}{1 + k/L_c} - \sum_{m=0}^{L_c-2} \left(\frac{-k}{L_c} \right)^m \left(1 - e^{-\gamma_{th}/\bar{\gamma}} \sum_{n=0}^m \frac{1}{n!} \left(\frac{\gamma_{th}}{\bar{\gamma}} \right)^n \right) \right) \right] \quad (6.111) \end{aligned}$$

6.9.2 Mean SNR Analysis

The mean SNR of generalized selection combining is

$$\begin{aligned} \bar{\gamma}_{gsc} &= L_c \bar{\gamma} + \sum_{k=L_c+1}^L \frac{L_c \bar{\gamma}}{k} \\ &= L_c \bar{\gamma} \left(1 + \sum_{k=L_c+1}^L \frac{1}{k} \right) \end{aligned}$$

The improvement in average SNR is

$$\frac{\bar{\gamma}_{gsc}}{\bar{\gamma}} = L_c \left(1 + \sum_{k=L_c+1}^L \frac{1}{k} \right)$$

Checking the extreme cases: $L_c = L$ (MRC)

$$\frac{\bar{\gamma}_{gsc}}{\bar{\gamma}} = L$$

Also for $L_c = 1$ (selection combining):

$$\frac{\bar{\gamma}_{gsc}}{\bar{\gamma}} = \left(1 + \sum_{k=2}^L \frac{1}{k}\right) = \left(\sum_{k=1}^L \frac{1}{k}\right)$$

6.10 Nakagami Fading

Consider the amplitude distribution

$$f_\alpha(\alpha) = \frac{2}{\Gamma(m)} \left(\frac{m}{2\sigma^2}\right)^m \alpha^{2m-1} e^{-m\alpha^2/2\sigma^2} \quad (6.112)$$

Note that $E\{\alpha^2\} = 2\sigma^2$. Note that $m = 1 \rightarrow$ Rayleigh. Again, if we let $\gamma = \alpha^2 \frac{E_s}{N_o}$ and $\sigma^2 = 1/2$, what is the distribution of γ ? Using the transformation of random variables described above we obtain

$$\begin{aligned} f_\gamma(\gamma) &= \frac{1}{2E_s/N_o \sqrt{\gamma/(E_s/N_o)}} \frac{2}{\Gamma(m)} \left(\frac{m}{2\sigma^2}\right)^m \left(\frac{\gamma}{E_s/N_o}\right)^{\frac{2m-1}{2}} e^{-\frac{m\gamma}{2\sigma^2 E_s/N_o}} \\ &= \frac{1}{\Gamma(m) E_s/N_o} \left(\frac{m}{2\sigma^2}\right)^m \left(\frac{\gamma}{E_s/N_o}\right)^{m-1} e^{-\frac{m\gamma}{2\sigma^2 E_s/N_o}} \end{aligned} \quad (6.113)$$

Letting $\bar{\gamma} = \frac{E_s}{N_o}$ and $\sigma^2 = 1/2$ we have

$$f_\gamma(\gamma) = \frac{1}{\Gamma(m)} \frac{m^m}{\bar{\gamma}^m} \gamma^{m-1} e^{-m\gamma/\bar{\gamma}}$$

(6.114)

which is a Gamma Distribution. If $m = N/2$ for integer N , this is a Chi-Square distribution. In this case, Nakagami behaves like m -fold diversity. If $N = 2$, $m = 1$, Nakagami fading reduces to Rayleigh fading.

6.10.1 Outage Probability

The outage probability in Nakagami fading can be found as

$$\begin{aligned} F_\gamma(\gamma) &= \int_0^\gamma \frac{1}{\Gamma(m)} \frac{m^m}{\bar{\gamma}^m} x^{m-1} e^{-mx/\bar{\gamma}} dx \\ &= \frac{1}{\Gamma(m)} \int_0^{m\gamma/\bar{\gamma}} y^{m-1} e^{-y} dy \\ &= \frac{\tilde{\gamma} \left(m, \frac{m\gamma}{\bar{\gamma}}\right)}{\Gamma(m)} \end{aligned} \quad (6.115)$$

An example of the outage probability for SNR in Nakagami fading is given in Figure 6.11 for $m = 1, 2, 4, 10$.

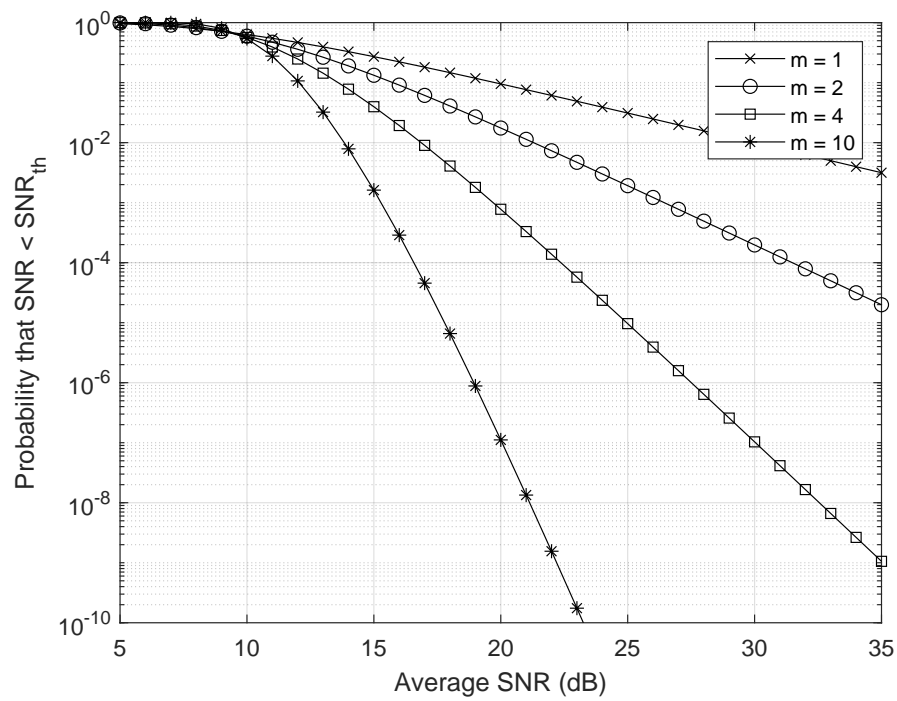


Figure 6.11: Outage Probability of Nakagami Fading for Various m Factors

6.11 MRC with Nakagami Fading

For MRC we know that

$$\gamma_{mrc} = \sum_{i=1}^L \gamma_i \quad (6.116)$$

If the γ_i are Gamma distributed and iid, then

$$f_\gamma(\gamma) = \frac{1}{\Gamma(m)} \frac{m^m}{\bar{\gamma}^m} \gamma^{m-1} e^{-m\gamma/\bar{\gamma}} \quad (6.117)$$

Thus, the moment generating function is

$$\Phi_\gamma(s) = \left(\frac{m/\bar{\gamma}}{m/\bar{\gamma} - s} \right)^m \quad (6.118)$$

Now, for MRC of L diversity branches the moment generating function is

$$\begin{aligned} \Phi_{\gamma_{mrc}}(s) &= \prod_{i=1}^L \Phi_{\gamma_i}(s) \\ &= \prod_{i=1}^L \left(\frac{m/\bar{\gamma}}{m/\bar{\gamma} - s} \right)^m \\ &= \left(\frac{m/\bar{\gamma}}{m/\bar{\gamma} - s} \right)^{mL} \end{aligned} \quad (6.119)$$

Note that this is the moment generating function of a Gamma random variable with $a = m/\bar{\gamma}$ and $b = mL$. Thus,

$$f_{\gamma_{mrc}}(\gamma) = \frac{1}{\Gamma(mL)} \left(\frac{m}{\bar{\gamma}} \right)^{mL} \gamma^{mL-1} e^{-m\gamma/\bar{\gamma}}$$

(6.120)

The cdf is

$$\begin{aligned} F_{\gamma_{mrc}}(\gamma) &= \int_0^\gamma \frac{1}{\Gamma(mL)} \left(\frac{m}{\bar{\gamma}} \right)^{mL} x^{mL-1} e^{-mx/\bar{\gamma}} dx \\ &= \frac{1}{\Gamma(mL)} \int_0^{m\gamma/\bar{\gamma}} y^{m-1} e^{-y} dy \\ &= \frac{\tilde{\gamma}(mL, m\gamma/\bar{\gamma})}{\Gamma(mL)} \end{aligned} \quad (6.121)$$

where again $\tilde{\gamma}$ is the incomplete gamma function. Examples of the probability of outage are given in Figures 6.12 and 6.13 for $m = 2$ and $m = 10$ respectively. We can see both from the pdf and the outage probability figure that the m -factor has the same impact as the diversity order.

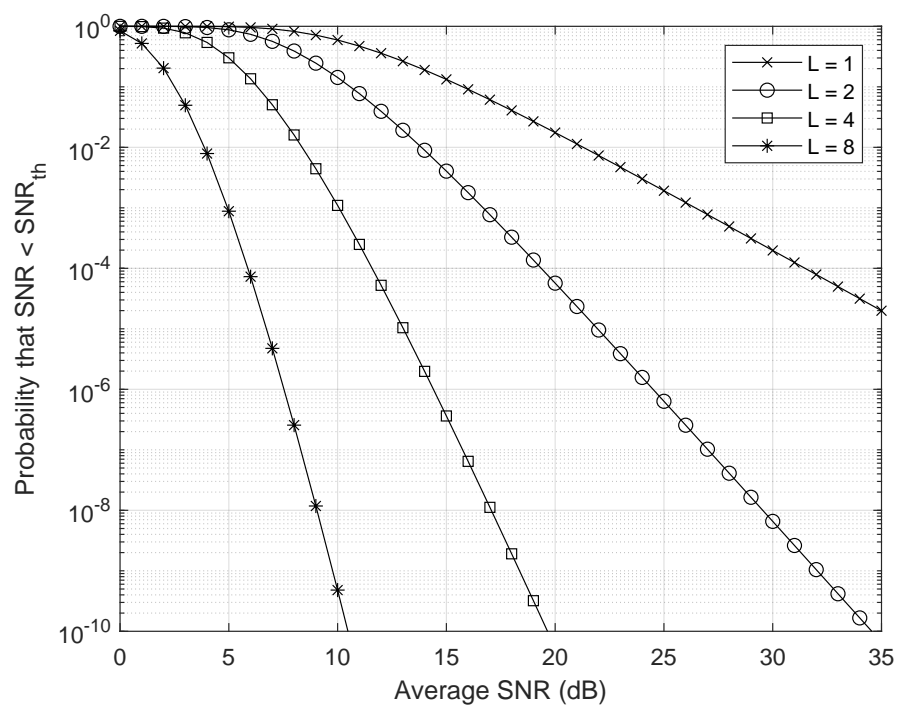


Figure 6.12: Outage Probability of Nakagami Fading for $m = 2$ and Various Numbers of Diversity Branches L

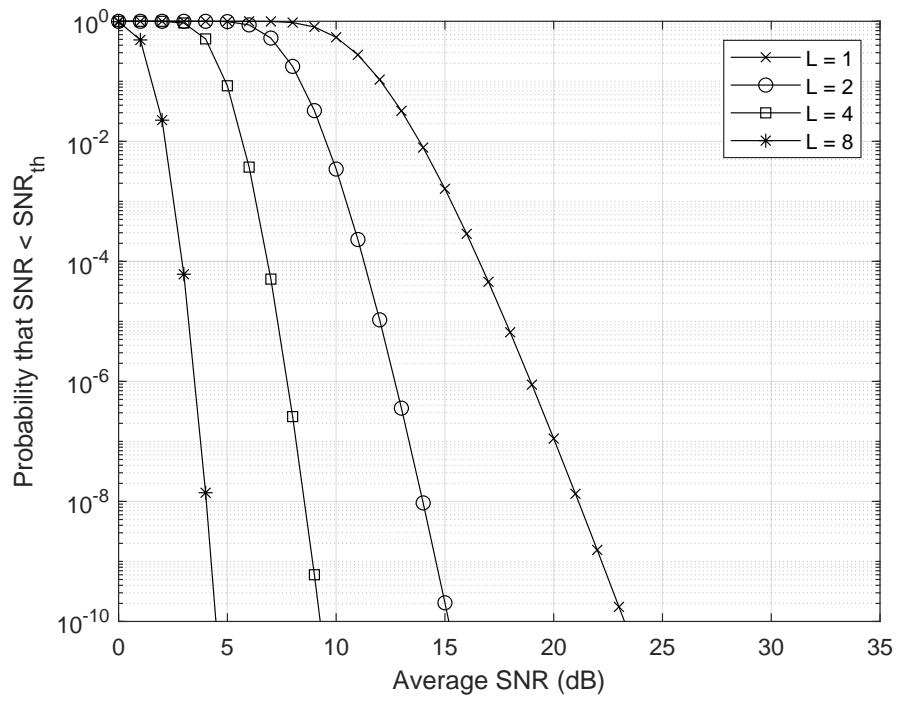


Figure 6.13: Outage Probability of Nakagami Fading for $m = 10$ and Various Numbers of Diversity Branches L

6.11.1 BER of BPSK in Nakagami Fading

It is shown in [11, 10] that the BER of BPSK in Nakagami fading can be written as

$$P_b = \frac{1}{2} \sqrt{\frac{\bar{\gamma}/m}{\pi(1+\bar{\gamma}/m)}} \frac{\Gamma(Lm+1/2)}{Lm+1} \left(\frac{1}{1+\bar{\gamma}/m}\right)^{Lm} {}_2F_1\left(1, Lm+1/2; Lm+1, \frac{1}{1+\bar{\gamma}/m}\right) \quad (6.122)$$

where ${}_2F_1(a, b; c, z)$ is the Gaussian hypergeometric formula. If Lm is an integer, SNR distribution simplifies to a Chi-Square distribution and the bit error rate simplifies to

$$P_b = \frac{1}{2} \left[1 - \sqrt{\frac{\bar{\gamma}/m}{1+\bar{\gamma}/m}} \sum_{k=0}^{Lm-1} \binom{2k}{k} \left(\frac{1}{4(1+\bar{\gamma}/m)}\right) \right] \quad (6.123)$$

which is essentially the BER of MRC in Rayleigh fading with Lm degrees of freedom and an SNR per branch of $\bar{\gamma}/m$. Example plots for $L = M_r = 1$ (no diversity) and $m = 1, 2, 4, 10$ are given in Figure 6.14. Note that $m = 1$ corresponds to Rayleigh fading and thus agrees with the plots in previous figures. The error rate improvement with $L = M_r = 2$ is shown in Figure 6.15. Again, note that the improvement due to diversity order and the improvement due to m factor (less severe fading) are analogous. Also note that in order to focus on the diversity benefit (as opposed to the average SNR improvement due to multiple antennas) the error rate is plotted against the SNR per bit $\gamma_b = \frac{E_b}{N_o} = \frac{\bar{\gamma}}{L}$. The performance for $L = M_r = 4$ is given in Figure 6.16.

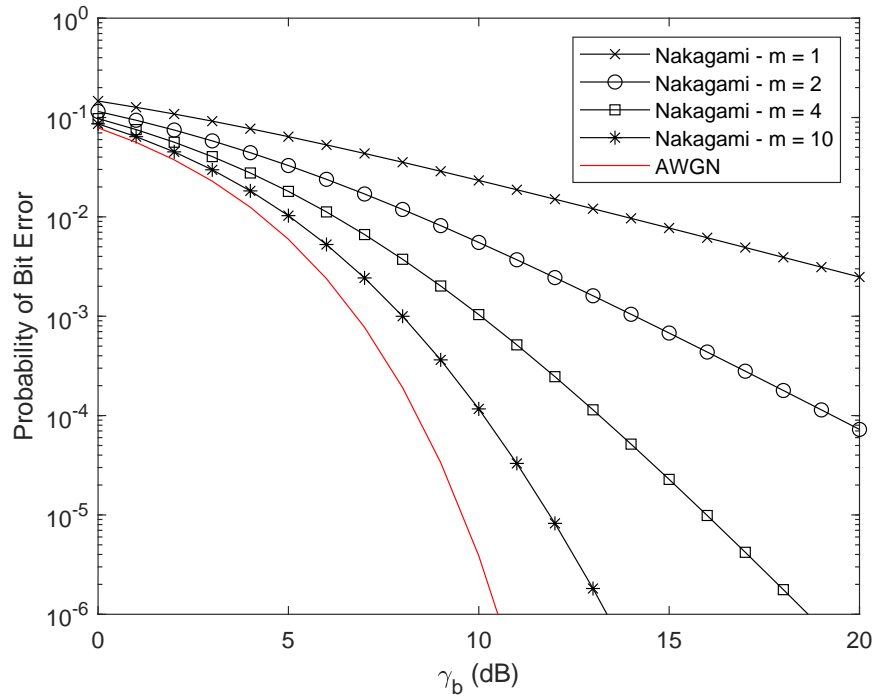


Figure 6.14: Bit Error Rate of BPSK in Nakagami Fading for Various m Factors

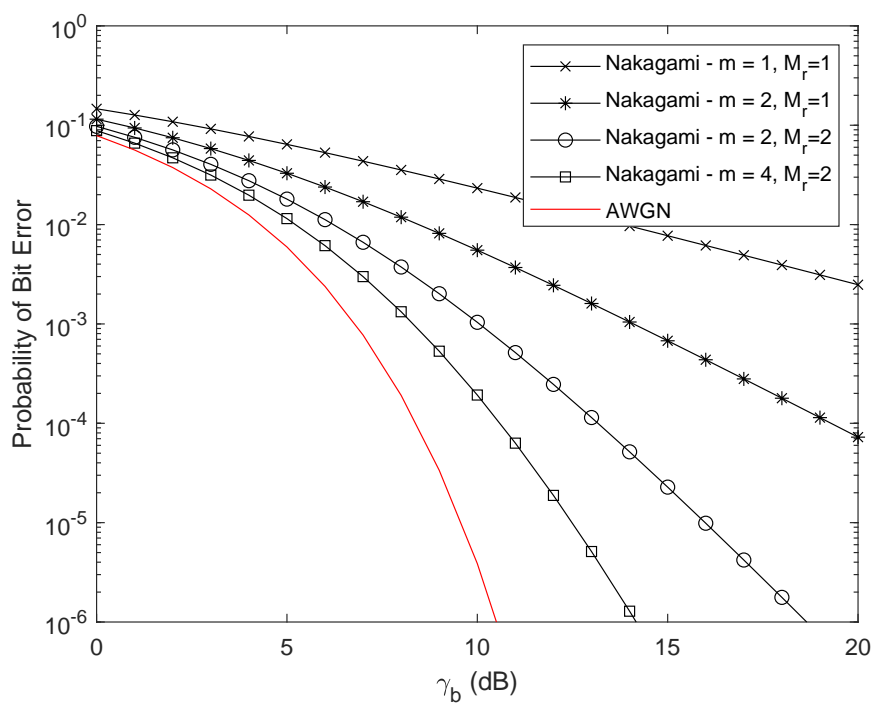


Figure 6.15: Bit Error Rate of BPSK in Nakagami Fading with MRC ($M_r = 2$) for Various m Factors

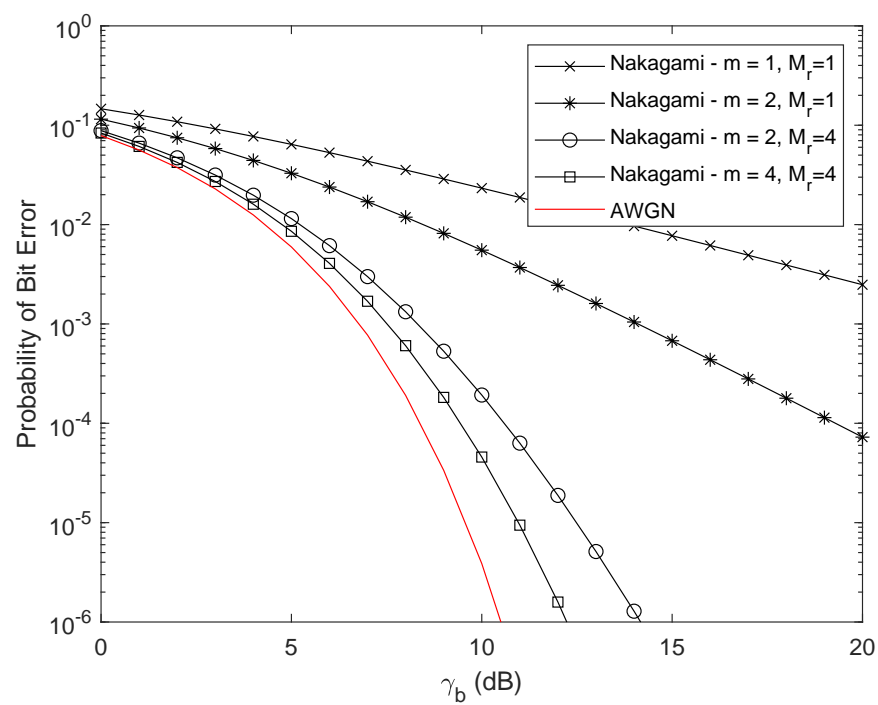


Figure 6.16: Bit Error Rate of BPSK in Nakagami Fading with MRC ($M_r = 4$) for Various m Factors

6.12 Correlated Branches with MRC in Rayleigh Fading

Up to this point we have assumed that all antennas experience independent fading. If fading on each antenna is correlated, we expect that the benefit of diversity will be diminished. To see this, consider MRC of L -branch diversity. The total received power $P = \alpha^2$ can be written as

$$\begin{aligned} P_t &= \sum_{i=1}^L \alpha_i^2 \\ &= \sum_{i=1}^L (X_i^2 + Y_i^2) \end{aligned}$$

where X_i and Y_i are the real and imaginary parts of the fading channel. For Rayleigh fading, X_i and Y_i are $GRV(0, \frac{P_i}{2})$. We can then group all $2L$ GRV into a single vector

$$\mathbf{x} = [X_1 Y_1 X_2 Y_2 \dots X_L Y_L] \quad (6.124)$$

The joint distribution function $f_{\mathbf{X}}(\mathbf{x})$ can be written as

$$f_{\mathbf{X}}(\mathbf{x}) = (2\pi)^{-L} |\mathbf{R}|^{-1/2} \exp\left(-\frac{1}{2} \mathbf{x} \mathbf{R}^{-1} \mathbf{x}^T\right) \quad (6.125)$$

where \mathbf{R} is the covariance matrix

$$\mathbf{R} = \begin{bmatrix} A_1 & B_{12} & B_{13} & \cdots & B_{1L} \\ B_{12}^T & A_2 & & & \vdots \\ \vdots & & & & \vdots \\ B_{1L}^T & \cdots & \cdots & \cdots & A_L \end{bmatrix} \quad (6.126)$$

where

$$A_i = \begin{bmatrix} \frac{1}{2}\bar{P}_i & 0 \\ 0 & \frac{1}{2}\bar{P}_i \end{bmatrix} \quad (6.127)$$

$$B_{ij} = \begin{bmatrix} \rho_{ij} & \beta_{ij} \\ -\beta_{ij} & \rho_{ij} \end{bmatrix} \quad (6.128)$$

$\rho_{ij} = E\{X_i X_j\}$ and $\beta_{ij} = E\{X_i Y_j\}$ and $|\mathbf{R}|$ is the determinant of \mathbf{R} .

Now, we wish to find the pdf of P_t . We will use the moment generating function approach. To do so, we can write P_t in terms of \mathbf{x} :

$$P_t = \mathbf{x} \mathbf{I} \mathbf{x}^T \quad (6.129)$$

Now, the moment generating function can be written as

$$\begin{aligned}
\Phi_{P_t}(s) &= \int_0^\infty e^{-sp} f_P(p) dp \\
&= \mathbb{E} \left\{ \exp(-s\mathbf{x}\mathbf{I}\mathbf{x}^T) \right\} \\
&= \underbrace{\int_{-\infty}^\infty \int_{-\infty}^\infty \cdots \int_{-\infty}^\infty}_{2L-fold} (2\pi)^{-L} |\mathbf{R}|^{-1/2} \exp \left(-\frac{1}{2} \mathbf{x}(\mathbf{R}^{-1} + 2sI)\mathbf{x}^T \right) dX_1 dY_1 \cdots dX_L dY_L \\
&= |\mathbf{R}|^{-1/2} |(\mathbf{R}^{-1} + 2sI)^{-1}|^{1/2} \times \\
&\quad \underbrace{\int_{-\infty}^\infty \int_{-\infty}^\infty \cdots \int_{-\infty}^\infty}_{=1 \text{ (integral of Gaussian pdf)}} (2\pi)^{-L} |(\mathbf{R}^{-1} + 2sI)^{-1}|^{-1/2} \exp \left(-\frac{1}{2} \mathbf{x}(\mathbf{R}^{-1} + 2sI)\mathbf{x}^T \right) dX_1 dY_1 \cdots dX_L dY_L \\
&= |\mathbf{R}|^{-1/2} \underbrace{|(\mathbf{R}^{-1} + 2sI)^{-1}|^{1/2}}_{|A^{-1}|=|A|^{-1}} \\
&= \underbrace{|\mathbf{R}|^{-1/2} |\mathbf{R}^{-1} + 2sI|^{-1/2}}_{|AB|=|A||B|} \\
&= |\mathbf{I} + 2s\mathbf{R}|^{-1/2}
\end{aligned} \tag{6.130}$$

Now, it can be shown that the final determinant is a perfect square so that

$$|\mathbf{I} + 2s\mathbf{R}|^{-1/2} = |\mathbf{I} + s\Psi|^{-1} \tag{6.131}$$

where

$$\Psi = \begin{bmatrix} \bar{P}_1 & \rho_{12} - j\beta_{12} & \cdots & \cdots & \rho_{1L} - j\beta_{1L} \\ \rho_{12} + j\beta_{12} & \bar{P}_2 & & & \vdots \\ \vdots & & & & \vdots \\ \rho_{1L} + j\beta_{1L} & \cdots & \cdots & \cdots & \bar{P}_L \end{bmatrix} \tag{6.132}$$

Thus, we can write

$$\begin{aligned}
\Phi(s) &= |\mathbf{I} + s\Psi|^{-1} \\
&= \frac{1}{\prod_{i=1}^L (1 + s\lambda_i)}
\end{aligned}$$

where λ_i is the i th eigenvalue of Ψ . If all eigenvalues are distinct, we can write (using partial fraction expansion)

$$\frac{1}{\prod_{i=1}^L (1 + s\lambda_i)} = \sum_{i=1}^L \frac{\eta_i}{1 + s\lambda_i} \tag{6.133}$$

where

$$\eta_i = \frac{\lambda_i^{L-1}}{\prod_{k \neq i} (\lambda_i - \lambda_k)} \tag{6.134}$$

Thus, making this substitution

$$\Phi(s) = \sum_{i=1}^L \frac{\lambda_i^{L-1}}{\prod_{k \neq i} (\lambda_i - \lambda_k)} \frac{1}{1 + s\lambda_i} \quad (6.135)$$

$$= \sum_{i=1}^L \frac{\lambda_i^{L-2}}{\prod_{k \neq i} (\lambda_i - \lambda_k)} \frac{1}{s + 1/\lambda_i} \quad (6.136)$$

and taking the inverse Laplace transform we have

$$f_{P_t}(p) = \sum_{i=1}^L \frac{\lambda_i^{L-2}}{\prod_{k \neq i} (\lambda_i - \lambda_k)} e^{-p/\lambda_i} \quad (6.137)$$

Now, we can find the distribution of the combined SNR γ_{MRC} assuming that the noise power is constant (our usual assumption). Additionally, we assume that the average received signal power on each antenna is the same: $\bar{P}_1 = \bar{P}_2 \dots = \bar{P}_L$. In other words $\bar{\gamma}_1 = \bar{\gamma}_2 \dots = \bar{\gamma}$. Let's define a matrix Λ

$$\Lambda = \frac{1}{\bar{P}_1} \Psi \quad (6.138)$$

with eigenvalues $\tilde{\lambda}_i$. Then, the distribution of SNR can be easily shown to be

$$f_{\gamma_{mrc}}(\gamma) = \sum_{i=1}^L \frac{\tilde{\lambda}_i^{L-2}}{\prod_{k \neq i} (\tilde{\lambda}_i - \tilde{\lambda}_k)} \frac{1}{\bar{\gamma}} e^{-\frac{\gamma}{\bar{\gamma}\tilde{\lambda}_i}} \quad (6.139)$$

Note that the distribution is identical to the case of independent, but non-identical SNRs. Thus, correlated branches will behave like independent SNRs with unequal branch SNRs. Example bit error rates are plotted in Figure 6.17 for $L = M_r = 4$. Note that independent channels and no diversity cases are also plotted for reference. For the correlated cases, we assume that

$$\Lambda = \begin{bmatrix} 1 & \rho & \rho & \rho \\ \rho & 1 & \rho & \rho \\ \rho & \rho & 1 & \rho \\ \rho & \rho & \rho & 1 \end{bmatrix} \quad (6.140)$$

We can see that the effect of correlation is to shift the curves to the right (analogous to an average SNR loss). The slope is not changed, confirming that there is no loss in diversity order.

6.13 Transmit Diversity - Concept

The previous sections examine the use of multiple antennas at the receiver to provide diversity gain in fading channels. Multiple antennas can also be used at the transmitter to achieve diversity, although it is somewhat different, especially in the absence of channel knowledge at the transmitter. In other words, transmit diversity is analogous to receive diversity when either (a) a time division duplex (TDD) system is employed with a slow fading channel (meaning that received channel information can be used on transmit) or (b) feedback is employed. We will not specifically discuss TDD systems, but the application to TDD should be obvious after reading the chapter. Instead, we will assume FDD and first examine open loop techniques (i.e., techniques which function in

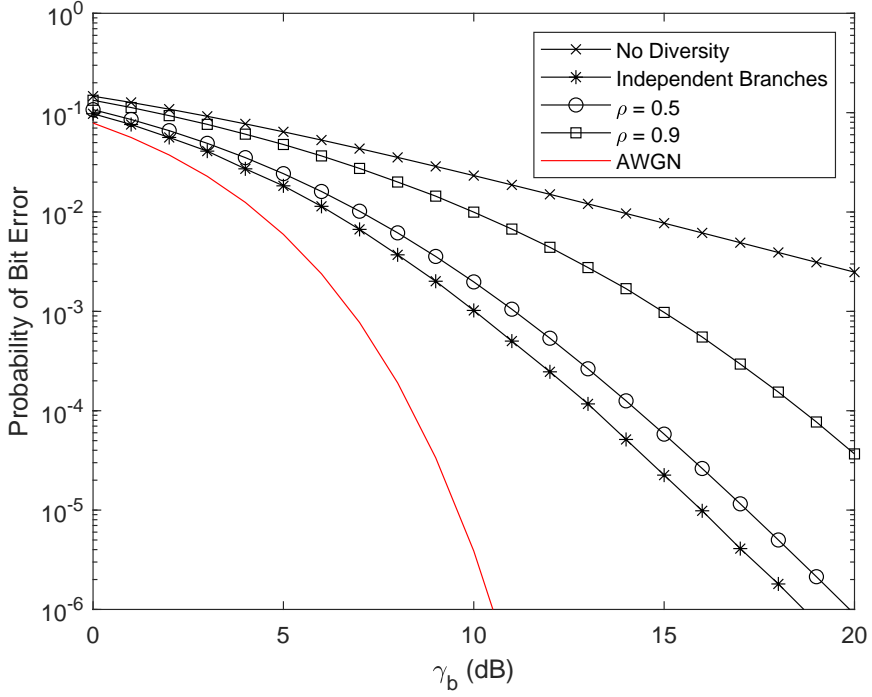


Figure 6.17: Bit Error Rate of BPSK in Correlated Rayleigh Fading for $L = M_r = 4$

the absence of channel knowledge at the transmitter) and then move on to closed-loop techniques (i.e., those techniques which feedback channel information to the transmitter).

The first question that might be asked is when not simply transmit from multiple widely-spaced antennas? To see why this isn't helpful, assume multiple transmit antennas with a single receive antenna and let $\tilde{\alpha}_i(t)$ be the complex channel from the i th antenna which is assumed to be a complex Gaussian random process (Rayleigh fading). Note that $E\{|\tilde{\alpha}_i(t)|^2\} = 1$ and that $E\{|\Re\{\tilde{\alpha}_i(t)\}|^2\} = E\{|\Im\{\tilde{\alpha}_i(t)\}|^2\} = 1/2$. Let the transmit signal $x(t) = \sum_{i=-\infty}^{\infty} s_i p(t - iT)$. If we transmit the same symbols from all antennas, but with $1/N_t$ of the power (keeping the total power the same as the single-antenna case), and assuming a narrowband channel, at the receiver we have

$$\begin{aligned} r(t) &= \sqrt{P_r} \sum_{i=1}^{N_t} \sqrt{\frac{1}{N_t}} x(t) \tilde{\alpha}_i(t) + n(t) \\ &= \sqrt{P_r} \left(\underbrace{\sqrt{\frac{1}{N_t}} \sum_{i=1}^{N_t} \tilde{\alpha}_i(t)}_{\tilde{\alpha}_T(t)} \right) x(t) + n(t) \end{aligned}$$

where $\tilde{\alpha}_T(t)$ is the sum of complex Gaussian random processes. It is thus another complex Gaus-

sian random process. Further, $E\{|\tilde{\alpha}_T(t)|^2\} = 1$ since the channels are independent with zero mean. Thus, the channel is still a Rayleigh fading channel with unit power. No improvement is obtained! Thus, we cannot simply transmit from multiple antennas and hope to obtain diversity benefit. However, there are various open-loop and closed-loop techniques to obtain diversity benefit with multiple transmit antennas, as we will discuss below.

6.14 Open Loop Transmit Diversity Techniques

6.14.1 Antenna Hopping

Let's assume slow fading such that $\tilde{\alpha}_i(t) = \tilde{\alpha}_i$. The received signal in this case is

$$r(t) = \sum_{i=-\infty}^{\infty} \sqrt{P_r} s_i p(t - iT) \tilde{\alpha}_{\lfloor i/N_t \rfloor} + n(t) \quad (6.141)$$

where P_r is the average received power (assumed to be the same on both channels) and $E\{|\tilde{\alpha}_i(t)|^2\} = 1$. Let's further assume that all channels are independent. Without any coding, the decision metric (after matched filtering) can be written as

$$z[\nu] = \sqrt{P_r} s_\nu |\tilde{\alpha}_{\lfloor i/N_t \rfloor}|^2 + n[\nu] \tilde{\alpha}_{\lfloor i/N_t \rfloor}^* \quad (6.142)$$

. The bit error rate for a specific instantiation of $\tilde{\alpha}$ is

$$P_b = Q\left(\sqrt{2 \frac{E_b}{N_o} |\tilde{\alpha}|^2}\right) \quad (6.143)$$

Since each symbol has a potentially different channel, the average BER is the same as in single-channel Rayleigh fading. If BPSK is used:

$$P_b \approx \frac{1}{4E_b/N_o} \quad (6.144)$$

where E_b/N_o is the average energy per bit divided by the noise power spectral density. Now, let us try using a simple rate $1/N_t$ repeat code. In this case, the decision variable (coherent combination of N_t consecutive received symbols) is

$$\begin{aligned} z[\lfloor \nu/N_t \rfloor] &= \sum_{i=1}^{N_t} \left(\sqrt{P_r/N_t} \tilde{\alpha}_i s_{\lfloor \nu/N_t \rfloor} + n[\lfloor \nu/N_t \rfloor + i] \tilde{\alpha}_i^* \right) \\ &= \sqrt{\frac{P_r}{N_t}} s_{\lfloor \nu/N_t \rfloor} \sum_{i=1}^{N_t} |\tilde{\alpha}_i|^2 + \sum_{i=1}^{N_t} \tilde{\alpha}_i^* n[\lfloor \nu/N_t \rfloor + i] \end{aligned} \quad (6.145)$$

$$P_b = Q\left(\sqrt{\frac{2}{N_t} \frac{E_b}{N_o} \sum_{i=1}^{N_t} |\tilde{\alpha}_i|^2}\right) \quad (6.146)$$

To determine the average error rate we recognize that

$$\eta = \frac{1}{N_t} \sum_{i=1}^{N_t} |\tilde{\alpha}_i|^2 \quad (6.147)$$

is a Chi Square R.V. with N_t degrees of freedom and average power $N_t/2$ in each of the underlying Gaussian random variables. Thus, we can write the BER as

$$P_b = \left[\left(1 - \sqrt{\frac{\bar{\gamma}_c}{1 + \bar{\gamma}_c}} \right) \right]^{N_t} \sum_{k=0}^{N_t-1} \binom{N_t - 1 + k}{k} \left[\frac{1}{2} \left(1 + \sqrt{\frac{\bar{\gamma}_c}{1 + \bar{\gamma}_c}} \right) \right]^k \quad (6.148)$$

where $\bar{\gamma}_c = \frac{1}{N_t} \frac{E_b}{N_o}$ and $\frac{E_b}{N_o}$ is the average energy per bit divided by the noise power spectral density. This can be approximated at high average $\frac{E_b}{N_o}$ as

$$P_b \approx \left(\frac{N_t}{4E_b/N_o} \right)^{N_t} \binom{2N_t - 1}{N_t} \quad (6.149)$$

This is identical to the probability of MRC with N_t receive antennas but without the N_t average SNR improvement.

6.14.2 Space Time Transmit Diversity

This is also known as a 2-dimensional Space-Time Block Code (STBC) or the Alamouti Code. During time slot #1, at the output of a matched filter we observe:

$$r_1 = \tilde{\alpha}_1 \sqrt{E_s/2} s_1 + \tilde{\alpha}_2 \sqrt{E_s/2} s_2 + n_1 \quad (6.150)$$

where n_1 is a GRV. During time slot #2

$$r_2 = -\tilde{\alpha}_1 \sqrt{E_s/2} s_2^* + \tilde{\alpha}_2 \sqrt{E_s/2} s_1^* + n_2 \quad (6.151)$$

where n_2 is a GRV. The decision metric for symbol one is created as

$$\begin{aligned} Z_1 &= \tilde{\alpha}_1^* r_1 + \tilde{\alpha}_2 r_2^* \\ &= \tilde{\alpha}_1^* \left(\tilde{\alpha}_1 \sqrt{E_s/2} s_1 + \tilde{\alpha}_2 \sqrt{E_s/2} s_2 + n_1 \right) + \dots \\ &\quad \tilde{\alpha}_2^* \left(-\tilde{\alpha}_1 \sqrt{E_s/2} s_2^* + \tilde{\alpha}_2 \sqrt{E_s/2} s_1^* + n_2 \right)^* \\ &= \underbrace{\sqrt{E_s/2} (|\tilde{\alpha}_1|^2 + |\tilde{\alpha}_2|^2) s_1}_{\text{desired energy}} + \underbrace{\sqrt{E_s/2} (\tilde{\alpha}_1^* \tilde{\alpha}_2 - \tilde{\alpha}_1 \tilde{\alpha}_2^*) s_2}_{\text{GRV with variance } (|\tilde{\alpha}_1|^2 + |\tilde{\alpha}_2|^2) \sigma^2} \\ &\quad \tilde{\alpha}_1^* n_1 + \tilde{\alpha}_2 n_2^* \\ &= \underbrace{\sqrt{E_s/2} (|\tilde{\alpha}_1|^2 + |\tilde{\alpha}_2|^2) s_1}_{\text{desired energy}} + \underbrace{\tilde{n}}_{\text{GRV with variance } (|\tilde{\alpha}_1|^2 + |\tilde{\alpha}_2|^2) \sigma^2} \end{aligned} \quad (6.152)$$

The per symbol SNR is

$$\gamma = \frac{E_s}{N_o} \frac{(|\tilde{\alpha}_1|^2 + |\tilde{\alpha}_2|^2)}{2} \quad (6.153)$$

And thus for BPSK (or QPSK) the BER is

$$Q \left(\sqrt{2 \frac{E_b}{N_o} \frac{(|\tilde{\alpha}_1|^2 + |\tilde{\alpha}_2|^2)}{2}} \right) \quad (6.154)$$

Averaged over Rayleigh fading we obtain:

$$\begin{aligned} P_b &= \left[\left(1 - \sqrt{\frac{\bar{\gamma}_c}{1 + \bar{\gamma}_c}} \right) \right]^2 \sum_{k=0}^1 \binom{2-1+k}{k} \left[\frac{1}{2} \left(1 + \sqrt{\frac{\bar{\gamma}_c}{1 + \bar{\gamma}_c}} \right) \right]^k \\ &= \left[\left(1 - \sqrt{\frac{\bar{\gamma}_c}{1 + \bar{\gamma}_c}} \right) \right]^2 \left(1 + \sqrt{\frac{\bar{\gamma}_c}{1 + \bar{\gamma}_c}} \right) \end{aligned} \quad (6.155)$$

where $\bar{\gamma}_c = \frac{1}{2} \frac{E_s}{N_o}$. This is the same BER that we would obtain from two-fold receive diversity with MRC. Note that it is easily shown (and we will verify this in the next chapter) that a similar decision metric and bit error rate are obtained for the second symbol.

Now, what if there are multiple antennas? Let's define $\tilde{\alpha}_{1i}$ as the channel between transmit antenna 1 and receive antenna i . Similarly, let r_{1i} and r_{2i} be the matched filter outputs on the i th antenna during time slots 1 and 2 respectively. The decision metric for the first symbol is found as

$$Z_1 = \sum_{i=1}^{M_r} (\tilde{\alpha}_{1i}^* r_{1i} + \tilde{\alpha}_{2i}^* r_{2i}^*) \quad (6.156)$$

The BER would be identical to that of $2M_r$ -fold diversity with MRC combining.

6.15 Closed-Loop Transmit Diversity Techniques

6.15.1 Antenna Selection

Assuming that all antennas are monitored (via pilot channels) and the best channel is fed back to the transmitter, the performance is equivalent to selection diversity. Specifically, for BPSK modulation and coherent detection the BER is

$$P_b = \frac{1}{2} \left[1 - \sum_{k=1}^{N_t} \binom{N_t}{k} (-1)^{k-1} \sqrt{\frac{\bar{\gamma}}{\bar{\gamma} + k}} \right] \quad (6.157)$$

where $\bar{\gamma} = \frac{E_b}{N_o}$. When bit errors occur, the performance can be approximated that in Rayleigh fading with no diversity¹.

$$P_{b|e} = \frac{1}{2} \left(1 - \sqrt{\frac{\bar{\gamma}}{\bar{\gamma} + 1}} \right) \quad (6.158)$$

Thus, the overall probability of bit error is

$$P_{b,t} = P_b(1-p) + P_{b|e}p \quad (6.159)$$

where p is the probability of feedback error.

6.15.2 Generalized Beamforming

Recall that in transmit beamforming, we weight the signals sent from multiple antennas so that they arrive at the mobile with the same phases and thus add coherently. When the channel can be approximated as plane wave propagation, we simply need to know the array geometry and

¹Due to the fact that the channel is NOT the maximum SNR channel, the performance would be slightly worse than that in standard Rayleigh fading.

the desired angle of departure to accomplish this. However, in a fading channel with non-zero angle spread, this is not true. We can still, however, co-phase the signals to cause them to sum coherently at the mobile. However, we require mobile feedback to accomplish this.

Let the channel from the i th antenna be $\tilde{\alpha}_i = \sqrt{P_r} \alpha_i e^{j\phi_i}$ where P_r is the average receive power in the channel. Assume that the mobile can feedback to the base station the measured values ϕ_i . The transmit signal from the i th antenna is

$$x_i(t) = e^{-j\phi_i} \sqrt{1/N_t} s(t) \quad (6.160)$$

where $s(t) = \sum_{i=-\infty}^{\infty} s_i p(t - iT)$. Thus, the received signal at the receiver is

$$r(t) = \sum_{i=1}^{N_t} \tilde{\alpha}_i x_i(t) + n(t) \quad (6.161)$$

$$= \sum_{i=1}^{N_t} \sqrt{P_r} \alpha_i e^{j\phi_i} e^{-j\phi_i} \sqrt{1/N_t} s(t) + n(t) \quad (6.162)$$

$$= \sqrt{P_r/N_t} \left(\sum_{i=1}^{N_t} \alpha_i \right) s(t) + n(t) \quad (6.163)$$

The instantaneous SNR is then

$$SNR = \frac{P_r \left(\sum_{i=1}^{N_t} \alpha_i \right)^2}{N_t \sigma_n^2} \quad (6.164)$$

where σ_n^2 is the variance of the noise signal $n(t)$. It is straightforward to show that the decision variable has the same statistics as equal gain combining with N_t receive antennas. To see this, consider the received signal on the i th receive antenna when there is one transmit antenna and M_r receive antennas:

$$r_i(t) = \sqrt{P_r} \alpha_i e^{j\phi_i} x(t) + n_i(t) \quad (6.165)$$

Now with equal gain combining we have:

$$r_T(t) = \sum_i e^{-j\phi_i} r_i(t) \quad (6.166)$$

$$= \sqrt{P_r} \left(\sum_i \alpha_i \right) x(t) + \sum_i e^{-j\phi_i} n_i(t) \quad (6.167)$$

$$= \sqrt{P_r} \left(\sum_i \alpha_i \right) x(t) + n_T(t) \quad (6.168)$$

Now, the SNR of this combined signal is then

$$SNR = \frac{P \left(\sum_i \alpha_i \right)^2}{M_r \sigma_n^2} \quad (6.169)$$

If instead of sending back only phase values, we instead send back normalized channel values we could create transmit weights

$$w_i = \frac{\tilde{\alpha}_i^*}{\sqrt{\sum_i |\tilde{\alpha}_i|^2}} \quad (6.170)$$

If we use these weights at the transmitter instead of phase only, we can show that the performance

is equivalent to maximal ratio combining with N_t receive antennas.

Note that although we have termed this “generalized beamforming”, there is no beampattern in this case, due to the fact that the channel is not coherent across the antenna array.

6.15.3 Maximal Ratio Transmission (MRT)

Maximal Ratio Transmission is a generalization of the previous idea when there are multiple transmit and receive antennas. Specifically, let's assume that we are transmitting a scalar signal $s(t)$ from N_t antennas and receiving that signal on M_r receive antennas. We wish to find a transmit weight vector \mathbf{v} to premultiply by the transmit signal so that the transmit vector is $\mathbf{s}(t) = \mathbf{v}s(t)$ and a receive vector \mathbf{w} to use for combining the received signals $\mathbf{r}(t)$ on M_r receive antennas. Specifically, ignoring time we have a receive vector each symbol time

$$\mathbf{r} = \mathbf{H}\mathbf{s} + \mathbf{n} \quad (6.171)$$

where \mathbf{H} is the $M_r \times N_t$ channel matrix and \mathbf{n} is the $M_r \times 1$ noise vector. Our decision variable is

$$z = \mathbf{w}^H \mathbf{r} \quad (6.172)$$

$$= \mathbf{w}^H (\mathbf{H}\mathbf{s} + \mathbf{n}) \quad (6.173)$$

$$= \mathbf{w}^H \mathbf{H}\mathbf{v}s + \mathbf{w}^H \mathbf{n} \quad (6.174)$$

Now, we wish to choose \mathbf{w} and \mathbf{v} to maximize SNR. Now, the SNR is

$$SNR = \frac{(\mathbf{w}^H \mathbf{H}\mathbf{v})^2 E_s}{\sum_i |w_i|^2 \sigma_n^2} \quad (6.175)$$

$$= \frac{\mathbf{w}^H \mathbf{H}\mathbf{v} \mathbf{v}^H \mathbf{H}^H \mathbf{w} E_s}{\mathbf{w}^H \mathbf{w}} \frac{E_s}{\sigma_n^2} \quad (6.176)$$

Note that $\frac{E_s}{\sigma_n^2}$ is the average SNR on a single antenna. Now, by definition MRT assumes that \mathbf{v} is a linear transformation of the channel matrix \mathbf{H} :

$$\mathbf{v} = \frac{(\mathbf{g}\mathbf{H})^H}{a} \quad (6.177)$$

where \mathbf{g} is a $1 \times M_r$ vector and $a = |\mathbf{g}\mathbf{H}|$ is a normalizing constant. Thus,

$$\mathbf{r} = \mathbf{H}\mathbf{H}^H \mathbf{g}^H \frac{s}{a} + \mathbf{n} \quad (6.178)$$

$$z = \mathbf{w}^H \mathbf{r} \quad (6.179)$$

$$= \mathbf{w}^H \mathbf{H}\mathbf{H}^H \mathbf{g}^H \frac{s}{a} + \mathbf{w}^H \mathbf{n} \quad (6.180)$$

Now, for a given value of \mathbf{g} , the optimal value of \mathbf{w} is $\mathbf{w} = \mathbf{g}^H$. Thus,

$$z = \mathbf{g}\mathbf{H}\mathbf{H}^H \mathbf{g}^H \frac{s}{a} + \mathbf{g}\mathbf{n} \quad (6.181)$$

The resulting SNR is

$$SNR = \frac{(\mathbf{g}\mathbf{H}\mathbf{H}^H\mathbf{g}^H)^2/a^2}{\mathbf{g}\mathbf{g}^H} \frac{E_s}{\sigma_n^2} \quad (6.182)$$

$$= \frac{\mathbf{g}\mathbf{H}\mathbf{H}^H\mathbf{g}^H E_s}{\mathbf{g}\mathbf{g}^H \sigma_n^2} \quad (6.183)$$

This is known as a Rayleigh quotient. It is well-known that the ratio is maximized when \mathbf{g} is chosen as the maximum eigenvector of $\mathbf{H}\mathbf{H}^H$. Further, the maximum SNR achieved is

$$SNR_{max} = \lambda_{max} \frac{E_s}{\sigma_n^2} \quad (6.184)$$

where λ_{max} is the maximum eigenvalue of $\mathbf{H}\mathbf{H}^H$.

Chapter 7

Space-Time Coding

7.1 Space-Time Block Codes

In the previous chapter we finished with a discussion of transmit diversity schemes. One of the open loop transmit diversity schemes considered was space-time transmit diversity. In that discussion we examined a two-antenna space-time block code known as the Alamouti code. In this chapter, we generalize the concept and discuss space-time block codes for numbers of antennas beyond $N_t = 2$. Consider a series of T code symbols \mathbf{s}_i of dimension $N_t \times 1$ transmitted from N_t transmit antennas. These T code symbols together form a codeword \mathbf{S} that is $N_t \times T$. More specifically, consider a $K \times 1$ vector of bits \mathbf{b} that is mapped to \mathbf{S} as shown in Figure 7.1. Although the space time encoder can map the bits to symbols in any desirable way, we will assume a simplified approach with the K bits are first mapped to $p = K/m$ M -ary PSK or QAM symbols ($M = 2^m$). These p symbols are then mapped to spatial symbols. That is we can write the space-time block as

$$\mathbf{S} = [\mathbf{s}_1 \mathbf{s}_2 \dots \mathbf{s}_T] \quad (7.1)$$

where $\mathbf{s}_i = M(\mathbf{s}, i)$ and $M(\cdot)$ is the mapping function with $\mathbf{S} = M(\mathbf{s})$. The rate of the space-time code is equal to $r = p/T$. If spatial symbols are transmitted at a rate R_{st} , then the symbol rate is $R_s = rR_{st}$ and the bit rate is $R_b = mR_{st}$.

7.1.1 Maximum Likelihood Detector

To determine the maximum likelihood detector, let us first consider an $N_t \times 1$ system with channel vector \mathbf{h} . The received symbol at the output of the matched filter during the i th time slot can be written as

$$r_i = \mathbf{s}_i^T \mathbf{h} + n_i \quad (7.2)$$

where n_i represents the AWGN component of the matched filter output and is a zero-mean Gaussian random variable with variance σ_n^2 . The matched filter outputs over T time slots corresponding to the space-time symbol can be written as a $T \times 1$ vector \mathbf{r} :

$$\mathbf{r} = \mathbf{S}^T \mathbf{h} + \mathbf{n} \quad (7.3)$$

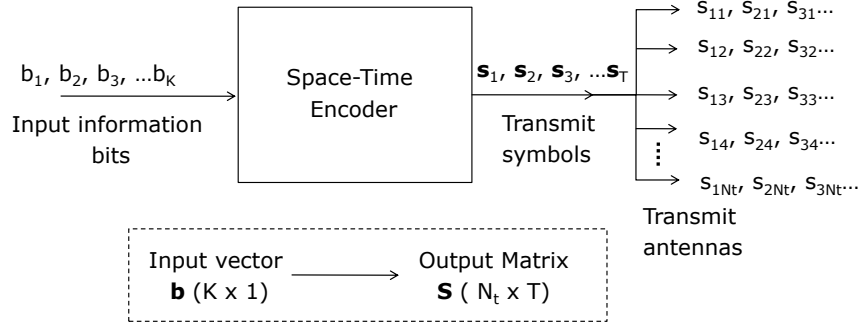


Figure 7.1: Block Diagram of General Space-Time Encoder

The probability density function of \mathbf{r} assuming Gaussian noise can be written as

$$p(\mathbf{r}|\mathbf{s}) = \frac{1}{(2\pi\sigma_n^2)^{T/2}} \exp\left(-\frac{1}{2\sigma_n^2} |\mathbf{r} - \mathbf{S}^T \mathbf{h}|^2\right) \quad (7.4)$$

The maximum likelihood detector is the one which maximizes $p(\mathbf{s}|\mathbf{r})$. However, for equally likely symbols, $p(\mathbf{s}|\mathbf{r}) \propto p(\mathbf{r}|\mathbf{s})$. Thus, the ML detector choose $\hat{\mathbf{S}}$ using the following rule

$$\begin{aligned} \hat{\mathbf{S}} &= \arg \max_{\mathbf{S}} p(\mathbf{r}|\mathbf{s}) = \frac{1}{(2\pi\sigma_n^2)^{T/2}} \exp\left(-\frac{1}{2\sigma_n^2} |\mathbf{r} - \mathbf{S}^T \mathbf{h}|^2\right) \\ &= \arg \min_{\mathbf{S}} \left\{ |\mathbf{r} - \mathbf{S}^T \mathbf{h}|^2 \right\} \end{aligned} \quad (7.5)$$

The transmit symbol vector $\hat{\mathbf{s}}$ is then determined from $\hat{\mathbf{S}}$, i.e., $\hat{\mathbf{s}} = M^{-1}(\hat{\mathbf{S}})$. Alternatively, we can describe an equivalent system where $\tilde{\mathbf{r}}$ has elements equal to either r_i or r_i^* :

$$\tilde{\mathbf{r}} = \mathcal{H}\mathbf{s} + \mathbf{n} \quad (7.6)$$

where the $N_t \times T$ matrix \mathcal{H} results from a mapping of the channel vector \mathbf{h} over each time slot which is analogous to the mapping from \mathbf{s} to \mathbf{S} . In this case, directly determine the ML estimate of the original vector \mathbf{s} :

$$\hat{\mathbf{s}} = \arg \min_{\mathbf{s}} \left\{ |\mathbf{r} - \mathcal{H}\mathbf{s}|^2 \right\} \quad (7.7)$$

7.1.2 Pairwise Error Probability

Assume that the spatial codewords are received on M_r receive antennas:

$$\mathbf{r}_i = \mathbf{H}\mathbf{s}_i + \mathbf{n}_i \quad (7.8)$$

Over T symbol times:

$$\begin{aligned} [\mathbf{r}_1, \mathbf{r}_2, \dots, \mathbf{r}_T] &= [\mathbf{Hs}_1, \mathbf{Hs}_2, \dots, \mathbf{Hs}_T] + [\mathbf{n}_1, \mathbf{n}_2, \dots, \mathbf{n}_T] \\ \mathbf{R} &= \mathbf{HS} + \mathbf{N} \end{aligned} \quad (7.9)$$

where \mathbf{S} is the space-time symbol. The maximum likelihood decoder estimates the space-time symbol as

$$\hat{\mathbf{S}} = \arg \min_{\mathbf{S}} \|\mathbf{R} - \mathbf{HS}\|_F^2$$

Further, the probability of pair-wise codeword error is

$$\begin{aligned} p(\mathbf{S}_i \leftarrow \mathbf{S}_j) &= Q\left(\sqrt{\frac{\|\mathbf{H}(\mathbf{S}_i - \mathbf{S}_j)\|_F^2}{2\sigma_n^2}}\right) \\ &= Q\left(\sqrt{\frac{\|\mathbf{HD}_S\|_F^2}{2\sigma_n^2}}\right) \end{aligned}$$

where σ_n^2 is the variance of the noise in each channel and $\mathbf{D}_S = \mathbf{S}_i - \mathbf{S}_j$. If we define $\langle \cdot \rangle = \text{vec}(\mathbf{H})$ and $\mathcal{D}_S = \mathbf{I}_{M_r} \otimes \mathbf{D}_S$, we can write

$$p(\mathbf{S}_i \leftarrow \mathbf{S}_j) = Q\left(\sqrt{\frac{\|\langle \mathcal{D}_S \rangle\|_F^2}{2\sigma_n^2}}\right)$$

If we assume a white channel, $E_{\mathbf{H}} \left\{ \langle \cdot \rangle^H \right\} = \mathbf{I}_{M_r N_t}$, when we can find the average probability of codeword error as

$$\begin{aligned} E_{\mathbf{H}} \{p(\mathbf{S}_i \leftarrow \mathbf{S}_j)\} &= \left(\frac{1}{\det \left[\mathbf{I}_{N_t} + \frac{\gamma}{4N_t} \mathbf{G}_{i,j} \right]} \right)^{M_r} \\ &= \prod_{k=1}^{R(\mathbf{G}_{i,j})} \left(1 + \frac{\gamma}{4N_t} \lambda_k(\mathbf{G}_{i,j}) \right)^{M_r} \end{aligned}$$

where $\mathbf{G}_{i,j} = \mathbf{D}_S^H \mathbf{D}_S$. For high SNR, $\gamma \gg 1$ we have

$$E_{\mathbf{H}} \{p(\mathbf{S}_i \leftarrow \mathbf{S}_j)\} \approx \frac{1}{\left(\prod_{k=1}^{R(\mathbf{G}_{i,j})} \lambda_k(\mathbf{G}_{i,j}) \right)^{M_r}} \left(\frac{\gamma}{4N_t} \right)^{-M_r R(\mathbf{G}_{i,j})} \quad (7.10)$$

We can see from this expression that the probability of codeword error decreases with $\gamma^{-M_r R(\mathbf{G}_{i,j})}$ where $M_r R(\mathbf{G}_{i,j})$ is termed the *diversity order*. To maximize the diversity order, we wish to design space-time codes for which $\mathbf{G}_{i,j}$ has maximum rank, i.e., $R(\mathbf{G}_{i,j}) = N_t$. This is termed the *rank criterion* for space-time codes. Further, the determinant of $\mathbf{G}_{i,j}$ provides a coding gain. Again, we wish to maximize the minimum value of this over all possible $\mathbf{G}_{i,j}$. This is termed the *determinant criterion* for space-time codes.

7.1.3 Orthogonal STBC's

Looking at the ML detector immediately provides a challenge to space-time block coding: complexity. The maximum likelihood detector must compare the received vector \mathbf{r} to all possible

transmit symbols \mathbf{S} or the equivalent $\tilde{\mathbf{r}}$ to all possible signal vector \mathbf{s} . Thus, for ML detection M^{N_t} different comparisons must be made, i.e., the decoding complexity is exponential in the number of transmit antennas N_t . This exponential complexity can be changed to a complexity that is linear in N_t by using what is termed an *orthogonal* design. An orthogonal design is one for which

$$\mathbf{SS}^H = c \left(\sum_{i=1}^p |s_i|^2 \right) \mathbf{I}_{N_t} \quad (7.11)$$

where s_i are the p symbols that are mapped to the various columns of \mathbf{S} . It can be shown that an orthogonal design also implies that

$$\mathcal{H}\mathcal{H}^H = c \left(\sum_{i=1}^k |h_i|^2 \right) \mathbf{I}_{N_t} \quad (7.12)$$

where k is the rank of the space-time block code. Recall that the equivalent system (found by conjugating specific values of the received vector \mathbf{r}) results in

$$\tilde{\mathbf{r}} = \mathcal{H}\mathbf{s} + \mathbf{n} \quad (7.13)$$

Since $\mathcal{H}\mathcal{H}^H = c \left(\sum_{i=1}^k |h_i|^2 \right) \mathbf{I}_{N_t}$, know that $\mathcal{H}^H\mathcal{H} = c \left(\sum_{i=1}^k |h_i|^2 \right) \mathbf{I}_{N_t}$. Further, we can create the decision metrics by applying \mathcal{H}^H to the equivalent received vector:

$$\begin{aligned} \mathbf{z} &= \mathcal{H}^H \mathbf{r} \\ &= \mathcal{H}^H (\mathcal{H}\mathbf{s} + \mathbf{n}) \\ &= \sum_{i=1}^{N_t} |h_i|^2 \mathbf{s} + \tilde{\mathbf{n}} \end{aligned} \quad (7.14)$$

where $\tilde{\mathbf{n}}$ is a zero-mean Gaussian vector with $\Sigma_n = \sigma_n^2 \left(\sum_{i=1}^{N_t} |h_i|^2 \right) \mathbf{I}_{N_t}$. Thus, we can see that each element of \mathbf{s} can be determined separately. This reduces the complexity from $O(M^{N_t})$ to $O(M \cdot N_t)$.

Generally $k = N_t$, i.e., orthogonal codes obtain full diversity. However, orthogonal designs are not guaranteed to have full rate. As we will show in the next section, the Alamouti code is one such design, and in fact does achieve full rate. However, it is the only such complex STBC that achieves full rate.

7.2 Alamouti Revisited

Let us consider the 2×1 transmit diversity scheme described in Section 6.14.2 known as the Alamouti code. In this case we can write the transmit code words as

$$\mathbf{S} = \begin{bmatrix} s_1 & -s_2^* \\ s_2 & s_1^* \end{bmatrix} \quad (7.15)$$

Note that

$$\begin{aligned}
\mathbf{S}\mathbf{S}^H &= \begin{bmatrix} s_1 & -s_2^* \\ s_2 & s_1^* \end{bmatrix} \begin{bmatrix} s_1^* & s_2^* \\ -s_2 & s_1 \end{bmatrix} \\
&= \begin{bmatrix} |s_1|^2 + |s_2|^2 & s_1 s_2^* - s_2^* s_1 \\ s_2 s_1^* - s_2 s_1^* & |s_1|^2 + |s_2|^2 \end{bmatrix} \\
&= (|s_1|^2 + |s_2|^2) \begin{bmatrix} 1 & 0 \\ 0 & 1 \end{bmatrix}
\end{aligned} \tag{7.16}$$

Thus, this is an orthogonal design.

7.2.1 Maximum Likelihood Decoding

For one receive antenna at two consecutive time slots assuming matched filtering and perfect sampling we have

$$\begin{aligned}
r_1 &= h_1 s_1 + h_2 s_2 + n_1 \\
r_2 &= -h_1 s_2^* + h_2 s_1^* + n_2
\end{aligned} \tag{7.17}$$

where h_1 and h_2 are the channels from the two transmit antennas to the one receive antenna and n_i are independent Gaussian noise samples. Define $\mathbf{r} = [r_1, r_2]^T$. We are interested maximizing the *a posteriori* probability $p(s_1, s_2 | \tilde{\mathbf{r}})$. If all symbol vectors $\mathbf{s} = [s_1, s_2]^T$ are equally likely

$$\begin{aligned}
p(\mathbf{s} | \mathbf{r}) &= p(\mathbf{r} | \mathbf{s}) \\
&= \frac{1}{2\pi\sigma_n^2} \exp\left(-\frac{1}{2\sigma_n^2} |\mathbf{r} - \mathbf{S}^T \mathbf{h}|^2\right) \\
&= \frac{1}{2\pi\sigma_n^2} \exp\left(-\left[\frac{|r_1 - h_1 s_1 - h_2 s_2|^2}{2\sigma_n^2} + \frac{|r_2 + h_1 s_2^* - h_2 s_1^*|^2}{2\sigma_n^2}\right]\right)
\end{aligned} \tag{7.18}$$

The ML detector minimizes the distance between the received signal vector $\tilde{\mathbf{r}}$ and the transmit signal vector \mathbf{s} .

$$\begin{aligned}
\hat{\mathbf{s}} &= \arg \min_{\mathbf{s}} \{|r_1 - h_1 s_1 - h_2 s_2|^2 + |r_2 + h_1 s_2^* - h_2 s_1^*|^2\} \\
&= \arg \min_{\mathbf{s}} \{(r_1 - h_1 s_1 - h_2 s_2)(r_1 - h_1 s_1 - h_2 s_2)^* + (r_2 + h_1 s_2^* - h_2 s_1^*)(r_2 + h_1 s_2^* - h_2 s_1^*)^*\} \\
&= \arg \min_{\mathbf{s}} \{|r_1|^2 - r_1 s_1^* h_1^* - r_1 s_2^* h_2^* - s_1 h_1 r_1^* + |s_1 h_1|^2 + s_1 h_1 s_2^* h_2^* - s_2 h_2 r_1^* + s_2 h_2 s_1^* h_1^* + |s_2 h_2|^2 \dots \\
&\quad + |r_2|^2 + r_2 s_2 h_1^* - r_2 s_1 h_2^* + s_2^* h_1 r_2^* + |s_2 h_1|^2 - s_2^* h_1 s_1 h_2^* - s_1^* h_2 r_2^* - s_1^* h_2 s_2 h_1^* + |s_1 h_2|^2\}
\end{aligned} \tag{7.19}$$

All terms with x_1 and x_2 together cancel. $|r_1|^2$ and $|r_2|^2$ are independent of \mathbf{s} . Thus,

$$\begin{aligned}
\hat{\mathbf{s}} &= \arg \min_{\mathbf{s}} \{-r_1 s_1^* h_1^* - r_1 s_2^* h_2^* - s_1 h_1 r_1^* + |s_1 h_1|^2 - s_2 h_2 r_1^* + |s_2 h_2|^2 \dots \\
&\quad + r_2 s_2 h_1^* - r_2 s_1 h_2^* + s_2^* h_1 r_2^* + |s_2 h_1|^2 - s_1^* h_2 r_2^* + |s_1 h_2|^2\}
\end{aligned} \tag{7.20}$$

Since there are no terms with s_1 and s_2 together, we can separate decisions

$$\begin{aligned}\hat{s}_1 &= \arg \min_{s_1} \left\{ -r_1 s_1^* h_1^* - s_1 h_1 r_1^* + |s_1 h_1|^2 - r_2 s_1 h_2^* + s_2^* h_1 r_2^* - s_1^* h_2 r_2^* + |s_1 h_2|^2 \right\} \\ &= \arg \min_{s_1} \left\{ |s_1|^2 (|h_1|^2 + |h_2|^2) + s_1 (-h_1 r_1^* - r_2 h_2^*) + s_1^* (-r_1 h_1^* - h_2 r_2^*) \right\}\end{aligned}\quad (7.21)$$

If all symbols have equal energy

$$\begin{aligned}\hat{s}_1 &= \arg \min_{s_1} \left\{ s_1 (-h_1 r_1^* - r_2 h_2^*) + s_1^* (-r_1 h_1^* - h_2 r_2^*) \right\} \\ &= \arg \min_{s_1} \left\{ \Re \{ s_1 (-h_1 r_1^* - h_2^* r_2) \} \right\} \\ &= \arg \min_{s_1} \left\{ \Re \{ -s_1 z_1^* \} \right\} \\ &= \arg \max_{s_1} \left\{ \Re \{ s_1 z_1^* \} \right\} \\ &= \arg \min_{s_1} \left\{ d^2(s_1, z_1) \right\}\end{aligned}\quad (7.22)$$

where

$$z_1 = h_1^* r_1 + h_2 r_2^* \quad (7.23)$$

Similarly, we can show that

$$\hat{s}_2 = \arg \min_{s_2} \left\{ d^2(s_2, z_2) \right\} \quad (7.24)$$

where $z_2 = h_2^* r_1 - h_1 r_2^*$. The variables z_1 and z_2 are the decision metrics where we have shown previously that

$$z_1 = \underbrace{(|h_1|^2 + |h_2|^2)}_{\text{two-fold diversity}} s_1 + h_1^* n_1 + h_2 n_2^* \quad (7.25)$$

There is no interference present in the decision variable. Something similar applies for z_2 . NOTE: Because of this separation instead of a complexity of M^2 the complexity is $2M$ where $M = 2^k$ is the number of symbols.

7.2.2 Equivalent System

As mentioned above, with orthogonal STBCs we can write the decision variable in terms of the symbol vector \mathbf{s} by using an *equivalent* system representation by conjugating specific elements of the matched filter output vector \mathbf{r} . In the case of the Alamouti code, we can formulate $\tilde{\mathbf{r}} = [r_1, r_2^*]^T$. In this case,

$$\tilde{\mathbf{r}} = \mathcal{H}\mathbf{s} + \mathbf{n} \quad (7.26)$$

where $\mathcal{H} = \begin{bmatrix} h_1 & h_2 \\ h_2^* & -h_1^* \end{bmatrix}$. Using this notation, the decision variables are created as

$$\mathbf{z} = \mathcal{H}^H \tilde{\mathbf{r}} \quad (7.27)$$

7.2.3 Multiple Receive Antennas

We now extend the decision variable calculation to multiple receive antennas. On the i th receive antenna we observe (after matched filtering and sampling):

$$\begin{aligned} r_{1i} &= h_{1i}s_1 + h_{2i}s_2 + n_{1i} \\ r_{2i} &= -h_{1i}s_2^* + h_{2i}s_1^* + n_{2i} \end{aligned} \tag{7.28}$$

The decision variables can be written as

$$\begin{aligned} z_1 &= \sum_{i=1}^{M_r} z_{1i} \\ &= \sum_{i=1}^{M_r} (h_{1i}^* r_{1i} + h_{2i}^* r_{2i}^*) \\ &= \frac{E_s}{2} \sum_{i=1}^{M_r} (|h_{1i}|^2 + |h_{2i}|^2) s_1 + \sum_{i=1}^{M_r} (h_{1i}^* n_{1i} + h_{2i}^* n_{2i}) \\ z_2 &= \sum_{i=1}^{M_r} z_{2i} \\ &= \sum_{i=1}^{M_r} (h_{2i}^* r_{1i} - h_{1i}^* r_{2i}^*) \end{aligned} \tag{7.29}$$

The Decision metrics are identical to those for $2M_r$ MRC diversity scheme with a 3dB loss. The probability of error can be written as

$$P_b = \left[\frac{1}{2}(1-\mu) \right]^{2M_r} \sum_{k=0}^{2M_r-1} \binom{2M_r-1+k}{k} \left[\frac{1}{2}(1+\mu) \right]^k \tag{7.30}$$

where $\mu = \sqrt{\frac{\bar{\gamma}_c}{2+\bar{\gamma}_c}}$ and $\bar{\gamma}_c$ is the average SNR per channel (assumed the same on all channels).

7.2.4 Impact of Channel Estimation Error

In order for properly designed STBC codes to be orthogonal, we assume that the know the channel at the receiver. Of course, in reality the channel is estimated at the receiver. Thus with orthogonal STBC's, channel estimation impacts performance in two distinct ways: (a) removing the channel effects in the individual symbols before ML detection and (b) removing the multi-antenna interference. We thus expect that orthogonal STBC's will be more sensitive to channel estimation. We examine that in this sub-section. Recall that the decision statistic for the first symbol (the second symbol can be found similarly) is:

$$z_1 = \hat{h}_1^* r_1 + \hat{h}_2 r_2^* \tag{7.31}$$

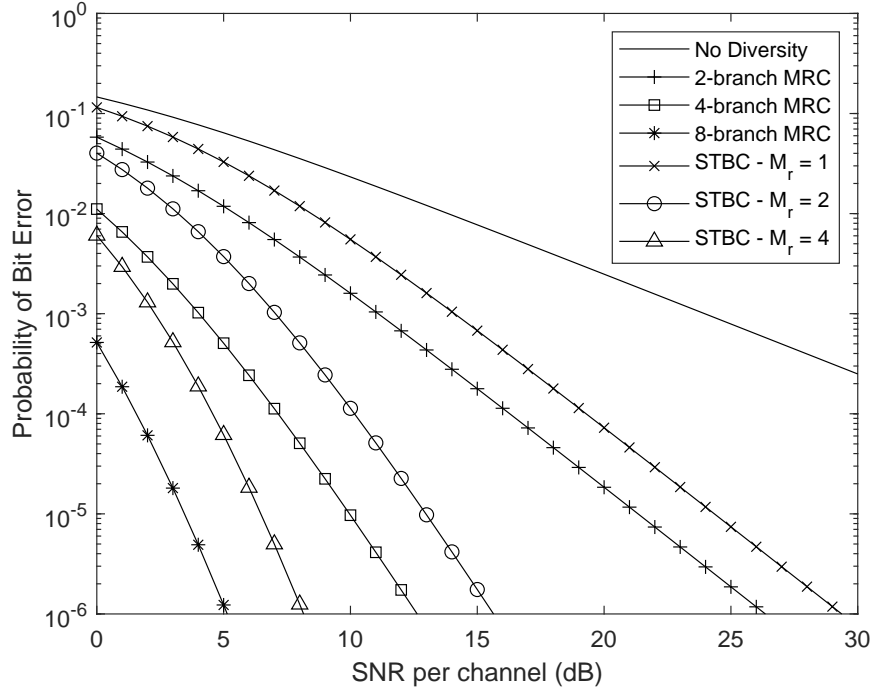


Figure 7.2: Performance of Two-Antenna STBC (Alamouti Code) with $M_r = 1, 2, 4$

where r_1 and r_2 are the matched filter outputs from time slots 1 and 2:

$$r_1 = h_1 s_1 + h_2 s_2 + n_1 \quad (7.32)$$

$$r_2 = h_2 s_1^* - h_1 s_2^* + n_2 \quad (7.33)$$

$$(7.34)$$

$\hat{h}_1 = h_1 + \nu_1$ and $\hat{h}_2 = h_2 + \nu_2$ are the channel estimates, and n_1 , n_2 , ν_1 , and ν_2 are zero mean Gaussian random variables with variance σ_n^2 , σ_n^2 , σ_e^2 , and σ_e^2 . Now substituting we have

$$z_1 = (h_1 + \nu_1)^*(h_1 s_1 + h_2 s_2 + n_1) + (h_2 + \nu_2)(h_2 s_1^* - h_1 s_2^* + n_2)^* \quad (7.35)$$

$$= (|h_1|^2 + |h_2|^2 + h_1 \nu_1^* + \nu_2 h_2^*)s_1 + (\nu_1^* h_2 - \nu_2 h_1^*)s_2 + h_1^* n_1 + \nu_1^* n_1 + h_2 \nu_2^* + \nu_2 n_2^* \quad (7.36)$$

We can see that the cross term s_2 is not completely eliminated in addition to an increase in the noise terms.

Now, the probability of bit error P_b for BPSK can be written as

$$P_b = \Pr \{ \Re(s_1 z_1^*) < 0 \} \quad (7.37)$$

$$= \Pr \{ \mathbf{x}^H \mathbf{M} \mathbf{x} < 0 \} \quad (7.38)$$

where

$$\mathbf{x} = \begin{bmatrix} h_1 \\ n_1 \\ \nu_1 \\ h_2 \\ n_2 \\ \nu_2 \end{bmatrix} \quad (7.39)$$

is a Gaussian vector with zero mean and covariance matrix

$$\mathbf{R}_{xx} = \begin{bmatrix} 1 & 0 & 0 & \rho & 0 & 0 \\ 0 & \sigma_n^2 & 0 & 0 & 0 & 0 \\ 0 & 0 & \sigma_e^2 & 0 & 0 & 0 \\ \rho^* & 0 & 0 & 1 & 0 & 0 \\ 0 & 0 & 0 & 0 & \sigma_n^2 & 0 \\ 0 & 0 & 0 & 0 & 0 & \sigma_e^2 \end{bmatrix} \quad (7.40)$$

where we have used the fact that the channel has mean power of one and correlation between channels of ρ . Further, it can be easily shown that the matrix \mathbf{M} is

$$\mathbf{M} = \begin{bmatrix} 1 & 1/2 & 1/2 & 0 & 0 & 1/2 \\ 1/2 & 0 & 1/2 & 0 & 0 & 0 \\ 1/2 & 1/2 & 0 & 1/2 & 0 & 0 \\ 0 & 0 & 1/2 & 1 & 1/2 & 1/2 \\ 0 & 0 & 0 & 1/2 & 0 & 1/2 \\ 1/2 & 0 & 0 & 1/2 & 1/2 & 0 \end{bmatrix} \quad (7.41)$$

Now, the characteristic function of the decision variable z can be shown to be

$$\Phi_z(s) = \mathbb{E} \{ e^{-sz} \} \quad (7.42)$$

$$= \frac{1}{\pi^2 |\mathbf{R}_{xx}|} \int_{\mathbf{x}} e^{-s\mathbf{x}^H \mathbf{M} \mathbf{x}} e^{-\mathbf{x} \mathbf{R}_{xx}^{-1} \mathbf{x}} d\mathbf{x} \quad (7.43)$$

$$= \frac{1}{\pi^2 |\mathbf{R}_{xx}|} \int_{\mathbf{x}} e^{-\mathbf{x} (s\mathbf{M} - \mathbf{R}_{xx}^{-1}) \mathbf{x}} d\mathbf{x} \quad (7.44)$$

$$= \frac{1}{|s\mathbf{M} - \mathbf{R}_{xx}^{-1}| |\mathbf{R}_{xx}|} \quad (7.45)$$

$$= \frac{1}{|s\mathbf{M}\mathbf{R}_{xx} - \mathbf{I}|} \quad (7.46)$$

Thus, the probability distribution of z can be written as

$$f(z) = \begin{cases} \sum_{i=1}^n -\frac{k_i}{\lambda_i} e^{-z/\lambda_i} & z < 0 \\ \sum_{i=n+1}^{n+p+1} -\frac{k_i}{\lambda_i} e^{-z/\lambda_i} & z > 0 \end{cases} \quad (7.47)$$

where λ_i $1 \leq i \leq n$ are the negative eigenvalues of $\mathbf{M}\mathbf{R}_{xx}$, λ_i $n+1 \leq i \leq n+p$ are the zero eigenvalues of $\mathbf{M}\mathbf{R}_{xx}$, λ_i $n+p \leq i \leq N$ are the positive eigenvalues of $\mathbf{M}\mathbf{R}_{xx}$, k_i are the residues

of $\Phi_z(s)$ evaluated at λ_i , $k_i = \prod_{j \neq i} \frac{\lambda_i}{\lambda_i - \lambda_j}$ for distinct eigenvalues. Now, the probability of error is then

$$P_b = \int_{-\infty}^0 f(z) dz \quad (7.48)$$

$$= \int_{-\infty}^0 \sum_{i=1}^n -\frac{k_i}{\lambda_i} e^{-z/\lambda_i} dz \quad (7.49)$$

$$= \sum_{i=1}^n k_i \quad (7.50)$$

The performance of orthogonal STBC with $N_t = 2$ (i.e., Alamouti code) in the presence of channel estimation is shown in Figures 7.3 and 7.4. Specifically, in Figure 7.3 we examine the impact of channel estimation as a function of SNR per channel. In this plot we assume two cases for STBC: (a) perfect channel estimation and (b) channel estimation with a pilot SNR of 20dB. In case (b) the pilot symbols (i.e., the known symbols used for channel estimation) are given enough power to ensure 20dB SNR regardless of the SNR per channel for the data. Also plotted are three other cases: (1) No diversity with perfect channel estimation, (2) two-branch receive diversity (with MRC combining) with perfect channel estimation, and (3) two-branch receive diversity (with MRC combining) with channel estimation SNR of 20dB. We can see that with perfect channel estimation receive diversity outperforms STBC by a constant 3dB. However, with channel estimation error, the loss is more pronounced. In fact, while the performance loss starts at 3dB, eventually STBC produces an error floor that is roughly 4-5x higher than receive diversity. At high SNR the residual interference between the two antennas dominates performance. In Figure 7.4 we plot the probability of bit error as a function of the channel estimation SNR when $\gamma_c = 20$ dB. We include the same curves for comparison.

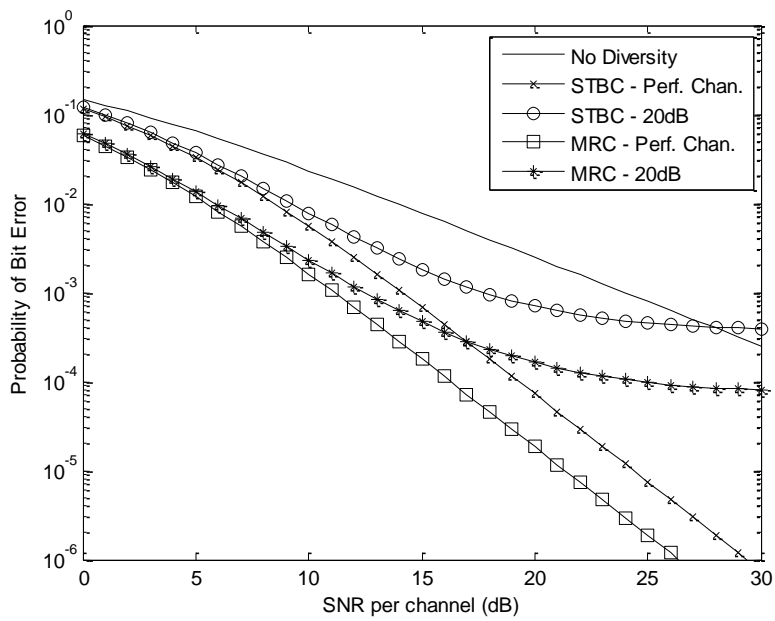


Figure 7.3: STBC with Channel Estimation Error

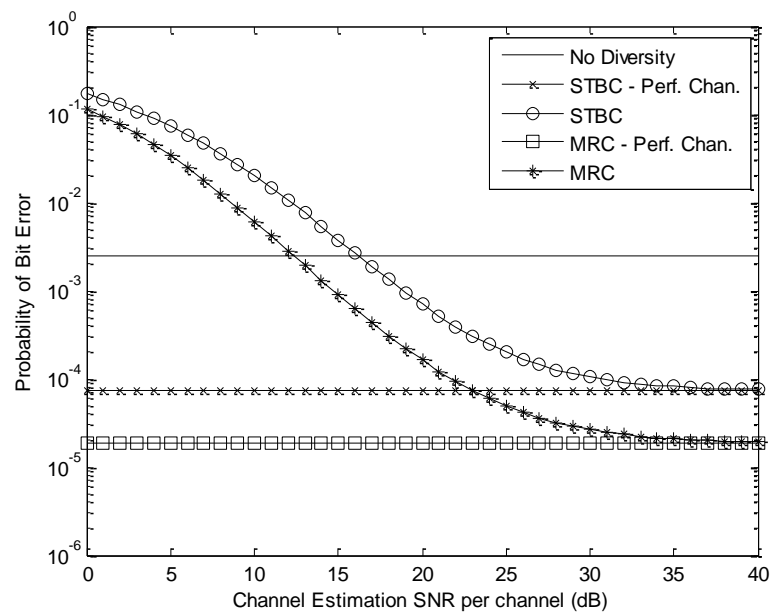


Figure 7.4: STBC with Channel Estimation Error ($\gamma_c = 20$ dB)

Table 7.1: Minimum block length T_{\min} for full diversity with real orthogonal designs

N_t	T_{\min}
2	2
3	4
4	5
5	6
6	8
7	8
8	8
9	16
10	32
11	64
12	64
14	128
15	128
16	128

7.3 General STBCs

7.3.1 General Orthogonal Designs

Real Designs

If the symbols are all real (e.g., BPSK), an orthogonal design can always be found. However, the minimum number of symbol periods needed to achieve full N_t diversity is

$$T_{\min} = \min (2^{4c+d}) \quad (7.51)$$

where $c \in \mathbb{Z}$, $d \in \mathbb{Z}$, $c > 0$, $0 \leq d \leq 4$, $8c + 2^d \geq N_t$. The value of T_{\min} is given in Table 7.1 for $2 \leq N_t \leq 16$. For $N_t \leq 8$, the value of $T_{\min} \approx N_t$. However, for $N_t > 8$, the value of T_{\min} grows dramatically.

Example 1: For $N_t = 3$, $r = 1$ and $T = 4$ we have

$$\mathbf{S} = \begin{bmatrix} s_1 & -s_2 & -s_3 & -s_4 \\ s_2 & s_1 & s_4 & -s_3 \\ s_3 & -s_4 & s_1 & s_2 \end{bmatrix} \quad (7.52)$$

Each symbol is transmitted on all three antennas (thus full $N_t = 3$ -fold diversity) and since four symbols are sent over four time slots, the rate is $r = 1$.

Example 2: For $N_t = 4$, $r = 1$ and $T = 4$ we have

$$\mathbf{S} = \begin{bmatrix} s_1 & -s_2 & -s_3 & -s_4 \\ s_2 & s_1 & s_4 & -s_3 \\ s_3 & -s_4 & s_1 & s_2 \\ s_4 & s_3 & -s_2 & s_1 \end{bmatrix} \quad (7.53)$$

Each symbol is transmitted on all four antennas (thus full $N_t = 4$ -fold diversity) and since four symbols are sent over four time slots, the rate is $r = 1$.

The performance of these real orthogonal designs using BPSK with $M_r = 1$ can be shown to be:

$$P_b = \left[\frac{1}{2} \left(1 - \sqrt{\frac{\gamma_c}{N_t/r + \gamma_c}} \right) \right]^{N_t} \sum_{k=0}^{N_t} \binom{N_t - 1 + k}{k} \left[\frac{1}{2} \left(1 + \sqrt{\frac{\gamma_c}{N_t/r + \gamma_c}} \right) \right]^k \quad (7.54)$$

However, if there are $M_r \geq 1$ receive antennas the performance is written as:

$$P_b = \left[\frac{1}{2} \left(1 - \sqrt{\frac{\gamma_c}{N_t/r + \gamma_c}} \right) \right]^{M_r N_t} \sum_{k=0}^{M_r N_t} \binom{N_t - 1 + k}{k} \left[\frac{1}{2} \left(1 + \sqrt{\frac{\gamma_c}{N_t/r + \gamma_c}} \right) \right]^k \quad (7.55)$$

Full-rate STBC's (with real symbols) that achieve N_t -fold diversity with simple linear processing and optimal delay ($T = N_t$) exist for $N_t = \{2, 4, 8\}$. If we are willing to accept non-optimal delay ($T > N_t$) we can construct an orthogonal code for any N_t . In general an $N_t \times p$ STBC with M-ary modulation requires the receiver to calculate $M(r * N_t)$ decision metrics (exponential complexity). However, with orthogonal designs, we only require $M \cdot r \cdot N_t$ decision metrics to be calculated (linear complexity). The major drawback with real designs is that they do not allow complex modulation which substantially reduces throughput.

7.3.2 Complex Designs

Unlike for real designs, there are very few complex designs that are full rate. In fact, the Alamouti scheme is the only one! Rate $\frac{1}{2}$ STBC's do exist for any value of N_t . However, this is not very effective since it requires a 50% loss in efficiency to obtain the diversity benefit. For some values of N_t higher rates ($r > 1/2$) exist. For example, a $r = \frac{3}{4}$ STBC exists for $N_t = 3$ and $N_t = 4$. Like real orthogonal designs, the rows are orthogonal and full N_t -fold diversity is achieved. One example is the $N_t = 3$ $r = 3/4$ block code defined by

$$\mathbf{S} = \begin{bmatrix} s_1 & -s_2^* & s_3^*/\sqrt{2} & s_3^*/\sqrt{2} \\ s_2 & s_1^* & s_3^*/\sqrt{2} & -s_3^*/\sqrt{2} \\ s_3/\sqrt{2} & s_3/\sqrt{2} & \frac{-s_1 - s_1^* + s_2 - s_2^*}{2} & \frac{s_2 + s_2^* + s_1 - s_1^*}{2} \end{bmatrix} \quad (7.56)$$

Note that each symbol is sent on all three transmit antennas over the course of a block (thus full diversity). A second example with $N_t = 4$ and $r = 3/4$ is

$$\mathbf{S} = \begin{bmatrix} s_1 & -s_2^* & s_3^*/\sqrt{2} & s_3^*/\sqrt{2} \\ s_2 & s_1^* & s_3^*/\sqrt{2} & -s_3^*/\sqrt{2} \\ s_3/\sqrt{2} & s_3/\sqrt{2} & \frac{-s_1 - s_1^* + s_2 - s_2^*}{2} & \frac{s_2 + s_2^* + s_1 - s_1^*}{2} \\ s_3/\sqrt{2} & -s_3/\sqrt{2} & \frac{-s_2 - s_2^* + s_1 - s_1^*}{2} & \frac{-s_1 + s_1^* - s_2 + s_2^*}{2} \end{bmatrix} \quad (7.57)$$

Again, each symbol is transmitted from each of the four antennas and all rows are orthogonal. The performance of N_t -fold STBC with rate r , one receive antenna $M_r = 1$ and QPSK modulation has performance that is identical to that with $M_r = N_t$ -fold receive diversity (with one transmit

antenna) except that a r/N_t SNR loss is incurred:

$$P_b = \frac{1}{2} \left[1 - \frac{\mu}{\sqrt{2 - \mu^2}} \sum_{k=0}^{N_t-1} \binom{2k}{k} \left[\frac{1 - \mu^2}{4 - 2\mu^2} \right]^k \right] \quad (7.58)$$

where $\mu = \sqrt{\frac{\gamma_c}{N_t/r + \gamma_c}}$.

Chapter 8

Spatial Multiplexing

In the previous chapters we have examined the usefulness of multiple antennas in wireless systems to increase SNR, combat Rayleigh fading and mitigate interference. The next use of multiple antennas that we want to discuss is *spatial multiplexing*. Spatial multiplexing is the ability to transmit multiple data streams in the same bandwidth at the same time by opening up spatial channels. Recall from equation (4.41) that the capacity of a MIMO link (in the absence of channel knowledge) can be written as

$$\frac{C}{B} = \log_2 \left(\prod_{i=1}^r \left(1 + \lambda_i \frac{\gamma}{N_t} \right) \right) b/s/Hz \quad (8.1)$$

where λ_i are the $r \leq \min\{M_r, N_t\}$ non-zero eigenvalues of $\mathbf{H}^H \mathbf{H}$. This expression explicitly shows that the capacity is made up of r parallel data streams each with SNR $\lambda_i \frac{\gamma}{N_t}$ where γ is the average SNR per channel. In this chapter we will examine spatial multiplexing both with and without channel information being available at the transmitter. We will always assume that channel information is available at the receiver through the use of pilot symbols or pilot channels. In the next section we consider techniques which do not require channel information at the transmitter (often called Channel Side Information at the Transmitter or CSIT).

8.1 Spatial Multiplexing in the Absence of CSIT

In the absence of CSIT, the transmitter will transmit equal power from each antenna and transmit a symbol vector \mathbf{s} at each time instance. We will assume that the transmit vector is a vector of standard PSK or QAM symbols. Again, without CSIT, there is no reason to use different modulation schemes on each transmitter. Thus, $s_i \in \mathcal{A}$ where \mathcal{A} is the symbol alphabet and the transmit signal for one symbol interval is

$$\mathbf{x}(t) = \mathbf{s}p(t) \quad (8.2)$$

where $p(t)$ is the pulse shape assumed.

8.1.1 Maximum Likelihood

At the receiver, we pass the received signal on each antenna through a pulse matched filter and sample it at the optimal sampling time. Assuming that the channel is constant over a symbol interval, the received signal vector for an arbitrary symbol time is

$$\mathbf{r} = \sqrt{\frac{E_s}{N_t}} \mathbf{H}\mathbf{s} + \mathbf{n} \quad (8.3)$$

where \mathbf{n} is assumed to be white noise with $E\{\mathbf{n}\mathbf{n}^H\} = \sigma_n^2 \mathbf{I}$.

Since \mathbf{n} is Gaussian with $\mathbf{R}_{nn} = \sigma_n^2 \mathbf{I}$, it is easy to show that the maximum likelihood receiver creates symbol vector estimates using

$$\hat{\mathbf{s}} = \arg \min_{\mathbf{s}} \left\| \mathbf{r} - \sqrt{\frac{E_s}{N_t}} \mathbf{H}\mathbf{s} \right\|^2 \quad (8.4)$$

which requires knowledge of \mathbf{H} and has a complexity that is on the order of M^{N_t} where $M = 2^k = |\mathcal{A}|$ is the number of possible symbols per stream and N_t is the number of transmit antennas. This complexity comes from the fact that we must do a brute force search over M^{N_t} symbol vectors \mathbf{s} .

8.1.2 Zero-forcing

Due to the exponential complexity of the ML receiver, we would like to examine less complex structures. Specifically, it would be preferable to find structures that had a linear complexity in the number of antennas and the symbol alphabet size. Let the decision variable be written as

$$\mathbf{z} = \mathbf{T}\mathbf{r} \quad (8.5)$$

A zero-forcing solution completely eliminates interference. This can be accomplished (assuming that $M_r \geq N_t$) using a linear transform

$$\mathbf{T}_{zf} = \sqrt{\frac{N_t}{E_s}} \mathbf{H}^\dagger = \sqrt{\frac{N_t}{E_s}} (\mathbf{H}^H \mathbf{H})^{-1} \mathbf{H}^H \quad (8.6)$$

Thus, the decision variable becomes

$$\begin{aligned} \mathbf{z} &= \sqrt{\frac{N_t}{E_s}} \mathbf{H}^\dagger \mathbf{r} \\ &= \sqrt{\frac{N_t}{E_s}} \mathbf{H}^\dagger \left(\sqrt{\frac{E_s}{N_t}} \mathbf{H}\mathbf{s} + \mathbf{n} \right) \\ &= \mathbf{s} + \sqrt{\frac{N_t}{E_s}} \mathbf{H}^\dagger \mathbf{n} \end{aligned} \quad (8.7)$$

Note that although the interference is eliminated, the noise covariance matrix is $\sigma_n^2 (\mathbf{H}^H \mathbf{H})^{-1}$. Since the eigenvalues of the psuedo-inverse are generally greater than one, the resulting noise power is enhanced and thus the SNR on some streams can be substantially worse than the SIMO case. Further, it can be shown that in independent Rayleigh fading, the resulting SNR has a distribution equal to

$$f_\Gamma(\gamma) = \frac{N_t}{\bar{\gamma}(M_r - N_t)!} e^{-\frac{N_t}{\bar{\gamma}}\gamma} \left(\frac{N_t}{\bar{\gamma}} \gamma \right)^{M_r - N_t}$$

which is the SNR expected from a diversity order of $M_r - N_t + 1$ with independent channels each with an average SNR of $\frac{\bar{\gamma}}{N_t}$. Thus, the probability of bit error of BPSK in independent Rayleigh fading is

$$P_b = \left[\frac{1}{2} \left(1 - \sqrt{\frac{\bar{\gamma}}{N_t + \bar{\gamma}}} \right) \right]^{M_r - N_t + 1} \sum_{k=0}^{M_r - N_t} \binom{M_r - N_t + k}{k} \left[\frac{1}{2} \left(1 + \sqrt{\frac{\bar{\gamma}}{N_t + \bar{\gamma}}} \right) \right]^k \quad (8.8)$$

The performance of zero-forcing (also sometimes termed a decorrelator) in a $N_t = 2 \times M_r = 2$ Rayleigh fading channel with QPSK modulation is plotted in Figure 8.1 (both simulated and the theoretical performance). We can see that the simulated performance matches the theoretical plots very well. Also plotted is the performance of the ML receiver which provides dramatic improvement over the zero-forcing receiver. Two comparison plots are also included: QPSK in a SIMO channel ($M_r = 2$) and 16-QAM in a SIMO channel ($M_r = 2$). The former provides a lower bound on the performance of spatial multiplexing, albeit one with half the spectral efficiency. The latter plot provides a comparison to SIMO with the same spectral efficiency. We can see that spatial multiplexing with an ML receiver provides substantial performance improvement over 16QAM without spatial multiplexing. However, the zero-forcing receiver outperforms 16-QAM only at low SNR.

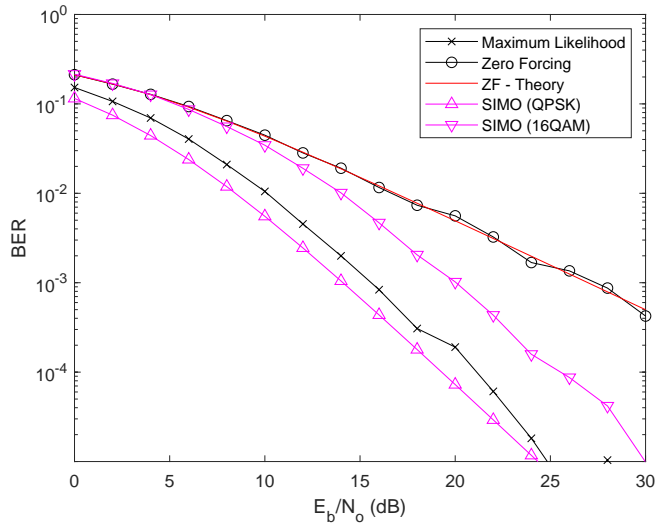


Figure 8.1: Performance of Spatial Multiplexing in Independent Rayleigh Fading Channel (QPSK, $N_t = 2$, $M_r = 2$)

8.1.3 MMSE

Since the performance of zero-forcing is substantially worse than the ML receiver, we would like to examine other structures that have linear complexity but improved performance. The MMSE receiver provides the linear transformation that minimizes the mean square error between the

received signal vector and the desired symbol vector:

$$\mathbf{T}_{mmse} = \arg \min_{\mathbf{T}} \mathbb{E} \left\{ \|\mathbf{Tr} - \mathbf{s}\|^2 \right\} \quad (8.9)$$

It is straightforward to show that the transformation which minimizes the MSE is

$$\mathbf{T}_{mmse} = \sqrt{\frac{N_t}{E_s}} \left(\mathbf{H}^H \mathbf{H} + \frac{N_t N_o}{E_s} \mathbf{I} \right)^{-1} \mathbf{H}^H \quad (8.10)$$

The performance of the MMSE receiver is better than zero-forcing since it balances the effects of enhanced noise and stream interference. One way to understand this is by looking at the inversion operation in (8.10). If the SNR (equivalently E_s/N_o) goes to infinity the receiver converges to the zero-forcing or decorrelating receiver. This is intuitive since for infinite SNR the MMSE is dominated by inter-stream interference. Alternatively, we can see that by adding a weighted diagonal to $\mathbf{H}^H \mathbf{H}$ prior to inverting it, we set a floor on the minimum eigenvalues of the matrix being inverted and thus a ceiling on the eigenvalues of its inverse. This limits the noise enhancement experienced.

8.1.4 Successive Interference Cancellation + Zero-Forcing/MMSE

As final structure we will examine a combination of successive interference cancellation (SIC) with a linear (ZF or MMSE) canceller. The successive interference cancellation approach does the following. Consider again the received vector \mathbf{r} . Rewriting the received vector we have

$$\mathbf{r} = \sqrt{\frac{E_s}{N_t}} \mathbf{H} \mathbf{s} + \mathbf{n} \quad (8.11)$$

$$= \sqrt{\frac{E_s}{N_t}} \sum_{i=1}^{N_t} s_i \mathbf{h} \quad (8.12)$$

where s_i is the symbol transmitted from the i th antenna and \mathbf{h}_i is the $M_r \times 1$ channel vector between the i th antenna and the receiver. The detector first estimates the symbol $s + i$ that is the most reliable. It then creates a new symbol vector by cancelling that symbol from the original received vector: $\mathbf{r}_1 = \mathbf{r} - \hat{s}_i \mathbf{h}_i$. The resulting signal vector is used to detect the second most reliable symbol. The estimate of this new symbol is then again used to cancel it from the received symbol vector. The process continues until all symbols are estimated. Note that it is important that the streams are detected and cancelled in decreasing order of reliability.

Unfortunately, successive cancellation alone is not very effective since even the most reliable stream is very difficult to detect in the presence of the inter-stream interference. However, if we apply a linear transformation such as \mathbf{T}_{zf} or \mathbf{T}_{mmse} prior to estimating the first symbol and cancelling it, we can obtain significantly better performance for the succeeding streams. Specifically, while the performance of the first stream is equivalent to that of zero-forcing (or MMSE), the succeeding layers are substantially better. For example, once the first signal is cancelled, in order to detect the second most reliable stream, we need only project away from $N_t - 2$ interfering streams (instead of $N_t - 1$) since there is one less interfering stream. Further, as we progress to the latter streams there are fewer and fewer interfering streams to cause degradation.

The specific algorithm for SIC + ZF is as follows:

1. Initialize
 - * $\mathbf{T}(1) = \mathbf{H}^\dagger$
 - * $i = 1$
 - * $\mathbf{r}_1 = \mathbf{r}$
 - * Set $\mathcal{A} = \{1, 2, 3, \dots, N_t\}$. Set $\mathcal{B} = \{\}$.
2. $k_i = \arg \min_{j \notin \mathcal{B}} \|[\mathbf{T}(i)]_{j,:}\|^2$
3. Remove k_i from \mathcal{A} . Add k_i to \mathcal{B} .
4. Create the nulling vector as $\mathbf{w}_{k_i} = [\mathbf{T}(i)]_{k_i,:}$
5. Apply the nulling vector to the k_i th stream to obtain the decision variable $z_{k_i} = \mathbf{w}_{k_i} \mathbf{r}_i$
6. Obtain a symbol estimate for the k_i th stream using an appropriate decision function: $\hat{s}_{k_i} = f(z_{k_i})$
7. Cancel the k_i th stream: $\mathbf{r}_{i+1} = \mathbf{r}_i - \hat{s}_{k_i} \mathbf{H}_{:,k_i}$
8. Determine the new transform $\mathbf{T}(i) = (\mathbf{H}_{\bar{\mathcal{B}}}^\dagger)$
9. Set $i = i + 1$ and go to 2

where $[\mathbf{A}]_{j,:}$ refers to the j th row of \mathbf{A} , $[\mathbf{A}]_{:,j}$ refers to the j th column of \mathbf{A} , and $\mathbf{A}_{\bar{\mathcal{B}}}$ refers to the matrix \mathbf{A} with columns whose indices are in set \mathcal{B} set to zero. Recall also that \mathbf{A}^\dagger is the pseudo-inverse of \mathbf{A} . It is important to use the pseudo-inverse in this process since \mathbf{H} and $\mathbf{H}_{\bar{\mathcal{B}}}$ will generally not be invertible.

Note that we can obtain even better performance if we replace zero-forcing with the MMSE receiver. The only change needed is to replace the zero-forcing transformation with the MMSE transformation in steps 1 and 7. The performance of the ZF+SIC receiver in a 2×2 channel is shown in Figure 8.2 (left). Also shown is the MMSE receiver. We can see that the MMSE receiver provides a modest benefit relative to the ZF receiver in this channel. Also, adding SIC to the ZF receiver also provides a modest improvement. All three (ZF, MMSE, SIC+ZF) provide the same diversity performance ($M_r - N_t + 1 = 1$). The ML receiver, on the other hand, provides M_r -fold diversity as indicated by its slope which matches the SIMO performance. The performance with $N_t = 2$ and $M_r = 4$ is also plotted in Figure 8.2 (right). With additional receive antennas, the ML receiver is nearly equivalent to QPSK with SIMO and within 4-6dB of AWGN performance of QPSK, while achieving twice the spectral efficiency. Further, SIC+ZF is within 1dB of ML, showing that strong performance can be achieved with reasonable complexity. This is expected since a diversity order of $M_r - N_t + 1 = 3$ can be achieved due to the additional antennas. Finally, we show the performance of $N_t = 4$ and $M_r = 4$ (8b/s/Hz) in Figure 8.3. Again, the ML performance is within 1-2dB of the interference free case with four times the capacity. The other

receiver structures suffer due to the lack of diversity since $M_r - N_t + 1 = 1$.

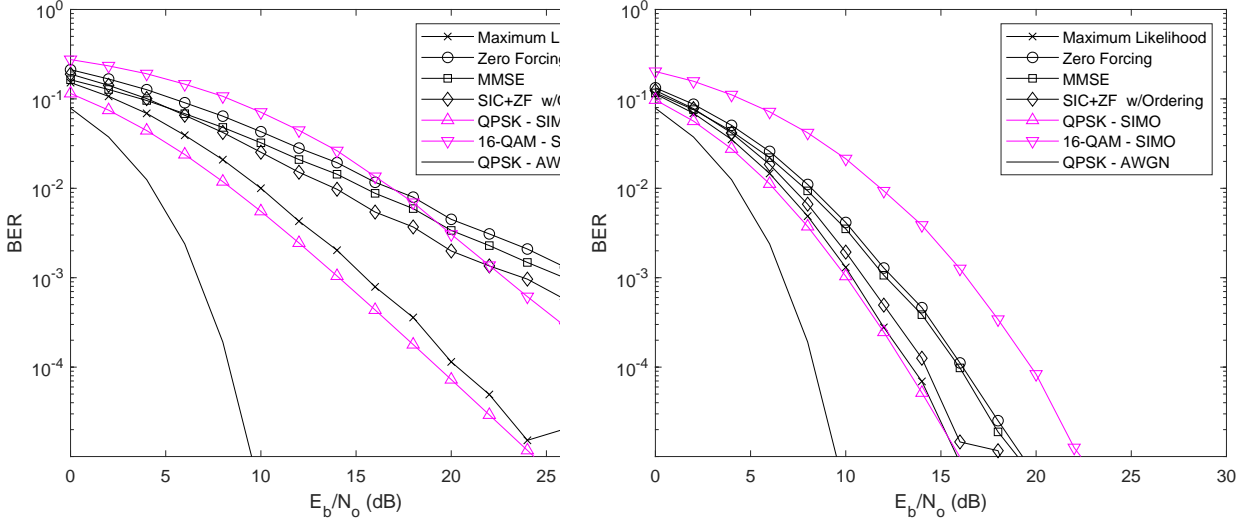


Figure 8.2: Performance of Spatial Multiplexing with $N_t = 2$ (4b/s/Hz) in Independent Rayleigh Fading Channel (left - $M_r = 2$, right $M_r = 4$)

8.2 Full Channel State Information at the Transmitter (CSIT)

Recall that the capacity of the MIMO channel with channel state information at the transmitter is

$$\frac{C}{B} = \log_2 \left(\prod_{i=1}^r \left(1 + \eta_i \lambda_i \frac{\gamma}{N_t} \right) \right) b/s/Hz \quad (8.13)$$

where $\eta_i = \left(\mu - \frac{1}{\lambda_i \gamma} \right)^+$ and μ is the water-filling level chosen to make $\sum_{i=1}^r \eta_i = 1$. Compared with the no CSIT case in (8.1), the only difference is the power allocation across modes in the CSIT case. When $N_t = M_r$ and the channels are independent, there is not much advantage from a capacity perspective as can be seen in Figure 8.4. As we will show later, this does not necessarily mean that practically speaking there isn't a benefit to having channel information at the transmitter. But from an information theory perspective, there is little to no benefit in this case. However, that is not the case when $N_t > M_r$ as can be seen in Figure 8.5. Since the spatial channel is more selective in this case, knowing which spatial mode(s) to place power in provides a substantial benefit.

In addition to the case where $N_t > M_r$, another scenario where CSIT provides a benefit is when the channel is correlated. For example, in Figure 8.6 the capacity of $N_t = M_r = 2$ (left) and $N_t = M_r = 4$ (right) when the channel at the receiver has an anglespread of 5° . We can see that in the two antenna case CSIT provides a 10 – 40% improvement in capacity, while in the four antenna case CSIT provides nearly double that improvement. Spatial correlation makes the channel more spatially selective, i.e., $\lambda_{max} \gg \lambda_{min}$. When this is the case, there is a bigger advantage to having channel knowledge. Thus, we can conclude that from a capacity perspective,

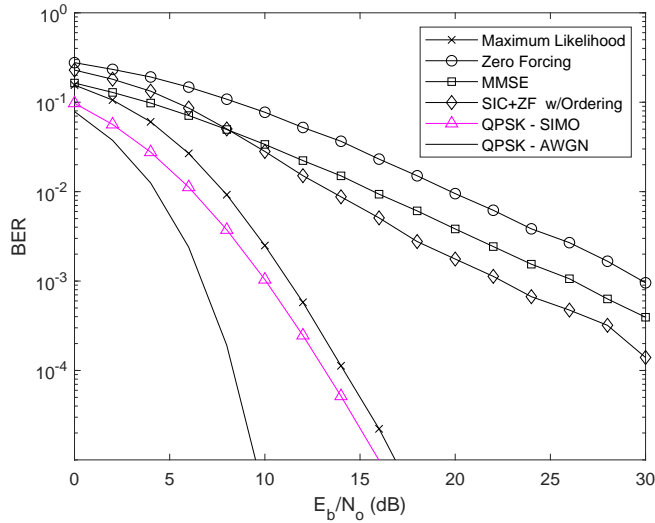


Figure 8.3: Performance of Spatial Multiplexing with $N_t = 4$ (8b/s/Hz) in Independent Rayleigh Fading Channel ($M_r = 4$)

CSIT provides a benefit in two general cases: (1) when $M_r > N_t$ and (2) when the channel is correlated.

8.2.1 Applying Channel Knowledge at the Transmitter

There are many ways to exploit channel knowledge at the receiver. The most straightforward way uses singular value decomposition. To see this recall that the received vector (after matched filtering) is written as

$$\mathbf{r} = \mathbf{H}\mathbf{s} + \mathbf{n} \quad (8.14)$$

Now, we can apply singular value decomposition to the channel matrix \mathbf{H} :

$$\mathbf{H} = \mathbf{U}\Sigma\mathbf{V}^H \quad (8.15)$$

where \mathbf{U} is an $M_r \times M_r$ matrix of left singular vectors, Σ is an $M_r \times N_t$ matrix of singular values (on the “diagonal”)¹ and \mathbf{V} is an $N_t \times N_t$ matrix of right singular vectors. The optimal use of channel state information at the transmitter (CSIT) is to “beamform” according to the eigenmodes of the channel (termed “eigenbeamforming”). In other words, we transmit along the right singular vectors:

$$\mathbf{x} = \mathbf{V}\mathbf{s} \quad (8.16)$$

¹The singular values are along the diagonal of the first N_t rows, that is the diagonal of the matrix formed by the first N_t rows and the N_t columns.

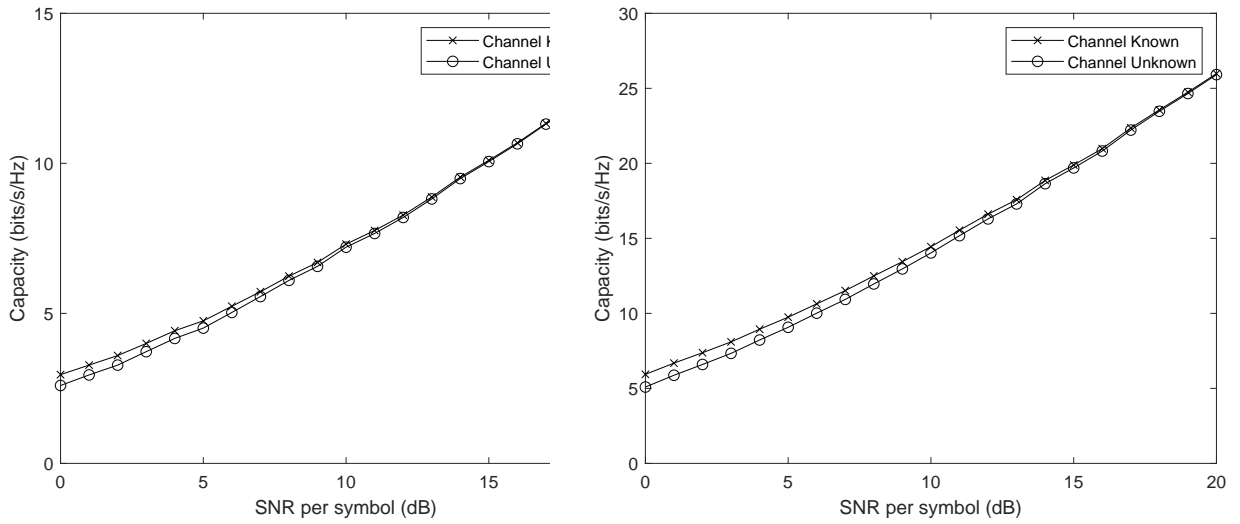


Figure 8.4: The Value of CSIT in Spatial Multiplexing with $M_r = N_t$ in Independent Rayleigh Fading Channel (left - $N_t = M_r = 2$, right $N_t = M_r = 4$)

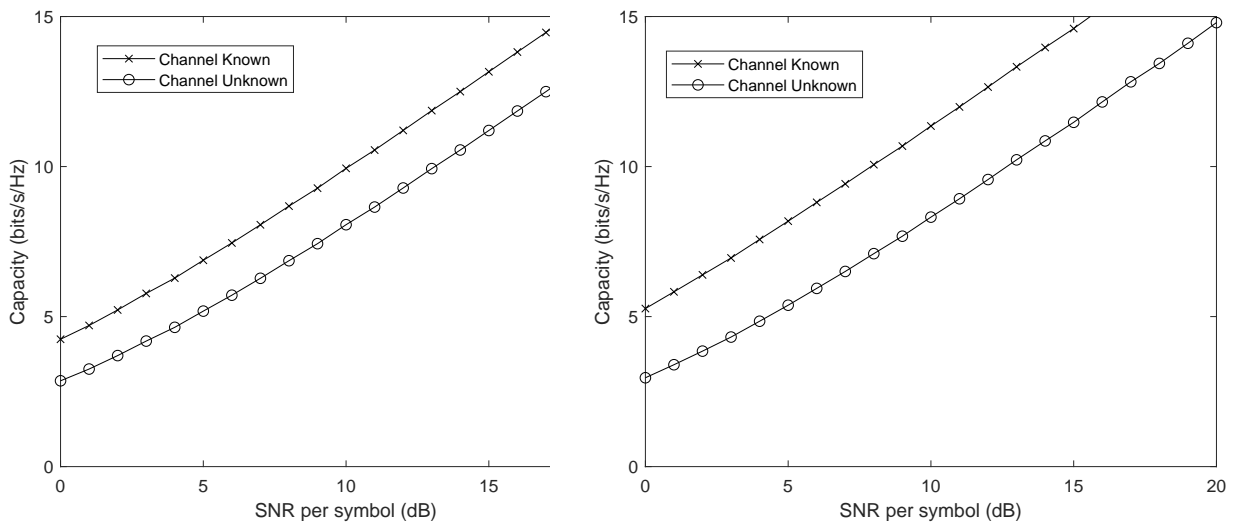


Figure 8.5: The Value of CSIT in Spatial Multiplexing with $M_r < N_t$ in Independent Rayleigh Fading ($d = 0.5\lambda$, Angle Spread = 5°) Channel (left - $N_t = 4, M_r = 2$, right - $N_t = 6, M_r = 2$)

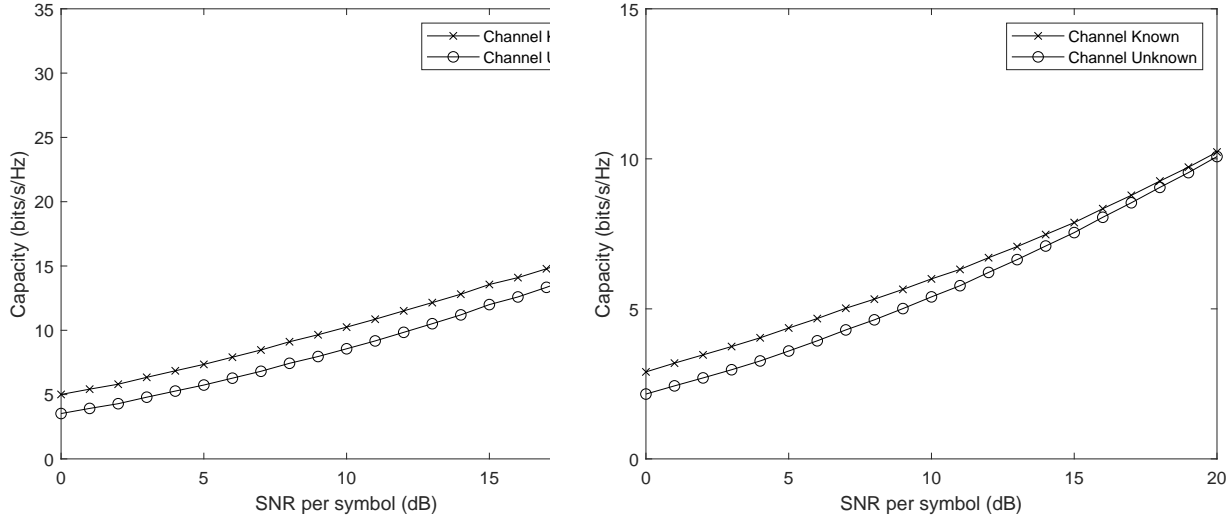


Figure 8.6: The Value of CSIT in Spatial Multiplexing with $M_r = N_t$ in Correlated Rayleigh Fading ($d = 0.5\lambda$, Angle Spread = 5°) Channel (left - $N_t = M_r = 2$, right - $N_t = M_r = 4$)

where \mathbf{x} is the transmit vector and \mathbf{s} is the vector of symbols we wish to transmit. At the receiver we “beamform” along the left singular vectors:

$$\mathbf{z} = \mathbf{U}^H \mathbf{r} \quad (8.17)$$

$$= \mathbf{U}^H \mathbf{U} \Sigma \mathbf{V}^H \mathbf{V} \mathbf{s} + \mathbf{U}^H \mathbf{n} \quad (8.18)$$

$$= \Sigma \mathbf{s} + \mathbf{n} \quad (8.19)$$

where we have completely eliminated any interference between sub-streams. Now, with full channel knowledge, we should allocate power (and thus bit rate) optimally among the spatial modes. This is accomplished via water-filling. Specifically, we use the diagonal matrix Γ to distribute the power among the eigenmodes:

$$\Gamma = \begin{bmatrix} \sqrt{\epsilon_1} & 0 & \cdots & 0 \\ 0 & \sqrt{\epsilon_1} & \cdots & 0 \\ \vdots & & & \\ 0 & 0 & \cdots & \sqrt{\epsilon_{N_t}} \end{bmatrix} \quad (8.20)$$

where η_i is the fraction of the transmit power in the i th eigenmode of the channel. Note that $\sum_i \eta_i = N_t$. How are these fractions found? Waterfilling.

8.3 Waterfilling

The concept of waterfilling represents the solution to a Lagrangian optimization problem as discussed in Chapter 4. Waterfilling can be accomplished using the following simple algorithm:

1. Initialize $p = 1$ ($r - p + 1$ modes will be used where r is the rank of the channel and is the number of available modes). Further, order the eigenvalues (or modes) from largest to smallest.

2. Calculate the “water level”:

$$\mu = \frac{N_t}{r - p + 1} \left[1 + \frac{N_o}{E_s} \sum_{i=1}^{r-p+1} \frac{1}{\lambda_i} \right] \quad (8.21)$$

where λ_i are the eigenvalues of the $\mathbf{H}\mathbf{H}^H$ and E_s/N_o is the average energy per symbol across all modes.

3. Determine the gain per mode:

$$\eta_i = \mu - \frac{N_t}{\lambda_i} \frac{N_o}{E_s} \quad i = 1, 2, \dots, r - p + 1 \quad (8.22)$$

4. Determine if $\eta_i < 0$ for any mode. If not, stop. If so, $p = p + 1$, go to 2.

8.4 Spatial Multiplexing with Partial Information

It may not always be feasible to feedback full channel state information. However, in the absence of full information, spatial multiplexing can benefit from *partial* information about the channel. To see this again consider the received signal after matched filtering:

$$\mathbf{r} = \mathbf{H}\mathbf{s} + \mathbf{n} \quad (8.23)$$

instead of feeding back \mathbf{H} to the transmitter we will consider two other approaches: (1) feeding back antenna indices and (2) feeding back a subset of the right eigenvectors.

8.4.1 Antenna Feedback

The $M_r \times N_t$ channel matrix can be written as a set of N_t column vectors:

$$\mathbf{H} = [\mathbf{h}_1 \mathbf{h}_2 \cdots \mathbf{h}_{N_t}] \quad (8.24)$$

where \mathbf{h}_i is the channel vector between the i th antenna and all M_r receive antennas. If we wish to only transmit on N of the N_t antennas, we can feedback the best N antennas. To do so, we examine all $\frac{N_t!}{(N_t-N)!N!}$ combinations of N vectors in the $M_r \times N$ matrix

$$\tilde{\mathbf{H}} = [\mathbf{h}_i \mathbf{h}_j \cdots \mathbf{h}_k] \quad (8.25)$$

where $i, j, k \in \{1, 2, \dots, N_t\}$ to determine which provides the maximum capacity

$$C = \sum_{i=1}^{\tilde{r}} \log_2 \left(1 + \frac{SNR}{\tilde{r}} \tilde{\lambda}_i \right) \quad (8.26)$$

where $\tilde{\lambda}_i$ are the eigenvalues of $\tilde{\mathbf{H}}$ and $\tilde{r} \leq N$ is the rank of $\tilde{\mathbf{H}}$. Note that rather than the entire channel matrix, we simply feedback the indices of the specific antennas chosen. For example,

if there are four antennas, we can sent back a four bit value where 1 indicates the use of that antenna and 0 indicates not using that antenna. This relies on using one of the various receiver techniques described earlier. The feedback simply allows for the optimization of the performance of the approach. A slightly better approach is to feedback eigenmode information.

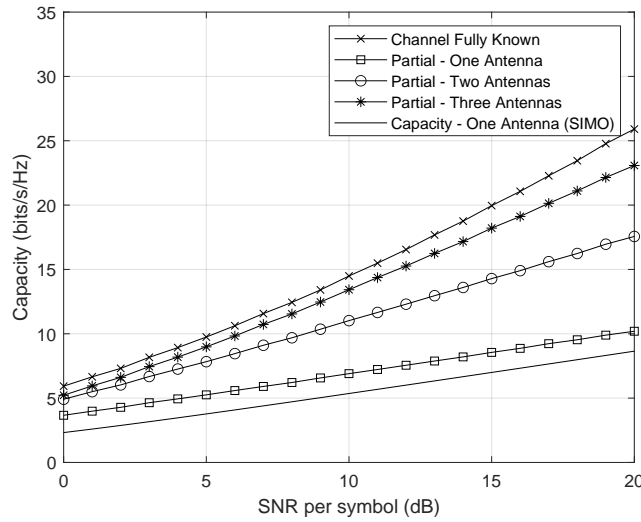


Figure 8.7: The Capacity of Spatial Multiplexing with Partial CSIT (Best Antennas) and $M_r = N_t = 4$ in Independent Rayleigh Fading

8.4.2 Eigenmode Feedback

With eigenmode feedback we wish to transmit on the best $N < N_t$ eigenmodes of the channel (rather than antennas as in the previous approach). Again, recall that we can use singular value decomposition to

$$\mathbf{H} = \mathbf{U}\Sigma\mathbf{V}^H \quad (8.27)$$

$$= [\mathbf{u}_1 \mathbf{u}_2 \dots \mathbf{u}_{M_r}] \begin{bmatrix} \sigma_1 & 0 & \dots & 0 \\ 0 & \sigma_2 & \dots & 0 \\ \vdots & & \ddots & \end{bmatrix} [\mathbf{v}_1 \mathbf{v}_2 \dots \mathbf{v}_{N_t}] \quad (8.28)$$

Let N be the number of chosen eigenmodes

$$\tilde{\mathbf{V}} = [\mathbf{v}_i \mathbf{v}_j \dots \mathbf{v}_N] \quad (8.29)$$

Then the effective channel is

$$\tilde{\mathbf{H}} = \mathbf{U}\tilde{\Sigma}\tilde{\mathbf{V}}^H \quad (8.30)$$

where $\tilde{\Sigma}$ is a diagonal matrix of N singular values. Thus, the received vector is then

$$\mathbf{r} = \tilde{\mathbf{H}}\tilde{\Lambda}\tilde{\mathbf{V}}\mathbf{s} + \mathbf{n} \quad (8.31)$$

and the decision statics are the first N values of the vector

$$\mathbf{z} = \mathbf{U}^H \mathbf{r} \quad (8.32)$$

The total information that is needed to feed back are the N maximum singular values and their associated N singular vectors.

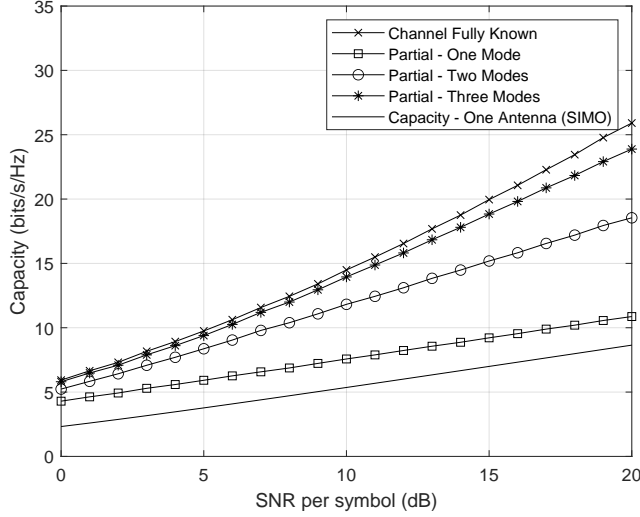


Figure 8.8: The Capacity of Spatial Multiplexing with Partial CSIT (Best Modes) and $M_r = N_t = 4$ in Independent Rayleigh Fading

The performance of spatial multiplexing with partial CSIT in Figure 8.9. More specifically, the figure provides the BER for several schemes with 4b/s/Hz including the use of BPSK on each of $N_t = 4$ antennas using SIC+ZF at the receiver, the use of QPSK on the best two antennas, the use of QPSK on the best two eigenmodes, the use of 16QAM on the best antenna, the use of 16QAM on the best eigenmode, and the SIMO case (16QAM on one antenna - no selection). We can see in this case, without CSIT, spatial multiplexing performs worse than SIMO. The loss of diversity is more detrimental than the increase of the constellation size from BPSK to 16QAM. However, with CSIT, we can provide substantial performance improvement. Using 16QAM on the best antenna (out of four antennas) instead of only a single antenna provides a 3-6dB improvement. Using the best mode instead of the best antenna provides an addition 2-3dB. Using the best two antennas or best two modes with QPSK modulation provides an additional 3-4dB improvement. Thus, the use of CSIT provides at least 10dB of improvement for spatial multiplexing.

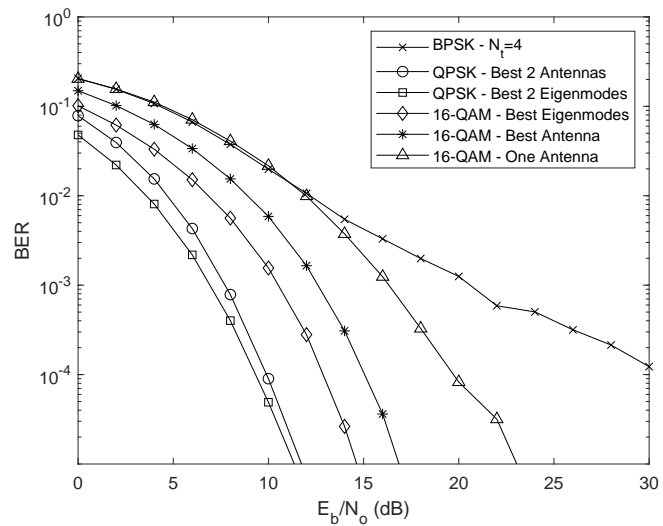


Figure 8.9: The Performance of Spatial Multiplexing with CSIT and $M_r = N_t = 4$ in Independent Rayleigh Fading (4b/s/Hz)

Chapter 9

Multi-user MIMO

9.1 Introduction

The gains due to multiple antennas in single user link capacity can be extended to multiple user settings. These gains are realized through (a) signal processing, (b) scheduling, and (c) channel feedback (i.e., CSIT). In this chapter, we will explore these gains.

MU-MIMO is the combination of MIMO theory which tells us that multiple spatial channels exist in rich scattering environment with the concept of Space Division Multiple Access. In other words, MU-MIMO applies the degrees of freedom in MIMO to multiuser transmission. Further, delay-tolerant traffic in wireless systems can allow for *multiuser scheduling* - the scheduling of users based on their current channel conditions. The combination of the two concepts provides a powerful tool for improving capacity and performance.

The difference between single user MIMO (SU-MIMO) and multiuser MIMO (MU-MIMO) is shown in Figure 9.1. In SU-MIMO with CSIT $\min\{N_t, M_r\}$ eigenbeams can be formed to transmit multiple spatial streams between the base station and a mobile. However, with multi-user MIMO we use the degrees of freedom to transmit to multiple users. More specifically, with MU-MIMO $\min(N_t, \sum_k M_r^{(k)})$ eigenbeams can be formed to transmit multiple spatial streams between the base station and multiple mobiles.

9.2 Benefits of MU-MIMO

MU-MIMO allows for direct gain in multiple access capacity (proportional to the number of base station antennas) due to multiuser multiplexing. Additionally, it is more immune to propagation limitations which impact SU-MIMO (i.e., low-rank channel loss or antenna correlation) due to decorrelated antennas across users and multiuser diversity gain. As an example, consider the SU-MIMO case with $N_t = M_r = 4$ with independent Rayleigh fading. We know that the relative strengths of the channel matrix singular values has a strong impact on the performance of MIMO. Figure 9.2 plots the distribution of the channel matrix condition number $\kappa = \frac{\sigma_{max}}{\sigma_{min}}$ where σ_{max} and σ_{min} are the maximum and minimum singular values of \mathbf{H} respectively. For SU-MIMO the average

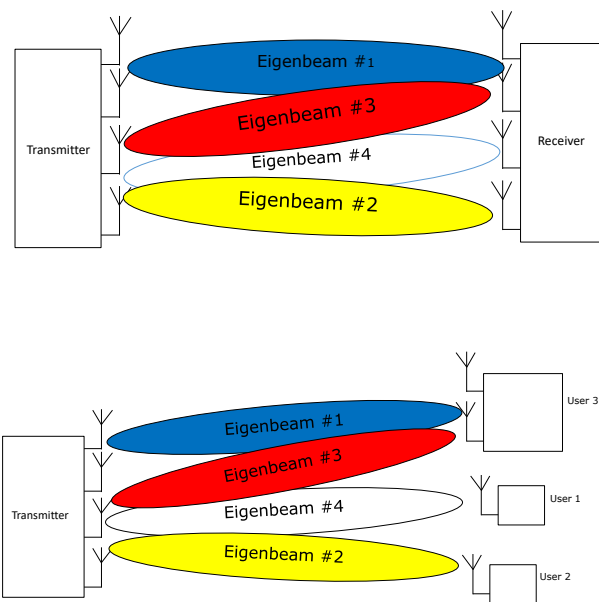


Figure 9.1: Single User MIMO (top) vs MultiUser MIMO (bottom) with Channel Knowledge at the Transmitter

condition number is approximately 11, and the condition number ranges from approximately 2 to well over 40. However, even when scheduling over 5 users, the condition number improves substantially with the mean value reducing to 5.4 and the range going from approximately 2 to roughly 20. When there are $K = 10$ users to choose from, the conditioning improves even more dramatically with an average condition number of 2.7 and a range of approximately 1.5 to 5. With $K = 15$ users, the average drops slightly more to 2.3, and the range is even tighter (approximately 1.5 to 3). Thus, the ability to choose from even a moderate pool of channel vectors allows for a dramatic improvement in channel quality as measured via the channel matrix condition number. In fact, even in the presence of LOS propagation MU-MIMO can be beneficial. This can be seen by the results shown in Figure 9.3 which examines the LOS case for $M_r = N_t = 4$. While it may take a much larger number of users, the condition number can be reduced dramatically with MU-MIMO.

In addition to the channel advantage, another major benefit is that, unlike SU-MIMO, MU-MIMO allows for spatial multiplexing gain at the base station without the need for multiple antennas at the user equipment. That is even with $M_r = 1$, spatial multiplexing gain can be realized.

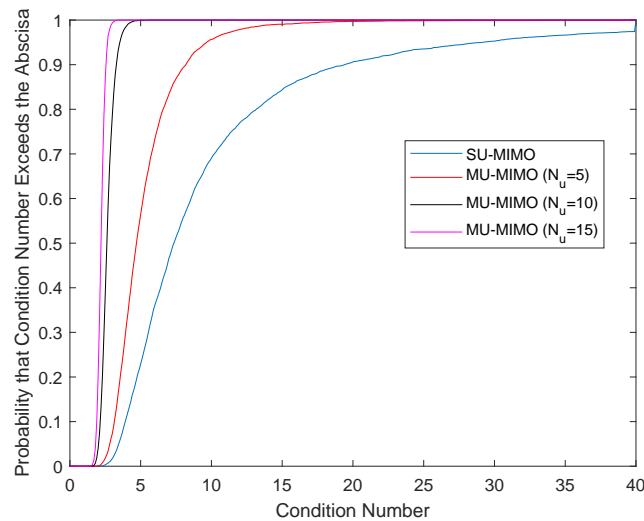


Figure 9.2: Impact of MultiUser MIMO (bottom) on Matrix Conditioning

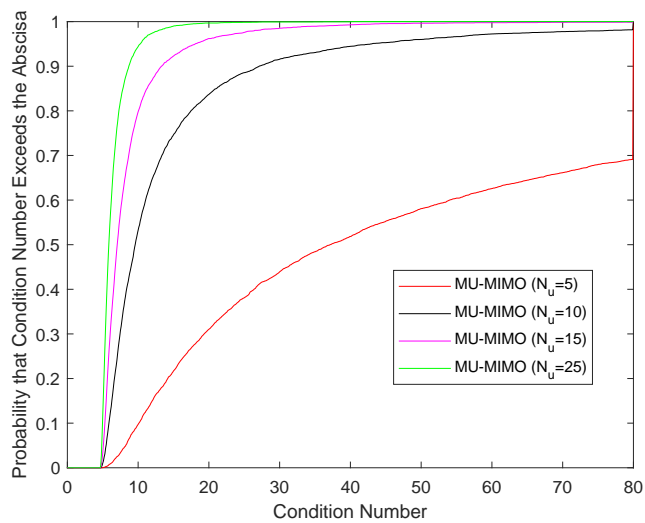


Figure 9.3: Impact of MultiUser MIMO (bottom) on Matrix Conditioning in LOS Channel with $N_t = M_r = 4$

9.3 Costs Associated with MU-MIMO

MU-MIMO, of course, does not come without costs. In general there are two primary costs associated with MU-MIMO:

- * The need for channel state information at the transmitter (CSIT)
- * Scheduling

Unlike SU-MIMO which can perform reasonably well without CSIT (recall that there is often very little difference between the capacity of SU-MIMO with and without CSIT), in the case of MU-MIMO CSIT is necessary for beneficial gains. Providing CSIT results in a loss of reverse link capacity due to the needed feedback (unless time-division duplexing is used).

There is also an associated complexity increased due to scheduling algorithms. That is, regardless of the metric applied for scheduling, the users chosen for transmission are always a subset of the available users. Thus, the base station must compare possible combinations for scheduled transmissions. If K users are connected to an N_t -antenna base station, and assuming that $N_u = N_t$, the scheduler must examine all possible N_t -user selections and all possible orders those users (since the order impacts the performance). In other words there are $\frac{K!}{(K-N_t)!}$ possible combinations that must be examined. Further, this doesn't include the impact of scheduling on specific Quality of Service (QoS) requirements for each user. Thus, the scheduling algorithm can be quite complex.

9.4 Uplink vs Downlink

As noted in the beginning of this chapter, MU-MIMO can be applied to either the uplink or downlink of a wireless system. In information theory studies, the uplink (link from the user equipment to base station or access point) is known as the Multiple Access Channel (MAC). In the MAC context, MU-MIMO techniques are generalizations of multiuser detection methods primarily studied in the context of CDMA. Additionally, the receiver structures are essentially the same as those discussed in the previous chapter on SU-MIMO.

However, the downlink (the channel from the base station to user equipment) is known as the Broadcast Channel (BC) and is the more challenging link theoretically, but also more interesting. Many applications have asymmetric traffic requirements with the downlink being more demanding. However, typically there is more complexity allowed at base station. In this chapter, we will focus on this link.

9.5 Downlink MU-MIMO

The key pieces of MU-MIMO on the downlink are

- * Precoding
- * Signal processing
- * Feedback

- * Scheduling

We will discuss each of these aspects in turn.

9.5.1 Precoding

Precoding is the signal processing at the base station transmitter to mitigate interference between streams to each user. This processing is analogous to SVD-based eigenbeamforming in SU-MIMO. The optimal precoding is a technique known as Dirty Paper Coding (DPC). Unfortunately, this processing is non-linear and fairly complex. Thus, sub-optimal approaches are typically applied. It should be noted that both linear and non-linear sub-optimal approaches have been examined, although linear approaches are simpler, as one would expect. The linear approaches include linear MMSE and Zero-Forcing approaches. The sub-optimal non-linear approaches include Vector Perturbation, DPC-based techniques and Tomlinson-Harishima Precoding.

9.5.2 Feedback

As discussed above, in order to provide CSIT in an FDD system, channel information needs to be intelligently fed back to the transmitter since perfect CSIT is impossible. This feedback depends on the rate of change of the channel (and thus the rate of the feedback) and the quantization applied. Ultimately, there is a trade-off between quality of the information and the loss of uplink data rate. There are many ways to feed back the channel state information. Common techniques include Vector Quantization, Adaptive feedback and statistical feedback.

9.5.3 Scheduling

The gains of MU-MIMO depend on which users are selected for transmission at any given time and which order they are placed in the precoding process. Optimal scheduling requires a search over all K users connected to the base station for the best ordered set of N_u users. Note that N_u need not be equal to N_t . In fact, $1 \leq N_u \leq N_t^2$. Thus, we not only need to examine all $\frac{K!}{(K-N_u)!}$ permutations, but we also need to consider multiple values of N_u . Thus, typically the optimal search is computationally impractical. However, there are also many sub-optimal techniques to schedule users that provide acceptable trade between complexity and performance including max-rate techniques, greedy user selection, random user selection, and proportionally fair scheduling.

9.6 MU-MIMO Signal Models

On the uplink, the $M_r \times 1$ received base station vector from N_u UEs can be written as

$$\mathbf{y} = \sum_{k=1}^{N_u} \mathbf{H}_k \mathbf{x}_k + \mathbf{n}$$

where \mathbf{x}_k is $N_t^{(k)}$ transmit vector and \mathbf{H}_k is the $M_r \times N_t^{(k)}$ channel matrix from the k th user and the base station.

On the downlink, the $M_r^{(k)} \times 1$ received UE vector from base station is written as

$$\mathbf{y}_k = \mathbf{H}_k \mathbf{x} + \mathbf{n}_k$$

where $\mathbf{x} = \sum_k \mathbf{x}_k$ and $J\mathbf{H}_k$ is the $M_r^{(k)} \times N_t$ channel matrix.

9.7 Capacity

In multiuser systems capacity is not a single number – it is instead characterized by a N_U -dimensional rate region. Each point is a vector of achievable rates by all users simultaneously. Capacity region (Gaussian BC) for unit noise power and channels \mathbf{H}_i :

$$C = \bigcup_{\sum_k P_k = P_T} \left\{ (R_1, R_2, \dots, R_{N_U}) \in \Re^{+N_U} : R_i \leq \log_2 \frac{\det [\mathbf{I} + \mathbf{H}_i(\Sigma_{j \geq i} \mathbf{Q}_j) \mathbf{H}_i^H]}{\det [\mathbf{I} + \mathbf{H}_i(\Sigma_{j > i} \mathbf{Q}_j) \mathbf{H}_i^H]} \right\}$$

where

$$\mathbf{Q}_k = E \{ \mathbf{x}_k \mathbf{x}_k^H \}$$

With CSIT and Dirty Paper Coding, the sum rate (assuming that all UEs have M_r antennas):

$$\lim_{N_U \rightarrow \infty} \frac{E\{R^{DPC}\}}{\log \log(N_U M_r)} = N_t$$

i.e., sum rate scales with the number of transmit antennas. However, without CSIT

$$E\{R^{NoCSIT}\} \approx \min\{N_t, M_r\} \log(SNR)$$

That is, the sum rate is essentially the same as in the SU-MIMO case. This emphasizes the fact that CSIT is absolutely critical to realizing the benefits of MU-MIMO.

In general, information theory teaches us several things about MU-MIMO. First, results advocate serving multiple users simultaneously in SDMA fashion (assuming that we choose a suitable precoding scheme at the transmitter). Second, these multiplexing gains can be achieved while receivers have only single antenna ($M_r = 1$). This means that the receivers can be low cost! Third, multiple antennas at the receiver would provide the capability of multiple streams per user or performance enhancements (i.e., SNR gains). Fourth, hte gains are immune to ill-behaved single user channels. Full rank of the global channel matrix $\tilde{\mathbf{H}}$ is nearly guaranteed by physical separation of users and a large number of users. Finally, a multiplexing gain of N_t comes with the condition of channel knowledge at the transmitter (unlike SU-MIMO case).

9.8 Resource Allocation

Resource allocation, i.e., scheduling techniques help exploit gains of multiuser MIMO. Thus, with MU-MIMO the PHY and MAC layers are necessarily tied together. However, this is no different than adaptive modulation and coding techniques which also allow for the optimization of link performance/capacity. The primary resources considered at the transmitter (in addition to frequency channels) are spatial stream and transmit power. These depend entirely on the channel conditions. The number of simultaneous users served is upper bounded by N_t^2 but practically is limited to N_t with linear precoding.

The structure of the scheduler depends on the metrics used. Common metrics are sum-rate, per-

user rate targets, and proportionally fair rate. Multiuser diversity (the various user SNR values) and user separability impact these metrics and thus must be considered in the scheduling process.

9.9 Signal Processing

In the uplink, we essentially apply multiuser detection, which is analogous to stream separation techniques used for uplink SU-MIMO. The uplink problem is not as interesting of a problem as the downlink and is not studied as much as the downlink.

On the downlink, the optimal approach is called Dirty Paper Coding and is essentially pre-canceling interference at the transmitter using CSIT and knowledge of the signals. DPC is difficult to implement in practice. This leads to the use of linear precoding which is a generalization of SDMA where users are assigned different precoding matrices.

The name dirty paper coding is attributed to Costa who showed that for a scalar discrete-time point-to-point memoryless channel,

$$y_i = x_i + s_i + n_i$$

x_i and y_i are the transmitted and the received signals respectively, the interfering signal s_i is known to the transmitter but not to the receiver, and n_i is the unknown noise. If both s_i and n_i are i.i.d. Gaussian, and if the entire non-causal realization of s_i is known to the transmitter prior to transmission, the channel capacity is the same as that of the AWGN channel i.e., as if the interference were not present. This tells us that knowing the interference non-causally at the transmitter is as powerful as knowing it at both the transmitter and the receiver. Costa's result was generalized to a vector point-to-point memoryless channel.

9.9.1 Zero Forcing Linear Precoding

Consider the received signal vector

$$\mathbf{y}_k = \mathbf{H}_k \mathbf{W}_k \mathbf{s}_k + \mathbf{H}_k \sum_{l \neq k} \mathbf{W}_l \mathbf{s}_l + \mathbf{n}_k \quad (9.1)$$

where \mathbf{W}_k is the precoding matrix and \mathbf{s}_k is the transmit symbol vector of the k th user.

Now, if $M_r^{(k)} = 1, \forall k$, $\mathbf{H}_k = \tilde{\mathbf{h}}_k$, i.e., the channel is a $1 \times N_t$ row vector, the precoding matrix \mathbf{W}_k is a vector $\mathbf{W}_k = \mathbf{w}_k$, and the received symbol is

$$y_k = \tilde{\mathbf{h}}_k \mathbf{w}_k \mathbf{s}_k + \tilde{\mathbf{h}}_k \sum_{l \neq k} \mathbf{w}_l \mathbf{s}_l + n_k \quad (9.2)$$

$$\tilde{\mathbf{H}} = \left[\tilde{\mathbf{h}}_1^T \tilde{\mathbf{h}}_2^T \cdots \tilde{\mathbf{h}}_{N_u}^T \right]^T \quad (9.3)$$

$$\begin{aligned}
\mathbf{W} &= [\mathbf{w}_1 \mathbf{w}_2 \cdots \mathbf{w}_{N_u}] \\
&= \tilde{\mathbf{H}}^\dagger \\
&= \tilde{\mathbf{H}}^H (\tilde{\mathbf{H}} \tilde{\mathbf{H}}^H)^{-1}
\end{aligned} \tag{9.4}$$

Note that the k th column will be orthogonal to all channels except the k th channel and is thus the precoding vector of the k th user.

Of course as with all zero-forcing type schemes, ZF for MU-MIMO can result in poor SNR for some users. Thus, there is also an MMSE version of the approach which improves the per user SNR. However, the scheduling algorithm can also help by choosing/grouping users that provide good SNR for all users.

9.9.2 Block Diagonalization

Note that if $M_r^{(k)} > 1$, the previous algorithm is not suitable. Thus, for $M_r^{(k)} > 1$, but $\sum_{k=1}^{N_u} M_r^{(k)} = N_t$ and $S_k = M_r^{(k)}$ we can use an approach known as *block diagonalization*. In this approach we choose weights such that

$$\mathbf{H}_l \mathbf{W}_k = 0 \quad \forall l \neq k$$

Specifically, define

$$\tilde{\mathbf{H}}_k = [\mathbf{H}_1^T \mathbf{H}_2^T \cdots \mathbf{H}_k^T \mathbf{H}_{k+1}^T \cdots \mathbf{H}_{N_u}^T]^T \tag{9.5}$$

Note that H_k is a $M_r^{(k)} \times N_t$ channel matrix of the k th user and thus, $\tilde{\mathbf{H}}_k$ is a $\sum_{j \neq k} M_r^{(j)} \times N_t$ matrix of all users except user k . We can decompose $\tilde{\mathbf{H}}_k$ using singular value decomposition:

$$\tilde{\mathbf{H}}_k = \tilde{\mathbf{U}}_k \tilde{\mathbf{D}}_k [\tilde{\mathbf{V}}_k^{(1)} \tilde{\mathbf{V}}_k^{(0)}]^T \tag{9.6}$$

where $\tilde{\mathbf{V}}_k^{(0)}$ are the $N_t \times M_r^{(k)}$ right singular vectors corresponding to the zero singular values. Thus, we choose the precoding matrix to be any combination of these singular vectors, but putting the k th users signal in the null-space of all other users.

While the SIR of ZF is good, the SINR may not be. What we would like to do is to maximize SINR for the k th user

$$SINR_k = \frac{\|\mathbf{H}_k \mathbf{W}_k\|^2}{M_r^{(k)} \sigma_n^2 + \sum_{l \neq k} \|\mathbf{H}_k \mathbf{W}_l\|^2}$$

We would like to choose \mathbf{W}_k for each user to maximize this for all users. However, this is a very challenging optimization problem. Instead it has been proposed to use signal-to-leakage plus noise ratio:

$$SINR_k = \frac{\|\mathbf{H}_k \mathbf{W}_k\|^2}{M_r^{(k)} \sigma_n^2 + \|\tilde{\mathbf{H}}_k \mathbf{W}_k\|^2}$$

This attempts to minimize the interference *caused to* other signals rather than *caused by* other signals while maximizing my received power.

Note that

$$\tilde{\mathbf{H}}_k = [\mathbf{H}_1^T, \mathbf{H}_2^T, \dots, \mathbf{H}_{k-1}^T, \mathbf{H}_{k+1}^T, \dots, \mathbf{H}_{N_u}^T]^T$$

is termed the “leakage channel”.

9.9.3 Non-linear Precoding - Tomlinson-Harishima Precoding

9.10 User Scheduling

Chapter 10

Massive MIMO

10.1 Introduction and Motivation

Information theory tells us that MIMO capacity increases with $\min\{N_t, M_r\}$ in single user (SU) MIMO and increases with N_t in multi-user (MU) MIMO (downlink with sufficient number of users and CSIT). What if we let the number of antennas at the base station N_t approach infinity? Would this dramatically increase capacity? Very possibly! That is the idea behind what is called *massive* MIMO. Not the obvious question is how can we fit a large number of antennas at the base station? The answer is to increase the frequency, specifically millimeter wave (mmWave) range. Thus, the primary motivation of massive MIMO is multiuser MIMO (MU-MIMO) which was discussed in the last chapter. While we cannot truly increase the capacity of our system infinitely, using massive MIMO as a MU-MIMO technique with realistic models of channel propagation and mutual coupling capacity increases of up to 10x can be achieved. Further, radiated energy efficiency increases of up to 100x can also be achieved, which is particularly important for cell-edge users and for overcoming the associated higher propagation losses at mmWave frequencies.

Other positive factors which make massive MIMO attractive include

- * Relatively simple signal processing - MRC/MRT as compared to ZF/SIC or DPC
- * Can be built with inexpensive, low-power components - Reduces the constraints on accuracy/linearity of each individual amplifier and RF chain since the Law of Large Numbers averages out noise, fading and hardware imperfections
- * Robust to failure of any one RF component
- * There is a surplus in the degrees of freedom ($N_t > N_u$) which can be used for hardware-friendly signal shaping
- * Channel tends towards an AWGN channel (fading resistance)

- * Fading resistance leads to the possibility of low latency
- * Channel-based scheduling is simplified since the Law of Large Numbers hardens the channel and every UE has roughly the same channel
- * Hardened channel also means that no fast power control is needed
- * Increases robustness against intentional and unintentional interference

10.2 Capacity Considerations

A simple example, consider the case of 6400 omni-direction antennas with half-wavelength spacing (an antenna area of $40m^2$) with 120W total tx power. In 20MHz BW and cell of radius 6km with 1000 terminals (UEs), simulations show that 95% of the terminals can receive a throughput of 21.2Mb/s for an overall throughput of 20Gbps []. This is roughly a spectral efficiency of 1000b/s/Hz!

Let's consider the Information Theory aspects of massive MIMO. Recall that the capacity (b/s/Hz) of MIMO can be written as

$$\begin{aligned} \frac{C}{B} &= \log_2 \det \left(\mathbf{I}_{N_t} + \frac{\gamma}{N_t} \mathbf{H} \mathbf{H}^H \right) \\ &= \sum_{k=1}^{\min(N_t, M_r)} \log_2 \left(1 + \frac{\gamma \sigma_k^2}{N_t} \right) \end{aligned}$$

where σ_k is the k th singular value of \mathbf{H} (i.e., $\lambda_k = \sigma_k^2$ is k th eigenvalue of $\mathbf{H} \mathbf{H}^H$). In MU-MIMO the capacity is in fact a region, rather than a value. However, we can write the Shannon sum-capacity of MU-MIMO which is analogous to that in point-to-point MIMO. More specifically, the capacity of the uplink assuming that the base station knows the channel and each of N_u users have $M_r = 1$ can be written as

$$\begin{aligned} \frac{C_{\text{sum-up}}}{B} &= \log_2 \det \left(\mathbf{I}_{N_u} + \frac{\gamma}{N_u} \tilde{\mathbf{H}} \tilde{\mathbf{H}}^H \right) \\ &= \sum_{k=1}^{\min(N_t, N_u)} \log_2 \left(1 + \frac{\gamma \tilde{\sigma}_k^2}{N_u} \right) \end{aligned} \quad (10.1)$$

where $\tilde{\mathbf{H}} = \begin{bmatrix} \mathbf{h}_1^T \\ \mathbf{h}_2^T \\ \vdots \\ \mathbf{h}_{N_u}^T \end{bmatrix}$ and \mathbf{h}_i is the $N_t \times 1$ channel vector from the i th user to the base station, and $\tilde{\sigma}_k$ is the k th singular value of $\tilde{\mathbf{H}}$. On the downlink, the Shannon sum-capacity is similar but

requires a search over the power allocation vectors:

$$\begin{aligned}\frac{C_{sum-dn}}{B} &= \sup_{\mathbf{g}} \left\{ \log_2 \det \left(\mathbf{I}_{N_t} + \gamma \tilde{\mathbf{H}}^H \mathbf{\Gamma} \tilde{\mathbf{H}} \right) \right\} \\ &= \sup_{\mathbf{g}} \left\{ \sum_{k=1}^{\min(N_t, N_u)} \log_2 \left(1 + \frac{\gamma \tilde{\sigma}_k^2 g_k}{N_t} \right) \right\}\end{aligned}$$

where $\mathbf{\Gamma}$ is a diagonal matrix with \mathbf{g} on the diagonal, $\mathbf{g} \geq \mathbf{0}, \mathbf{1}^T \mathbf{g} = 1$ represents the power allocation across N_u users.

Of course in both cases, the capacity depends on the singular values of \tilde{H} or equivalently the eigenvalues of $\tilde{H}^H \tilde{H}$. As we discussed in Chapter 4 in the context of single user MIMO, the worst case capacity occurs when there is a single non-zero eigenvalue and the best case occurs when there are $\min\{N_t, M_r\}$ eigenvalues of equal value. For the multiuser case, equating M_r with the total number of antennas N_u (assuming all users have a single antenna), let's normalize the channel coefficients such that

$$\sum_{k=1}^{\min(N_t, N_u)} \tilde{\sigma}_k^2 = \text{trace} \left(\tilde{\mathbf{H}} \tilde{\mathbf{H}}^H \right) \approx N_t N_u$$

Then, in the worst case scenario, there is only one singular value

$$\tilde{\sigma}_1^2 = \text{trace} \left(\tilde{\mathbf{H}} \tilde{\mathbf{H}}^H \right) \approx N_t N_u$$

However, in the best case, all singular values are the same

$$\tilde{\sigma}_i^2 = \approx \max(N_t, N_u) \quad \forall i$$

Thus, on the uplink we have

$$\log_2 (1 + \gamma N_u) \leq \frac{C_{sum-up}}{B} \leq \min(N_t, N_u) \log_2 \left(1 + \frac{\gamma \max(N_t, N_u)}{N_t} \right)$$

Now, let's consider the behavior of $\tilde{\mathbf{H}} \tilde{\mathbf{H}}^H$ as the number of antennas at base station grows large. Figure 10.1 plots the correlation between channel vectors for $N_t = 4, 10, 100, 1000$. The top plot shows the CDF of the channel correlation for independent identically distributed Rayleigh fading channels. For a large number of antennas we can see that the probability of low correlation between the channels is extremely high. The bottom plot shows that even with some correlation between the channels, there is high probability that the channels have low correlation. Thus, we can conclude that when the number of antennas is large we have $\tilde{\mathbf{H}} \tilde{\mathbf{H}}^H \approx \mathbf{I}_{N_t}$

More specifically, if we hold N_s fixed but allow N_t to grow large:

$$\left(\frac{\tilde{\mathbf{H}} \tilde{\mathbf{H}}^H}{N_t} \right)_{N_t >> N_u} \approx \mathbf{I}_{N_u}$$

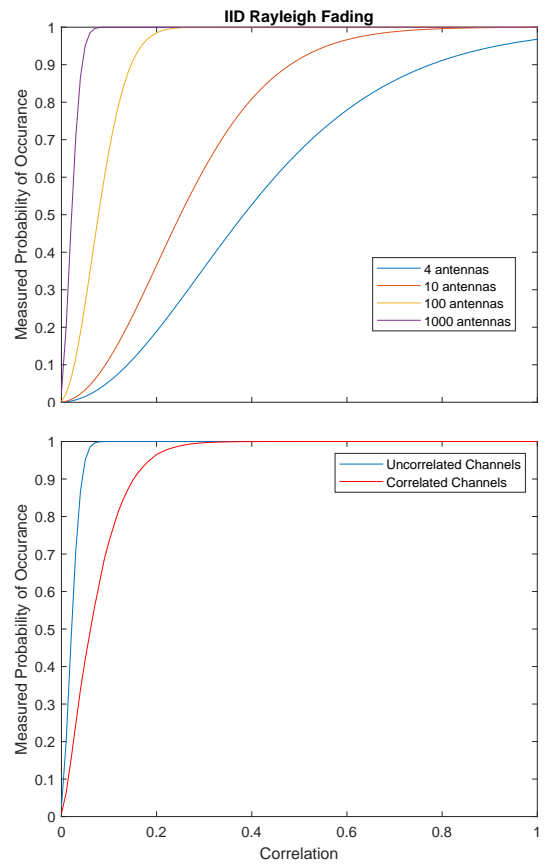


Figure 10.1: Correlation Between Channel Vectors for IID Rayleigh Fading for $N_t = 4, 10, 100, 1000$ (top) for Uncorrelated and Correlated Channels with $N_t = 1000$ (bottom)

and thus

$$\begin{aligned} C &\approx \log_2 \det(\mathbf{I}_{N_u} + \gamma \mathbf{I}_{N_u}) \\ &= N_u \log_2 (1 + \gamma) \end{aligned}$$

This matches the capacity upper bound described earlier!

As an example consider an IID Rayleigh fading channel with $N_u = 16, 32, 64, 128$. The ergodic uplink sum capacity (in terms of spectral efficiency b/s/Hz) is plotted versus the number of antennas is plotted in Figure 10.2. The sum-capacity calculation uses (eq:upcap) and averages over random values of $\tilde{\mathbf{H}}$. We can see that although capacity doesn't scale linearly with the number of antennas, it is close, especially for a large number of users.

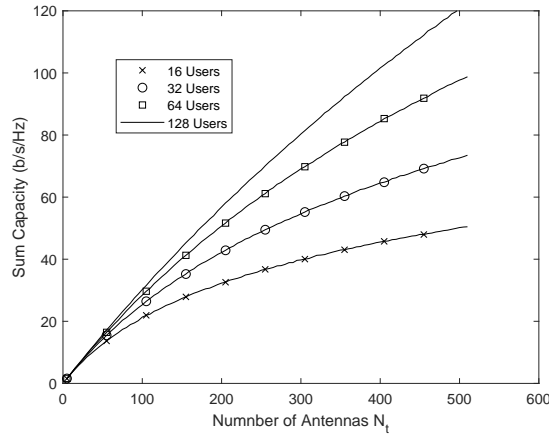


Figure 10.2: Simulated Capacity for IID Rayleigh Fading for $N_u = 16, 32, 64, 128$ for SNR = -6dB

10.3 Energy Efficiency

Massive MIMO uses eigenbeamforming as opposed to classic (open loop) beamforming. That is, the beamforming weights are $\mathbf{w} = \mathbf{h}/\|\mathbf{h}\|$. This is accomplished by measuring the uplink channel and using it for both transmit and receive beamformers. Of course, this assumes reciprocity which we will discuss more later. This allows the array gain to continue even past the point where the array beamwidth is smaller than the angular spread. Since all channels have some non-zero angular spread, eigenbeamforming will provide larger gain whenever the beamwidth is more narrow than the angle spread. As an example, consider a channel with 5° angle spread (following a Gaussian distribution). Figure 10.3 plots the beamforming gain for both classical beamforming (linear array) and eigenbeamforming (also linear array). Clearly eigenbeamforming is able to achieve the full gain of N_t . However, when the beamwidth ($\approx \frac{720}{N_t}$) is less than the angle spread the gain drops quickly.

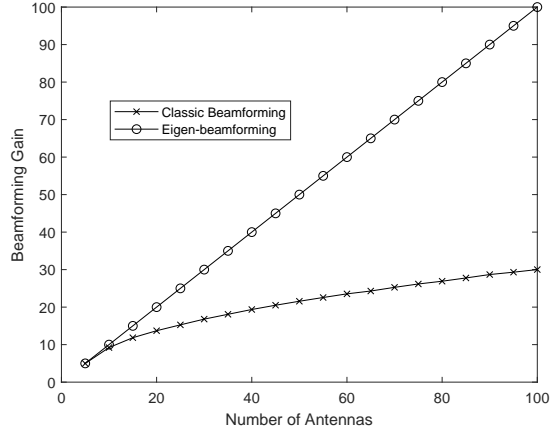


Figure 10.3: Beamforming Gain for Classical Beamforming and Eigenbeamforming for a Channel with 5° Angle Spread (Gaussian Distribution)

10.4 Signal Processing

The fact that the correlation between channel vectors also allows relatively simple signal processing approaches. Of course this is very important since the number of antennas is so large. On the uplink processing becomes simple maximal ratio combining (same as eigenbeamforming). On the downlink the transmission uses Maximal Ratio Transmission (which is again eigenbeamforming). Neither approach requires complex processing, just knowledge of channel, as $\mathbf{w} = \mathbf{h}$.

10.4.1 Downlink

As we discussed Chapter 9, precoding approaches for MU-MIMO include Zero-Forcing (ZF) and Block-Diagonalization (BD). However, as N_t grows, \mathbf{H} tends towards orthogonal columns, which means that the performance of ZF will tend towards an interference free system. The received symbol for the k th user is the k th element of the $N_u \times 1$ vector \mathbf{y} :

$$\mathbf{y} = \mathbf{H}\mathbf{W}\mathbf{s} + \mathbf{n}$$

where \mathbf{H} is the $N_u \times N_t$ complete channel matrix to all users, \mathbf{W} is the precoding matrix and \mathbf{s} is the vector of transmit symbols. Now the ZF solution uses $\mathbf{W} = \mathbf{H}^\dagger = \tilde{\mathbf{H}}^H (\tilde{\mathbf{H}}\tilde{\mathbf{H}}^H)^{-1}$. However, as we have discussed, for a large number of antennas $\tilde{\mathbf{H}}\tilde{\mathbf{H}}^H \approx \mathbf{I}$ and thus $\mathbf{W} = \tilde{\mathbf{H}}^H$. Thus, we have what is often called Matched Filter Transmission or downlink eigenbeamforming.

Again, given the large dimensionality of the channel

$$\left(\frac{\mathbf{H}\mathbf{H}^H}{N_t} \right)_{N_t > > M_r} \approx \mathbf{I}_{M_r}$$

Thus,

$$\begin{aligned}\mathbf{y} &= \mathbf{H}\mathbf{W}\mathbf{s} + \mathbf{n} \\ &= \mathbf{H}\mathbf{H}^H\mathbf{s} + \mathbf{n} \\ &\approx N_t\mathbf{s} + \mathbf{n}\end{aligned}$$

10.5 Fading and Power Control

As the large number of channels (antennas) grows, the channel exhibits what is termed “hardening”. That is, the combined channel approaches a constant value. Thus, fading is eliminated. This can be seen by the distribution of the normalized channel value after eigenbeamforming in a Rayleigh fading channel as shown in Figure 10.4.

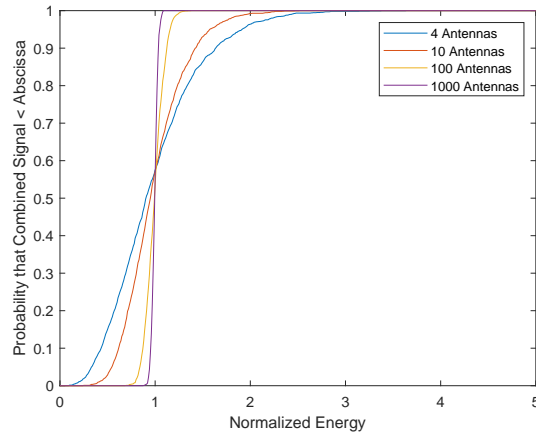


Figure 10.4: CDF of the Channel Gain after Eigenbeamforming for Varying Numbers of Antennas

Two major impacts of this channel hardening are (1) multiuser diversity is no longer needed (or useful) since all channels are roughly the same simplifying the scheduler and (2) fast power control is no longer needed since fading is not present (after eigenbeamforming).

10.6 Challenges

Although Massive MIMO is very promising, it is not without its challenges. Those challenges are centered around the need for CSIT. As with standard MU-MIMO the big requirement of Massive MIMO is channel knowledge. How can we estimate the channel for a large number of users simultaneously? Won't we run out of bandwidth just transmitting pilots? Additionally, there is the problem of pilot contamination. Specifically, since there are a limited number of orthogonal pilot sequences in a limited bandwidth, eventually pilot sequences across cells will need to be reused. When the sequences are reused the channel estimates will be contaminated by transmissions from other cells. Finally, with very large arrays we cannot ignore channel correlation and mutual coupling. How do correlation and coupling impact the gains of massive MIMO?

10.6.1 Channel Estimation

As with standard MU-MIMO the big requirement is channel knowledge. A major challenge is estimating the channel for a large number of users simultaneously. The challenge is substantially different in the Frequency Division Duplexing (FDD) and TDD cases.

For FDD, with uplink beamforming, channel estimation requires that each mobile transmits a pilot sequence. In order for the pilot sequences to be received without interference between them, they must be orthogonal. Orthogonal transmission of K pilot sequences requires K time slots. However, for downlink beamforming channel estimation requires that we send a pilot for each transmit antenna. This requires N_t time slots for orthogonality. Additionally, this channel knowledge needs to be fed back to the transmitter requiring that we use time slots for this purpose. Ultimately, channel estimation results in a massive uplink capacity loss due to the need for $K + N_t$ orthogonal time slots pulse feedback slots.

However, with TDD we can exploit channel reciprocity. In this case, we require only that the UEs transmit K pilots in K time slots. This channel estimation can be used for both uplink beamforming and downlink beamforming and there is no need for feedback. Thus, substantially less bandwidth is needed in this case!

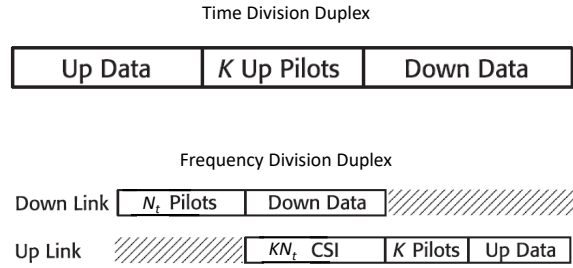


Figure 10.5: Frame Structure Requirements for Channel Estimation in Massive MIMO in TDD and FDD Cases

10.6.2 Pilot Contamination

All users within a cell transmit orthogonal pilot signals to the base station. This allows uplink channel estimation that is free from interference. There is a limited number of orthogonal pilot sequences for limited transmit time. Pilot sequences will inevitably be reused in other cells. Frequency reuse can mitigate the problem but causes capacity loss. Repeated pilot sequences means that channel estimates will be linear (weighting based on relative SINRs) combination of target UE channel and other UE channels. Effectively steering beams partially at the correct user and partially at an incorrect user in another cell.

Consider a K time-slot pilot sequence:

$$\Psi = \begin{bmatrix} p_1 & 0 & \dots & 0 \\ 0 & p_2 & \dots & 0 \\ \dots & \dots & & \dots \\ 0 & 0 & \dots & p_K \end{bmatrix}$$

At the base station we receive

$$\mathbf{Y}^{(p)} = \mathbf{H}\Psi^T + \mathbf{N}$$

To estimate the channel, we simply apply the pilot matrix:

$$\begin{aligned} \mathbf{Y}^{(p)}\Psi^* &= \mathbf{H}\Psi^T\Psi^* + \mathbf{N}\Psi^* \\ &= \mathbf{H} + \mathbf{N}\Psi^* \end{aligned}$$

When we include the impact of other cells, received signal at the base station becomes

$$\mathbf{Y}^{(p)} = \sum_{k=1}^L \mathbf{H}_k \Psi^T + \mathbf{N}$$

Again, to estimate the channel, we simply apply the pilot matrix:

$$\begin{aligned} \mathbf{Y}^{(p)}\Psi^* &= \sum_{k=1}^L \mathbf{H}_k \Psi^T \Psi^* + \mathbf{N}\Psi^* \\ &= \mathbf{H}_i + \underbrace{\sum_{k \neq i} \mathbf{H}_k}_{\text{Pilot Contamination}} + \mathbf{N}\Psi^* \end{aligned}$$

There are several techniques to mitigate this problem including:

- * Time slotting pilot transmissions from different cells
- * Precoding (e.g., ZF-beamforming instead of MRT)
- * Spatial-based pilot assignment

Time slotting still results in some interference, but at least the interference should not be correlated with pilots. However, due to the TDD nature of transmission, interference may now come from base stations which may be worse! Precoding could be a solution, but it is obviously more complex and perhaps even prohibitively complex. Spatially assigning pilots is essentially assigning pilots in each cell so that their channels are close to orthogonal (i.e., in different directions). Unfortunately, this is difficult to realize in practice since you need to know directions/channels to some degree in advance. Each of these techniques has some promise, but also serious challenges. Thus, pilot

contamination remains an active research area.

10.7 Channel Correlation and Mutual Coupling

10.8 Conclusions

In this chapter we have briefly discussed Massive MIMO. Massive MIMO is an approach to multi-user MIMO that assumes the use of a large number of base station antennas. Most gains/benefits are due to the asymptotic behavior of the channel vectors when they grow large. There is the potential for dramatic capacity increases with modest processing requirements and hardware complexity.

Part III

Orthogonal Frequency Division Multiplexing

Chapter 11

The Wireless Channel Revisited - Frequency Selectivity

11.1 Introduction

In Chapter 2 we reviewed the basic aspects of the wireless channel. Recall that there were three aspects of the wireless channel that led to three essential effects:

- * Doppler spread → temporally selective fading
- * Angle spread → spatially selective fading
- * Delay spread → frequency selective fading

These aspects of the wireless channel directly lead to specific techniques that are used in modern wireless communications. In the previous chapters we focused on MIMO systems which directly exploit spatially selective fading. Although we don't specifically address error correction coding, it is the primary technique used to mitigate temporal fading. In this chapter we will discuss the frequency selective nature of the wireless channel which motivates the second half of this manuscript Orthogonal Frequency Division Multiplexing (OFDM).

11.2 The Power Delay Profile (Power Spectrum)

Ignoring spatial aspects we can write the time-varying specular channel impulse response as

$$h(\tau, t) = \sum_{i=1}^N \alpha_i(t) e^{-j\phi_i(t)} \delta(\tau - \tau_i(t)) \quad (11.1)$$

For static channels this becomes

$$h(\tau) = \sum_{i=1}^N \alpha_i e^{-j\phi_i} \delta(\tau - \tau_i) \quad (11.2)$$

The power delay profile (power delay spectrum) can be written as

$$\varphi_h(\tau) = E_t \{ h(\tau, t) h^*(\tau, t) \} \quad (11.3)$$

which for static, specular channels becomes:

$$\varphi_h(\tau) = \sum_{i=1}^N \alpha_i^2 \delta(\tau - \tau_i) \quad (11.4)$$

The total power can be written as

$$P_T = \int_0^\infty \varphi(\tau) d\tau \quad (11.5)$$

$$= \sum_{i=1}^N \alpha_i^2 \quad (11.6)$$

The Ricean K -factor for a channel is

$$K = \frac{\alpha_1^2}{P_T - \alpha_1^2} \quad (11.7)$$

This measures the severity of the fading. The rms delay spread of the channel is

$$\tau_{rms} = \sqrt{\bar{\tau}^2 - (\bar{\tau})^2} \quad (11.8)$$

For static, specular channels we have

$$\bar{\tau} = \frac{\sum_{i=1}^N \alpha_i^2 \tau_i}{P_T} \quad (11.9)$$

$$\bar{\tau}^2 = \frac{\sum_{i=1}^N \alpha_i^2 \tau_i^2}{P_T} \quad (11.10)$$

11.3 The Channel Transfer Function

The channel transfer function is the Fourier Transform of the time-varying impulse response where the transform is taken with respect to τ . More specifically, we have

$$H(f, t) = \mathcal{F}_\tau \{h(\tau, t)\} \quad (11.11)$$

$$= \int_{-\infty}^{\infty} h(\tau, t) e^{-j2\pi f\tau} d\tau \quad (11.12)$$

$$= \int_{-\infty}^{\infty} \left(\sum_{i=1}^N \alpha_i(t) e^{-j\phi_i(t)} \delta(\tau - \tau_i(t)) \right) e^{-j2\pi f\tau} d\tau \quad (11.13)$$

$$= \sum_{i=1}^N \alpha_i(t) e^{-j\phi_i(t)} \int_{-\infty}^{\infty} \delta(\tau - \tau_i(t)) e^{-j2\pi f\tau} d\tau \quad (11.14)$$

$$= \sum_{i=1}^N \alpha_i(t) e^{-j\phi_i(t)} e^{-j2\pi f\tau_i(t)} \quad (11.15)$$

$$= \sum_{i=1}^N \alpha_i(t) e^{-j(2\pi f\tau_i(t) + \phi_i(t))} \quad (11.16)$$

For a large number of multipath components, for a specific moment in time t , $H(f, t)$ is the sum of a large number of random variables (this includes both specular and diffuse components). In this case $H(f, t)$ will approach a complex Gaussian distribution. If the distribution has zero mean, the magnitude $|H(f, t)|$ will approach Rayleigh, otherwise Ricean. The Ricean distribution:

$$p_R(r) = \frac{r}{\sigma^2/2} e^{-(r^2+\rho^2)/\sigma^2} I_0 \left(\frac{r\rho}{\sigma^2/2} \right) \quad (11.17)$$

where $I_0(x)$ is the zeroth order modified Bessel function of the first kind, $\sigma^2 = P_T - \alpha_1^2 = \frac{P_T}{K-1}$ is the diffuse power, and $\rho^2 = \alpha_1^2 = \frac{P_T K}{K+1}$ is the power of the LOS component.

11.4 Correlation Functions

For a Wide Sense Stationary Uncorrelated Scattering (WSSUS) channel, $h(\tau, t)$ is wide sense stationary. WSS implies that the first and second order statistics of $h(\tau, t_o)$ are independent of t_o . US implies that α_i, ϕ_i are uncorrelated with α_k, ϕ_k for all $i \neq k$. In a WSSUS channel we can write the correlation function as

$$R_h(\Delta f, \Delta t) = \mathbb{E} \{ H(f, t) H^*(f + \Delta f, t + \Delta t) \} \quad (11.18)$$

11.5 Modeling the Frequency Selective Fading Channel

The modeling of the frequency selective fading channel typically focuses on the modeling of two things $\mathbb{E} \{\alpha_i^2(t)\}$ and τ_i . The power of each discrete multipath component and its delay are what ultimately determine the delay power spectrum and the rms delay spread. The time-variation of each path tends to follow models analogous to the models described in Chapter 2. Thus, in this chapter we focus on modeling the power delay spectrum and the resulting frequency correlation.

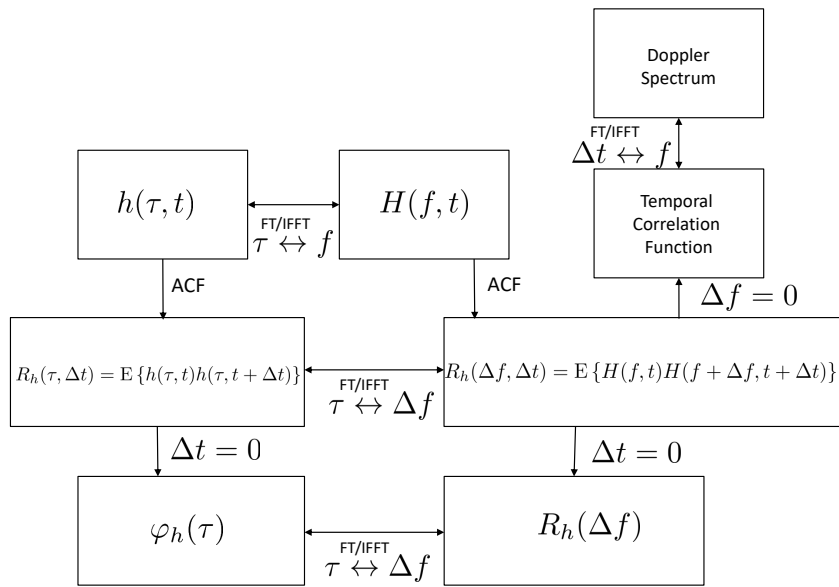


Figure 11.1: Relationships Between Various Views of the WSSUSS Channel

Note that for channel vector of multipath components

$$\mathbf{h} = \begin{bmatrix} h_0 \\ h_1 \\ \vdots \\ h_{L-1} \end{bmatrix}$$

$$\begin{aligned} h_i &= h(\tau)|_{\tau=iT_s} \\ &= \alpha_i e^{j\phi_i} \end{aligned}$$

we can compute the frequency response using

$$\begin{aligned} \mathbf{H} &= \mathbf{D}_{NL}\mathbf{h} \\ &= \begin{bmatrix} H_0 \\ H_1 \\ \vdots \\ H_{N-1} \end{bmatrix} \end{aligned}$$

where \mathbf{D}_{NL} is the first L columns of the DFT matrix:

$$\mathbf{D}_{NL} = \frac{1}{\sqrt{N}} \begin{bmatrix} 1 & 1 & 1 & \dots & 1 \\ 1 & e^{-j2\pi/N} & e^{-j2\pi2/N} & \dots & e^{-j2\pi(L-1)/N} \\ 1 & \vdots & & \dots & e^{-j2\pi2(L-1)/N} \\ \vdots & & & & \vdots \\ 1 & e^{-j2\pi(N-1)/N} & e^{-j2\pi2(N-1)/N} & \dots & e^{-j2\pi(L-1)(N-1)/N} \end{bmatrix}$$

Note that each element of the frequency vector is the transfer function sampled (in frequency) at intervals of $\frac{f_s}{N}$:

$$H_i = H(f)|_{f=i\frac{f_s}{N}}$$

There are two fundamental approaches to modeling the power of discrete multipath components α_i^2 at specific delays τ_i . The first uses a model for the power decay versus delay while the second uses a specific table of values.

11.5.1 Exponential Decay Model for PDP

The frequency selective channel is typically comprised of a finite number of resolvable (and potentially time varying) multipath components. Note that these resolvable components are often assumed to themselves be made up of many unresolvable components which leads to their time-varying amplitude/phase. In order to model both Rayleigh and Ricean fading, we separate the channel into two pieces: (a) diffuse multipath and (b) a single, specular LOS path. For Rayleigh fading, there is no LOS. For Ricean fading, there is. That is, we model the power delay profile

(PDFP) as

$$\varphi_h(\tau) = \underbrace{\frac{P_T\gamma}{K+1}e^{-\gamma\tau}u(\tau)}_{\text{diffuse}} + \underbrace{\frac{P_TK}{K+1}\delta(\tau)}_{\text{specular}} \quad (11.19)$$

where for Rayleigh fading, $K = 0$, while for Ricean fading $K > 0$. The rms delay spread for this model can be found from

$$\begin{aligned} \bar{\tau} &= \frac{1}{P_T} \int_0^\infty \varphi_h(\tau)\tau d\tau \\ &= \frac{1}{P_T} \frac{P_T\gamma}{K+1} \int_0^\infty \tau e^{-\gamma\tau} d\tau + \frac{1}{P_T} \frac{P_TK}{K+1} \underbrace{\int_0^\infty \tau \delta(\tau) d\tau}_{=0} \\ &= \frac{\gamma}{K+1} e^{-\gamma\tau} \left[-\frac{\tau}{\gamma} - \frac{1}{\gamma^2} \right]_0^\infty \\ &= \frac{1}{\gamma(K+1)} \end{aligned} \quad (11.20)$$

$$\begin{aligned} \bar{\tau^2} &= \frac{1}{P_T} \int_0^\infty \varphi_h(\tau)\tau^2 d\tau \\ &= \frac{1}{P_T} \frac{P_T\gamma}{K+1} \int_0^\infty \tau^2 e^{-\gamma\tau} d\tau \\ &= \frac{\gamma e^{-\gamma\tau}}{K+1} \left[-\frac{\tau^2}{\gamma} - \frac{2\tau}{\gamma^2} - \frac{2}{\gamma^3} \right]_0^\infty \\ &= \frac{2}{\gamma^2(K+1)} \end{aligned} \quad (11.21)$$

And thus, the rms delay spread is

$$\tau_{rms} = \frac{1}{\gamma} \sqrt{\frac{2K+1}{(K+1)^2}} \quad (11.22)$$

For Rayleigh channels, $K = 0$ and $\tau_{rms} = \frac{1}{\gamma}$. For large values of K (strong LOS component), we have

$$\tau_{rms} \approx \frac{1}{\gamma} \sqrt{\frac{2}{\gamma K}} \quad (11.23)$$

Thus, as K increases τ_{rms} decreases and as γ increases, τ_{rms} decreases.

The frequency correlation function for this model is found to be:

$$R_h(\Delta f) = \mathcal{F}\{\phi_h(\tau)\} \quad (11.24)$$

$$= \int_0^\infty \frac{P_T\gamma}{K+1} e^{-\gamma\tau} e^{-j2\pi\Delta f\tau} d\tau + \int_{-\infty}^\infty \frac{P_TK}{K+1} \delta(\tau) e^{-j2\pi\Delta f\tau} d\tau \quad (11.25)$$

$$= \frac{P_T\gamma/(K+1)}{\gamma + j2\pi\Delta f} + \frac{P_TK}{K+1} \quad (11.26)$$

$$= \frac{P_T}{K+1} \left(K + \frac{\gamma}{\gamma + j2\pi\Delta f} \right) \quad (11.27)$$

Now, if we want to express the correlation function in terms of the rms delay spread, we can use

the relationship

$$\gamma = \frac{\sqrt{(2K+1)/(K+1)^2}}{\tau_{rms}} \quad (11.28)$$

Defining $K_1 = \sqrt{(2K+1)/(K+1)^2}$, we have

$$R_h(\Delta f) = \frac{P_T}{K+1} \left(K + \frac{1}{1 + j2\pi\Delta f \tau_{rms}/K_1} \right) \quad (11.29)$$

This makes it clear that increasing τ_{rms} narrows $R_h(\Delta f)$.

11.5.2 Generating the Exponential Decay PDP

In the following sections we present two methods for generating multipath profiles that follow the exponential decay PDP. NOTE: In the models described below, best performance (i.e., most accurate modeling) is obtained when the sampling frequency $f_s \geq \frac{N}{16}\gamma$ which corresponds to $f_s \geq \frac{N}{16}\frac{1}{\tau_{rms}}$ in Rayleigh fading ($K = 0$).

Frequency Domain Approach

The first approach that we will provide starts with samples in the frequency domain. These samples are simulated as Gaussian random variables in order to obtain Rayleigh (or Ricean) fading. The general approach is illustrated in Figure 11.2.

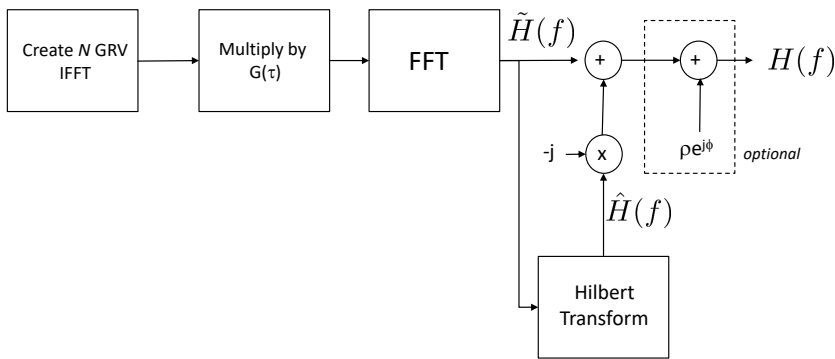


Figure 11.2: Overview of Frequency Domain Approach to Modeling Frequency Domain Channel

A step-by-step approach is as follows (see Figure 11.2):

1. Create N real unit variance Gaussian Random variables. These represent uncorrelated frequency channel values.
2. Transform the values into the time domain using the IDFT (or IFFT). Note that this result is two-sided in time, i.e., it is non-causal since the original values are all real.
3. Multiply the result by $G(\tau) = \sqrt{\varphi(\tau)} = \beta e^{-\gamma|\tau|/2}$ where β is a constant chosen to normalize the *average* power. (Again, this is two-sided in time.)
4. Take the Fourier Transform of the result. Make sure that this is all real (i.e., throw away in small imaginary components). Call this $\tilde{H}(f)$.
5. Take the Hilbert Transform of the result to obtain a real sequence. If using Matlab, take `imag(hilbert(x))`. Call this $\hat{H}(f)$.
6. The frequency domain channel is then $H(f) = \tilde{H}(f) + j\hat{H}(f)$. This will have the proper frequency domain correlation.
7. For verification purposes take the inverse DFT to verify the result matches the desired PDP.

As an example consider the case when the desired sampling frequency $f_s = 20\text{MHz}$, $N = 128$ frequency domain samples, $\tau_{rms} = 100\text{ns}$ ($\gamma = 10/\mu\text{s}$) with $P_t = 1$ and $K = 0$. An example simulated channel is plotted in Figures 11.3 and 11.4. In this case the measured rms delay spread is 96.8ns. We can see from Figure 11.4 that the simulated channel follows the desired delay spread.

Time Domain Approach

A second, perhaps more direct approach is to create hte samples directly in the time domain. Steps:

1. Determine the sampling period in time. Specifically, if we desire N components of the frequency domain channel with frequency spacing Δf , then $f_s = 2(N/2 * \Delta f) = N\Delta f$. Thus, $T_s = \frac{1}{N\Delta f}$.
2. Generate N complex Gaussian random variables $\{h_k\}$ where each Gaussian (both real and imaginary components) has zero mean and variance $\sigma_k^2 = \frac{1}{2} \left(\frac{1-e^{-T_s/\tau_{rms}}}{1-e^{-NT_s/\tau_{rms}}} \right) e^{-kT_s/\tau_{rms}}$ for $k = 0, 1, 2, \dots, N-1$. Note that this provides normalized average power.
3. $H(f) = \mathcal{F}\{h_k\}$

As an example consider the case when the desired sampling frequency $f_s = 20\text{MHz}$, $N = 128$ frequency domain samples, $\tau_{rms} = 50\mu\text{s}$ ($T_s = 5\mu\text{s}$) with $P_t = 1$ and $K = 0$. An example simulated channel is plotted in Figures 11.5 and 11.6. In this case the measured rms delay spread is $53.5\mu\text{s}$. We can see from Figure 11.5 that the simulated channel follows the desired delay spread.

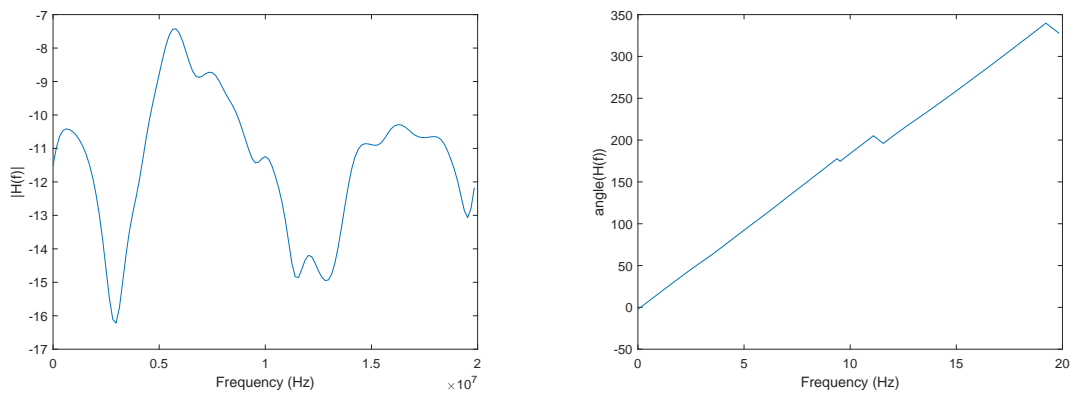


Figure 11.3: Example Frequency Domain Plots (Magnitude and Phase) of Simulated Channel Using Frequency Domain Approach

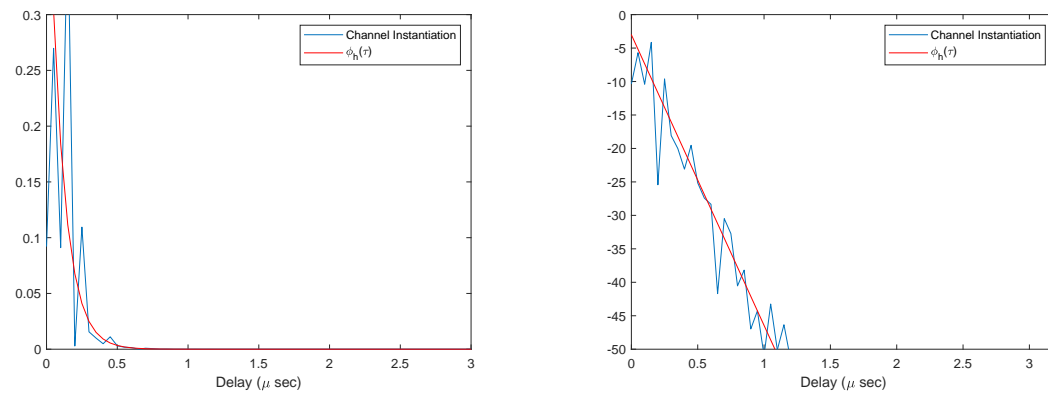


Figure 11.4: Example Time Domain Plots (Power Delay Profile) of Simulated Channel Using Frequency Domain Approach

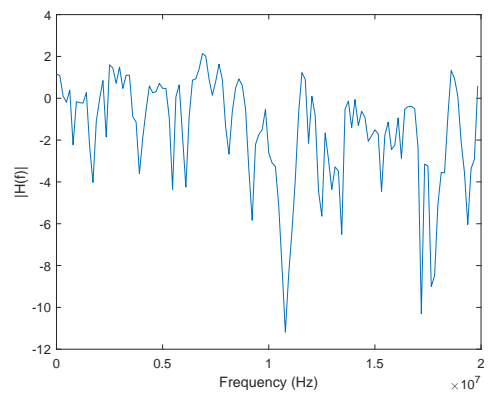


Figure 11.5: Example Frequency Domain Plots (Magnitude and Phase) of Simulated Channel Using Time Domain Approach

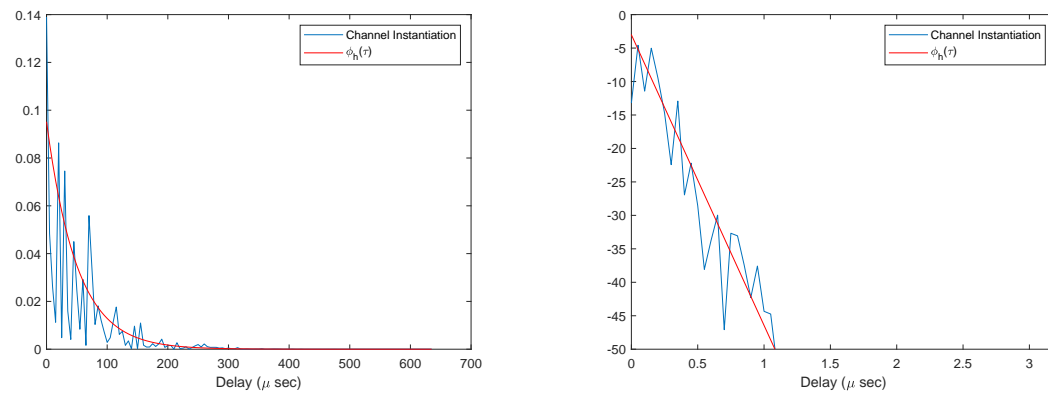


Figure 11.6: Example Time Domain Plots (Power Delay Profile) of Simulated Channel Using Time Domain Approach

Table 11.1: PDP Tap Values for the ITU Indoor Model

Tap	Channel A		Channel B		Doppler Spectrum
	Relative Delay (ns)	Avg. Power (dB)	Relative Delay (ns)	Avg. Power (dB)	
1	0	0	0	0	Flat
2	50	-3.0	100	-3.6	Flat
3	110	-10.0	200	-7.2	Flat
4	170	-18.0	300	-10.8	Flat
5	290	-26.0	500	-18.0	Flat
6	310	-32.0	700	-25.2	Flat

Table 11.2: PDP Tap Values for the ITU Outdoor-to-Indoor Model

Tap	Channel A		Channel B		Doppler Spectrum
	Relative Delay (ns)	Avg. Power (dB)	Relative Delay (ns)	Avg. Power (dB)	
1	0	0	0	0	Classic
2	110	-9.7	200	-0.9	Classic
3	190	-19.2	800	-4.9	Classic
4	410	-22.8	1200	-8.0	Classic
5			2300	-7.8	Classic
6			3700	-23.9	Classic

11.5.3 Standard Models

Another set of models that is commonly used is the models developed by the International Telecommunications Union (ITU) and 3GPP. These models specify the power and delay of various paths for different scenarios.

ITU Models

There are three primary ITU models for frequency selective fading channels based on the scenario they represent: Indoor, Pedestrian, and Vehicular. The model uses the following general equation:

$$y(t) = \sum_{i=1}^{N_p} \sqrt{p_i} \gamma_i(t) x(t - \tau_i)$$

where $p_i = E\{\alpha_i^2(t)\}$ and τ_i are defined by Tables 11.1-11.3. To model the time-varying nature of each path they use a sum-of-sinusoids model with one of two Doppler spectra: (a) the classic spectrum

$$S(f) = \frac{1}{\pi} \frac{1}{\sqrt{(V/\lambda)^2 - f^2}} \quad |f| < V/\lambda$$

and (b) a flat Doppler spectrum

$$S(f) = \frac{\lambda}{2V} \quad |f| < V/\lambda$$

Table 11.3: PDP Tap Values for the ITU Vehicular Model

Tap	Channel A		Channel B		Doppler Spectrum
	Relative Delay (ns)	Avg. Power (dB)	Relative Delay (ns)	Avg. Power (dB)	
1	0	0	0	-2.5	Classic
2	310	-1.0	300	0	Classic
3	710	-9.0	8900	-12.8	Classic
4	1090	-10.0	12900	-10.0	Classic
5	1730	-15.0	17100	-25.2	Classic
6	2510	-20.0	20000	-16.0	Classic

Table 11.4: PDP Tap Values for the 3GPP EPA Model

Tap	Delay (ns)	Relative Power (dB)
1	0	0.0
2	30	-1.0
3	70	-2.0
4	90	-3.0
5	110	-8.0
6	190	-17.2
7	410	-20.8

3GPP

The Third Generation Partnership Project (3GPP) specified three models Extended Pedestrian A (EPA) shown in Table 11.4, Extended Vehicular A (EVA) shown in Table ?? and Extended Typical Urban (ETU) shown in Table 11.6.

Table 11.5: PDP Tap Values for the 3GPP EVA Model

Tap	Delay (ns)	Relative Power (dB)
1	0	0.0
2	30	-1.5
3	150	-1.4
4	310	-3.6
5	370	-0.6
6	710	-9.1
7	1090	-7.0
8	1730	-12.0
9	2510	-16.9

Table 11.6: PDP Tap Values for the 3GPP ETU Model

Tap	Delay (ns)	Relative Power (dB)
1	0	-1.0
2	50	-1.0
3	120	-1.0
4	200	0.0
5	230	0.0
6	500	0.0
7	1600	-3.0
8	2300	-5.0
9	5000	-7.0

Chapter 12

Introduction to OFDM

12.1 Introduction

In the previous chapter we described the frequency selective channel - a channel where the channel has resolvable multipath. However, frequency selective fading is actually relative to the bandwidth of the signal of interest. That is, a channel is considered frequency selective, if the bandwidth of the signal is larger than the coherence bandwidth of the channel. When this is true, the channel will cause distortion to the signal spectrum and degrade performance. This is perhaps easier to understand in the time domain. Specifically, a frequency selective channel is one for which $\tau_{rms} \approx T_s$. That is, if the rms delay spread is on the order of the symbol period. Channels for which this is true will exhibit intersymbol interference (ISI). This ISI is self-interference and limits the performance of the channel. Since higher symbol rates are the means to higher data rates, frequency selective fading is a major impediment to high data rate wireless transmission. As we will see, this is a primary motivation for Orthogonal Division Multiple Access (OFDM).

Another motivation for OFDM comes from Information Theory. Information Theory tells us that in a frequency selective fading channel, the optimal capacity comes from creating parallel channels and allocating power across frequency using water-filling. For example, consider a block fading model as shown in Figure 12.1. Information Theory tells us that the capacity of this channel is

$$C = \max_{P_j: \sum_j P_j \leq P} \sum_{j=1}^{N_b} B \log_2 \left(1 + \frac{|H_j|^2 P_j}{N_o B} \right)$$

where the optimal power allocation is found via water-filling. More specifically, the optimal power per sub-band is found to be

$$\frac{P_j}{P} = \begin{cases} \frac{1}{\gamma_o} - \frac{1}{\gamma_j} & \gamma_j \geq \gamma_o \\ 0 & \gamma_j < \gamma_o \end{cases}$$

where $\gamma_j = \frac{|H_j|^2 P}{N_o B}$ is the SNR per channel (assuming full power transmission per band) and γ_o is

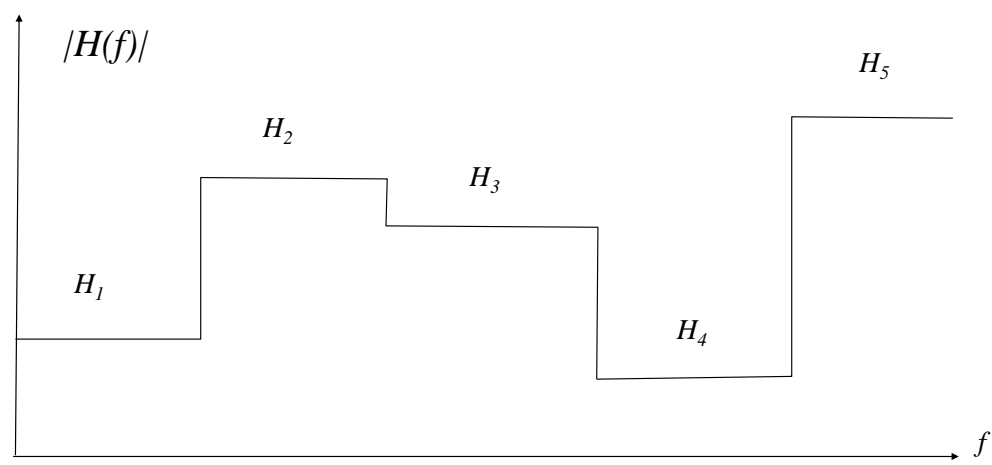


Figure 12.1: Block Fading Model of a Frequency Selective Channel

the SNR cut-off value which is chosen such that

$$\sum_j \left(\frac{1}{\gamma_o} - \frac{1}{\gamma_j} \right) = 1$$

Using water-filling, the capacity becomes

$$C = \sum_{j: \gamma_j \geq \gamma_o} B \log_2 \left(\frac{\gamma_j}{\gamma_o} \right)$$

Thus, information theory suggests that to achieve capacity we must place different power in different sub-bands – something which is difficult (if not impossible) to do with classic digital modulation. This is true regardless of the number of sub-bands. In fact we can show that this also applies to a continuous frequency fading model $H(f)$. In this case, capacity is

$$C = \max_{P(f): \int P(f) df \leq P} \int \log_2 \left(1 + \frac{|H(f)|^2 P(f)}{N_o} \right)$$

where the power allocation is

$$\frac{P(f)}{P} = \begin{cases} \frac{1}{\gamma_o} - \frac{1}{\gamma(f)} & \gamma(f) \geq \gamma_o \\ 0 & \gamma(f) < \gamma_o \end{cases}$$

and $\gamma(f) = \frac{|H(f)|^2 P}{N_o}$. As in the block fading case, we can simplify the capacity as

$$C = \int_{f: \gamma(f) \geq \gamma_o} \log_2 \left(\frac{\gamma(f)}{\gamma_o} \right) df$$

Both of the above arguments (impact of ISI and information theory motivations) suggest that performance would be enhanced (both from a BER and capacity point of view) if we used a set of parallel channels in the frequency domain as shown in Figure 12.2. Each parallel channel would ideally undergo flat fading. Additionally, we could partition the power among the parallel channels based on the individual channel SNRs. The difficulty of creating parallel channels is that they would typically require substantially more bandwidth than a single carrier signal and a set of narrow filters which can be challenging to implement. However, both of these problems can be solved by choosing *orthogonal* subcarriers for each parallel channel. This can be accomplished by restricting modulation on each subcarrier (i.e., parallel channel) to be linear (PSK or QAM). To see this, consider two channels $s_1(t)$ and $s_2(t)$ defined at complex baseband as

$$\begin{aligned} s_1(t) &= s_1 e^{j2\pi f_1 t} & 0 \leq t \leq T \\ s_2(t) &= s_2 e^{j2\pi f_2 t} & 0 \leq t \leq T \end{aligned} \tag{12.1}$$

where s_1 and s_2 are complex symbols which impart amplitude and/or phase modulation on the two signals and conveys the information. For these two signals to be orthogonal, both signals need

to go through an integer number of cycles over the symbol interval T . That is

$$f_1 T = j \quad (12.2)$$

$$f_2 T = k \quad (12.3)$$

for $j, k \in \mathbb{Z}$. Further, this means that $f_1 - f_2 = \frac{j-k}{T} = \frac{m}{T}$ for integer m . Thus, we can create a set of N orthogonal sub-channels with frequencies $k\Delta f$ for $k = -\frac{N/2}{}, -\frac{N}{2} + 1, \dots, \frac{N}{2} - 1$ and $\Delta f = \frac{1}{T}$. This is the essential concept behind OFDM.

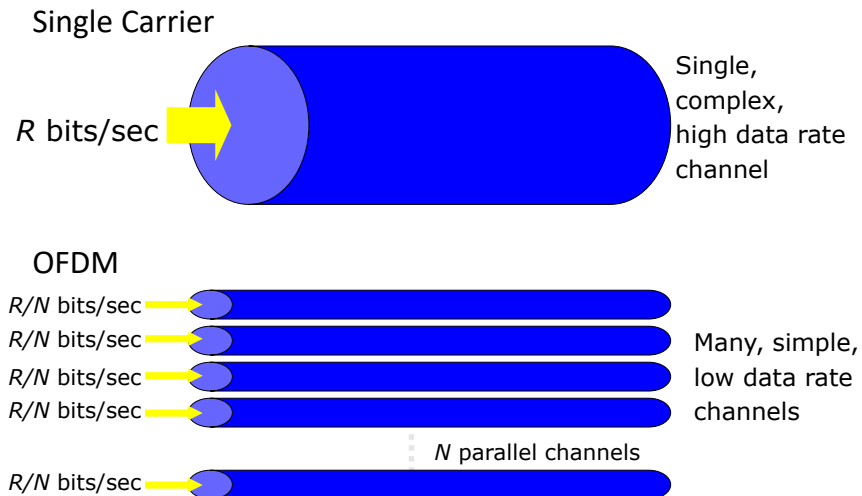


Figure 12.2: Concept Behind OFDM

To be more clear, a single OFDM symbol is defined as a set of N orthogonal subcarriers where each subcarrier is modulated by a different modulation symbol s_i and consecutive subcarriers are separated by $\Delta f = \frac{1}{T}$:

$$s(t) = \sum_{i=-N/2}^{N/2-1} s_i e^{j2\pi i t/T} \quad (12.4)$$

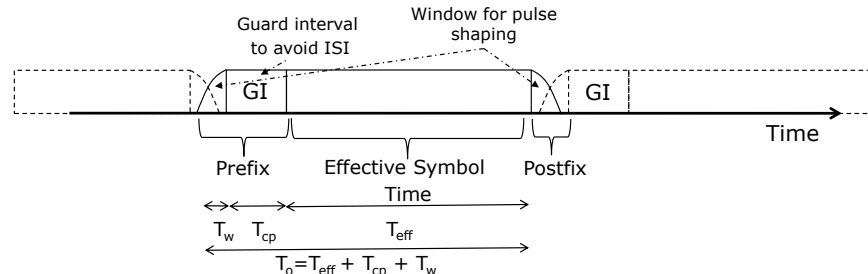
One can view this as the Fourier Transform of the discrete set of symbols $\mathbf{s} = [s_{-N/2}, \dots, s_{N/2-1}]^T$. This is a somewhat simplistic view of the OFDM symbol as we will show shortly, but it provides the basic idea. At the receiver we correlate the signal with the complex conjugate of each of the

subcarriers to obtain the symbol estimates:

$$\begin{aligned}
 z_i &= \frac{1}{T} \int_0^T s(t) e^{-j2\pi it/T} dt \\
 &= \frac{1}{T} \int_0^T \sum_{k=-N/2}^{N/2-1} s_k e^{j2\pi kt/T} e^{-j2\pi it/T} dt \\
 &= \sum_{i=-N/2}^{N/2-1} s_i \frac{1}{T} \int_0^T e^{j2\pi(k-i)t/T} dt \\
 &= s_i
 \end{aligned} \tag{12.5}$$

where we have exploited the orthogonality between subcarriers.

At the transmitter



At the receiver

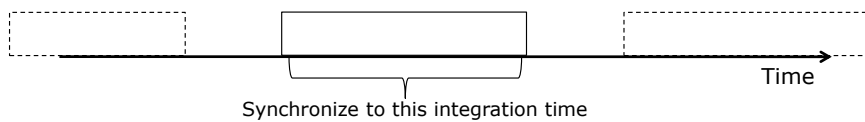


Figure 12.3: Full OFDM Symbol Description in the Time Domain

12.2 OFDM Signal Model

The above description doesn't quite provide the entire picture of the OFDM symbol. A more complete picture is provided in Figure fig:timing. Specifically, in order to eliminate the impact of multipath a guard interval (GI) is added to the beginning of the symbol. We define this to be T_{cp} seconds long. Additionally, there is a windowing interval T_w that is used to shape the spectrum. The actual symbol integration time is termed the *effective* symbol duration and is defined to be T_{eff} . Thus, the total symbol duration (and thus the time between OFDM symbols) is defined to be T_o .

Thus, the transmit signal equal can be written as

$$x(t) = \sum_{k=-\infty}^{\infty} s_k(t - kT_o)$$

where $w(t)$ is the windowing function (which we will define shortly), $s_k(t)$ is the transmitted OFDM symbol and T_o is the time between OFDM symbols. The OFDM symbol is defined as

$$s_k(t) = w(t) \sum_{i=-N/2}^{N/2-1} s_{i,k} e^{j2\pi it/T_{eff}} \quad (12.6)$$

where $s_{i,k}$ is the data symbol modulating the i th subcarrier of the k th OFDM symbol and $T_{eff} = \frac{1}{\Delta f}$ is the effective symbol rate. Note that the subcarrier separation is defined relative to this effective symbol duration. In the absence of guard time, cyclic prefix or a window, $T_{eff} = T_o$. However, normally we have

$$T_o = T_{eff} + T_{cp} + T_w \quad (12.7)$$

where T_{cp} is the guard time (also called the guard interval) or duration of the cyclic prefix and T_w is the window duration. Note that the signal exists on

$$-T_w - T_{cp} \leq t \leq T_{eff} + T_w \quad (12.8)$$

Note that this is identical to a Fourier Series representation of the OFDM symbol. The received signal can be written as

$$\begin{aligned} r(t) &= x(t) * h(\tau, t) + n(t) \\ &= \int_0^{\tau_{max}} h(\tau, t)x(t - \tau)d\tau + n(t) \end{aligned} \quad (12.9)$$

where τ_{max} is the max delay in the channel impulse response. For now, we will assume that

$$1. \tau_{max} < T_{cp}$$

$$2. h(\tau, t) = h(\tau)$$

Now at the receiver, we have a “matched” filter during the effective symbol interval:

$$\begin{aligned} z_{i,k} &= \frac{1}{T_{eff}} \int_{kT_o}^{kT_o + T_{eff}} r(t) e^{-j2\pi i(t - kT_o)/T_{eff}} dt \\ &= \frac{1}{T_{eff}} \int_{kT_o}^{kT_o + T_{eff}} \left(\int_0^{\tau_{max}} h(\tau, t)x(t - \tau)d\tau + n(t) \right) e^{-j2\pi i(t - kT_o)/T_{eff}} dt \end{aligned}$$

Since $\tau_{max} < T_{cp}$ and $w(t) = 1$ over the integration period:

$$\begin{aligned} z_{i,k} &= \frac{1}{T_{eff}} \int_{kT_o}^{kT_o + T_{eff}} \left(\int_0^{\tau_{max}} h(\tau) \sum_{m=-N/2}^{N/2-1} s_{m,k} e^{j2\pi m(t - kT_o - \tau)/T_{eff}} d\tau \right) e^{-j2\pi i(t - kT_o)/T_{eff}} dt + \dots \\ &\quad \frac{1}{T_{eff}} \int_{kT_o}^{kT_o + T_{eff}} n(t) e^{-j2\pi i(t - kT_o)/T_{eff}} dt \end{aligned}$$

Interchanging the integration and summation and letting $u = t - kT_o$

$$\begin{aligned}
z_{i,k} &= \sum_{m=-N/2}^{N/2-1} s_{m,k} \frac{1}{T_{eff}} \int_0^{T_{eff}} \left(\int_0^{\tau_{max}} h(\tau) e^{j2\pi m(u-\tau)/T_{eff}} d\tau \right) e^{-j2\pi i u/T_{eff}} du + n_{i,k} \\
&= \sum_{m=-N/2}^{N/2-1} s_{m,k} \frac{1}{T_{eff}} \int_0^{T_{eff}} \underbrace{\left(\int_0^{\tau_{max}} h(\tau) e^{-j2\pi m\tau/T_{eff}} d\tau \right)}_{\mathcal{F}\{h(\tau)\}|_{f=m/T_{eff}} \triangleq H_m} e^{-j2\pi(i-m)u/T_{eff}} du + n_{i,k} \\
&= \sum_{m=-N/2}^{N/2-1} H_m s_{m,k} \underbrace{\frac{1}{T_{eff}} \int_0^{T_{eff}} e^{-j2\pi(i-m)u/T_{eff}} du}_{= \begin{cases} 1 & i = m \\ 0 & i \neq m \end{cases}} + n_{i,k} \\
&= H_i s_{i,k} + n_{i,k}
\end{aligned}$$

Thus, for perfectly synchronized OFDM we have N parallel Gaussian channels. Modulation and demodulation are performed by the IFFT and DFT respectively.

The SNR per channel is

$$\gamma_i = \frac{\mathbb{E}\{|s_{i,k}|^2\} |H_i|^2}{\sigma_n^2} \quad (12.10)$$

where $\sigma_n^2 = \mathbb{E}\{|n_{i,k}|^2\}$ which is the same on all channels. Under our assumptions of perfect synchronization, a static channel, and $\tau_{max} < T_{cp}$ (i.e., delay spread less than the cyclic prefix), the performance of OFDM depends only on the statistics of the channel H_i . If the channel is fixed over time and frequency, the performance will be similar to AWGN. If the delay spread is very small and the channel varies slowly over time with Rayleigh or Ricean statistics, performance will follow that of flat Rayleigh or Ricean fading. If the delay spread is large, but smaller than the cyclic prefix, each carrier will appear to have flat fading (either Rayleigh or Ricean). Coding can then be used to exploit the frequency diversity available.

12.3 Performance of OFDM in AWGN and Rayleigh Fading

As derived above, the decision variable in OFDM can be written as

$$z_{i,k} = H_i s_{i,k} + n_{i,k} \quad (12.11)$$

For an AWGN channel, H_i is a complex constant and the performance of BPSK is the same as in a single carrier system:

$$P_b = Q \left(\sqrt{2 \frac{E_b}{N_o}} \right) \quad (12.12)$$

where $\frac{E_b}{N_o} = 2\gamma_i$ is the SNR per bit and is constant over all subcarriers. In a flat Rayleigh fading channel $H_i = H$, $\forall i$ will be a complex Gaussian random variable and again constant over all subcarriers. The SNR on each subcarrier will follow a exponential distribution as discussed in Chapter 6. The resulting BER for BPSK can be approximated as

$$P_b \approx \frac{1}{4E_b/N_o} \quad (12.13)$$

where $\overline{E_b/N_o}$ is the average SNR per bit. The probability of bit error in frequency selective fading will be the same. This is because although the overall channel is frequency selective, each individual subcarrier will experience flat fading. Further, while for a particular instantiation of the channel, some subcarriers will experience higher (or lower) BER than other subcarriers, when averaged over all fading realizations, the subcarriers will all experience the same *average* performance.

12.4 Frequency Domain Representation

The OFDM symbol is the summation of subcarriers as shown in (12.6). The spectrum is thus the spectrum of a single OFDM symbol over the effective symbol time can be written as

$$\begin{aligned} S(f) &= \mathcal{F} \left\{ \sum_{i=-N/2}^{N/2-1} s_i e^{j2\pi i t / T_{eff}} \Pi \left(\frac{t}{T_{eff}} \right) \right\} \\ &= \sum_{i=-N/2}^{N/2-1} s_i \mathcal{F} \left\{ e^{j2\pi i t / T_{eff}} \Pi \left(\frac{t}{T_{eff}} \right) \right\} \\ &= \sum_{i=-N/2}^{N/2-1} s_i \mathcal{F} \left\{ e^{j2\pi i t / T_{eff}} \right\} * \mathcal{F} \left\{ \Pi \left(\frac{t}{T_{eff}} \right) \right\} \end{aligned}$$

where $*$ is the convolution operation. Taking the two Fourier Transforms we have

$$\begin{aligned} S(f) &= \sum_{i=-N/2}^{N/2-1} s_i \delta(f - k\Delta f) * T_{eff} \text{sinc}(fT_{eff}) \\ &= \sum_{i=-N/2}^{N/2-1} s_i \text{sinc}(T_{eff}(f - k\Delta f)) \end{aligned}$$

Thus, the spectrum of a single OFDM symbol is the sum of frequency shifted sinc functions in the frequency domain. Note that due to the definition of the sinc function, the spectrum of individual subcarriers goes to zero when the other subcarriers peak. Thus, provided that we are “sampling” the spectrum at the peaks, there is no interference between subcarriers (i.e., no Inter Carrier Interference or ICI). This is shown in Figure 12.4.

As discussed earlier, OFDM symbols often include window functions to help further shape the spectrum. Even though the spectrum is comprised of narrow sinc functions, it is still desireable to reduce sidelobe levels through windowing. One such window function is defined as

$$w(t) = \begin{cases} \frac{1}{2} \left[1 - \cos \left(\left(\frac{\pi(t+T_w+T_{cp})}{T_w} \right) \right) \right] & -T_w - T_{cp} \leq t \leq -T_{cp} \\ 1 & -T_{cp} \leq t \leq T_{eff} \\ \frac{1}{2} \left[1 - \cos \left(\left(\frac{\pi(t-T_w-T_{eff})}{T_w} \right) \right) \right] & T_{eff} \leq t \leq T_{eff} + T_w \end{cases}$$

The effect of the window length is shown in Figure 12.5. Clearly increasing the window size benefits the spectrum by reducing sidelobes. However, the window interval (like the guard interval) represents a waste of time resources since no useful signal is transmitted during this interval. Thus, we wish to reduce T_w for energy efficiency purposes, while spectral characteristics are benefited by increasing T_w creating a trade-off that must be considered.

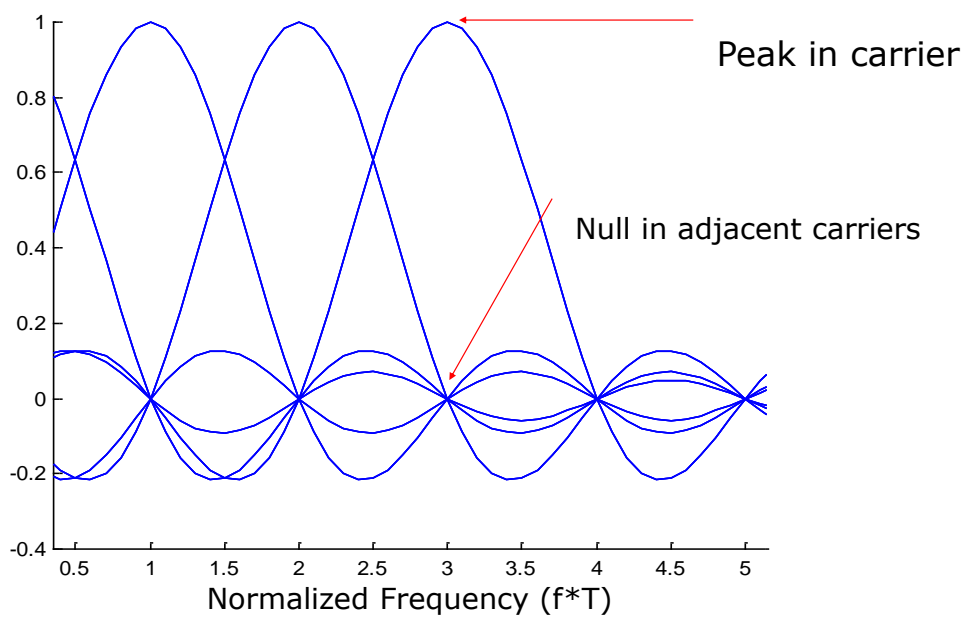


Figure 12.4: subcarriers in the Frequency Domain

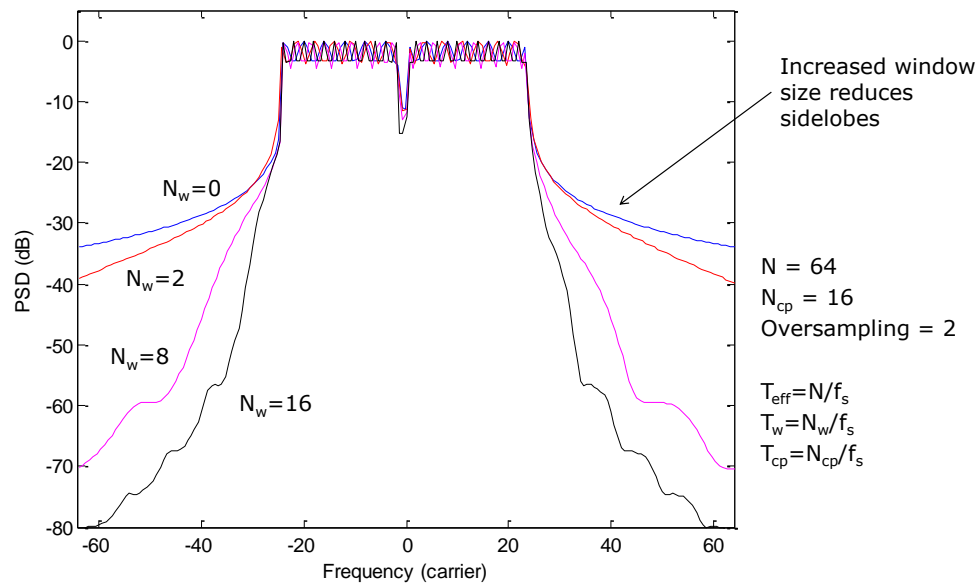


Figure 12.5: Impact of Windowing on OFDM Spectrum

12.5 Impact of Timing Error

The impact of timing error can be seen by assuming a timing difference of δt between the received signal $r(t)$ and the local reference and integration time:

$$z_{i,k} = \frac{1}{T_{eff}} \int_{kT_o + \Delta t}^{kT_o + T_{eff} + \Delta t} r(t) e^{-j2\pi i(t - kT_o - \Delta t)/T_{eff}} dt$$

If $\Delta t < T_{cp}$, no ISI results. Otherwise, ISI can occur. In the case $\Delta t < T_{cp}$:

$$\begin{aligned} z_{i,k} &= \sum_{m=-N/2}^{N/2-1} s_{m,k} \frac{1}{T_{eff}} \int_0^{T_{eff}} \underbrace{\left(\int_0^{\tau_{max}} h(\tau) e^{-j2\pi m\tau/T_{eff}} d\tau \right)}_{H_m} e^{-j2\pi(i-m)u/T_{eff} + m\Delta t/T_{eff}} du + n_{i,k} \\ &= H_i s_{i,k} \underbrace{e^{-j2\pi i \Delta t/T_{eff}}}_{\text{Progressive phase rotation}} + n_{i,k} \end{aligned} \quad (12.14)$$

Thus, for $\Delta t > T_{cp}$ ISI occurs, but if $\Delta t \leq T_{cp}$ only a phase shift is experienced. ADDITIONAL NOTES:

- * If $\Delta t = T_{eff}/N$, phase rotation reaches $\pm\pi/2$ for largest subcarriers.
- * This phase rotation will appear to be part of the channel and equalized via channel estimation and compensation (provided that the pilot symbol spacing is sufficient).

12.6 Impact of Frequency Error

Let f_{co} be the frequency offset (frequency error) due to imperfect frequency estimation.

$$r(t) = e^{j(2\pi f_{co}t + \theta)} x(t) * h(\tau) + n(t)$$

$$\begin{aligned} z_{i,k} &= \frac{1}{T_{eff}} \int_{kT_o}^{kT_o + T_{eff}} r(t) e^{-j2\pi i(t - kT_o)/T_{eff}} dt \\ &= \frac{e^{j\theta}}{T_{eff}} \int_{kT_o}^{kT_o + T_{eff}} \left(\int_0^{\tau_{max}} h(\tau) x(t - \tau) e^{-j2\pi f_{co}\tau} d\tau + n(t) \right) e^{j(2\pi f_{co}t + \theta)} e^{-j2\pi i(t - kT_o)/T_{eff}} dt \\ &= e^{j(\theta + 2\pi f_{co}kT_o)} \sum_{m=-N/2}^{N/2-1} \tilde{H}_m s_{m,k} \frac{1}{T_{eff}} \int_0^{T_{eff}} \underbrace{e^{-j2\pi \left(\frac{i-m}{T_{eff}} - f_{co} \right) u}}_{\neq \begin{cases} 1 & i = m \\ 0 & i \neq m \end{cases}} du + n_{i,k} \\ &= \underbrace{e^{j(\theta + 2\pi f_{co}kT_o)} \tilde{H}_i s_{i,k} \frac{1}{T_{eff}} \int_0^{T_{eff}} e^{j2\pi f_{co}u} du}_{\text{desired term}} + \underbrace{\sum_{m=-N/2, m \neq i}^{N/2-1} \tilde{H}_m s_{m,k} \frac{1}{T_{eff}} \int_0^{T_{eff}} e^{j2\pi \left(\frac{i-m}{T_{eff}} - f_{co} \right) u} du}_{ICI} + n_{i,k} \end{aligned}$$

where \tilde{H}_m is the channel response seen in the m th subcarrier bin after the frequency shift. The desired term is degraded by

$$\frac{1}{T_{eff}} \int_0^{T_{eff}} e^{j2\pi f_{co} u} du = e^{j\pi f_{co} T_{eff}} \text{sinc}(f_{co} T_{eff}) \quad (12.15)$$

12.7 Discrete Time Notation

In order to continue our analysis, it is helpful to work in the discrete domain (i.e., use vectors and matrices in our analysis). To do so, it will be helpful to define some useful matrices. Those definitions follow. First, we define the vector of symbols \mathbf{s} as a $N_s \times 1$ vector defining the complex PSK or QAM symbols. The transmit signal samples for one OFDM symbol is defined as a $N \times 1$ vector \mathbf{x}

$$\begin{aligned} \mathbf{x}[n] &= x(nT_s) \\ &= \sum_{k=-\infty}^{\infty} s_k(nT_s - kT_o) \end{aligned}$$

If we restrict ourselves to a single OFDM symbol, we can write

$$\begin{aligned} \mathbf{x}[n] &= x(nT_s) \\ &= s(nT_s) \\ &= \sum_{k=0}^{N-1} s_k e^{j2\pi knT_s/T_{eff}} \\ &= \sum_{k=0}^{N-1} s_k e^{j2\pi kn/N} \end{aligned}$$

where $n = 0, 1, \dots, N-1$ and $T_s = \frac{1}{f_s} = \frac{T_{eff}}{N}$ is the sampling interval (the inverse of the sampling frequency f_s). Note that the k th OFDM symbol is represented as $\mathbf{x}[k]$. The received signal during the k th OFDM symbol interval will be represented by the vector $\tilde{\mathbf{r}}[k]$. Often we will focus on a generic symbol interval and simply use the notation $\tilde{\mathbf{r}}$.

12.7.1 DFT Matrices

Define \mathbf{D}_N as the $N \times N$ DFT matrix with n, m th element $\mathbf{D}_N[n, m] = e^{-j2\pi(n-1)(m-1)/N}$

$$\mathbf{D}_N = \frac{1}{\sqrt{N}} \begin{bmatrix} 1 & 1 & 1 & \dots & 1 \\ 1 & e^{-j2\pi/N} & e^{-j2\pi 2/N} & \dots & e^{-j2\pi(N-1)/N} \\ 1 & \vdots & & \dots & e^{-j2\pi 2(N-1)/N} \\ \vdots & & & & \vdots \\ 1 & e^{-j2\pi(N-1)/N} & e^{-j2\pi 2(N-1)/N} & \dots & e^{-j2\pi(N-1)(N-1)/N} \end{bmatrix} \quad (12.16)$$

Further, we will need special cases of the DFT matrix. Specifically, define $N \times L$ matrix \mathbf{D}_{NL} as the first L columns of the DFT matrix:

$$\mathbf{D}_{NL} = \frac{1}{\sqrt{N}} \begin{bmatrix} 1 & 1 & 1 & \dots & 1 \\ 1 & e^{-j2\pi/N} & e^{-j2\pi2/N} & \dots & e^{-j2\pi(L-1)/N} \\ 1 & \vdots & & \dots & e^{-j2\pi2(L-1)/N} \\ \vdots & & & & \vdots \\ 1 & e^{-j2\pi(N-1)/N} & e^{-j2\pi2(N-1)/N} & \dots & e^{-j2\pi(L-1)(N-1)/N} \end{bmatrix} \quad (12.17)$$

Further, let's define two additional versions of the DFT matrix which correspond to the locations of the N_p pilots. Define the set $\mathcal{P} = \{k_1, k_2, \dots, k_{N_p}\}$ as the set of frequency indices where the pilots are located, with $|\mathcal{P}| = N_p$. Further define the set N_s symbol locations as: $\mathcal{S} = \{\kappa_1, \kappa_2, \dots, \kappa_{N_s}\}$. Again, note that $|\mathcal{S}| = N_s$. Note that $N_s + N_p \leq N$ with the inequality due to the fact that there may be null-subcarriers. Thus, we will define two matrices \mathbf{Q}_{N_pL} and \mathbf{Q}_{N_sN} :

$$\mathbf{Q}_{N_pL} = \frac{1}{\sqrt{N}} \begin{bmatrix} 1 & e^{-j2\pi k_1/N} & e^{-j2\pi2 k_1/N} & \dots & e^{-j2\pi(L-1) k_1/N} \\ 1 & e^{-j2\pi k_2/N} & & \dots & e^{-j2\pi(L-1) k_2/N} \\ \vdots & & & & \vdots \\ 1 & e^{-j2\pi k_{N_p}/N} & e^{-j2\pi2 k_{N_p}/N} & \dots & e^{-j2\pi(L-1) k_{N_p}/N} \end{bmatrix} \quad (12.18)$$

$$\mathbf{Q}_{N_sN} = \frac{1}{\sqrt{N}} \begin{bmatrix} 1 & e^{-j2\pi \kappa_1/N} & e^{-j2\pi2 \kappa_1/N} & \dots & e^{-j2\pi(N-1) \kappa_1/N} \\ 1 & e^{-j2\pi \kappa_2/N} & & \dots & e^{-j2\pi(N-1) \kappa_2/N} \\ \vdots & & & & \vdots \\ 1 & e^{-j2\pi \kappa_{N_s}/N} & e^{-j2\pi2 \kappa_{N_s}/N} & \dots & e^{-j2\pi(N-1) \kappa_{N_s}/N} \end{bmatrix} \quad (12.19)$$

12.7.2 Defining the Signal and Pilots

We shall define the vector of total transmitted symbols \mathbf{s}_t as an N -length vector which is the sum of both the data and pilot symbols where the locations (i.e., subcarriers) of the symbols are defined by the set \mathcal{S} and the locations of the pilots are defined by the set \mathcal{P} . Specifically,

$$\mathbf{s}_t = \mathbf{I}_{N\mathcal{S}}\mathbf{s} + \mathbf{I}_{N\mathcal{P}}\mathbf{p} \quad (12.20)$$

where $\mathbf{I}_{N\mathcal{S}}$ is $N \times N$ identity matrix where only the $N_s = |\mathcal{S}|$ columns corresponding the elements in the set \mathcal{S} are retained resulting in an $N \times N_s$ matrix. Similarly, $\mathbf{I}_{N\mathcal{P}}$ is $N \times N$ identity matrix where only the $N_p = |\mathcal{P}|$ columns corresponding the elements in the set \mathcal{P} are retained resulting in an $N \times N_p$ matrix. Note that $N_s + N_p \leq N$ with equality occurring only if all subcarriers are used. As an example, consider $N = 4$ with pilot locations $\mathcal{P} = \{2\}$ and symbol locations $\mathcal{S} = \{1, 3, 4\}$. In this case

$$\mathbf{I}_{N\mathcal{S}} = \begin{bmatrix} 1 & 0 & 0 \\ 0 & 0 & 0 \\ 0 & 1 & 0 \\ 0 & 0 & 1 \end{bmatrix} \quad (12.21)$$

and

$$\mathbf{I}_{N\mathcal{P}} = \begin{bmatrix} 0 \\ 1 \\ 0 \\ 0 \end{bmatrix} \quad (12.22)$$

Note that during much of the development we will ignore the pilots and simply let $\mathbf{s}_t = \mathbf{s}$. When we explicitly consider channel estimation, we will use the notation described above. If we want to obtain the pilot symbols or data symbols from \mathbf{s}_t we simply apply the transpose:

$$\begin{aligned} \mathbf{s} &= \mathbf{I}_{N\mathcal{S}}^T \mathbf{s}_t \\ \mathbf{p} &= \mathbf{I}_{N\mathcal{P}}^T \mathbf{s}_t \end{aligned}$$

Note that $\mathbf{I}_{N\mathcal{S}}^T \mathbf{I}_{N\mathcal{S}} = \mathbf{I}_{N_s}$ and $\mathbf{I}_{N\mathcal{P}}^T \mathbf{I}_{N\mathcal{P}} = \mathbf{I}_{N_p}$.

12.7.3 Notation for Zero Padding

If we wish to add zero-padding (simple guard interval of length N_{zp} zeros instead of using a cyclic prefix), we apply the $(N_{zp} + N) \times N$ matrix transformation

$$\mathbf{T}_{zp} = \left[\mathbf{0}_{N_{zp} \times N}^T \mathbf{I}_N^T \right]^T \quad (12.23)$$

and we remove it using the $N \times (N + N_{zp})$ matrix transformation

$$\mathbf{R}_{zp} = [\mathbf{0}_{N \times N_{zp}} \mathbf{I}_N] \quad (12.24)$$

12.7.4 Notation for the Cyclic Prefix

Often we will wish to use a cyclic prefix (simple pre-extension of the symbol at the beginning). Define \mathbf{T}_{cp} as the matrix transform to add the cyclic prefix. This can be written as

$$\mathbf{T}_{cp} = \left[\mathbf{I}_{N_{cp}N}^T \mathbf{I}_N^T \right]^T \quad (12.25)$$

where \mathbf{I}_N is an $N \times N$ identity matrix, \mathbf{I}_{kN} is the last k columns of \mathbf{I}_N , and N_{cp} is the number of samples in the cyclic prefix. Note that \mathbf{T}_{cp} is an $(N_{cp} + N) \times N$ matrix. Finally, if \mathbf{s}_t is an N -length vector of symbols (both data and pilots) in the frequency domain, we convert to the time domain and add the cyclic-prefix using the linear transformation:

$$\mathbf{x}_{cp} = \mathbf{T}_{cp} \mathbf{D}_N^H \mathbf{s}_t \quad (12.26)$$

Note that \mathbf{x}_{cp} is a $(N_{cp} + N) \times 1$ vector of time samples. Removing the cyclic prefix at the receiver is accomplished by applying the appropriate matrix transform to the received vector $\mathbf{r}_{cp} = \tilde{\mathbf{H}} \mathbf{x}_{cp} + \mathbf{n}$:

$$\tilde{\mathbf{r}} = \mathbf{R}_{cp} \mathbf{r}_{cp} \quad (12.27)$$

where $\mathbf{R}_{cp} = [\mathbf{0}_{N \times N_{cp}} \mathbf{I}_N]$ and $\mathbf{0}_{m \times n}$ is an $m \times n$ matrix of zeros. Note that \mathbf{R}_{cp} is an $N \times (N + N_{cp})$ matrix.

12.7.5 Circulant Matrices

An $N \times N$ circulant matrix \mathbf{C} is one which is completely defined by the vector \mathbf{c} which is equal to the first column. We can show this by writing $\mathbf{C}(\mathbf{c})$. Further, the 2nd through N th columns are circularly shifted versions of the previous column. Note that the last row is a reversed order version of the first column \mathbf{c} .

$$\mathbf{C} = \begin{bmatrix} c_0 & c_{N-1} & \dots & c_2 & c_1 \\ c_1 & c_0 & c_{N-1} & \dots & c_2 \\ \vdots & c_1 & c_0 & \ddots & \vdots \\ c_{N-2} & & \dots & & c_{N-1} \\ c_{N-1} & c_{N-2} & \dots & c_1 & c_0 \end{bmatrix} \quad (12.28)$$

An important property of circulant matrices is that their eigenvectors are equivalent to the columns of the DFT matrix. As a result, a circulant matrix is diagonalized by the DFT and IDFT matrices:

$$\mathbf{D}_N \mathbf{C} \mathbf{D}_N^H = \mathbf{D}_N^H \mathbf{C} \mathbf{D}_N = \text{diag}(\lambda) \quad (12.29)$$

where λ is the vector of eigenvalues of \mathbf{C} . Note that these eigenvalues are equal to $\mathbf{D}_N \mathbf{c}$.

12.8 The Impact of Multipath

Let's first examine what occurs without zero padding or a cyclic prefix. The transmit signal can be written in terms of the symbol vector \mathbf{s}_t :

$$\mathbf{x} = \mathbf{D}_N^H \mathbf{s}_t \quad (12.30)$$

Consider the channel impulse response $\tilde{\mathbf{h}} = [h_0, h_1, h_2, \dots, h_{L-1}]^T$ where the impulse response is sampled at the same rate as the transmit signal $f_s = N\Delta f$. Define the $N \times N$ matrix $\tilde{\mathbf{H}}$:

$$\tilde{\mathbf{H}} = \begin{bmatrix} h_0 & 0 & 0 & \dots & 0 \\ h_1 & h_0 & 0 & \dots & 0 \\ h_2 & h_1 & h_0 & \dots & 0 \\ \vdots & \vdots & \vdots & \dots & \vdots \\ h_{L-1} & h_{L-2} & h_{L-3} & & 0 \\ 0 & h_{L-1} & h_{L-2} & & 0 \\ \vdots & \vdots & \vdots & \dots & \vdots \\ 0 & 0 & 0 & \dots & h_0 \end{bmatrix} \quad (12.31)$$

The receive signal (ignoring intersymbol interference for now) can be written as

$$\mathbf{r} = \tilde{\mathbf{H}} \mathbf{D}_N^H \mathbf{s}_t + \mathbf{n} \quad (12.32)$$

After applying the Discrete Fourier Transform:

$$\mathbf{e} = \mathbf{D}_N \mathbf{r} = \underbrace{\mathbf{D}_N \tilde{\mathbf{H}} \mathbf{D}_N^H}_{\neq \alpha \mathbf{I}} \mathbf{s} + \mathbf{D}_N \mathbf{n} \quad (12.33)$$

Note that because $\tilde{\mathbf{H}}$ is not circulant, the product $\mathbf{D}_N \tilde{\mathbf{H}} \mathbf{D}_N^H$ is not diagonal and thus we have interference between the symbol streams (i.e., the subcarriers). Note that this interference between subcarriers is termed inter-carrier interference or ICI. Focusing only on a generic symbol doesn't illustrate that there is another form of interference, that is interference between consecutive OFDM symbols, or inter-symbol interference (ISI). This can be seen by examining the k th symbol interval. The received samples can be written as

$$\mathbf{r}[k] = \tilde{\mathbf{H}} \mathbf{D}_N^H \mathbf{s}_t[k] + \underbrace{\tilde{\mathbf{H}}_{isi} \mathbf{D}_N^H \mathbf{s}_t[k-1]}_{ISI} + \mathbf{n}[k]$$

where the second term is the ISI and $\tilde{\mathbf{H}}_{isi}$ (which we will define shortly) represents the channel terms causing that ISI. Applying the DFT matrix we obtain

$$\begin{aligned} \mathbf{e}[k] &= \mathbf{D}_N^H \mathbf{r}[k] \\ &= \mathbf{D}_N^H \tilde{\mathbf{H}} \mathbf{D}_N^H \mathbf{s}_t[k] + \mathbf{D}_N^H \tilde{\mathbf{H}}_{isi} \mathbf{D}_N^H \mathbf{s}_t[k-1] + \mathbf{D}_N^H \mathbf{n}[k] \end{aligned}$$

where now we see that there is ICI in the first term and ISI in the second term unless $\mathbf{D}_N^H \tilde{\mathbf{H}} \mathbf{D}_N^H$ is diagonal (no ICI) or $\mathbf{D}_N^H \tilde{\mathbf{H}}_{isi} \mathbf{D}_N^H$ is a matrix of zeros. To eliminate these two effects, we will examine zero-padding and the cyclic prefix.

12.8.1 Impact of a Zero-padded Guard Interval

Let \mathbf{s} be our transmitted symbol vector (ignore pilots for now). Without zero-padding the transmit signal is $\mathbf{x} = \mathbf{D}_N^H \mathbf{s}$ which is an $N \times 1$ vector. With zero-padding we transmit

$$\mathbf{x}_{zp} = \mathbf{T}_{zp} \mathbf{x} = \mathbf{D}_{Nzp} \mathbf{s}_t \quad (12.34)$$

where $\mathbf{D}_{Nzp} = \mathbf{T}_{zp} \mathbf{D}_N^H = \begin{bmatrix} \mathbf{0}_{N_{zp}N} \\ \mathbf{D}_N^H \end{bmatrix}$. Now, to consider intersymbol interference (ISI) let's define the i th time interval of $N + N_{zp}$ received samples:

$$\mathbf{r}_{zp}[i] = \tilde{\mathbf{H}}_g \mathbf{x}_{zp}[i] + \tilde{\mathbf{H}}_{isi} \mathbf{x}_{zp}[i-1] + \mathbf{n}[i] \quad (12.35)$$

where $\tilde{\mathbf{H}}_g$ is an $(N + N_{zp}) \times (N + N_{zp})$ matrix

$$\tilde{\mathbf{H}}_g = \begin{bmatrix} h_0 & 0 & 0 & \dots & 0 \\ h_1 & h_0 & 0 & \dots & 0 \\ h_2 & h_1 & h_0 & \dots & 0 \\ \vdots & \vdots & \vdots & \dots & \vdots \\ h_{L-1} & h_{L-2} & h_{L-3} & & 0 \\ 0 & h_{L-1} & h_{L-2} & & 0 \\ \vdots & \vdots & \vdots & \dots & \vdots \\ 0 & 0 & 0 & \dots & h_0 \end{bmatrix} \quad (12.36)$$

Note that the only difference between $\tilde{\mathbf{H}}_g$ and $\tilde{\mathbf{H}}$ is that the former has an additional N_{zp} rows and N_{zp} columns. The matrix $\tilde{\mathbf{H}}_{isi}$ is also $(N + N_{zp}) \times (N + N_{zp})$ but defined as

$$\tilde{\mathbf{H}}_{isi} = \begin{bmatrix} 0 & \dots & 0 & h_{L-1} & h_{L-2} & \dots & h_0 \\ 0 & 0 & 0 & h_{L-1} & \dots & h_1 \\ \vdots & \vdots & \vdots & \vdots & & \vdots \\ 0 & \dots & 0 & & & 0 & h_{L-1} \\ 0 & 0 & 0 & \dots & & 0 & 0 \\ & & & & & \vdots & \\ 0 & 0 & 0 & \dots & & 0 & 0 \end{bmatrix} \quad (12.37)$$

We can rewrite this as

$$\mathbf{r}_{zp}[i] = \tilde{\mathbf{H}}_g \mathbf{D}_{Nzp} \mathbf{s}[i] + \tilde{\mathbf{H}}_{isi} \mathbf{D}_{Nzp} \mathbf{s}[i-1] + \mathbf{n}[i] \quad (12.38)$$

Now, examining the second term

$$\tilde{\mathbf{H}}_{isi} \mathbf{D}_{Nzp} \quad (12.39)$$

we can see that only the last L columns and first L rows of $\tilde{\mathbf{H}}_{isi}$ are non-zero. Since when removing the zero-padding, we will throw away the first N_{zp} values, if $N_{zp} \geq L$ there is no ISI. Since there is no ISI, we can momentarily drop the symbol index. Further, let's partition $\tilde{\mathbf{H}}_g$ into the first N_{zp} columns (term this part $\tilde{\mathbf{H}}_{ex}$) and the last N columns (term this part $\tilde{\mathbf{H}}_{eff}$). We can then rewrite the received samples as

$$\begin{aligned} \mathbf{r}_{zp} &= [\tilde{\mathbf{H}}_{ex} \tilde{\mathbf{H}}_{eff}] [0_{N_{zp}N}^T \mathbf{D}_N^H]^T \mathbf{s}_t + \mathbf{n} \\ &= \tilde{\mathbf{H}}_{eff} \mathbf{D}_N^H \mathbf{s}_t + \mathbf{n} \end{aligned}$$

where \mathbf{r}_{zp} is an $(N + N_{zp}) \times 1$ vector.

12.8.2 Recevier

At the receiver we need to (a) remove the zero padding and (b) apply the matched filter (DFT):

$$\begin{aligned}\tilde{\mathbf{r}} &= \mathbf{R}_{zp} \mathbf{r}_{zp} \\ &= \mathbf{R}_{zp} \tilde{\mathbf{H}}_{eff} \mathbf{D}_N^H \mathbf{s}_t + \mathbf{R}_{zp} \mathbf{n}\end{aligned}\quad (12.40)$$

Now, the decision variables are

$$\mathbf{e} = \mathbf{D}_N \tilde{\mathbf{r}} = \mathbf{D}_N \mathbf{R}_{zp} \tilde{\mathbf{H}}_{eff} \mathbf{D}_N^H \mathbf{s}_t + \mathbf{D}_N \mathbf{R}_{zp} \mathbf{n} \quad (12.41)$$

Unfortunately, although there is no ISI, the matrix $\mathbf{D}_N \mathbf{R}_{zp} \tilde{\mathbf{H}}_{eff} \mathbf{D}_N^H$ is not diagonal since $\mathbf{R}_{zp} \tilde{\mathbf{H}}_{eff}$ is not circulant. We could alternatively apply an MMSE or zero forcing receiver to $\tilde{\mathbf{r}}$ instead of a simple matched filter. We will come back to this later.

12.9 Cyclic Prefix

Let's define the $N \times (N + N_{cp})$ matrix

$$\mathbf{D}_{Ncp} = \mathbf{T}_{cp} \mathbf{D}_N^H = [\underbrace{\mathbf{q}_{N-N_{cp}+1}, \dots, \mathbf{q}_N}_{\text{last.N}_{cp}.\text{columns.of.}\mathbf{D}_N^H} \mathbf{D}_N^H] \quad (12.42)$$

The transmit signal is then

$$\begin{aligned}\mathbf{x}_{cp} &= \mathbf{T}_{cp} \mathbf{x} \\ &= \mathbf{T}_{cp} \mathbf{D}_N^H \mathbf{s}_t \\ &= \mathbf{D}_{Ncp} \mathbf{s}_t\end{aligned}\quad (12.43)$$

12.9.1 Receiver

At the receiver we have

$$\mathbf{r}_{cp}[i] = \tilde{\mathbf{H}}_g \mathbf{x}_{cp}[i] + \tilde{\mathbf{H}}_{isi} \mathbf{x}_{cp}[i-1] + \mathbf{n}[i] \quad (12.44)$$

To remove the cyclic prefix we apply \mathbf{R}_{cp} :

$$\tilde{\mathbf{r}}[i] = \mathbf{R}_{cp} \mathbf{r}_{cp}[i] \quad (12.45)$$

Now, let's assume that $N_{cp} \geq L$:

* Examining $\tilde{\mathbf{H}}_{isi}$, since only the first L rows have non-zero entries, only the first L samples of $\tilde{\mathbf{H}}_{isi} \mathbf{x}_{cp}$ will be non-zero. Thus,

$$\mathbf{R}_{cp} \tilde{\mathbf{H}}_{isi} \mathbf{x}_{cp}[i-1] = \mathbf{0} \quad (12.46)$$

and ISI is eliminated.

* Examining the first term (and dropping the symbol index):

$$\tilde{\mathbf{r}} = \mathbf{R}_{cp}\mathbf{r}_{cp} = \mathbf{R}_{cp}\tilde{\mathbf{H}}_g\mathbf{x}_{cp} + \mathbf{R}_{cp}\mathbf{n} \quad (12.47)$$

Now, we can show that $\mathbf{R}_{cp}\tilde{\mathbf{H}}_g\mathbf{T}_{cp} = \mathbf{C}_N(\tilde{\mathbf{h}})$ is a circulant matrix with $[h_0, 0, 0, \dots, 0, h_{L-1}, \dots, h_1]$ as the first row. Thus, we have

$$\tilde{\mathbf{r}} = \mathbf{R}_{cp}\mathbf{r}_{cp} = \mathbf{C}_N(\tilde{\mathbf{h}})\mathbf{x} + \mathbf{R}_{cp}\mathbf{n} \quad (12.48)$$

Thus, applying the matched filter:

$$\mathbf{e} = \mathbf{D}_N\tilde{\mathbf{r}} \quad (12.49)$$

$$= \mathbf{D}_N\mathbf{C}_N(\tilde{\mathbf{h}})\mathbf{D}_N^H\mathbf{s} + \mathbf{D}_N\mathbf{R}_{cp}\mathbf{n} \quad (12.50)$$

$$= \Gamma\mathbf{s}_t + \nu \quad (12.51)$$

where Γ is a diagonal matrix with $D_{NL}\tilde{\mathbf{h}}$ on the diagonal.

12.10 Advanced Receiver Techniques

Up to this point we have only considered a single receiver structure - the DFT, also known as the matched filter solution (this view considers the subcarriers as pulse shapes, so that correlating with the subcarriers is essentially matched filtering). Let's define a time-varying channel impulse response

$$h(\tau, t) = \sum_{i=0}^{L-1} \alpha_i(t) e^{j\theta_i(t)} \delta(\tau - \tau_i) \quad (12.52)$$

After sampling we can write a matrix of coefficients where the columns represent time t and the rows represent delay τ :

$$\mathbf{h}_t = \begin{bmatrix} h_{1,1} & h_{1,2} & \dots & h_{1,N} \\ h_{2,1} & h_{2,2} & \dots & h_{2,N} \\ \vdots & \vdots & \vdots & \vdots \\ h_{L,1} & h_{L,2} & \dots & h_{L,N} \end{bmatrix} \quad (12.53)$$

Now, due to the use of the cyclic prefix we can define an $N \times N$ matrix

$$\mathbf{H}_{cp} = \begin{bmatrix} h_{1,1} & 0 & 0 & \dots & h_{3,1} & h_{2,1} \\ h_{2,2} & h_{1,2} & 0 & \dots & h_{4,2} & h_{3,2} \\ h_{3,3} & h_{2,3} & h_{1,3} & \dots & h_{5,3} & h_{4,3} \\ \vdots & \vdots & & & & \\ h_{L,L} & h_{L-1,L} & & \ddots & & \\ 0 & h_{L,L-1} & & & & \\ 0 & 0 & h_{L-2,L} & & & \\ \vdots & \vdots & \vdots & \ddots & \vdots & h_{1,N-1} & 0 \\ 0 & 0 & 0 & \dots & h_{2,N} & h_{1,N} \end{bmatrix} \quad (12.54)$$

where $\mathbf{H}[m, n] = h_{mod(m-n, N)+1, m}$. At the receiver, after removing the cyclic prefix we can write:

$$\tilde{\mathbf{r}} = \mathbf{H}_{cp} \mathbf{D}_N^H \mathbf{s} + \mathbf{R}_{cp} \mathbf{n} \quad (12.55)$$

Taking the DFT (matched filter) we have

$$\mathbf{e} = \mathbf{D}_N \tilde{\mathbf{r}} = \Gamma \mathbf{s}_t + \nu \quad (12.56)$$

If the channel is static, we have already shown that Γ is diagonal and we obtain the decision statistics (in the case of PSK modulation) by applying Γ^H : $\mathbf{z} = \Gamma^H \mathbf{e}$. Note that $\Gamma^H \Gamma$ is diagonal with all real elements on the diagonal allowing simple detection of PSK.

If the channel is time-varying, ICI occurs. We can apply a zero-forcing (LS) approach in this case:

$$\mathbf{z} = (\Gamma^H \Gamma)^{-1} \Gamma^H \mathbf{e} \quad (12.57)$$

$$= (\Gamma^H \Gamma)^{-1} \Gamma^H \Gamma \mathbf{s}_t + (\Gamma^H \Gamma)^{-1} \Gamma^H \nu \quad (12.58)$$

Alternatively, we could apply MMSE filtering:

$$\mathbf{z} = \left(\Gamma^H \Gamma + \frac{1}{SNR} \mathbf{I}_N \right)^{-1} \Gamma^H \mathbf{e} \quad (12.59)$$

Finally, an SIC approach uses the following algorithm:

- * $\tilde{\Gamma} = \Gamma, \tilde{\eta} = \mathbf{e}$
- * $\mathbf{G} = \left(\tilde{\Gamma}^H \tilde{\Gamma} + \frac{1}{SNR} \mathbf{I}_N \right)^{-1}$
- * $\mathbf{T} = \mathbf{G} \tilde{\Gamma}^H$
- * for $i = 1:N$
- * $a_i = \arg \min \text{diag}(\mathbf{G})$
- * \mathbf{t} is the a_i th row of \mathbf{T}
- * $z_{a_i} = \mathbf{t} \tilde{\eta}, \hat{s}_{a_i} = f(z_{a_i})$
- * $\tilde{\eta} = \tilde{\eta} - \hat{s}_{a_i} h_{a_i}$ (h_{a_i} is the a_i th column of $\tilde{\Gamma}$)
- * $[\tilde{\Gamma}]_{a_i} = \mathbf{0}$
- * $\mathbf{G} = \left(\tilde{\Gamma}^H \tilde{\Gamma} + \frac{1}{SNR} \mathbf{I}_N \right)^{-1}$
- * $\mathbf{T} = \mathbf{G} \tilde{\Gamma}^H$

Chapter 13

Parameter Estimation

13.1 OFDM Channel Estimation

In any wireless communication system, a key aspect of coherent detection is *channel estimation*, that is estimating the complex gain observed by the receiver due to the wireless channel. Of course estimating and removing the effect of this complex gain (hereafter termed the “channel”) is vitally important in order to detect the data. We spent a significant amount of time discussing the wireless channel in Chapter 2 and again in Chapter 11. In this section we discuss channel estimation techniques that are particular to OFDM.

13.1.1 The Problem

Let \mathbf{s}_t be the vector of transmitted symbols including data symbols \mathbf{s} and pilots \mathbf{p} where $\mathbf{s}_t = \mathbf{I}_{N\mathcal{S}}\mathbf{s} + \mathbf{I}_{N\mathcal{P}}\mathbf{p}$. The transmit signal with cyclic prefix is written as

$$\begin{aligned}\mathbf{x}_{cp} &= \mathbf{T}_{cp}\mathbf{D}_N^H\mathbf{s}_t \\ &= \mathbf{D}_{N_{cp}}\mathbf{s}_t\end{aligned}$$

At the receiver we observe

$$\mathbf{r}_{cp} = \tilde{\mathbf{H}}_g\mathbf{x}_{cp} + \mathbf{n} \quad (13.1)$$

We first remove the cyclic prefix:

$$\tilde{\mathbf{r}} = \mathbf{R}_{cp}\mathbf{r}_{cp} \quad (13.2)$$

$$= \mathbf{R}_{cp}\tilde{\mathbf{H}}_g\mathbf{x}_{cp} + \mathbf{R}_{cp}\mathbf{n} \quad (13.3)$$

$$= \mathbf{R}_{cp}\tilde{\mathbf{H}}_g\mathbf{T}_{cp}\mathbf{x} + \mathbf{R}_{cp}\mathbf{n} \quad (13.4)$$

$$= C_N(\tilde{\mathbf{h}})\mathbf{x} + \mathbf{R}_{cp}\mathbf{n} \quad (13.5)$$

Secondly, we apply the DFT:

$$\mathbf{e} = \mathbf{D}_N \tilde{\mathbf{r}} \quad (13.6)$$

$$= \mathbf{D}_N C_N(\tilde{\mathbf{h}}) \mathbf{x} + \mathbf{D}_N \mathbf{R}_{cp} \mathbf{n} \quad (13.7)$$

$$= \mathbf{D}_N C_N(\tilde{\mathbf{h}}) \mathbf{D}_N^H \mathbf{s}_t + \nu \quad (13.8)$$

$$= \Gamma \mathbf{s}_t + \nu \quad (13.9)$$

where $\Gamma = \text{diag}(D_{NL}\tilde{\mathbf{h}})$ ¹. Defining \mathbf{H} to be the DFT of the channel impulse response we have $\Gamma = \text{diag}(\mathbf{H})$. Now, to obtain the final decision metrics \mathbf{z} , we must remove the channel effects. For PSK that means:

$$\mathbf{z} = \hat{\Gamma}^H \mathbf{e} \quad (13.10)$$

while for QAM that means

$$\mathbf{z} = \hat{\Gamma}^{-1} \mathbf{e} \quad (13.11)$$

where $\hat{\Gamma} = \text{diag}(\hat{\mathbf{H}})$ and $\hat{\mathbf{H}}$ is the estimate of our frequency domain channel. Thus, we are concerned we means to create the estimate $\hat{\mathbf{H}}$.

13.1.2 Channel Estimation from Pilots Symbols

The received, noisy pilot symbols can be written as

$$\mathbf{e}_p = \mathbf{I}_{NP}^T \mathbf{e} \quad (13.12)$$

while the channel values at those same sub-carrier locations can be written as

$$\mathbf{H}_p = \mathbf{I}_{NP}^T \mathbf{H} \quad (13.13)$$

Ultimately, we wish to estimate \mathbf{H} from \mathbf{e}_p .

13.1.3 Least Squares Estimate of \mathbf{H}_p

The channel at the pilot symbol locations are related to the received pilot symbols as

$$\mathbf{e}_p = \text{diag}(\mathbf{H}_p) \mathbf{p} + \nu_p \quad (13.14)$$

$$= \text{diag}(\mathbf{p}) \mathbf{H}_p + \nu_p \quad (13.15)$$

$$= \mathbf{P} \mathbf{H}_p + \nu_p \quad (13.16)$$

where $\mathbf{P} \triangleq \text{diag}(\mathbf{p})$. This is a classic scenario where the observed vector is a linear function of the vector parameter to be estimated plus Gaussian noise. Since \mathbf{P} is a square matrix the least squares estimate of \mathbf{H}_p is

$$\mathbf{H}_p^{(LS)} = \mathbf{P}^{-1} \mathbf{e}_p \quad (13.17)$$

We could then obtain the channel estimates at the other sub-carriers through interpolation if desired. Alternatively, we can find the least squares or maximum likelihood solutions, which we consider next.

¹ $\text{diag}(\mathbf{x})$ is a diagonal matrix with \mathbf{x} on the diagonal.

Least Squares Estimate of \mathbf{H}

First, we should note that due to the linear relationship between $\tilde{\mathbf{h}}$ and \mathbf{H} , i.e., since $\mathbf{H} = \mathbf{D}_{NL}\tilde{\mathbf{h}}$, it can be shown that $\hat{\mathbf{H}}^{(LS)} = \mathbf{D}_{NL}\hat{\mathbf{h}}^{(LS)}$. Further, we should mention that in Gaussian noise the maximum likelihood estimate is equivalent to the least squares estimate $\hat{\mathbf{h}}^{(MLE)} = \hat{\mathbf{h}}^{(LS)}$ and $\hat{\mathbf{H}}^{(MLE)} = \hat{\mathbf{H}}^{(LS)}$. Now, we can re-write the received pilot symbols \mathbf{e}_p as

$$\mathbf{e}_p = \mathbf{P}\mathbf{H}_p + \nu_p \quad (13.18)$$

$$= \mathbf{P}\mathbf{Q}_{N_p L}\tilde{\mathbf{h}} + \nu_p \quad (13.19)$$

First, we can remove the modulation by multiplying (in the case of PSK) or dividing (in the case of QAM) the symbols:

$$\mathbf{y} = \mathbf{P}^{-1}\mathbf{e}_p \quad (13.20)$$

$$= \mathbf{Q}_{N_p L}\tilde{\mathbf{h}} + \epsilon \quad (13.21)$$

where $\epsilon = \mathbf{P}^{-1}\nu_p$ is a Gaussian random vector. Again, we have the standard relationship between an observed vector and the parameter vector to be estimated. Since the matrix $\mathbf{Q}_{N_p L}$ isn't square we must apply the pseudo-inverse:

$$\hat{\mathbf{h}}^{(LS)} = \mathbf{Q}_{N_p L}^\dagger \mathbf{y} \quad (13.22)$$

$$= (\mathbf{Q}_{N_p L}^H \mathbf{Q}_{N_p L})^{-1} \mathbf{Q}_{N_p L}^H \mathbf{P}^{-1} \mathbf{e}_p \quad (13.23)$$

It is important to note that this estimate relies on the inversion of the matrix $\mathbf{Q}_{N_p L}^H \mathbf{Q}_{N_p L}$. This matrix will only be invertable if $N_p \geq L$. **Thus, we see that in order to estimate an L -tap frequency selective channel we must use $N_p \geq L$ pilots.** Finally, we have the least squares estimate of \mathbf{H} as

$$\hat{\mathbf{H}}^{(LS)} = \mathbf{D}_{NL}\hat{\mathbf{h}}^{(LS)} \quad (13.24)$$

$$= \mathbf{D}_{NL}\mathbf{Q}_{N_p L}^\dagger \underbrace{\mathbf{P}^{-1}\mathbf{e}_p}_{\hat{\mathbf{H}}_p^{(LS)}} \quad (13.25)$$

Note that we then apply this to the data symbols by using $\hat{\Gamma} = \text{diag}(\hat{\mathbf{H}}^{(LS)})$ in (13.10) or (13.11).

13.1.4 The MMSE Estimator

The General MMSE Solution

Consider a set of noisy observations \mathbf{x} which are related to a parameter to be estimated θ . We wish to estimate the parameter using a linear combinations of the observations

$$\hat{\theta} = \mathbf{w}^H \mathbf{x} \quad (13.26)$$

where \mathbf{w} are the combining weights. The error between the estimate and the true parameter can be written as

$$\epsilon = \theta - \hat{\theta} \quad (13.27)$$

$$= \theta - \mathbf{w}^H \mathbf{x} \quad (13.28)$$

The squared error is then

$$\epsilon^2 = \theta^2 - 2\theta\mathbf{w}^H\mathbf{x} + \mathbf{w}^H\mathbf{x}\mathbf{x}^H\mathbf{w} \quad (13.29)$$

The cost function to be considered is the mean square error which can be written as

$$\mathbf{E}\{\epsilon^2\} = \mathbf{E}\{\theta^2\} + \mathbf{w}^H\mathbf{E}\{\mathbf{x}\mathbf{x}^H\}\mathbf{w} - 2\mathbf{w}^H\mathbf{E}\{\theta^*\mathbf{x}\} \quad (13.30)$$

$$= \mathbf{E}\{\theta^2\} + \mathbf{w}^H\Phi_{xx}\mathbf{w} - 2\mathbf{w}^H\Phi_{\theta x} \quad (13.31)$$

where $\Phi_{xx} = \mathbf{E}\{\mathbf{x}\mathbf{x}^H\}$ and $\Phi_{\theta x} = \mathbf{E}\{\theta^*\mathbf{x}\}$. Taking the gradient gives

$$\nabla\mathbf{E}\{\epsilon^2\} = 2\Phi_{xx}\mathbf{w} - 2\Phi_{\theta x} \quad (13.32)$$

Now, setting the gradient equal to zero and solving for \mathbf{w} provides the Minimum Mean Square Error weights:

$$\mathbf{w}_{mmse} = \Phi_{xx}^{-1}\Phi_{\theta x} \quad (13.33)$$

We will apply this solution to a few different OFDM channel estimators.

The Two-Dimensional MMSE Filter for OFDM Channel Estimation

Consider the time-frequency plane pictured in Figure 13.1 where the columns represent consecutive OFDM symbols in time and the rows represent sub-carriers in each OFDM symbol. We desire to find the channel estimate for each point in the time-frequency grid in order to perform data detection. Now the time-domain channel can be written as a time-varying impulse response (assuming that the multipath delays τ_i are static)

$$h(\tau, t) = \sum_{i=1}^L \alpha_i(t)\delta(\tau - \tau_i) \quad (13.34)$$

where we model the time-variation using a Jakes' model:

$$\alpha_i(t) = \frac{\sigma_i}{\sqrt{S}} \sum_{m=1}^S e^{j(2\pi f_{i,m}t + \phi_{i,m})} \quad (13.35)$$

where σ_i^2 is the average power of the i th path (normalized such that $\sum_i \sigma_i^2 = 1$), S is the number of scatterers, and $f_{i,m}$ and $\phi_{i,m}$ are the frequency and phase due to the i th scatterer. Note that $f_{i,m} = f_{dmax}\cos(\theta_{i,m})$ where $\theta_{i,m}$ is the angle of arrival of the i th path's m th scatterer (assumed uniformly distributed on $[0, 2\pi]$). Now, taking the Fourier Transform along τ results in

$$H(f, t) = \sum_{i=1}^L \alpha_i(t)e^{-j2\pi f\tau_i} \quad (13.36)$$

Now, sampling in time every T seconds (i.e., at every OFDM symbol) and in frequency at Δf (i.e., at every sub-carrier) we have

$$H[k, n] = \sum_{i=1}^L \alpha_i(nT)e^{-j2\pi k\Delta f\tau_i} \quad (13.37)$$

Now, again considering Figure 13.1, we wish to estimate each channel value in the time-frequency

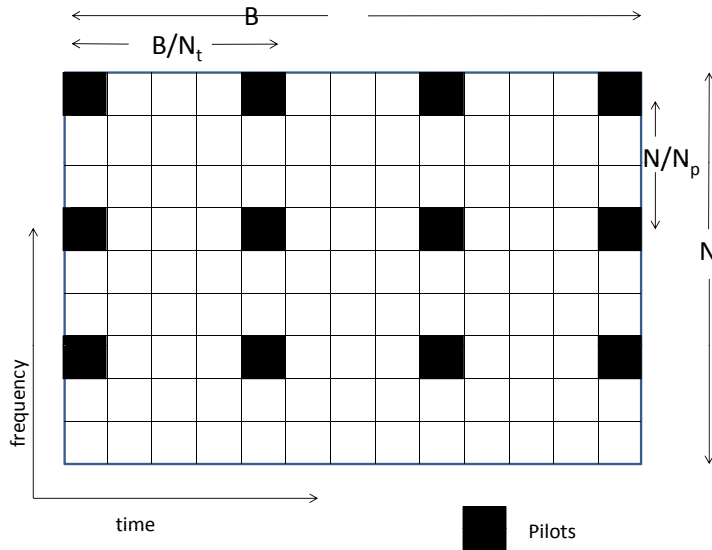


Figure 13.1: Illustration of the Time-Frequency Plane for OFDM Channel Estimation

plane $\hat{H}[k, n]$ based on pilots placed at various locations in time and frequency. In other words, we wish to estimate the $N \times B$ channel matrix \mathbf{H} based on the $N_p N_{pt}$ values obtained via pilots, i.e., N_p pilots are equally spaced in N_{pt} out of B OFDM symbols where each OFDM symbol has N sub-carriers. The N_p pilots in each OFDM symbol are spaced $\frac{N}{N_p} \Delta f$ Hz apart where $\Delta f = 1/T$ is the sub-carrier spacing. The pilots are spaced $\frac{B}{N_{pt}} T$ seconds apart in time. Note that The $N_p N_{pt}$

pilot locations are defined by the set $\mathcal{P}^2 = \begin{bmatrix} k_i \\ n_i \end{bmatrix}$ where k_1, k_2, \dots, k_{N_p} are the N_p frequency locations in terms of sub-carrier number and $n_1, n_2, \dots, n_{N_{pt}}$ are the N_{pt} time locations in terms of OFDM symbol number. Note that for proper estimation the spacing between pilots should obey Nyquist's sampling theorem. Specifically, in the frequency domain $\frac{N}{N_p} < \frac{1}{2\tau_{max} \Delta f}$ where τ_{max} is the maximum multipath delay. Similarly, in the time domain $\frac{B}{N_{pt}} < \frac{1}{2f_d T_s}$.

At each pilot location, by dividing by the known symbol, we obtain the least squares estimates of the channel values:

$$\begin{aligned} \mathbf{H}_p^{(LS)} &= \mathbf{P}^{-1} \mathbf{e}_p \\ &= \mathbf{H}_p + \tilde{\nu}_p \\ &\triangleq \mathbf{R} \end{aligned}$$

Each element of \mathbf{R} is simply the channel value sampled at $k\Delta f$ in frequency and nT_s in time corrupted by Gaussian noise:

$$R[k, n] = H[k, n] + \tilde{\nu}[k, n] \quad (13.38)$$

where again $\tilde{\nu} = \mathbf{P}\nu$. for $\begin{bmatrix} k \\ n \end{bmatrix} \in \mathcal{P}^2$ and where $\nu[n, k]$ is AWGN with variance $\sigma^2 = \frac{N_o}{E_s}$.

Now, we wish to estimate the channel at all NB locations using the $N_p N_{pt}$ pilot values using a linear transformation. In other words, we want to find

$$\hat{H}[k, n] = \sum_{k'} \sum_{n'} w^*[n, k; n', k'] R[k', n'] \quad (13.39)$$

where $\begin{bmatrix} k' \\ n' \end{bmatrix} \in \mathcal{P}^2$. Note that the weights are summed over $N_p N_{pt}$ pilots and are different for each value of $[n, k]$. This is illustrated in Figure 13.2.

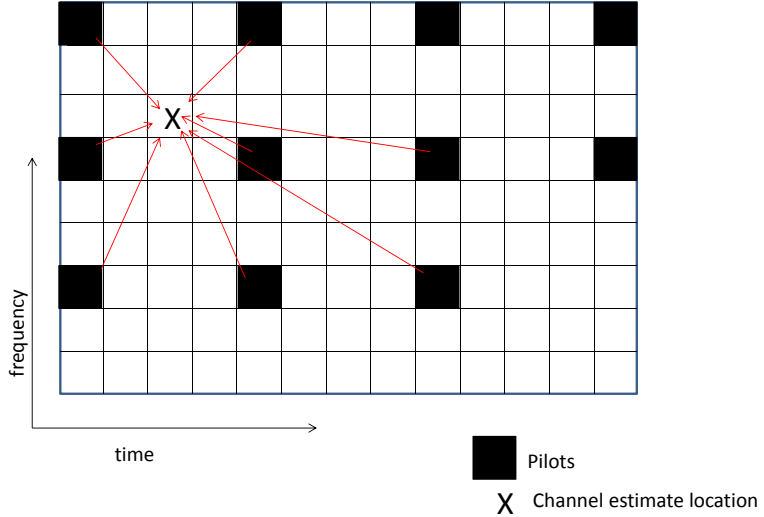


Figure 13.2: Illustration of Two-Dimensional MMSE OFDM Channel Estimation

To find the MMSE weights, we first define a vector version of R :

$$\mathbf{r}^{(p)} = \text{vec}(R) = \begin{bmatrix} R(k_1, n_1) \\ R(k_2, n_1) \\ \vdots \\ R(k_{N_p}, n_1) \\ R(k_1, n_2) \\ \vdots \\ R(k_{N_p}, n_{N_{pt}}) \end{bmatrix} \quad (13.40)$$

where $\mathbf{r}^{(p)}$ is a $N_{pt}N_p \times 1$ vector and $\begin{bmatrix} k_i \\ n_j \end{bmatrix} \in \mathcal{P}^2$. Now we can define a $N_{pt}N_p \times 1$ vector $\mathbf{w}_{k,n}$ applied to $\mathbf{r}^{(p)}$ to obtain $\hat{H}[k, n]$. That is

$$\hat{H}[k, n] = (\mathbf{w}_{k,n})^H \mathbf{r}^{(p)} \quad (13.41)$$

For a 2-dimensional MMSE filter we have

$$\mathbf{w}_{k,n} = \Phi_{rr}^{-1} \Phi_{rH}^{k,n} \quad (13.42)$$

where $\Phi_{rr} = \mathbf{E}\{\mathbf{r}^{(p)}(\mathbf{r}^{(p)})^H\}$ is an $N_{pt}N_p \times N_{pt}N_p$ covariance matrix and $\Phi_{rH}^{k,n} = \mathbf{E}\{\mathbf{r}^{(p)} H^*[k, n]\}$ is an $N_{pt}N_p \times 1$ correlation vector.

The covariance matrix elements can be determined based on the assumed channel model:

$$\mathbf{E}\{R[k, n]R^*[m, l]\} = \mathbf{E}\{(H[k, n] + \nu[k, n])(H[m, l] + \nu[m, l])^*\} \quad (13.43)$$

$$= \mathbf{E}\{H[k, n]H[m, l]^*\} + \delta(k - m)\delta(n - l)\sigma^2 \quad (13.44)$$

where

$$\delta(x) = \begin{cases} 1 & x = 0 \\ 0 & \text{else} \end{cases} \quad (13.45)$$

and

$$\mathbf{E}\{H[k, n]H[m, l]^*\} = \mathbf{E}\left\{\sum_{i=1}^L \sum_{u=1}^L \alpha_i(nT)\alpha_u^*(lT)e^{-j2\pi k\Delta f\tau_i}e^{j2\pi m\Delta f\tau_u}\right\} \quad (13.46)$$

$$= \sum_{i=1}^L \mathbf{E}\{\alpha_i(nT)\alpha_i^*(lT)\} e^{-j2\pi(k-m)\Delta f\tau_i} \quad (13.47)$$

$$= \underbrace{J_o(2\pi f_{dmax}|n-l|T)}_{\phi_t(nT-lT)} \underbrace{\sum_{i=1}^L \sigma_i^2 e^{-j2\pi(k-m)\Delta f\tau_i}}_{\phi_f(k\Delta f-m\Delta f)} \quad (13.48)$$

where we have assumed uncorrelated scattering and $\sigma_i^2 = \mathbf{E}\{|\alpha_i(t)|^2\}$, i.e., the average power of the i th resolvable multipath component with delay τ_i . Further, the m th element of the correlation vector $\Phi_{rH}^{k,n}$ can be found as

$$\Phi_{rH}^{k,n}[m] = \mathbf{E}\{\mathbf{r}^{(p)}[m]H^*[k, n]\} \quad (13.49)$$

$$= \mathbf{E}\{R[rem(m, N_p), \lceil m/N_p \rceil]H^*[k, n]\} \quad (13.50)$$

$$= \mathbf{E}\{H[rem(m, N_p), \lceil m/N_p \rceil]H^*[k, n]\} \quad (13.51)$$

where $rem(x, N) = x - \lfloor \frac{x}{N} \rfloor N$, $\lfloor x \rfloor$ is the floor operation and $\lceil x \rceil$ is the ceiling operation. Thus, the procedure for estimating the block channel is to (a) find the channel estimates at the pilot locations and create the vector $\mathbf{r}^{(p)}$. Then, using the known channel statistics, create the pilot covariance matrix Φ_{rr} . Then for every channel location $1 \leq k \leq N_p$, $1 \leq n \leq B$, find the cross-correlation matrix $\Phi_{rH}^{k,n}$ (again assuming that the channel statistics are known or can be estimated) and estimate the channel as

$$\hat{H}[k, n] = (\Phi_{rr}^{-1} \Phi_{rH}^{k,n})^T \mathbf{r}^{(p)} \quad (13.52)$$

The basic concept is illustrated in Figure 13.2.

Separable 1-D MMSE Filters for OFDM

A second option is to filter in the time and frequency domains separately. This is less complex and suffers very little in terms of performance. Although due to the linear nature of the filters, it doesn't matter whether one filters in time first or frequency first, we will present the concept by showing frequency domain filtering first.

Frequency Domain Recall that pilots exist at the $N_p N_{pt}$ values $\begin{bmatrix} k_i \\ n_i \end{bmatrix}$ in the set \mathcal{P}^2 . For the n_i th OFDM symbol, we estimate the frequency domain channel as shown in Figure 13.3

$$\tilde{H}[k, n_i] = \sum_{m=1}^{N_p} \mathbf{w}_k^f[m] R[k_m, n_i] \quad (13.53)$$

where \mathbf{w}_k^f is the vector of frequency domain weights needed to estimate the k th channel estimate in frequency. Now, let's define the following $N_p \times 1$ vector of noisy channel estimates at the pilots of the n_i th OFDM symbol

$$\mathbf{r}_{n_i}^{(N_p)} = \begin{bmatrix} R[k_1, n_i] \\ R[k_2, n_i] \\ \vdots \\ R[k_p, n_i] \end{bmatrix} \quad (13.54)$$

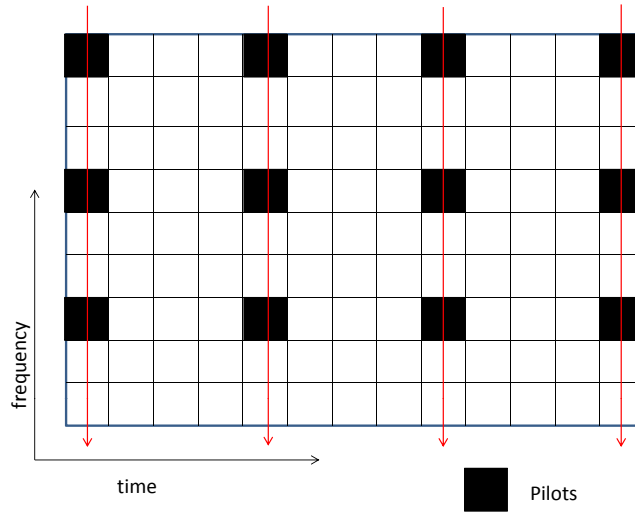


Figure 13.3: Illustration of One-Dimensional MMSE OFDM Channel Estimation in Frequency Domain

Now, following the MMSE criterion, the weights can be calculated as

$$\mathbf{w}_k^f = (\Phi_{rr}^f)^{-1} \Phi_{rH}^{f,k} \quad (13.55)$$

where

$$\Phi_{rr}^f = \mathbf{E} \left\{ \mathbf{r}_{n_i}^{(N_p)} (\mathbf{r}_{n_i}^{(N_p)})^H \right\} \quad (13.56)$$

where the choice of n_i doesn't influence the weights since the frequency correlation is assumed to be stationary. Using the previous definitions, we can show that the k, m th element can be found as

$$\Phi_{rr}^f[k, m] = \phi_f \left(\frac{N}{N_p} (k - m) \Delta f \right) + \frac{N_o}{E_s} \delta(k - m) \quad (13.57)$$

Further, the correlation vector can be found to be

$$\Phi_{rH}^{f,k} = \mathbf{E} \left\{ \mathbf{r}_{n_i}^{(N_p)} H^*[k, n_i] \right\} \quad (13.58)$$

where again, the choice of n_i doesn't matter. The m th element of this $N_p \times 1$ vector is found as

$$\Phi_{rH}^{f,k}[m] = \phi_f \left(\left(\frac{N}{N_f} m - k \right) \Delta f \right) \quad (13.59)$$

Time Domain Once all channel values have been estimated in each OFDM symbol with pilots (as shown in Figure 13.3), the channel values can be estimated across OFDM symbols i.e., in the time-domain as shown in Figure 13.4. Note that the estimates $\tilde{H}[k, n]$ in equation (13.53) are preliminary estimates since they do not include time domain correlation. That is, for each value of k, n (including those previously estimated) we create

$$\hat{H}[k, n] = \sum_{m=1}^{N_{pt}} \mathbf{w}_n^t[m] \tilde{H}[k, n_m] \quad (13.60)$$

Again, the weights are chosen to satisfy the MMSE criterion. Thus, they are found as

$$\mathbf{w}_n^t = (\Phi_{rr}^t)^{-1} \Phi_{rH}^{t,n} \quad (13.61)$$

where

$$\Phi_{rr}^t = \mathbf{E} \left\{ \mathbf{r}_k^{(N_{pt})} (\mathbf{r}_k^{(N_{pt})})^H \right\} \quad (13.62)$$

and

$$\mathbf{r}_k^{(N_{pt})} = \begin{bmatrix} R[k, n_1] \\ R[k, n_2] \\ \vdots \\ R[k, n_{N_{pt}}] \end{bmatrix} \quad (13.63)$$

and

$$\Phi_{rH}^{t,n} = \mathbf{E} \left\{ \mathbf{r}_k^{(N_{pt})} H[k, n] \right\} \quad (13.64)$$

Note, that $\Phi_{rr}^t = \Phi_{HH}^t + \frac{N_o}{E_s} \mathbf{I}$ where

$$\Phi_{HH}^t[n, k] = \phi_t(|n - k| T_o N_{pt}) \quad (13.65)$$

where T_o is the OFDM symbol duration. Further note that

$$\Phi_{rH}^{t,n}[k] = \phi_t(|n - kN_{pt}|T_o) \quad (13.66)$$

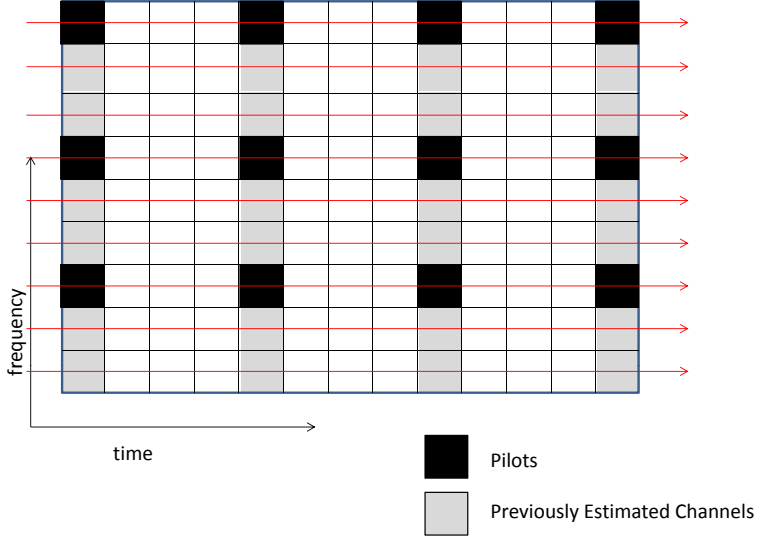


Figure 13.4: Illustration of One-Dimensional MMSE OFDM Channel Estimation in Time Domain

For a more detailed discussion of this filter, please see [3].

13.2 Synchronization

In addition to channel estimation, a major parameter estimation problem at the receiver is to estimate and remove timing offset and frequency offset. This process is known as synchronization and can also be considered aligning the local timing/frequency reference to the incoming signal. For timing offset estimation, there are two typical aspects: symbol timing and frame timing. The former involves determining where each OFDM symbol starts (symbol offset k_o), while the latter involves determining where a frame of OFDM symbols starts. In terms of frequency offset estimation/removal, there are also two general parts: the fine estimation which removes any fractional offset and the coarse estimation which removes an integer offset. In other words, the frequency offset in continuous time can be written as

$$f_{co} = (z + \phi) \Delta f \quad (13.67)$$

where $z \in \mathbb{Z}$ is the integer multiple of the subcarrier spacing (integer offset) and ϕ is the fractional offset. Note that the digital frequency offset is defined as $f_o = f_{co}T_{eff} = \frac{f_{co}}{\Delta f}$. Thus, $f_o = z + \phi$ where z is the integer offset and ϕ is the fractional offset. We will discuss all four items in the remainder of this chapter. One last note: In equation() there are two different ways we could choose z and ϕ . For example if $f_{co} = 1.2\Delta f$ we could choose $z = 1$ and $\phi = 0.2$ or we could choose

$z = 2$ and $-\phi = 0.8$. Similarly if $f_{co} = -2.3\Delta f$ we could choose $z = -2$ and $\phi = -0.3$ or we could choose $z = -3$ and $\phi = 0.7$. For consistency and later convenience, we will always require that $|\phi| < 1/2$. The reason for this will become more clear later.

13.2.1 Maximum Likelihood Estimation of $f_o = \phi$ and k_o

Let us consider the case where $z = 0$ and thus $f_o = \phi$. Consider received signal samples with time offset k_o and frequency offset f_o :

$$r[k] = x[k - k_o]e^{j2\pi f_o k/N} + n[k] \quad (13.68)$$

When using a cyclic prefix

$$x[k] = x[k + N] \quad k \in \mathcal{I} \quad (13.69)$$

where $\mathcal{I} = \{k_o, k_o + 1, \dots, k_o + L - 1\}$, $\mathcal{I}' = \{k_o + N, k_o + N + 1, \dots, k_o + N + L - 1\}$. Consider a $2N + L \times 1$ vector of samples $\mathbf{r} = [r[1], r[2], \dots, r[k_o], \dots, r[2N + L]]^T$. The likelihood function can be found to be

$$\begin{aligned} f(\mathbf{r}|k_o, f_o) &= \prod_{k \in \mathcal{I}} f(r[k], r[k + N]) \prod_{k \notin \mathcal{I} \cup \mathcal{I}'} f(r(k)) \\ &= \prod_{k \in \mathcal{I}} \frac{f(r[k], r[k + N])}{f(r[k])f(r[k + N])} \prod_k f(r[k]) \end{aligned}$$

Note that the second term does not depend on k_o or on f_o and can thus be ignored. The vector $\tilde{\mathbf{r}}$ is a complex Gaussian vector. The mean of each sample is zero and the variance is $\sigma_s^2 + \sigma_n^2$ (the sum of the signal power and noise power). Further, for $k \in \mathcal{I}$

$$\mathbb{E}\{r[k]r^*[k + m]\} = \begin{cases} \sigma_s^2 + \sigma_n^2 & m = 0 \\ \sigma_s^2 e^{j2\pi f_o} & m = N \\ 0 & \text{else} \end{cases} \quad (13.70)$$

It can be shown that

$$f(r[k], r[k + N]) = \frac{1}{\pi^2(\sigma_s^2 + \sigma_n^2)(1 - \rho^2)} \exp\left(-\frac{(|r[k]|^2 - 2\rho\Re\{e^{j2\pi f_o}r[k]r^*[k + N]\} + |r[k + N]|^2)}{(\sigma_s^2 + \sigma_n^2)(1 - \rho^2)}\right) \quad (13.71)$$

and

$$f(r[k]) = \frac{1}{\pi(\sigma_s^2 + \sigma_n^2)(1 - \rho^2)} \exp\left(-\frac{|r[k]|^2}{\sigma_s^2 + \sigma_n^2}\right) \quad (13.72)$$

The log-likelihood function can then be written as

$$\begin{aligned} \Lambda(k_o, f_o) &= \log\left(\prod_{k \in \mathcal{I}} \frac{f(r[k], r[k + N])}{f(r[k])f(r[k + N])}\right) \\ &= \sum_{k \in \mathcal{I}} \log\left(\frac{f(r[k], r[k + N])}{f(r[k])f(r[k + N])}\right) \\ &= c_1 + c_2 (|\gamma(k_o)|\cos(2\pi f_o + \angle\gamma(k_o)) - \rho\Psi(k_o)) \end{aligned} \quad (13.73)$$

The constants c_1 and c_2 do not depend on k_o or f_o , and

$$\gamma(m) = \sum_{k=m}^{m+N_{cp}-1} r[k]r^*[k+N] \quad (13.74)$$

$$\Phi(m) = \frac{1}{2} \sum_{k=m}^{m+N_{cp}-1} (r[k]|^2 + |r[k+N]|^2) \quad (13.75)$$

and

$$\rho = \left| \frac{\mathbb{E}\{r[k]r^*[k+N]\}}{\sqrt{\mathbb{E}\{|r[k]|^2\}\mathbb{E}\{|r[k+N]|^2\}}} \right| \quad (13.76)$$

Ignoring the two constants we have

$$\Lambda(k_o, f_o) = |\gamma(k_o)|\cos(2\pi f_o + \angle\gamma(k_o)) - \rho\Psi(k_o) \quad (13.77)$$

Note that only one term depends on f_o , the center term. That term can be maximized if we set $f_o = -\frac{1}{2\pi}\angle\gamma(k_o) + n$ for an integer n . This creates a log likelihood function depending only on k_o :

$$\Lambda(k_o, \hat{f}_o^{ML}) = |\gamma(k_o)| - \rho\Psi(k_o) \quad (13.78)$$

Thus, the maximum likelihood estimate for k_o is

$$\hat{k}_o^{ML} = \arg \max_{k_o} |\gamma(k_o)| - \rho\Psi(k_o) \quad (13.79)$$

and the maximum likelihood estimate for f_o is then

$$\hat{f}_o^{ML} = -\frac{1}{2\pi}\angle\gamma(\hat{k}_o^{ML}) + z \quad (13.80)$$

If we can assume that a coarse frequency offset estimator brought such that $f_o = \phi < \frac{1}{2}$, we can set $z = 0$ and thus

$$\hat{f}_o^{ML} = -\frac{1}{2\pi}\angle\gamma(\hat{k}_o^{ML}) \quad (13.81)$$

Note now the reason for requiring absolute fractional offset being less than 1/2. The range of $\angle\gamma(\hat{k}_o^{ML})$ is 2π :

$$-\pi < \angle\gamma(\hat{k}_o^{ML}) \leq \pi \quad (13.82)$$

Thus, we can only estimate ϕ in the range of $-\frac{1}{2} < \phi \leq \frac{1}{2}$. Due to the ambiguity in angles greater than π or less than $-\pi$, we will map such frequency offsets incorrectly and essentially push the offset to the next integer multiple of Δf .

Note the intuition behind this overall estimator. The offset estimate is that value corresponding to the beginning of an N_{cp} sample window that maximizes the correlation between that window of N_{cp} samples and another window spaces N samples away (after normalizing by the energy in those samples). In other words, it finds the beginning of the samples corresponding to the cyclic prefix. The frequency estimator finds the phase rotation between the two windows which corresponds to the frequency offset. As an example, consider a received signal with an SNR of 10dB and $N = 256$ sub-carriers and a cyclic prefix length of $N_{cp} = 48$. In this example let $k_o = 90$ and $f_o = 0.3$. An example timing metric is shown in Figure 13.5. We can see a distinct peak at $k_o = 90$ as is expected. The angle of the metric (divided by 2π) is shown in Figure . We can see that in the

region of $k_o = 90$ the metric (and thus estimate) is very close to the true value. The performance of the joint ML approach is shown in Figure 13.7 for the case $N = 256$, $N_{cp} = 48$ and $|f_o| < \frac{1}{2}$. We can see that the performance is very good. Even at 0dB the RMSE of the timing error is only two samples, well within the cyclic prefix. The frequency estimate at 0dB is approximately 2% of the OFDM symbol rate. As SNR increases the performance of both estimators improves as expected.

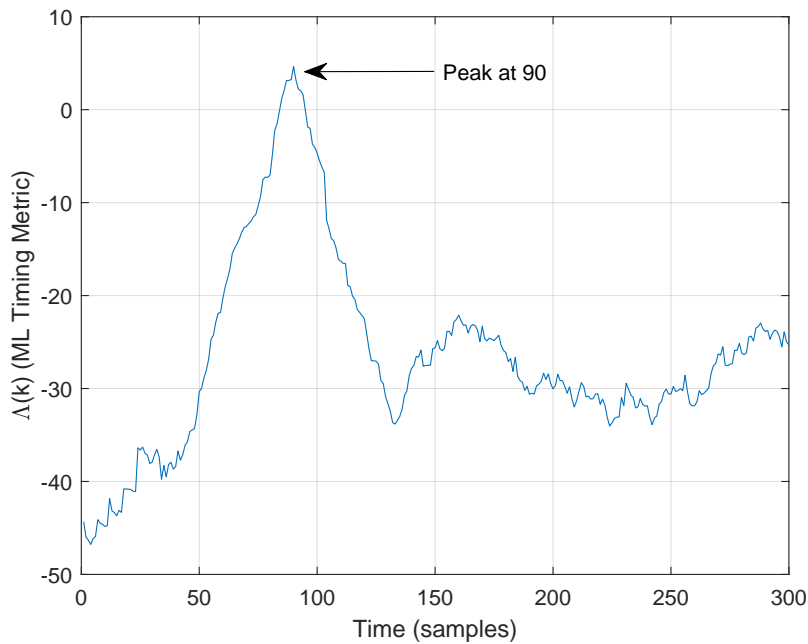


Figure 13.5: Example Timing Metric for Maximum Likelihood Timing Estimation (SNR = 10dB, $N = 256$, $N_{cp} = 48$, $k_o=90$)

13.2.2 Frame and Symbol Offset Estimation

The previously described estimator provides timing at the OFDM symbol level. However, it cannot tell one OFDM symbol from another. If we have a stream of OFDM symbols, we likely want to know where we are in that stream. This is typically known as frame synchronization. To accomplish frame synchronization, we can put known symbol patterns into the stream and simply look for those patterns. An alternative approach allows us to achieve both symbol synchronization and frame synchronization simultaneously. This involves putting one special known symbol (i.e., a special type of pilot symbol) at the beginning of the frame. This special symbol has the same samples in the second half of the symbol as the first half of the symbol. This effectively creates an increased range of samples with correlation (as compared to the cyclic prefix) and is sufficiently different from other symbols that it allows us to both estimate symbol timing and the beginning of the frame.

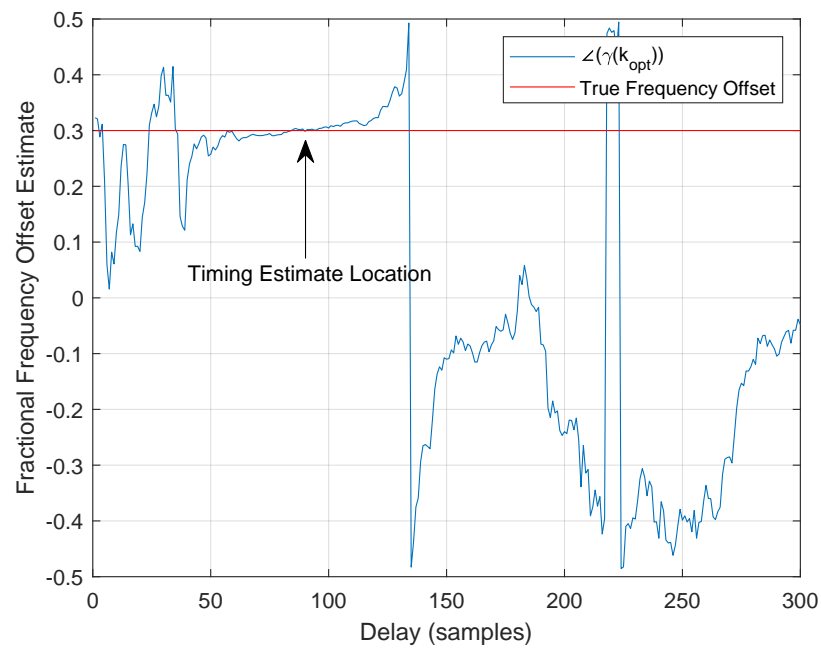


Figure 13.6: Example Frequency Estimate at Different Delays for Maximum Likelihood Frequency Estimation (SNR = 10dB, $N = 256$, $N_{cp} = 48, f_o=0.3$)

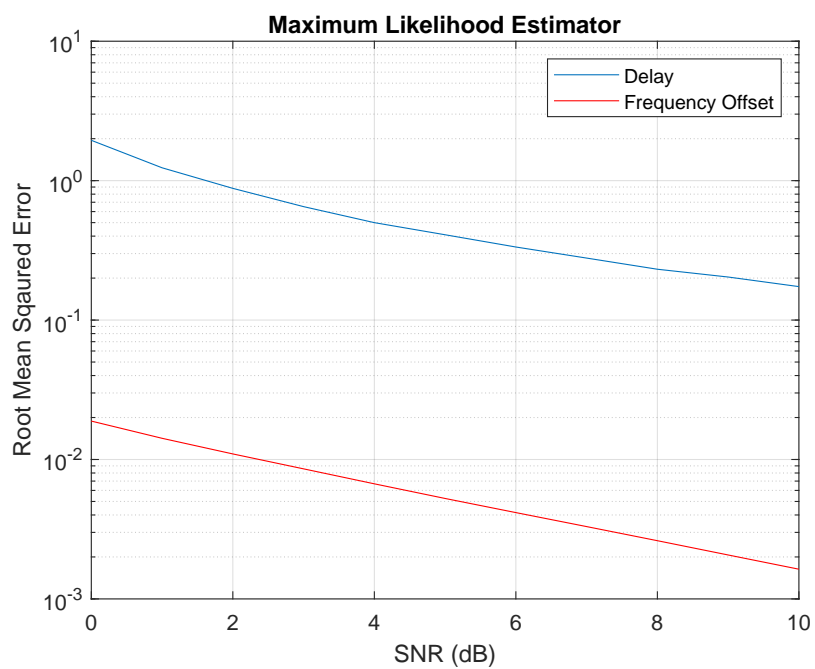


Figure 13.7: RMSE of Timing and Frequency Offset Using the Joint ML Estimator ($N = 256, N_{cp} = 48, |f_o| < \frac{1}{2}$)

The OFDM symbol samples are can written as

$$\begin{aligned} x[n] &= \frac{1}{\sqrt{N}} \sum_{k=0}^{N-1} s[k] e^{j2\pi kn/N} \\ &= \underbrace{\frac{1}{\sqrt{N}} \sum_{k=0,2}^{N-2} s[k] e^{j2\pi kn/N}}_{\text{even terms}} + \underbrace{\frac{1}{\sqrt{N}} \sum_{k=1,3}^{N-1} s[k] e^{j2\pi kn/N}}_{\text{odd terms}} \end{aligned} \quad (13.83)$$

Now, the second half of the symbol can be written as

$$\begin{aligned} x[n+N/2] &= \frac{1}{\sqrt{N}} \sum_{k=0}^{N-1} s[k] e^{j2\pi k(n+N/2)/N} \\ x[n+N/2] &= \frac{1}{\sqrt{N}} \sum_{k=0}^{N-1} s[k] e^{j2\pi kn/N} \underbrace{e^{j2\pi kN/(2N)}}_{\substack{1 \quad k \quad \text{even} \\ -1 \quad k \quad \text{odd}}} \\ &= \underbrace{\frac{1}{\sqrt{N}} \sum_{k=0,2}^{N-2} s[k] e^{j2\pi kn/N}}_{\text{even terms}} - \underbrace{\frac{1}{\sqrt{N}} \sum_{k=1,3}^{N-1} s[k] e^{j2\pi kn/N}}_{\text{odd terms}} \end{aligned} \quad (13.84)$$

Thus, we can force $x[n] = x[n+N/2]$ by setting $s[k] = 0$ for k odd. Now, let the received samples be equal to

$$r[n] = x[n] e^{j2\pi f_o n/N} + \nu[n] \quad (13.85)$$

where $\nu[n]$ are samples of Gaussian noise. We define the following two metrics as

$$\begin{aligned} P(n) &= \sum_{k=0}^{N/2-1} r[n+k] r^*[n+k+N/2] \\ R(n) &= \sum_{k=0}^{N/2-1} |r[n+k+N/2]|^2 \end{aligned}$$

Further, we set our synchronization metric to be

$$\begin{aligned} M(n) &= \frac{|P(n)|^2}{R^2(n)} \\ &= \frac{\left| \sum_{k=0}^{N/2-1} r[n+k] r^*[n+k+N/2] \right|^2}{\left(\sum_{k=0}^{N/2-1} |r[n+k+N/2]|^2 \right)^2} \end{aligned}$$

When $-N_{cp} \leq n \leq 0$, we will have $r[n+k] = r[n+k+N/2]$ (ignoring noise) and $M(n) = 1$. Outside of this interval, $M(n)$ will be a Central Chi-Square random variable with two degrees of freedom (or four dof with noise).

13.2.3 Frequency Offset Estimation

Using the same synchronization symbol described above (i.e., one for which $x[n+N/2] = x[n]$), we can estimate the frequency offset from the offset between samples from the first half of the

symbol and samples from the second half of the symbol *assuming the frequency offset is less than the OFDM symbol rate*². Specifically,

$$\hat{f}_o = \frac{\angle(P(n_{opt}))}{\pi} \quad (13.86)$$

where n_{opt} is the optimal sample offset from the timing synchronization and the frequency offset is defined in terms of the OFDM symbol rate. Note that if the frequency offset is greater than the OFDM symbol rate, $\angle(P(n_{opt})) > \pi$ and an ambiguity arises. We will address this later.

However, to understand the theory behind this estimator, consider a set of samples with a frequency offset (ignoring noise for simplicity):

$$r[n] = x[n]e^{j(2\pi f_o n/N + \theta_o)} \quad (13.87)$$

where f_o is the normalized frequency offset $f_o = f_{co}T_{eff}$, f_{co} is the continuous time (i.e., non-normalized) offset and f_s is the sampling rate. Now, the samples in the second half of the received symbol are

$$r[n + N/2] = \underbrace{x[n + N/2]}_{=x[n]} e^{j(2\pi f_o(n+N/2)/N + \theta_o)} \quad (13.88)$$

Thus, if we multiply samples by the complex conjugate of a sample $N/2$ samples away we have:

$$r[n]r^*[n + N/2] = x[n]x^*[n]e^{j(2\pi f_o n/N + \theta_o)}e^{-j(2\pi f_o(n+N/2)/N + \theta_o)} \quad (13.89)$$

$$= |x[n]|^2 e^{-j(\pi f_o)} \quad (13.90)$$

Thus,

$$P(n_{opt}) = \sum_k |x[n+k]|^2 e^{-j(\pi f_o)} \quad (13.91)$$

and $\angle(P(n_{opt})) = \pi f_o$. This leads to the estimator in equation (13.86). Again this ignores noise. In the presence of noise, the estimator will obviously not be perfect, and will improve with the number of synchronization symbols used. Note that since

$$-\pi < \angle(P(n_{opt})) \leq \pi$$

we can allow a larger range on ϕ than we could with the ML estimator based only on the CP. More specifically, we can now handle

$$-1 < f_o \leq 1$$

If however $|f_o| > 1$, this estimator will not work, as we will see in the next section.

As an example, consider a received signal with an SNR of 10dB and $N = 256$ sub-carriers and a cyclic prefix length of $N_{cp} = 48$. In this example let $k_o = 90$ and $f_o = 0.3$. An example of the timing metric is shown in Figure 13.8. We can see that rather than having a distinct peak at $k_o = 90$ as in the ML estimator, we obtain a flat region corresponding to the cyclic prefix. To estimate the symbol timing, we need to estimate the beginning or end of that region. The angle of the metric (divided by π) is shown in Figure . We can see that in the region of $k_o = 90$ the metric (and thus estimate) is very close to the true value. Note that the estimate is somewhat better than the ML estimate, simply because it uses more samples. In other words, this is in fact

²Note that this is the a slightly looser assumption than we made previously. We will discuss this further shortly.

the ML estimator if the cyclic prefix length were $N/2$ rather than N_{cp} . Figure 13.8 shows one shortcoming of this estimator - it identifies the entire CP region. We still need some means to identify the beginning of the CP (or equivalently the end). For example, we could find the earliest sample that exceeds 95% of the max value. An alternative is to adjust the metric so that it is similar to the ML metric. Specifically, we could create a metric

$$P'(n) = \sum_{k=0}^{N/2-1} r[n+k]r^*[n+k+N_{cp}+N/2]$$

This metric searches for a region of $N/2 + N_{cp}$ samples that is correlated with another group of the same size $N/2$ samples away. By adding the N_{cp} samples, the region of maximum correlation is reduced to one sample, rather than N_{cp} samples. A comparison of the two metrics is shown in Figure 13.10. We can see that the metric specifically identifies the beginning of the CP region or the first sample as desired. The performance of the frame-timing-based estimators are shown in Figure 13.11. The figure plots the performance of the case of $N = 256$, $N_{cp} = 48$ and $|f_o| < \frac{1}{2}$. We can see that the original frame timing estimator is significantly worse than the ML estimator. The estimate is well within the cyclic prefix, which will avoid ICI, but it is still not as accurate as the ML approach. Modifying the approach as in (13.92) results in substantially improved performance, but still not equivalent to the ML approach, despite using more samples. However, the frequency estimator (which is essentially the same as the ML approach) is nearly equivalent to ML performance.

13.2.4 Impact of $f_{co} = \frac{z}{T_{eff}}$

Before discussing the estimator, let us examine the impact of a frequency offset which is an integer multiple of the OFDM symbol rate. Specifically, let $f_{co} = \frac{z}{T_{eff}}$ where $z \in \mathbb{Z}, z \neq 0$. Further, for simplicity let $\theta_o = 0$. If we don't correct the frequency offset, a signal sample (ignoring noise) can be written as

$$x[n]e^{j2\pi f_o n/N} = \frac{1}{\sqrt{N}} \sum_{k=0}^{N-1} s[k]e^{j2\pi kn/N} e^{j2\pi f_o n/N} \quad (13.92)$$

$$= \frac{1}{\sqrt{N}} \sum_{k=0}^{N-1} s[k]e^{j2\pi kn/N} e^{j2\pi nz/N} \quad (13.93)$$

$$= \frac{1}{\sqrt{N}} \sum_{k=0}^{N-1} s[k]e^{j2\pi(k+z)n/N} \quad (13.94)$$

At the receiver, the decision metric for symbol $s[k]$ is then (again ignoring noise for simplicity)

$$z[k] = \frac{1}{\sqrt{N}} \sum_{n=0}^{N-1} x[n]e^{-j2\pi kn/N} \quad (13.95)$$

$$= \frac{1}{\sqrt{N}} \sum_{n=0}^{N-1} \left(\frac{1}{\sqrt{N}} \sum_{k=0}^{N-1} s[k]e^{j2\pi(k+z)n/N} \right) e^{-j2\pi kn/N} \quad (13.96)$$

$$= s[k-z] \quad (13.97)$$

Thus, we can see that an frequency offset which is an integer multiple of a the OFDM symbol rate results in the symbols being shifted by the integer multiple z .

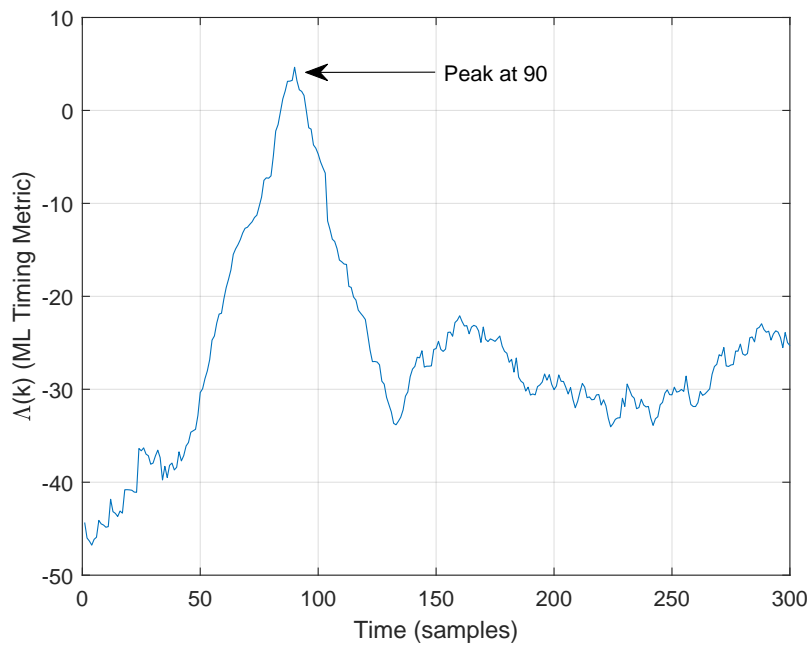


Figure 13.8: Example Timing Metric for Frame/Symbol Timing Estimation (SNR = 10dB, $N = 256$, $N_{cp} = 48$, $k_o=90$)

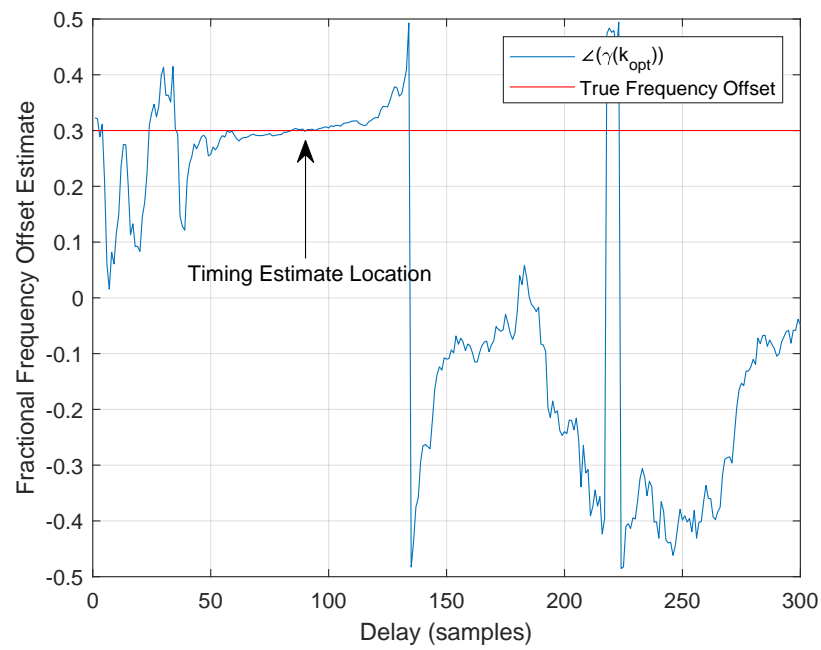


Figure 13.9: Example Timing Metric for Frequency Estimation when using the Frame/Symbol Timing Estimator (SNR = 10dB, $N = 256$, $N_{cp} = 48$, $f_o=0.3$)

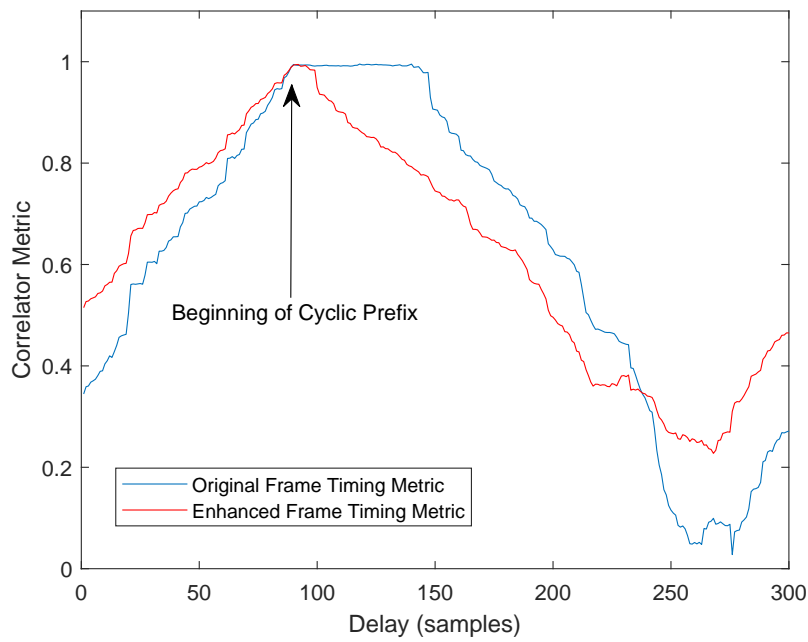


Figure 13.10: Comparison of Two Timing Metrics for Frame/Symbol Timing Estimation (SNR = 10dB, $N = 256$, $N_{cp} = 48$, $k_o=90$)

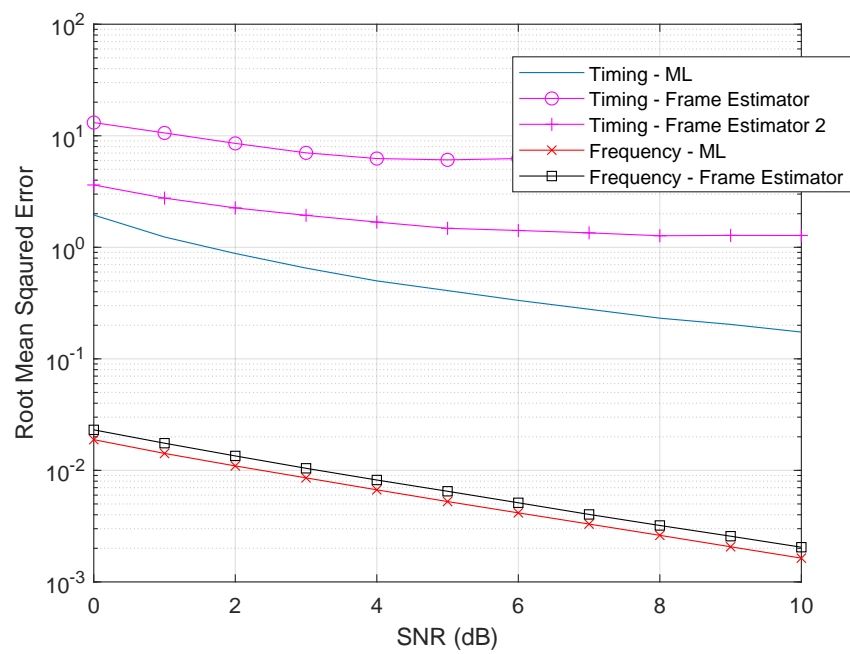


Figure 13.11: RMSE of Timing and Frequency Offset Using Frame Estimator and ML Estimator ($N = 256$, $N_{cp} = 48, |f_o| < \frac{1}{2}$)

13.2.5 Impact of $|f_{co}| > \frac{1}{T_{eff}}$ on the Estimator

Let the normalized frequency offset be greater than the OFDM symbol rate. Further, writing it in terms of the integer and fractional (relative to the symbol rate) components:

$$f_o = \underbrace{z}_{\text{integer}} + \underbrace{\frac{\phi}{\pi}}_{\text{fractional}} \quad (13.98)$$

where $\phi < \pi$ is the fractional digital offset. We can then rewrite (13.89) as

$$r[n]r^*[n+N/2] = x[n]x^*[n]e^{j(2\pi(\frac{z}{N} + \frac{\phi}{\pi N})n + \theta_o)}e^{-j(2\pi(\frac{z}{N} + \frac{\phi}{\pi N})(n+N/2) + \theta_o)} \quad (13.99)$$

$$= |x[n]|^2 e^{-j(\pi(\frac{z}{N} + \frac{\phi}{\pi N})N)} \quad (13.100)$$

$$= |x[n]|^2 e^{-j\phi} e^{j(z\pi)} \quad (13.101)$$

Thus, if we use the previous estimator, we will not obtain the appropriate result since we cannot know z or even that z is present. Instead, we should use the previous estimator and remove the fractional frequency offset, followed by an estimator for the integer offset.

13.2.6 Integer Offset Estimation

The above discussion of symbol, frame and fractional frequency offset estimation assumes the use of a single special OFDM symbol at the beginning of a frame. To handle the case of integer frequency offsets (i.e., $z \neq 0$ in 13.2), we use two special OFDM symbols. The first OFDM symbol is defined as $\mathbf{x}_1 = \mathbf{D}_N^H \mathbf{s}_1$ where

$$\mathbf{s}_1 = \begin{bmatrix} s_1 & 0 & s_2 & 0 & \dots & s_{N/2} & 0 \end{bmatrix}$$

while the second symbol is defined $\mathbf{x}_2 = \mathbf{D}_N^H \mathbf{s}_2$ where

$$\mathbf{s}_2 = \begin{bmatrix} s_1 v_1 & 0 & s_2 v_2 & 0 & \dots & s_{N/2} v_{N/2} & 0 \end{bmatrix}$$

where \mathbf{v} is a length $N/2$ pseudo-random sequence with good autocorrelation properties. Let's assume that symbol timing has already been performed and the fractional frequency offset ϕ has been estimated and removed. Define $\tilde{\mathbf{r}} = \mathbf{T}_{cp}\tilde{\mathbf{r}}$. Then we have

$$\begin{aligned} \eta_1 &= \mathbf{D}_N \tilde{\mathbf{r}}_1 \\ &= \Gamma \mathbf{s}_1 + \nu_1 \\ \eta_2 &= \mathbf{D}_N \tilde{\mathbf{r}}_2 \\ &= \Gamma \mathbf{s}_2 + \nu_2 \end{aligned} \quad (13.102)$$

Let $\mathbf{a} \cdot \mathbf{b} = [a_1 b_1, a_2 b_2, \dots, a_N b_N]^T$. Let $\mathbf{b} = \text{sgn}(\Re(\Gamma_1 \cdot \Gamma_2^*))$. Then $\hat{\mathbf{v}} = \mathbf{b}(1 : 2 : N)$. Finally our estimate of z is

$$\hat{z} = 2 \left(\arg \max_z \sum_{k=0}^{N/2-1} \mathbf{v}_k \hat{\mathbf{v}}_{k+z} \right) \quad (13.103)$$

And the integer frequency offset estimate is

$$\hat{f}_o = \hat{z} \quad (13.104)$$

13.2.7 Overall Frequency Offset Estimator

The overall frequency offset estimator would then follow these steps:

1. Estimate fractional frequency offset $\hat{\phi}/\pi$ using the estimator defined in (13.86).
2. Remove this fractional offset using $r[n] = r[n]e^{-j\hat{\phi}}$.
3. Estimate the integer frequency offset z using the second estimator (13.103)
4. Remove the integer frequency offset

13.3 Conclusions

In this chapter we have examined parameter estimation in OFDM systems including channel estimation, frequency offset estimation, and timing offset estimation.